University of Washington
Department of Civil and Environmental Engineering

REGIONALIZATION OF A MACROSCALE HYDROLOGICAL MODEL

Fayez Abdulla

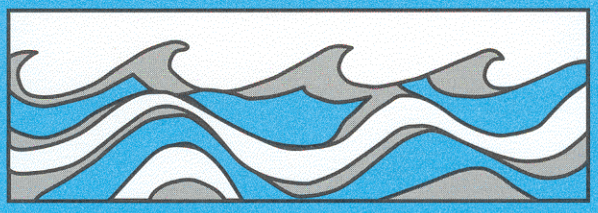

Water Resources Series
Technical Report No.144
July 1995

Seattle, Washington
98195

Department of Civil Engineering
University of Washington
Seattle, Washington 98195

REGIONALIZATION OF A MACROSCALE HYDROLOGICAL MODEL

Fayez Abdulla

Water Resources Series
Technical Report No. 144

July 1995

ABSTRACT

A methodology is presented for regionalization of the parameters of a macroscale land surface hydrologic model (the two-layer variable infiltration capacity model, VIC-2L) for the Arkansas-Red River basin using station hydrological and meteorological data and distributed land surface characteristics from digital elevation data and the SCS STATSGO soil data base. The approach is developed using a search procedure to provide catchment estimates of the parameters of the VIC-2L model for a set of catchments of intermediate size (drainage areas 100 to 10,000 km^2) within the Arkansas-Red River basin. Regional equations are developed to relate the VIC-2L model parameters to measurable physical quantities. The optimum parameters of the VIC-2L model for 34 catchments in the Arkansas-Red River basin are the dependent variables in the regional regression equations. The independent variables are catchment characteristics derivable for digital elevation, soils, climatalogical, and land cover data. The approach is validated by comparing observed and simulated runoff records from 6 catchments not in the 34 calibration catchments. The model performance was generally quite good, especially for humid and sub-humid catchments.

Three applications of a grid-based version of the VIC-2L model to the Arkansas-Red River basin at the one degree spatial scale are described, using variations of the regionally estimated parameters. In the first application, the water balance components for the basin were estimated using a simple spatial interpolation scheme applied to the parameters from the 40 calibration catchments. In the second application, the regional parameter estimation equations were used to compute the water balance components. In the third application, the VIC-2L model was run in a full energy and water balance mode, and was tested for its ability to simulate large-scale sensible and latent heat fluxes using the regional parameter estimation scheme. Simulated monthly hydrographs for the Arkansas-Red River basin using the regional parameters are in reasonably good agreement with the observed hydrographs. The average absolute relative error in the simulated annual runoff for ten gaging stations is about 10 percent in the case of the regional parameters and about 20 percent in the case of the interpolated parameters. The magnitude of the bias is less for the humid eastern part of the basin than the arid west.

Spatially averaged evaporative fluxes predicted by the VIC-2L model are in good agreement with those estimated using an atmospheric water budget for the Arkansas-Red River basin. The budgets are relatively insensitive to the two forms of regional parameter estimates that were tested. However, significant differences in the temporal means of the water balance components for individual grid cells are observed. The largest relative differences in the runoff ratios occur in the most arid part of the region, while the largest differences in the evaporation ratios occur in the humid area. The results indicate that the surface hydrological cycle in the Arkansas-Red River basin is mainly water rather than energy limited, especially at the annual scale.

ACKNOWLEDGMENTS

The research described in this report is based on the doctoral dissertation of the author. The author wish to express his sincere appreciation and thanks to his adviser, Professor Dennis P. Lettenmaier for his advice and encouragement throughout the course of my research. It can be very honestly said that without his support and encouragement this work would not have been undertaken. The author also would like to thank Professor Stephen J. Burges, whose candid suggestions have substantially improved this work, Professor Eric F. Wood at Princeton University for his advice and encouragement throughout this work, and Professor David R. Montgomery for his many insights and suggestions. It was his honor and privilege to have Professors Dennis P. Lettenmaier, Stephen J. Burges, Eric F. Wood, Nicholas R. Chrisman, David R. Montgomery, and Finbarr S. O'Sullivan as members of his supervisory committee. He is indebted to his committee members who have been considerate and helpful throughout this research.

Special thanks are due to his parents, for their great care and encouragement during his study and throughout his life, and to his wife Manal, for her great support. Without their constant love, care and support, the completion of this thesis would not have been possible. He would also like to thank his three children, Ahmad, Ibrahim, and Omar; they have brought him great joy. Special thanks to my host family, Jean McGrew and Claire McGrew for their help and encouragement. Many thanks to all his fellow graduate students in Room 159 Wilcox Hall for their help and encouragement. Special thanks to Dr. Reiner Schnur for his valuable comments and suggestions during this research.

The author was supported by a fellowship from the Deans Council at Jordan University of Science and Technology during most of his tenure at the University of Washington. This research was also supported in part by the National Oceanic and Atmospheric Administration under Grants NA36GP0483 and NA56GP0198, and by the U.S. National Science Foundation under Grant EAR-9318898.

TABLE OF CONTENTS

LIST OF FIGURES

LIST OF TABLES

CHAPTER 1 INTRODUCTION

1.1 Background

Global atmospheric general circulation models (GCMs) have been developed to simulate the present climate and to predict future climate change. The limited predictive capability of existing GCMs, and the complexity of land-ocean-atmosphere interactions prevent reliable assessments of hydrologic cycle modifications, such as those resulting from possible global warming. The importance of these issues have been documented by Mahfouf et al. (1987), Avissar and Pielke (1989), and Wood (1991). Furthermore, at the scale of watersheds or river basins, the resolution of GCMs does not permit detailed assessments of changes in the water balance that must accompany climate change (Wood, 1991). In addition, modeling experiments have revealed the magnitude and persistence of the influence of land-atmosphere interactions upon regional climatology (Delworth and Manabe 1989, Shuttleworth 1991, Wood 1991). This finding was especially far-reaching for surface hydrology as it lead to the general acknowledgement of the importance of multiscale dependence between large-scale and regional climate, and regional climate and field-scale hydrology. Questions about the global water balance (the spatial and temporal characteristics of water in all compartments of the global system: atmosphere, oceans, and continents) have therefore become more important in modern hydrologic science (Eagleson, 1986).

The problem of how to represent land surface processes in GCMs has drawn the interest of climate modelers, and increasingly, hydrologists and systems ecologists. Early generation GCMs did not include representations of land surface hydrology, instead they used fixed boundary conditions, prescribed surface wetness and temperature (Manabe et al., 1969), and thus could not account for the feedbacks between the land surface and atmosphere. Subsequent numerical experiments (Charney et al. 1977, Mintz 1984, and Rowntree 1988)

demonstrated the sensitivity of modeled climate to the land surface moisture state and brought concerted effort to incorporate more realistic hydrology algorithms within the very real constraints of computation time (Eagleson, 1986)

In view of the limitations of GCMs in predicting regional climatic conditions, climate modelers have devised limited-area-meteorological (LAM) models, whereby fine-mesh models are imbedded in a coarse-resolution GCM over an area of interest (Giorgi and Mearns, 1991). The GCM provides initial and boundary conditions for the LAM, which in turn, produces high-resolution hydroclimatic predictions. Hydrologists have used nesting approaches whereby GCM outputs, such as average temperature and precipitation over the area of interest are used to drive numerical models of the regional hydrologic cycle (Lettenmaier and Sheer, 1991).

Predicting variations in the earth's climate system has been recognized by the international scientific community to require improved understanding of interactions between the atmosphere, land surface, and oceans. Since 1979, the World Climate Research Programme (WCRP) science committees have fostered efforts aimed at quantitative understanding of climate and predictions of global and regional climate changes on all time scales. The recognition that water and energy budgets were inadequately understood on regional and global scales led to establishment of the Global Energy and Water Cycle Experiment (GEWEX) in 1987. The GEWEX Continental-Scale International Project (GCIP) initiative is the first major project under GEWEX. GCIP is designed to improve understanding and the ability to model for climate prediction purposes the coupling between the atmosphere and the land surface on a continental scale. The GCIP program is focused on the Mississippi River Basin to take maximum advantage of the existing meteorological and hydrological networks.

A primary objective of GCIP is to determine the space-time variability of water and energy fluxes at continental scales. The GCIP Science Plan (1992) recommends that the research program be organized along a multi-scale framework which includes small scale areas (SSA) with dimensions ranging from

10^0 to 10^2 km^2; intermediate scale areas (ISA) with dimensions ranging from 10^2 to 10^4 km^2; and large scale areas (LSA) with dimensions ranging from 10^5 to 10^6 km^2. The initial focus of the GCIP program is the Southwest Large Scale Area (LSA-SW) which essentially comprises the Arkansas-Red River basins.

An important scientific objective of GCIP is the development and testing of macroscale hydrological models appropriate for modeling the water and energy budgets at the LSA scales. The GCIP science plan identifies an implementation strategy consisting of model development and testing at the SSA and ISA scales, and up-scaling to the LSA scale. It is expected that land surface hydrologic model-based estimates of the space-time variability of water and energy fluxes at the LSA scale will be compared to similar water budget estimates from atmospheric analysis. For this modeling strategy to be successful and to provide reliable estimates of the LSA water and energy fluxes, the macroscale hydrologic model must be calibrated using data from smaller regions within the LSA.

Recent field experiments such as the First International Satellite Land Surface Climatology Project (ISLSCP) Field Experiment (FIFE) (Sellers, et al., 1989) have led to a better understanding of the physical relationships which govern land surface-atmosphere interactions (Betts et al., 1993). This understanding, along with the highly detailed data provided by field experiments has, in turn, led to the development and improvement of hydrologic models used to simulate these interactions.

1.2 Effects of hydrological processes on climate

Hydrological processes at the land surface play an important role in understanding global climate change. From the point view of atmospheric models, the role of surface hydrological processes is to partition the radiative energy reaching the land surface, essentially into latent and sensible heat, which are controlled by the temperature and wetness of the surface. Reasonable representations of hydrologic processes are required at scales similar to those of GCMs (currently hundreds of km). Global data appropriate for specifying hydrologic parameters of GCM surface hydrology schemes are at present

virtually nonexistent. Furthermore, measurement of individual processes in medium to large river basins using site instrumentation poses practical difficulties. Use of large hydrologic data bases (e.g. Wallis, et al., 1991; Slack et al., 1992) offers one possibility for implementation of regional parameter estimation methods. However this implies application of parameter estimation schemes for a large number (i.e., hundreds to thousands) of catchments, which necessitates the use of computationally efficient parameter estimation algorithms.

Soil moisture has been shown to have an important role in atmospheric circulation (Ookouchi et al. 1984, Mahfouf et al. 1987). The ratio of sensible to latent heat, the Bowen Ratio, depends directly upon the availability of water at the land surface (Mintz 1984, Sud et al. 1989). Surface properties, such as topography, geology, and vegetation, affect the partitioning of incoming solar energy and hence moisture fluxes. Soil properties can vary widely over scales much smaller than the resolution of atmospheric models (Dooge, 1986). The scientific issue is, therefore, how to describe hydrologic processes at large scales, when much of the knowledge is from smaller scales.

Among the components of the global hydrologic cycle, groundwater is one of the most difficult to quantify. The reasons are obvious: monitoring of ground water fluxes is difficult and expensive to implement (Zektser and Loaiciga, 1989). Many of the early studies of the global water cycle excluded the analysis of ground water. The quantification of baseflow, which is closely related to groundwater for large river basins and at a global scale is nonetheless an important issue. Baseflow is related to the state of soil moisture which affects the energy and momentum fluxes. It participates in the hydrologic cycle as the subsurface component of river runoff, or baseflow, and as direct ground-water flow from land to large lakes, seas, and oceans. Modeling baseflow and evaluating related parameters (for example, the maximum soil moisture and maximum baseflow) is necessary to model the processes of transpiration, soil evaporation, runoff, and heat transport within the soil. Each of these processes affects the heat exchange between the atmosphere and land surface.

The role of the river runoff in the global hydrologic cycle is clearly a significant one and it is important that the runoff process are adequately represented. Knowledge of the spatial location of discharge within river catchments is essential for many hydrological applications such as the assessment of the sensitivity of water resources to climate change. Furthermore, in climate studies, there is a need for reliable global estimates of surface runoff on a regular grid to test the outputs of GCMs. Runoff information at large scale in conjunction with climatological data would lead to better understanding of the physical basis of climate models.

Various approaches have been used for the computation of grid estimates of hydrological variables. Among these methods are isoline interpolation, Thiessen polygons, weighted averaging and Kriging. But these methods are applicable only when a dense network of observations is available or when the spatial variation in the parameters of interest is modest. Clearly, what is needed is an approach which takes into account as much ancillary information as possible, in addition to the limited number of direct observations.

One alternative to the simple approaches referred to in the previous paragraph is to use a water balance model such as the two-layer variable infiltration capacity model (VIC-2L) to extend the observational information. Such models can be applied to grid cells in such a way as to obtain estimates for the water balance components.

1.3 Hydrological land-surface models and their regional transferability

Hydrological land-surface process models can be classified into two groups. The first group includes simple conceptual models (lumped or semi-distributed). Among these models are Arno model (Francini and Pacciani, 1991) and VIC model (Wood et al., 1992). These models have been successfully applied for different purposes over a range of spatial scales. However, the state of their parameterization, and accordingly their regional transferability, is limited, since the parameters are usually estimated on the basis of existing streamflow records.

The second group includes detailed distributed, grid based and physically-based models. Examples on these models are the System Hydrologique Europeen (SHE) (Abbott et al., 1986) and the Institute of Hydrology Distributed Model (IHDM) (Beven et al., 1987). They are fully parameterized and accordingly, at least in principle, are regionally transferable. Becker and Pfuetzner (1990) argue that such models should be applicable to ungaged basins. However, especially for large-scale applications, intensive computations are required, and assembling the necessary input data for the elementary units of the chosen grid (meteorological, physiographic, soil, vegetation data) requires enormous effort and time. At smaller scales, detailed hydrological models are required, while at larger scales simple models have often proved to be quite adequate. In this context, land surface schemes such as the bucket model (Manabe et al., 1965) and the variable infiltration capacity (VIC) model (Wood et al., 1992) can be classified as belonging to the first group. Our intent is to study the transferability of such a model using regionalization schemes applicable to large scale catchments.

Bucket algorithms were used to represent land-surface hydrology in many first generation GCMs (e.g. Manabe et al., 1965). These parameterization ignored the role of vegetation algorithm, using instead a so-called beta function to relate actual evapotranspiration to bulk aerodynamic potential evapotranspiration and soil moisture. Recently, bucket models have been replaced by soil-vegetation schemes (SVATS). Of these, SiB (Simple Biosphere model) (Sellers et al., 1986) and BATS (Biosphere-Atmosphere Transfer Scheme) (Dickinson et al., 1986) are the best known. These models, which represent the role of vegetation explicitly, require specification of a large number of parameters. Wood et al (1992) developed the variable infiltration capacity (VIC) model which requires estimation of three parameters: an infiltration parameter, an evaporation parameter, and a base flow parameter. Liang et al. (1994) generalized the VIC model to include multiple soil layers and spatially varying vegetation and evapotranspiration with a corresponding increase in the number of parameters.

In most cases, the parameters of SVATS schemes, such as SiB, BATS,

and VIC-2L, have been estimated using data from small scale meteorological studies (Sellers et al., 1989), and there are questions as to whether the use of point or small-scale parameters are valid at the GCM grid scale (Wood et al., 1992). Avissar and Pielke (1989), Entekhabi and Eagleson (1989), and Famiglietti and Wood (1991) have attempted to develop simpler land surface models that still incorporate important features of the governing hydrological processes.

In previous large scale applications of the VIC or (Arno) model, (e.g. Stamm et al, 1994; Rowntree and Lean, 1994) parameters have been selected subjectively, e.g., from ranges suggested by Dumenil and Todini (1992) based on streamflow calibration for a few catchments. Obviously, for application in GCMs, global parameter estimation using streamflow data is infeasible. In this study, we will focus on regionalization of the VIC-2L model parameters in order to improve our understanding of the hydrological cycle at large scales. This implies application of parameter estimation methods for a large number of catchments.

Hydrological regionalization is mainly concerned with transfer of information, typically from gaged to ungaged catchments (e.g. Riggs, 1972; Mosley, 1981). Regionalization of the parameters of rainfall-runoff models for prediction at ungaged catchments is not an easy task. A few attempts have been made, including studies by Jarboe and Haan (1974), Magette et al. (1976), Weeks and Ashkenasa (1985), and Weeks and Boughton (1987). Most of these approaches are similar to the extent that regression relationships are developed between the optimized parameters and catchment characteristics for a set of gaged catchments. These regionalization studies have varying limitations. There are two main reasons for the limited success in the regionalization of the rainfall-runoff models. The first is that, at the catchment level, the parameters may be poorly determined (e.g. Kuczera (1983)), which makes the task of developing useful regionalization relationships more difficult. The second reason is that some parameters may not be well estimated by regional relationships.

1.4 Research objectives

The goal of this research is to develop a methodology for regionalization of the parameters of a deterministic soil-vegetation-atmosphere transfer scheme (SVAT) based on hydrologic principles. This is to be achieved by first identifying efficient estimation procedures for hydrological parameter estimation at gaged sites and then extending these estimates using multivariate techniques to develop relationships between the site specific parameters, and climate and land surface characteristics. Initially, the approach will be developed by estimating the parameters of the VIC-2L model as a case study. A relatively simple methodology (regression-based regionalization) will be explored that makes use of land surface characteristics that are readily obtainable from maps, tables, and an archival data base that do not require field surveys. Once the methodology is developed, the ultimate intent is to use it in parameterization of a land surface scheme appropriate for GCMs used in numerical weather prediction and climate simulation.

The specific objectives of this research are:

1) To explore two alternative approaches for estimation of the parameters of the VIC-2L model. The first method, complete optimization, estimates all model parameters simultaneously using a search procedure. The second method uses spatially distributed soils data directly to determine selected parameters of the VIC-2L model with the remaining parameters determined using a search procedure;

2) To develop regional relationships for parameterization of the VIC-2L land surface scheme in GCMs. This objective will be achieved through development of regional equations using multiple linear regression based on the assumption that all the catchments are from the same hydrologically homogeneous group;

3) To investigate different possibilities for applying the regionalized VIC-2L

model for large river basins. Three applications will be investigated: i) the VIC-2L model parameters estimated via a search procedure will be used in conjunction with a distributed soil database linearly interpolated and overlaid on a spatial grid to evaluate the water balance of the Arkansas-Red River basin; ii) regional equations of the VIC-2L model will be used to evaluate the water balance of the Arkansas-Red River basin; and iii) large scale surface energy fluxes in the Arkansas-Red River basin will be estimated using the regionalized VIC-2L model. Chapters 2, 3, 4, 5 of this dissertation provide a thorough account of the descriptive, analytical, and quantitative components of the work completed to the fulfill these objectives.

1.5 Thesis Structure

The study area, as well as station hydrologic and meteorological data bases, land surface characteristics estimated from digital elevation data, the distributed soils (SCS STATSGO) data base, and vegetation data bases are described in Chapter 2. The VIC-2L model, and adaptations for grid-based implementation as well as parameter estimation strategy are presented in Chapter 3. Chapter 4 introduces the parameter regionalization methodology for the VIC-2L model. Generally, the structure of the thesis is that chapters or groups of chapters represent stand alone contributions that either will be or have been submitted for journal publication.

Chapter 5 describes three applications of the VIC-2L grid-based model for the Arkansas-Red River basin. Section 5.2 is essentially identical to a paper that will appear in the Journal of Geophysical Research (Abdulla et al., 1995); it describes an application of VIC-2L parameters for 44 catchments in the Arkansas-Red River basin which were linearly interpolated, and overlaid on a one degree grid. The model-dervied evapotranspiration spatially integrated over the entire Arkansas-Red basin is also compared to evapotranspiration estimated independently from an atmospheric moisture budget. Section 5.3, along with part of Chapter 4, constitutes the major portion of a second manuscript. This section describes the application of the regionalized VIC-2L parameters for large

scale grids. Finally, Section 5.4 composes a paper presented at the European Geophysical Society 1995 meeting (Abdulla et al., 1995b) in which the VIC-2L model is tested for its ability to simulate large scale sensible and latent heat fluxes in the Arkansas-Red River basin. Conclusions and recommendations of future work are given in Chapter 6.

CHAPTER 2 STUDY AREA AND DATA SELECTION

In this chapter, the study area and data used in this study are described.

2.0 Overview of the adopted approach

Figure 2.1 illustrates schematically the methodology that will be followed in regionalization and application of macroscale hydrological model for both the intermediate scale areas (ISA) with dimensions ranging from 10^2 to 10^4 km^2 and the large scale areas (LSA) with dimensions ranging from 10^5 to 10^6 km^2. The first step in the methodology is to identify a number of ISA catchments for which long records of climatological and streamflow data are available. In this study the LSA represents the entire Arkansas-Red River basin, while ISA represents a number of catchments within the Arkansas-Red River basin.

The second step is to calibrate the hydrologic model (described in Chapter 3) to these catchments to determine the locally optimized hydrological parameters. Since the purpose of this study is to regionalize the parameters of a hydrologic model, physical characteristics of the catchments must be known. At this point, we do not know which of the catchment attributes should be considered. From a hydrological standpoint, surface runoff and baseflow are affected by climatological, morphological, geological, and hydrogeological factors. Unfortunately, only a few characteristics are available for some of the catchments in published sources, such as USGS reports. Therefore, a detailed study was conducted to select catchment attributes that are most useful for predicting hydrologic response.

Once the optimum parameters of the hydrological model and the explanatory variables for the ISA calibration catchments are known, the regional relationships may be developed using a multiple linear regression. Then, these regional relationships may be applied either to ungauged ISA catchments to simulate streamflows or to the LSA to evaluate the water and energy budgets.

In the following sections a description of the LSA and ISA calibration catchments is presented. This is followed by a description of the physical characteristics used in the parameter estimation strategy.

2.1 Study area

The study area is the Arkansas-Red River basin of the U.S. Southern Great Plains (Figure 2.2). The Arkansas-Red River basin is the first large scale study area of the GEWEX (Global Energy and Water Exchange) GCIP (GEWEX Continental-Scale International Project) which seeks to quantify the water and energy budget of the Mississippi River basin. For the purposes of identifying ISAs (intermediate scale areas with dimension ranging from 10^2 to 10^4 km^2), we also included the White River, because it is hydrologically similar to the Arkansas and Red Rivers, and is included with the Arkansas and Red in the US Water Resources Council Hydrological Region 11. This region includes all of Oklahoma, and parts of Arkansas, Colorado, Kansas, Louisiana, Missouri, New Mexico, and Texas. The total area of this region is 637,000 km^2. For application of VIC-2L at the LSA scale, we subdivided the Arkansas and Red basins into 61 $1^o \times 1^o$ grid cells, 45 of which lie in the Arkansas River basin, and 16 cells in the Red River basin (for this purpose, the White River was excluded). Figure 2.3 shows the one degree by one degree schematization of the basin, and the flow directions as represented in the model, along with locations at which naturalized flows (reservoir effects removed) were available.

2.2 Selected catchments

Forty catchments were selected for the preliminary study (see Figure 2.4). Table 2.1 lists the watersheds used in the study. These catchments are divided into two groups. The first group contains thirty-four catchments to be used in the development of the regional equations. The second group is comprised of six catchments to be used to test the regionalization methodology. The area of these catchments ranges from 285 to 5278 km^2, and the stream gage elevations range from 53 to 2344 m above mean sea level. These catchments are taken from three

different sources i) A subset of the list of continental U.S. stations with long-term unregulated streamflow records assembled by Wallis et al., (1991; hereafter referred to as WLW); ii) The USGS Hydroclimatological Data Network (HCDN; Slack et al., 1992); iii) regulated catchments for which naturalized streamflows (regulation effects removed) have been estimated by the Tulsa District of the Department of the Army Corps of Engineers (see Figure 2.3 for the location of the naturalized streamflow gages). Combination of these three data sources allows representation of a wider range of catchment areas than the WLW catchments, which are mostly relatively small. The third source includes several large catchments that are of size comparable to the grid cells in the one degree representation (about 9000 km^2).

2.3 Estimation and selection of the catchments physical characteristics

It is necessary to decide from a hydrological standpoint which hydrological, hydrogeological and climatological variables should form the basis for development of the regional parameter estimation methodology. Many factors that affect the hydrologic response such as baseflow are mentioned in the literature. The most important variables can be classified into three groups: I) Climatological factors; II) Morphological factors; III) Geological and hydrogeological factors. These characteristics, which are not directly available for most of the catchments, can be calculated from ancillary data such as the closest rainfall stations (for mean annual precipitation and intensity), digital elevation files (for elevation, total stream length, slope) and soil reports and data bases.

2.3.1 Climatological factors

Climatological factors govern the potential for recharge of ground water and the importance of direct runoff relative to infiltration and baseflow. The principal meteorological influence on baseflow is precipitation (Riggs, 1972). Another important factor is evapotranspiration, which depends on temperature, wind, humidity, available water, and the nature of vegetation cover.

Daily precipitation, minimum, and maximum temperatures were taken from National Climatic Data Center cooperator stations, available from two sources (see Figure 2.5). An initial data set was assembled consisting of all of the WLW stations (originally screened by Karl et al. (1990) as part of the Hydroclimatological Data Network (HCN) of Oak Ridge National Laboratories). For the grid based model of the entire Arkansas-Red basin, we tried to have at least one precipitation station for each grid cell, and preferably two. This was accomplished by supplementing the WLW stations using additional NCDC cooperator station data available from commercial CD-ROMs. The supplemental stations were selected based on the length of records, record completeness, station locations, and, for the headwaters grid cells, giving preference to higher elevation locations which are otherwise poorly represented. The supplemental stations were processed for estimation of missing data using methods similar to those employed by WLW. In the case of the smaller calibration catchments, a single precipitation station, located as close as possible to the catchment centroid, was used.

One hundred and twenty precipitation stations were selected for the analysis from the sources noted above. These stations are located over the entire study area. Thirty years of daily rainfall during the period 1948 to 1977 were analyzed for the 120 stations. Preliminary analysis of ten of these stations suggested that three seasons are sufficient for representing the rainfall characteristics. These seasons are: Season 1, from November to May, Season 2, from June to August; and Season 3, from September to October. Different statistical properties of rainfall are considered: mean seasonal interarrival times defined as the mean of the time between the rainfall events; seasonal daily mean rainfall amounts, mean annual rainfall amount, annual number of events, and mean annual intensity of rainfall define as the annual precipitation divided by the total number of events. An event is defined as the occurrence of a day with a total rainfall amount exceeding a specified threshold (0.25 mm). Figure 2.6 shows histograms of the mean annual rainfall, mean annual intensity, and mean annual number of events. Figures 2.7 and 2.8 show the ranges of the seasonal mean and coefficient of variation of storm depth and interarrival time.

2.3.2 Morphological factors

In this study, all the catchments were delineated using GRASS (the Geographic Analysis Support System) which is a geographic information system (GIS) developed by the U.S. Army Construction Engineering Research Laboratory, Champigan, IL, (USACERL). Two different resolutions were used: 3 arc seconds (about 90 m N-S) for the smaller catchments, and 30 arc seconds (about 1 km N-S) for the larger catchments. Digital elevation data were also used to determine the elevation bands in headwater catchments needed to run the snow accumulation and melt algorithm, which was the temperature index model of the National Weather Service River Forecast System, developed by Anderson (1973).

2.3.3 Geological and hydrological factors

The third group of characteristics includes geological and hydrogeological factors. Among these are soil hydraulic characteristics, and the thicknesses and composition of the rocks overlying the aquifers. Riggs (1972) noted that the most important factors influencing low flow are the aquifer hydraulic conductivity and hydraulic gradient. The underlying basin formation is also an important determinant of base flow. According to McMahon and Diaz (1982), basins that have more impervious formations will have lower baseflow during drought periods. Many investigators report that streamflow characteristics are associated with geological variations between catchments (Lull and Sopper 1965, Grant 1971, and Riggs 1973, 1972).

The soil data used in this study were extracted from the U. S. Soil Conservation Service (SCS) STATSGO (State Soil Geographic data base). The soil data extracted from STATSGO are the average available water capacity, the average permeability, the areal coverage of soil hydrologic group index (which refers to the soils grouped according to their runoff-producing characteristics). In the following Section more details information about STATSGO and the derived soil data.

2.3.4 Derived soil attributes from STATSGO data base

The USDA-Soil Conservation Service is in the process of developing soil geographic data bases to improve access to soils information. At the regional level, a State Soil Geographic Database (STATSGO) has been developed for river basin, multi-state, state, and multi-county resources planning. STATSGO is a GIS-compatable data base that confirms information from SCS soil surveys using the USGS 1:250,000-scale topographic quadrangles as base maps. The widespread availability of a soil geographic data base is a recent development, data bases such as, STATSGO have not, as yet, been widely used in parameterization of hydrologic models. The STATSGO data base is utilized in this thesis as one of the key elements in a regionalization scheme for the VIC-2L model. Soil information from STATSGO were extracted for each of the eight states lying within the Arkansas-Red River basins (Colorado, New Mexico, Texas, Kansas, Oklahoma, Arkansas, Missouri, and Louisiana). In the case of the VIC-2L model, the extracted soil information were used for:

i) determining three of the VIC-2L model parameters (the saturated hydraulic conductivity, the residual moisture content, and the pore size distribution index) directly using the method of Rawls and Brakensiek (1985) and the Kozeny-Carman equation (Ahuja et al., 1989); and

ii) providing candidate attributes for use in regional equations to determine the remaining VIC-2L drainage and infiltration parameters (see Chapter 4).

Techniques were adapted to use GRASS to manage and interpret the multi-component attributes associated with STATSGO. These interpretation techniques focus on forms of aggregation that generalize the more detailed component attribute values to either a single value or probability values that are then mapped using GIS according to the composition of individual STATSGO

map units (Lytle et al., 1994).

The STATSGO/GRASS Interface developed by USDA-SCS (Minzenmayer, 1992) was used to prepare multiple probability maps for a given interpretation rating (one map per class of interpretation criteria) which consider the rating of each STATSGO component. The methodology used for extracting the soil data from STATSGO is illustrated in an example in Appendix A.

The procedure described in Appendix A was used to extract the map unit averages for the following soil properties:

. bulk density,
. available water capacity (Awc),
. percent clay (PC),
. percent passing sieve number 4,
. percent passing sieve number 10,
. percent passing sieve number 200,
. permeability (Pr),
. soil hydrologic groups (Hgb, Hgc, and Hgd)

Some of the soil characteristics so estimated are described briefly below.

A) average available water capacity

STATSGO gives the capacity of soils to hold water available for consumption by plants. It is commonly defined as the difference between the amount of soil water at field capacity and the wilting point. It is commonly expressed as inches of water per inch of soil. Results for the available water capacity are shown in Figure 2.9.

b) Hydrologic group index

Soils are assigned to one of four groups according to their runoff-producing characteristics. Group A soils are considered to have a high infiltration rate.

They are mainly deep, well drained, and sandy or gravelly. Group D soils have very low infiltration rates. Soils in hydrologic groups B and C are intermediate. Jarboe and Haan (1974) assigned an integer value for each hydrologic group as follows: 4 for soils in group A, 3 for soils in group B, 2 for soils in group C, and 1 for soils in group D. An average group index was calculated for each catchment similar to the above soil characteristics. For this application the percent areal coverage of each of the soil groups was calculated. Figure 2.10 shows the areal coverage of soil groups B and D.

The following derived soil properties were calculated for each catchment and grid cell using the information extracted from STATSGO:

1) percent sand (PS) (defined as percent passing sieve no. 10 – percent passing sieve no. 200),
2) percent silt (percent passing sieve no. 200 – percent clay),
3) soil porosity (TP) (total volume occupied by pores per unit volume of soil)
4) saturated hydraulic conductivity (K_s),
5) Brooks-Corey pore size distribution index (B_p),
6) Brooks-Corey residual water content (h_r), and
7) field capacity (FC).

Results for percent sand are shown in Figure 2.11.

The factors to be considered in this study are listed in Table 2.3. The following procedure was used to determine the average value of the soil characteristics for each catchment:

1) the map units that are related to each catchment were identified;
2) the fraction of the catchment covered by each map unit was determined;
3) the mean of each soil characteristics was determined for each map unit as described in Appendix A;
4) the soil data for each catchment were determined using the map

unit means weighted according to their fractional area in that catchment.

The same approach is used to determine the average soil attributes for each grid cell shown in Figure 2.3.

2.4 Vegetation

Six vegetation classes were generated for the Arkansas-Red River basin from the data sets developed by Olson et al. (1983). Figure 2.12 shows the areal coverage of each vegetation class. These data are at one-half degree resolution, so that there can be at most four vegetation classes for each grid cell. A fractional coverage of the grid box, as well as some prescribed canopy characteristics, is associated with each of these vegetation types.

NOAA monthly 10 minute Normalized Difference Vegetation Index (NDVI) data for the period April 1985 to December 1988 (taken from EPA/NOAA/NGDC (1991)) were used to calculate the monthly average NDVI for each 1 degree by 1 degree grid cell. For details information about how this index is estimated, the reader is referred to Kidwell (1990). Figure 2.13 shows the average NDVIs for both January and June. The monthly average Leaf Area Index (LAI[n,m]) (where n=1, 2,....., 6 is the land cover class, and m=1, 2,....., 12 is the month index) were derived from the average normalized difference vegetation index (NDVIs) as follows:

$$\mathrm{LAI[n,m]} = \mathrm{LAI_{min}[n]} + \frac{(\mathrm{LAI_{max}[n]} - \mathrm{LAI_{min}[n]})}{(\mathrm{NDVI_{max}[m]} - \mathrm{NDVI_{min}[m]})} (\mathrm{NDVI[m]} - \mathrm{NDVI_{min}[m]})$$

where $\mathrm{LAI_{min}}$ and $\mathrm{LAI_{max}}$ are the minmum and maximum values of the leaf area index for each vegetation cover, and $\mathrm{NDVI_{min}}$ and $\mathrm{NDVI_{max}}$ are the minimum and maximum values for each month over the entire region. The $\mathrm{LAI_{min}}$ and $\mathrm{LAI_{max}}$ were the values suggested for the Simple Biosphere Model (SiB) by Sellers et al. (1989).

Table 2.1 Calibration and validation catchments

	Catchment Number	Catchment Name	Calibration Period	Area sq.km	Lat degree	Long.
Calbiraton catchments						
1	7057500	NORTH FORK R, MO	1948-53	1452	36.62	92.25
2	7069500	SPRING R, AR	1948-53	3063	36.20	91.17
3	7071500	ELEVEN POINT R, MO	1948-53	2053	36.65	91.20
4	7095000	GRAPE CREEK, CO	1948-53	828	38.19	105.48
5	7152000	CHIKASKIA R, OK	1971-76	4814	36.81	97.28
6	7153000	BLACK BEAR CR, OK	1971-76	1491	36.34	96.80
7	7167500	OTTER CREEK, KS	1971-76	334	37.71	96.22
8	7172000	CANEY R, KS	1948-53	1152	37.00	96.31
9	7180500	CEDAR CREEK, OK	1948-53	284	38.20	96.82
10	7186000	SPRING RIVER, MO	1948-53	3014	37.25	94.56
11	7187000	SHOAL CREEK, MO	1970-75	1105	37.02	94.52
12	7189000	ELK RIVER, MO	1948-53	2258	36.63	94.59
13	7196500	ILLINOIS R, OK	1948-53	2483	35.92	94.92
14	7199000	CANADIAN R,NM	1970-75	593	36.79	104.46
15	7208500	RAYADO CK, NM	1970-75	168	36.37	104.97
16	7243500	DEEP FORK, OK	1971-76	5226	35.67	96.06
17	7250000	LEE CREEK , AR	1948_53	1103	35.49	94.45
18	7252000	MULBERRY R, AR	1971-76	966	35.58	94.02
19	7263000	SO FOURCHE R, AR	1948-53	543	34.91	93.06
20	7335000	CLEAR BOGGY, OK	1948-53	1864	34.25	96.20
21	7346070	LIT CYPRESS, TX	1948-53	1748	32.71	94.35
22	7147070	WHITEWATER R, KS	1970-75	1103	37.80	97.01
23	7147800	WALNUT R, KS	1970-75	4869	37.22	96.99
24	7195000	OSAGE CREEK, AR	1955-60	336	36.22	94.29
25	7221000	MORA RIVER, NM	1970-75	2859	35.80	104.78
26	7229300	WALNUT CREEK, OK	1975-80	523	35.00	97.37
27	7243000	DRY CREEK, OK	1970-75	178	35.78	96.85
28	7301410	SWEETWATER CK, TX	1970-75	743	35.47	100.12
29	7304500	ELK CREEK, OK	1970-75	1421	34.91	99.11
30	7311500	DEEP RED, OK	1955-60	1598	34.22	98.45
31	7311700	NORTH WICHITA R,TX	1975-80	2426	33.82	99.79
32	7332500	BLUE RIVER, OK	1970-75	1232	34.00	96.24
33	7342500	S. SULPHUR R, TX	1970-75	1364	33.36	95.59
34	7343000	N. SULPHUR R, TX	1980-85	714	33.47	95.59
Validation Catchments						
35	7068000	CURRENT R, MO	1948-53	5278	36.62	90.85
36	7191000	BIG CABIN CK,OK	1948-53	1165	36.57	95.15
37	7207500	PONIL CREEK, NM	1948-53	442	36.57	104.95
38	7218000	COYOTE CREEK,	1970-75	556	35.92	105.16
39	7340000	LITTLE RIVER, AR	1948-53	6894	33.92	94.39
40	7343500	WHITE OAK CREEK, TX	1970-75	1279	33.32	95.09

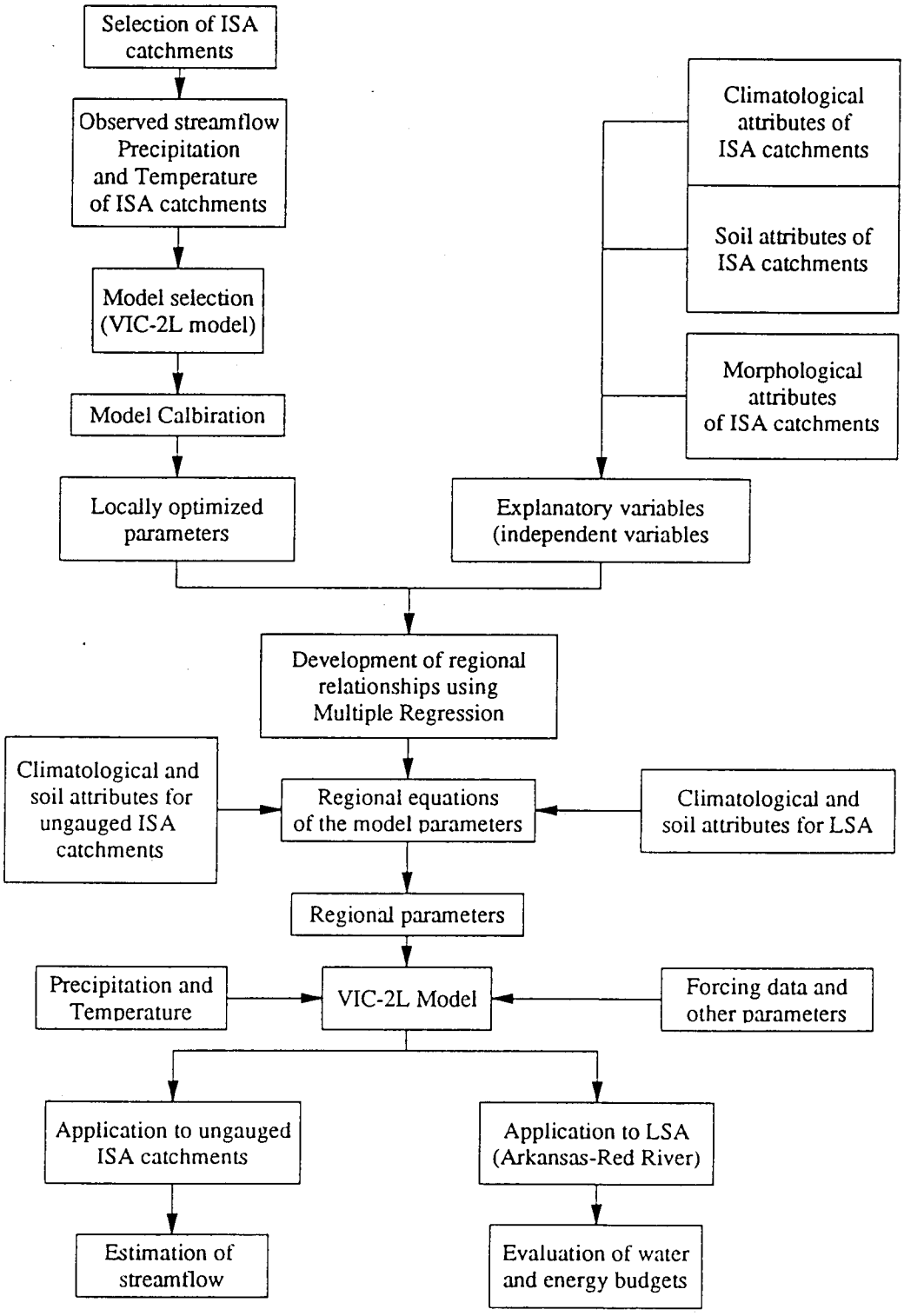

Fig. 2.1 Schematic diagram of research approach

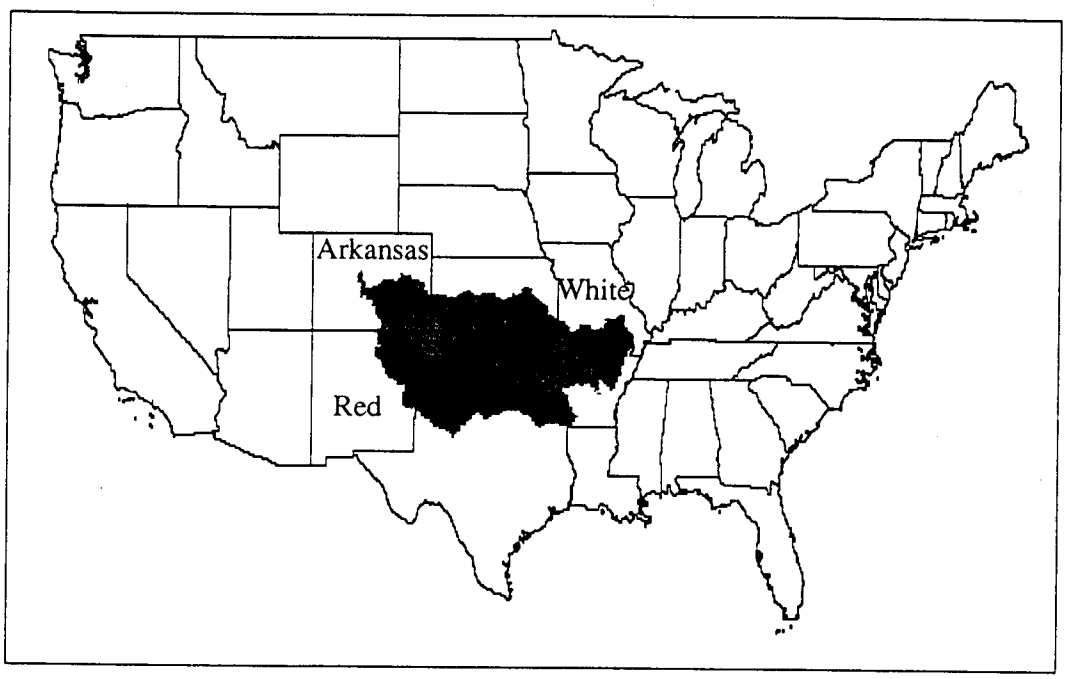

Fig. 2.2 Location of the study area.

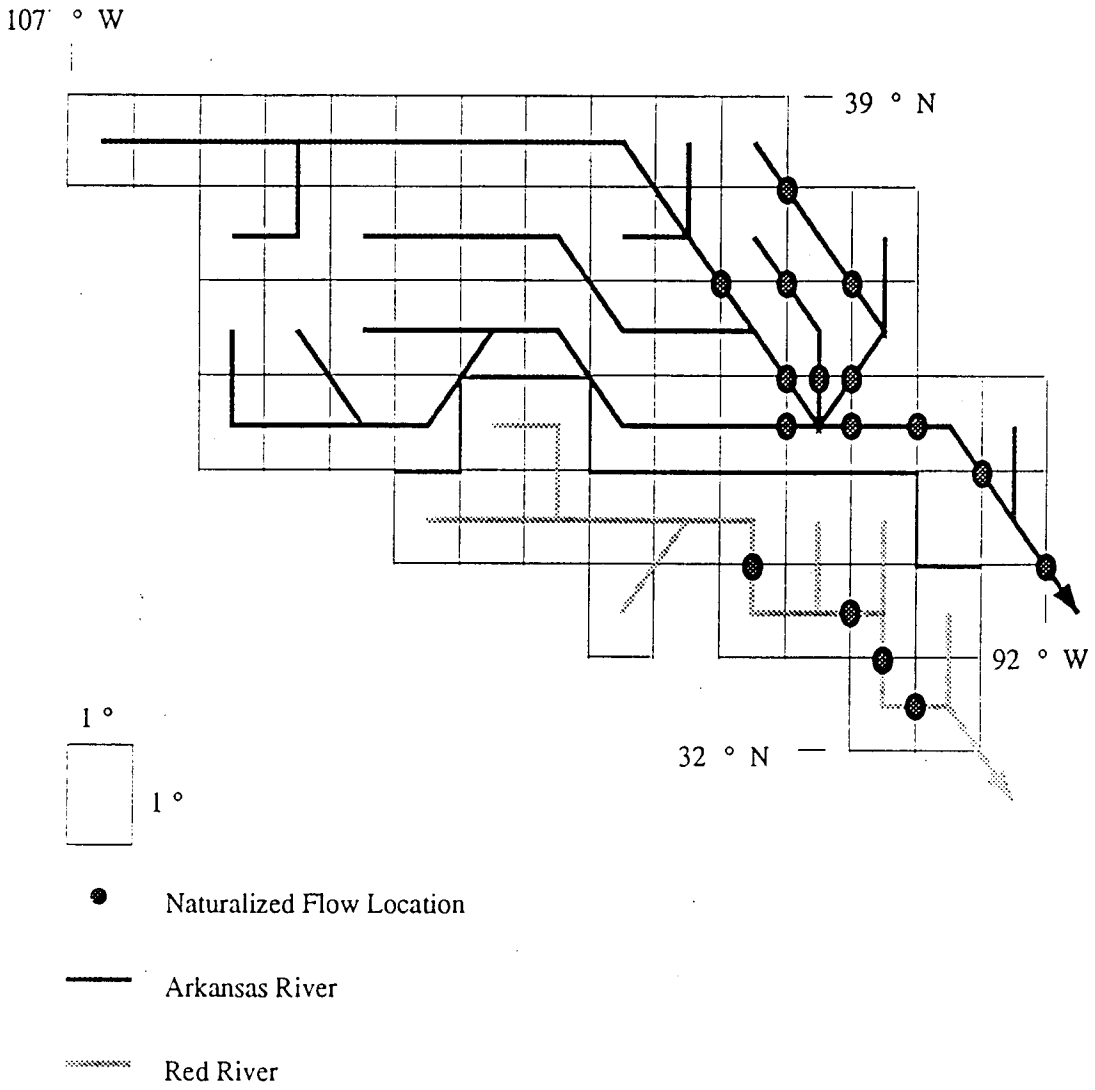

Fig. 2.3 Schematic diagram of 1°×1° flow network for the Arkansas-Red River basin.

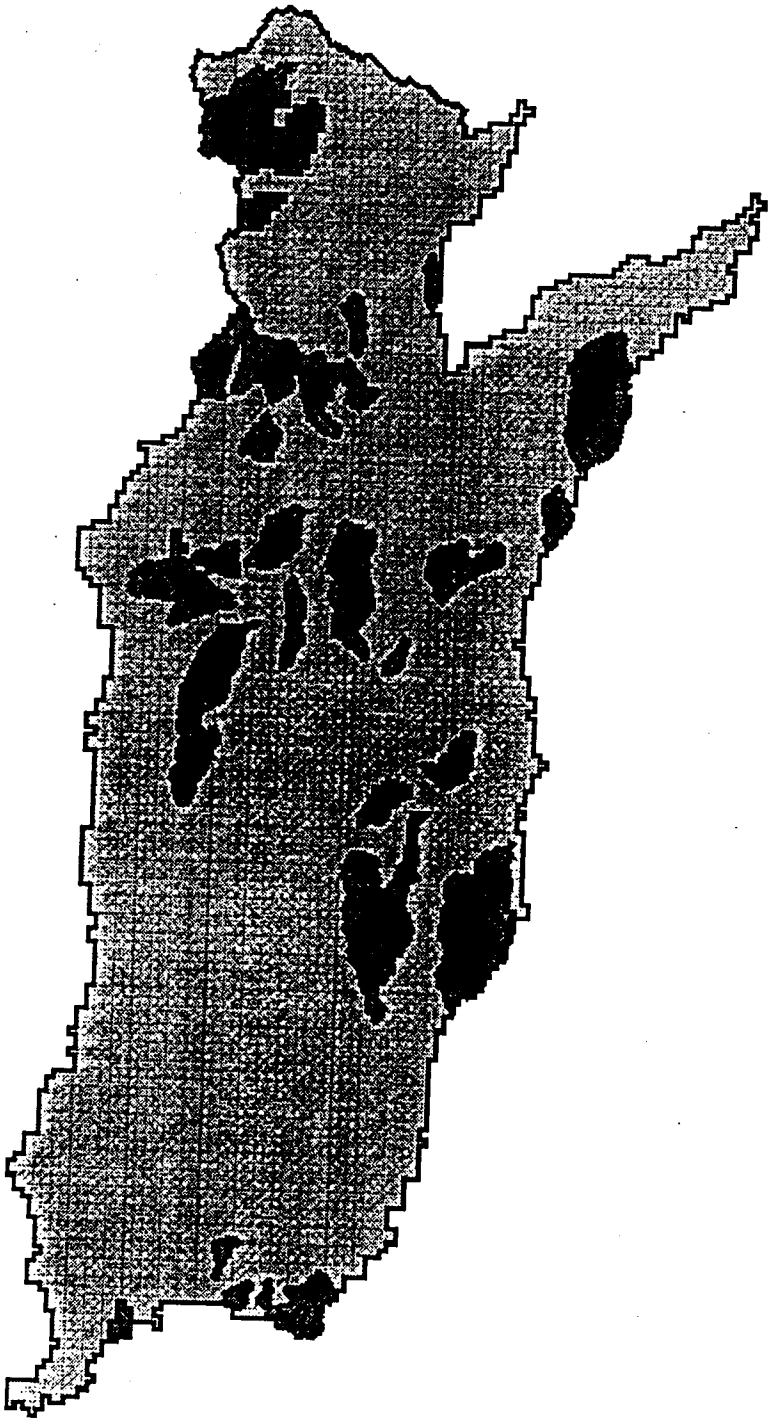

Fig. 2.4 Location of the calibration and validation catchments

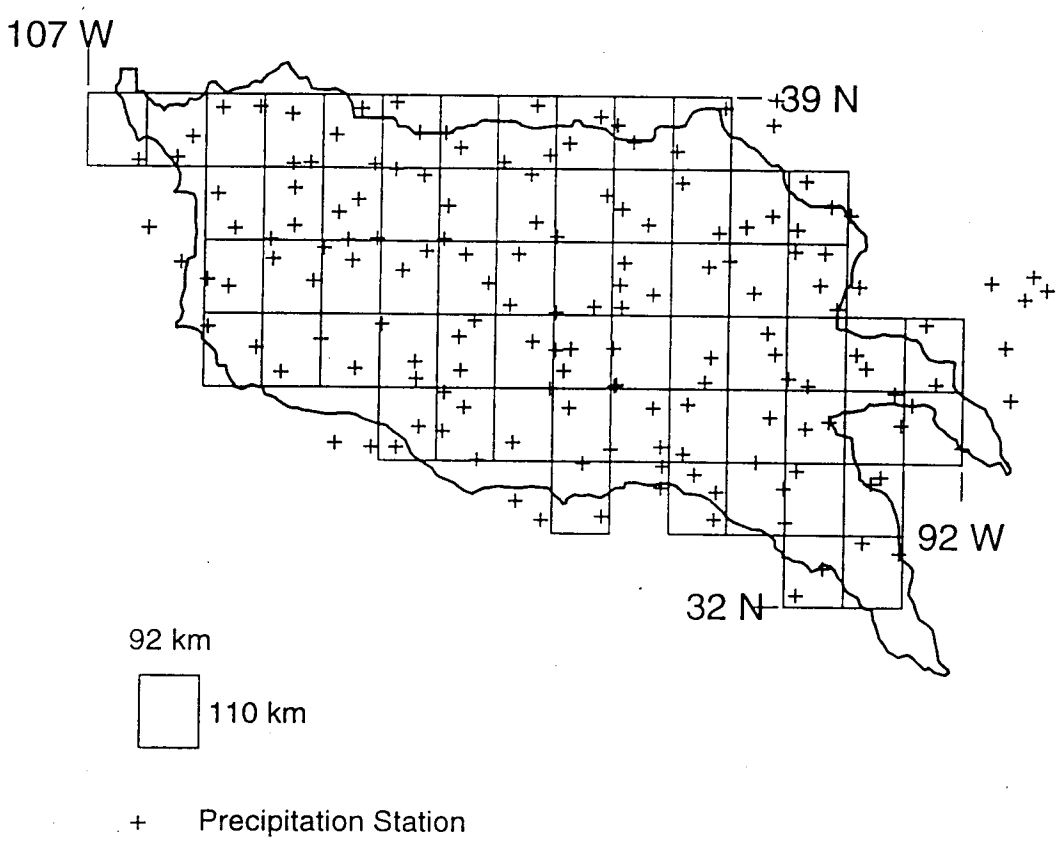

Fig 2.5 Location of the precipitation stations in the Arkansas-Red River basin

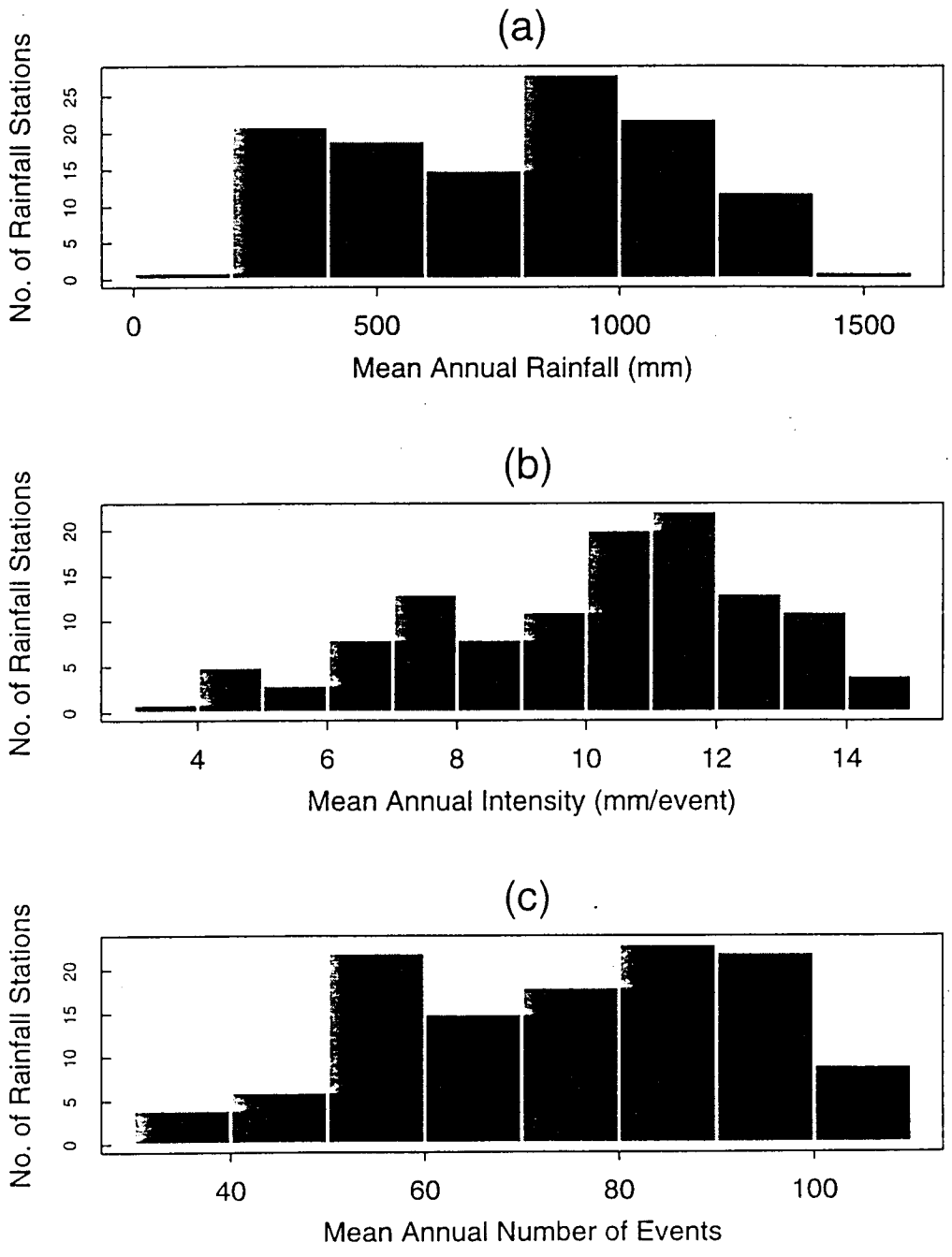

Fig. 2.6 Mean annual a) precipitation amount (mm); b) intensity (mm/day); and c) number of events for all the rainfall stations

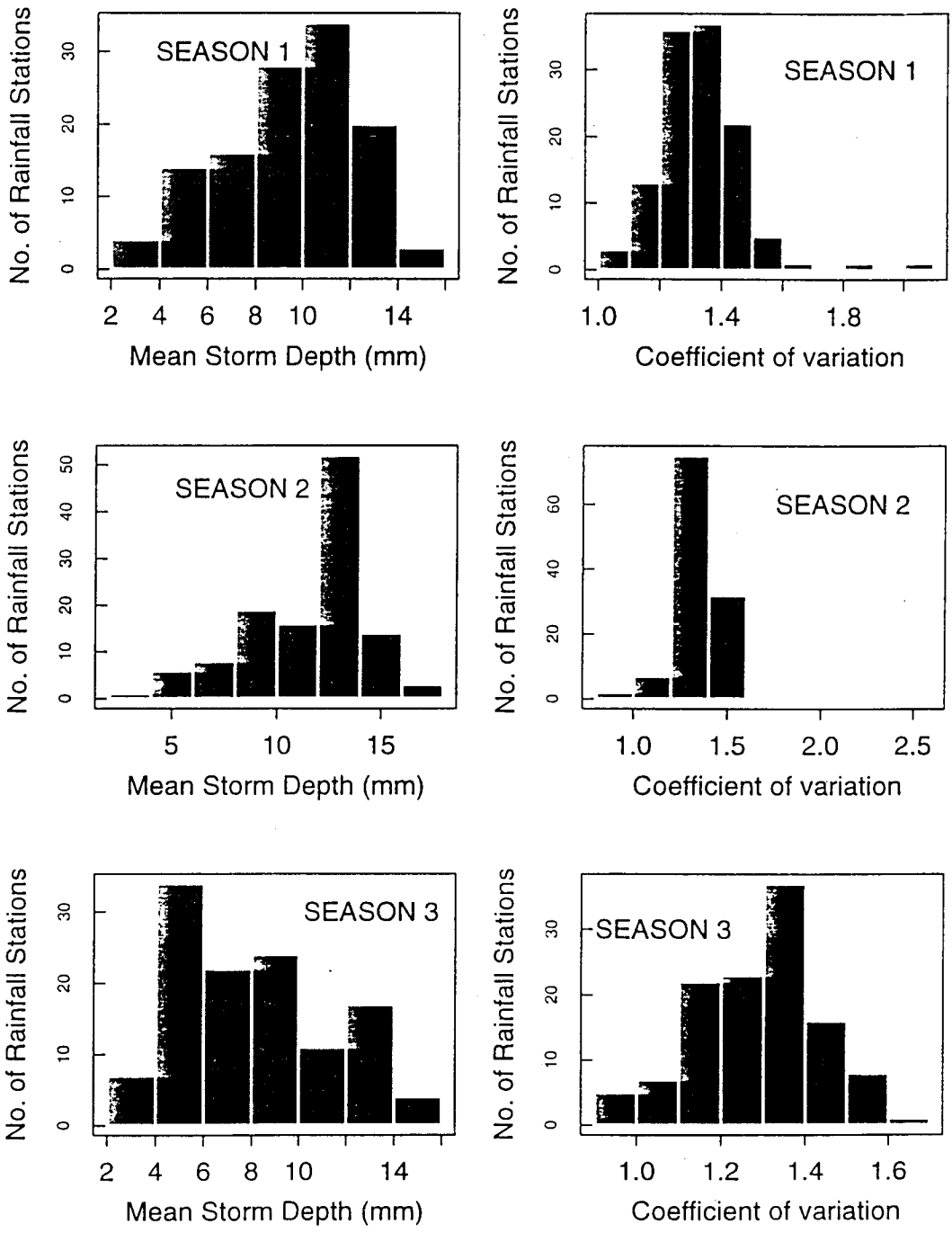

Fig. 2.7 Mean and coefficient of variation of storm depth for a) Season 1 (from November to May); b) Season 2 (from June to August); and c) Season 3 (from September to October)

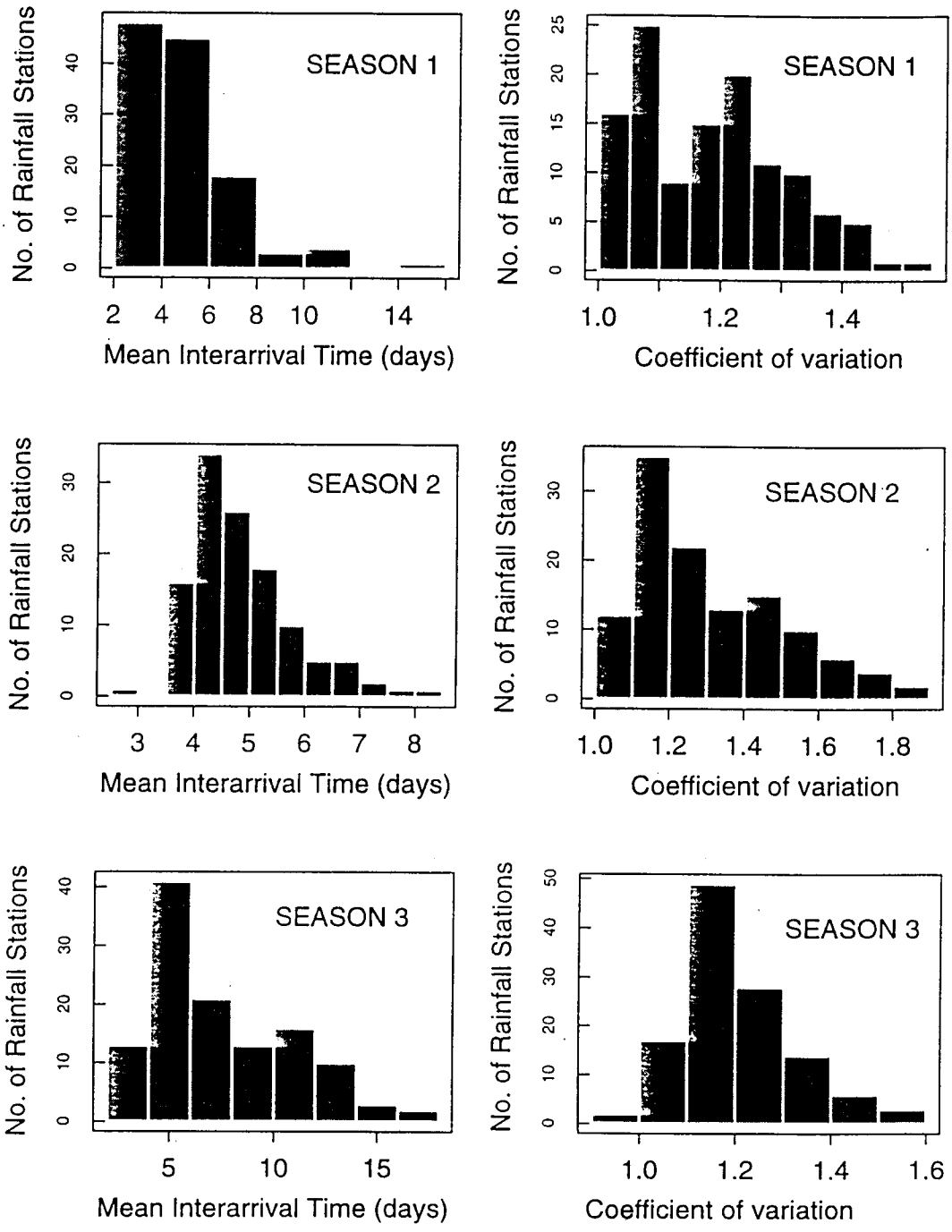

Fig. 2.8 Mean and coefficient of variation of storm interarrival times for a) Season 1 (from November to May); b) Season 2 (from June to August); and c) Season 3 (from September to October)

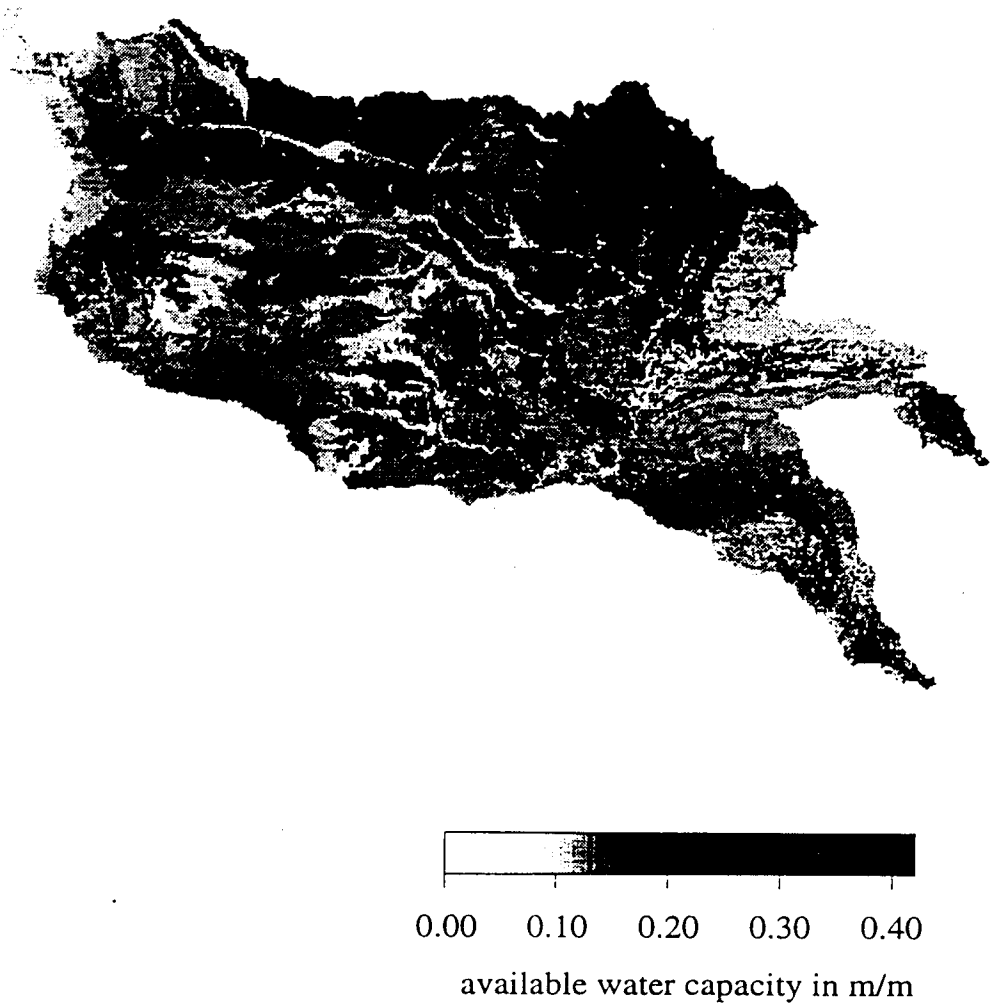

Fig. 2.9 Available water capacity of the surface layer for the Arkansas-Red River basin.

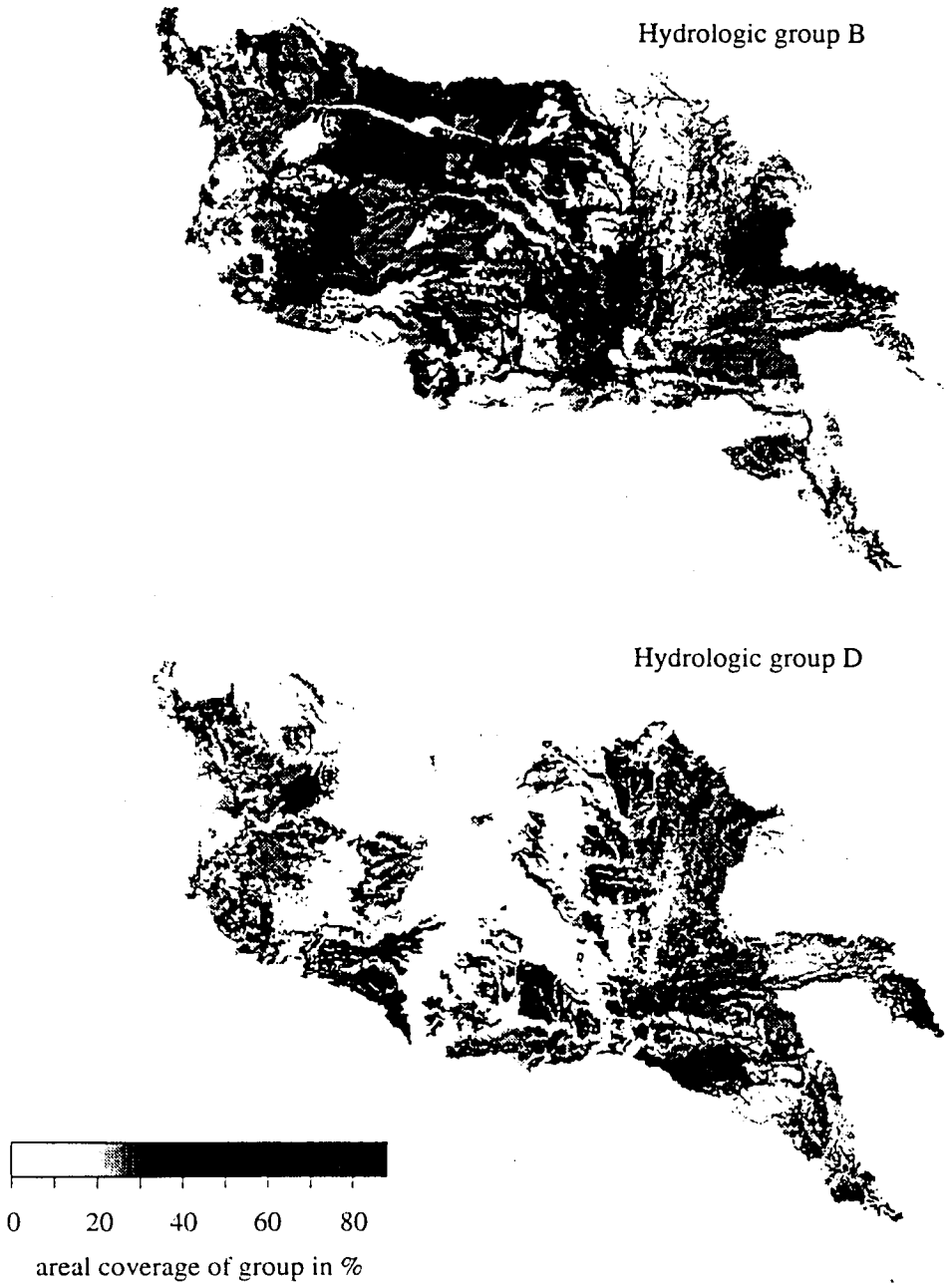

Fig. 2.10 Soil hydrologic group for the Arkansas-Red River basin.

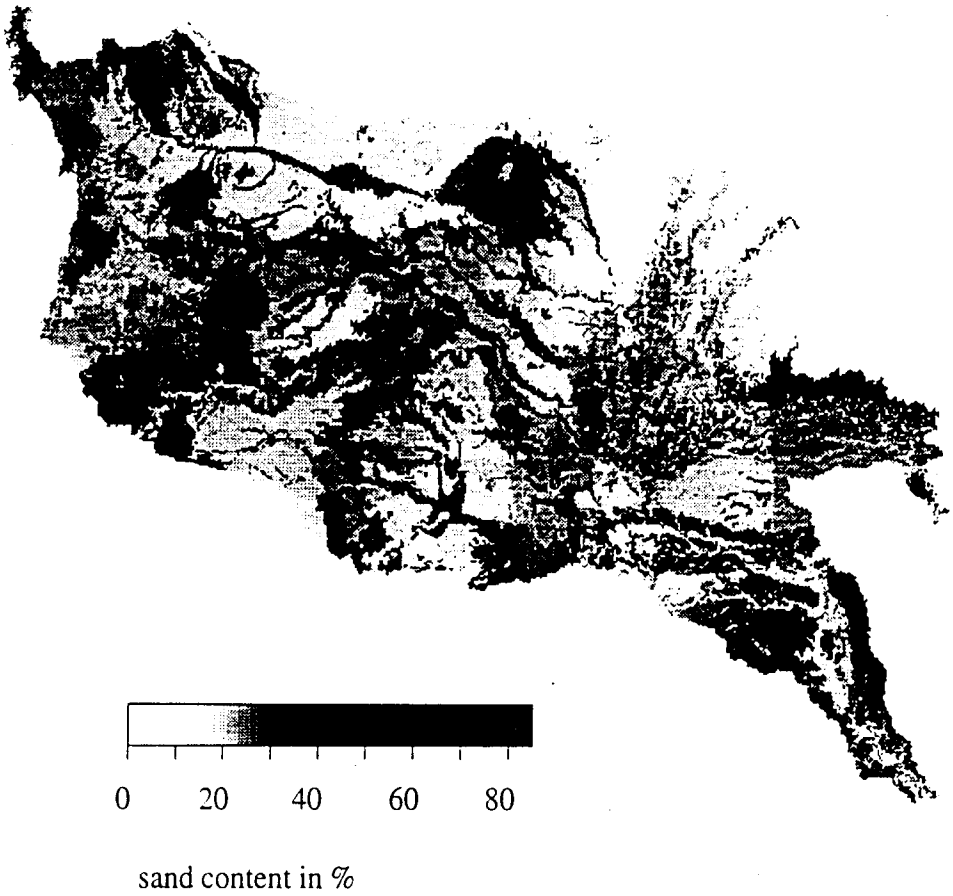

Fig. 2.11 Sand content of the surface layer for the Arkansas-Red River basin.

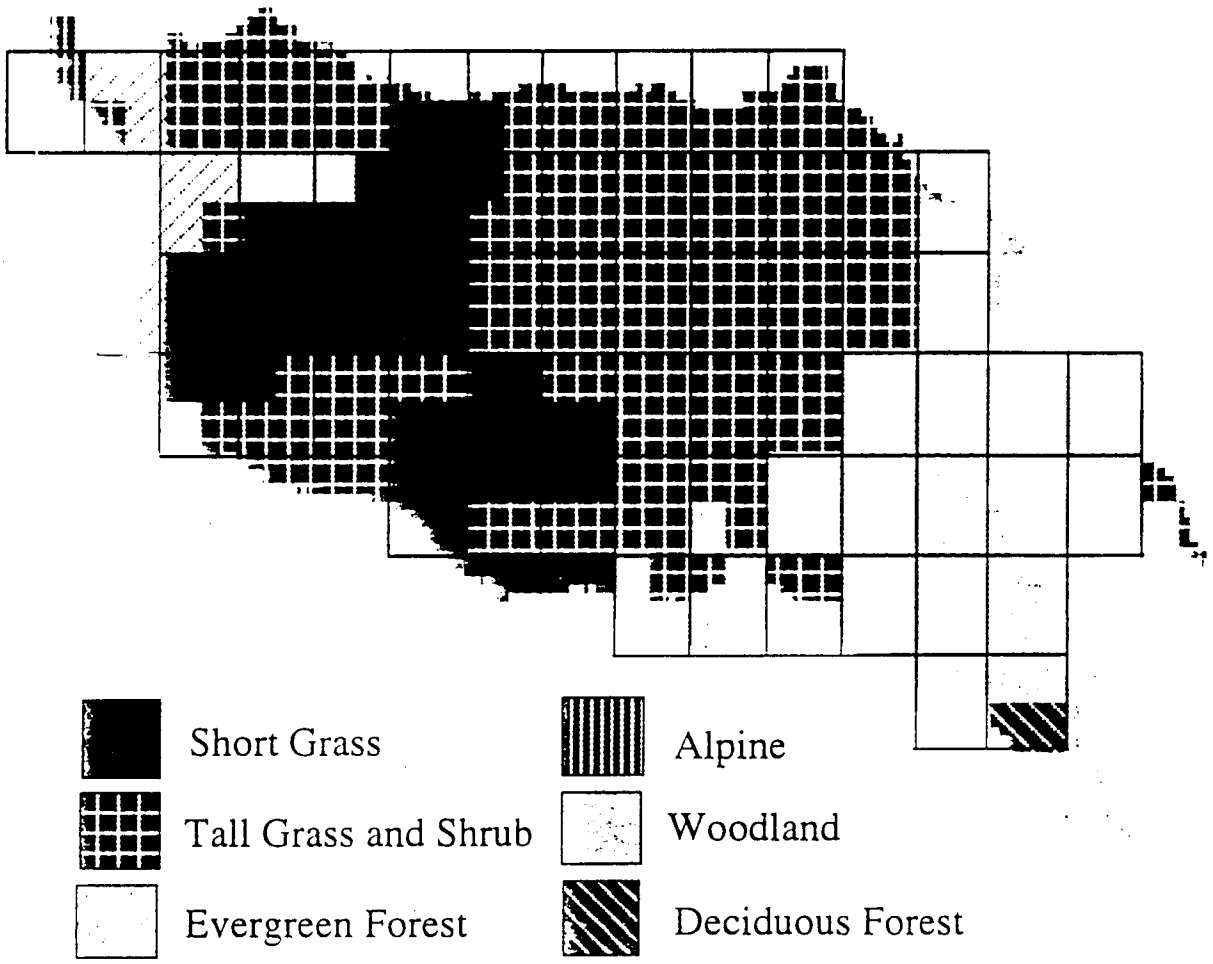

Fig. 2.12 Vegetation classes in the Arkansas-Red River basin

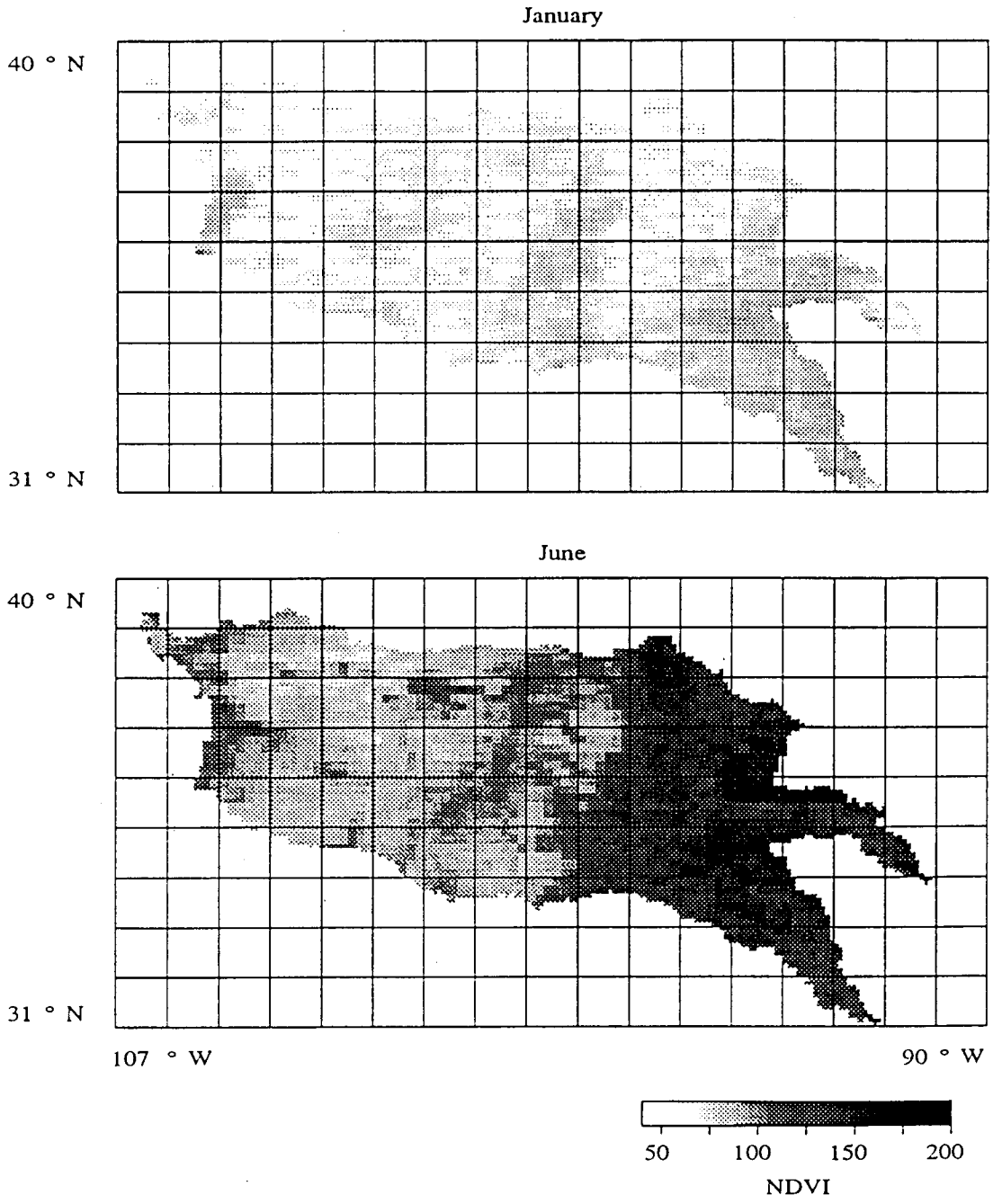

Fig. 2.13 Average monthly NDVI value for the Arkansas-Red River basin.

CHAPTER 3 MODEL DESCRIPTION AND PARAMETER ESTIMATION

This chapter describes the functional elements of the chain of models used for simulating the components of the water and energy budgets in a multi-scale framework (i.e. intermediate scale areas (ISA) with area ranging from 10^2 to 10^4 km^2 and large scale areas (LSA) with area ranging from 10^5 to 10^6 km^2) as well as alternative approaches for estimation of the parameters of a macroscale hydrologic model.

3.1 Introduction

This chapter describes a modeling strategy that will allow validating of macroscale energy-water balance models appropriate for modeling the water and energy budgets at the LSA scale (see Chapter 2 for description of terms). For this modeling strategy to be successful and to provide reliable estimates of the LSA water and energy fluxes, the macroscale hydrologic model must be calibrated using data at smaller scales within the LSA. This will also permit the development and testing of the regional equations for the VIC-2L model parameters, which is the primary goal of this thesis. For this purpose, alternative approaches for direct estimation of the hydrologic parameters of the VIC-2L model using station hydrologic and meteorologic data for a set of intermediate scale areas (ISA) is described.

This study involves two different scales: the intermediate or catchment scale and large or continental scale. Certain processes which do not play an important role at the catchment scale need to be explicitly represented at the larger scale. Therefore, it is necessary to construct two frameworks based on simple conceptual models that are sufficient to maintain a realistic description across a variety of physiographic and climate settings, and that account for the spatial scale differences between the ISA and LSA as well.

The first framework is the application of the VIC-2L model to a set of ISA calibration catchments within the LSA. In this application, the VIC-2L model is calibrated using station hydrologic, meteorological and distributed soil data for a number of ISA catchments.

The second framework is the application of the grid-based VIC-2L model to the LSA. In this application, a series of models are needed which calculate the snow melt and the runoff, and route the flow through stream channels and reservoirs. Three models were selected and combined to form an overall modeling strategy for the LSA application. These models are the National Weather Service River Forecast System (NWSRFS) snowmelt model (Anderson, 1973), the macro-scale land surface hydrology model (VIC-2L) (Liang et al., 1994), and the routing model of Wetzel (1994). The approach we followed can be summarized as follows: i) the snow accumulation and ablation model is run for each grid cell; ii) the VIC-2L model is run for each grid cell, using the snow model output as input; iii) the runoff from each grid cell is then routed from grid cell to grid cell through the LSA channel network using simple travel time assumptions.

In the following sections a brief description of these models is given. This is followed by description of the parameter estimation strategy for ISA catchments. The strategy used for estimation of the parameters for the LSA application is deferred to Chapter 5.

3.2 Review of hydrologic models

The relationship between rainfall and runoff is highly complex, and is dependent upon many geomorphological and climatic factors that are only imperfectly known and understood. There are a wide range of rainfall-runoff models in existence (see for example, STANFORD WATERSHED model, Crawford and Linsley, 1966; SACRAMENTO model, Burnash et al. 1973; TANK model, Sugawara et al. 1983; XINANJIANG model, Zhao 1977; and ARNO model, Francini and Todini 1991). Although many rainfall-runoff models have been reported in the hydrological literature, their implementation in GCMs has

been limited by the lack of data for calibration and initialization at large scale (Dumenil and Todini, 1992). In addition, the hydrologic process included in these models have focused traditionally on the water balance and moisture fluxes at the catchment scale which is much smaller than the scale of atmospheric phenomena. This has led to somewhat different representation of the land surface hydrology in atmospheric models than those to which hydrologists are accustomed.

The first attempts to parameterize the land hydrology in atmospheric models are attributed to Manabe et al. (1965). They used the so-called 'bucket' model. Bucket algorithms were used to represent land-surface hydrology in many of the first generation of GCMs (e.g. Manabe et al., 1965). The bucket model assumes that all the precipitation is infiltrated until the saturation capacity is exceeded. After that overflow contributes to runoff. Evaporation occurs at the potential rate when soil moisture is near saturation, and below some critical value, it is proportional to the potential evaporation, with a proportionality factor equal to the ratio of current soil moisture to saturation soil moisture. These parameterizations ignored the role of vegetation algorithm, using instead a so-called beta function to relate actual evapotranspiration to bulk aerodynamic potential evapotranspiration and soil moisture. The bucket model is clearly simplistic with respect to infiltration and runoff production, in addition to evaporation, and ignores vegetation effects on evapotranspiration.

Most current land surface parameterizations (LSPs) belong to the class of soil-vegtation schemes (SVATS). Of these, SiB (Simple Biosphere model) (Sellers et al., 1986) and BATS (Biosphere-Atmosphere Transfer Scheme) (Dickinson et al., 1986, Dickinson et al., 1993)) are best known. SVATS are recent alternatives to the previously dominant highly simplified representations of the land surface in GCMs. These models require specification of a large number of parameters. A distinguishing feature of SVATS, which is evident in both BATS and SiB, is that they have a high level of vertical resolution and structure, but a low level of horizontal resolution (Wood 1991). For example, the parameters for the soil and vegetation properties are assumed constant

within a GCM grid by which the spatial heterogeneity is ignored. Furthermore, most SVATS use a flat surface representation of the land surface which neglects the effects of topography on runoff production and soil moisture dynamics.

One of the few operational hydrologic models that has found use in coupled land-atmosphere applications is the Xinanjiang model (Zhao, 1977), variations of which have also have been termed Arno model by Francini (1991) and Pacciani, and the variable infiltration capacity model, or VIC, by Wood et al. (1992). Francini and Pacciani (1991) describe a variation of Xinanjiang model which incorporates a simple scheme for describing the spatial variability of infiltration and runoff production, and nonlinear base flow recessions. Wood et al. (1992) describe a single layer version of the VIC model, while Liang et al. (1994) generalized the VIC model to include multiple soil layers and spatially varying vegetation and evapotranspiration. Recently, Rowntree and Lean (1994) tested the Arno model using a one-dimensional version of the UK Meteorological Office GCM. They reported a runoff deficiency in summer, which they related to the difficulty in representing ground water storage. Variations of this model, which is sometimes termed the Arno model, have been implemented in GCMs by Dumenil and Todini (1992) in the Max Planck Institute model, and by Stamm et al. (1994) in the GFDL model.

In most previous large scale applications, the VIC or (Arno) model parameters have been selected subjectively, e.g., from ranges suggested by Dumenil and Todini (1992) based on streamflow calibration for a few catchments. Obviously, for application in GCMs, global parameter estimation using streamflow data is infeasible. In this study, we will focus on regionalization of the VIC-2L model parameters in order to improve our understanding of the hydrological cycle at large scales. This implies application of parameter estimation methods for a large number of catchments.

3.3 Snowmelt model

The snowmelt model used in this research is the temperature index model of Anderson (1973). It is an approximate energy balance method, in which the

form and temperature of precipitation and the components of the snowpack energy budget are indexed to surface air temperature. The model uses a 6-hourly computational time step to represent the daily cycle. The only data requirements are precipitation, surface air temperature, and elevation data. The model continuously accounts for the snowpack heat content, surface layer temperature, melt in the surface layer, and liquid water content. The rain-plus-melt output becomes the input to the soil moisture accounting model (VIC-2L model).

3.4 VIC-2L model

The VIC-2L model described by Liang et al. (1994) accounts for the spatial variability of soil moisture, evaporation, and infiltration within an area. In the VIC-2L model, the surface is described by N+1 land cover types, where n = 1,.., N represents N different vegetation, and n = N+1 represents bare soil. Associated with each land cover types is a single canopy layer, soil layer 1 (upper zone) and soil layer 2 (lower zone). The vertical and horizontal characterizations are shown schematically in Figure 3.1. The land cover types are specified by their leaf area index (LAI), canopy resistance, and relative fraction of roots in each of the soil layers. The evapotranspiration from each vegetation type is characterized by potential evapotranspiration together with canopy resistance, aerodynamic resistance to the transfer of water, and architectural resistance. In the following subsection the hydrologic part of the VIC-2L model, which includes the parameters to be regionalized, is described.

3.4.1 Surface and subsurface runoff

The model assumes that the infiltration capacity of the soil is not uniform, and therefore runoff generation and evapotranspiration vary within an area due to variations in topography, soil, and vegetation. The infiltration capacity varies within an area an can be expressed as

$$i = i_m[1 - (1 - A)^{1/b_i}] \qquad (3.1a)$$

$$A = 1 - (1 - \frac{i}{i_m})^{b_i} \tag{3.1b}$$

where i and i_m are the infiltration capacity and maximum infiltration capacity respectively, A ($0 \leq A \leq 1$) represents the fraction of the grid cell (or catchments) for which the infiltration capacity is less than i, and b_i is the infiltration parameter.

If the relationship between the maximum soil moisture averaged over the area (expressed as a depth) and i_m can be derived by calculating the shaded area in Figure 3.2 as follows:

$$W_{c1} = i_m - \int_0^{i_m} A \, di = i_m - \int_0^{i_m} [1 - (1 - \frac{i}{i_m})^{b_i}] \, di$$

$$= \frac{i_m}{b_i + 1} \tag{3.2}$$

The VIC model assumes that runoff is generated by those areas for which precipitation, when added to soil moisture storage at the end of the previous time step, exceeds the storage capacity of the soil. The direct runoff Q_d from these areas is given by

$$Q_d = P - W_{c1} + W^-_1 \qquad i_0 + P \geq i_m$$

$$Q_d = P - W_{c1} + W^-_1 + W_{c1}[1 - \frac{i_0 + P}{i_m}]^{1+b_i} \qquad i_0 + P \leq i_m \tag{3.3}$$

Where W^-_1 is the soil moisture content in layer 1 at beginning of the time step and i_0 represents the infiltration capacity of the saturated area.

For bare soil the water balance in layer 1 is

$$W^+_1 = W^-_1 + P - Q_d - Q_{12} - E \tag{3.4}$$

where W^+_1 is the soil moisture content in layer 1 at the end of each time step, Q_{12} is the drainage from layer 1 to layer 2. Assuming that the drainage is driven by gravity, the Brooks and Corey (1964) formulation gives

$$Q_{12} = K_s \left(\frac{W^-_1 - \theta_r}{W_c - \theta_r}\right)^{\frac{2}{B_p}+3} \tag{3.5}$$

where K_s is the saturated hydraulic conductivity, θ_r is the residual moisture content and B_p is the pore size distribution index.

The formulation of subsurface runoff (baseflow) follows the Arno model conceptualization (Fig. 3.3) (Francini and Pacciani 1991), which is applied only to the lower soil layer. The baseflow Q_b is given by:

$$Q_b = \frac{D_s D_m}{W_s W_{c2}} W^-_2 \qquad 0 \le W^-_2 \le W_s W_{c2} \tag{3.6a}$$

$$Q_b = \frac{D_s D_m}{W_s W_{c2}} W_2^- + (1-\frac{D_s}{W_s}) D_m \left(\frac{W^-_2 - W_s W_{c2}}{W_{c2} - W_s W_{c2}}\right)^2 \quad \text{for } W^-_2 \ge W_s W_{c2} \tag{3.6b}$$

where D_m, D_s , W_s and W_{c2} are the drainage parameters and W^-_2 is the soil moisture content at the beginning of the time step in layer 2. Table 3.1 lists the hydrologic parameters of the VIC-2L model which need to be regionalized.

Evapotranspiration can be estimated using a representation similar to that employed by Wood et al. (1992) and Liang et al (1994). In the case of Wood et al. (1992), the evaporation is represented by:

$$E = E_p \left\{ 1 - \left(1 - \left(\frac{W_0}{W_c}\right)\right)^{1/B_e} \right\} \tag{3.7}$$

where E_p is the potential evapotranspiration, and B_e is an evapotranspiration parameter. On the other hand, Liang et al. (1994) used the representation suggested by Francini and Pacciani (1991) which reduced the number of parameters by one. In this representation, it is assumed that when the soil is saturated it evaporates at a rate equal to the potential, E_p. When it is unsaturated, it evaporates at rate E computed using the equation

$$E = E_p \times \left[\int_0^{A_s} dA + \int_{A_s}^{1} \frac{i_0}{i_m \left[1 - (1 - A)^{1/b_i}\right]} \, dA \right] \tag{3.8}$$

The first integral represents the part of evaporation from the saturated area, which evaporates at the potential rate. Since there is no analytical expression for the second integral in Eq. 3.11 Liang et al. (1994) approximated the above equation via a power series expansion:

$$E = E_p \times \left\{ A_s + \frac{i_0}{i_m} (1 - A_s) \left[1 + \frac{b_i}{1 + b_i} (1 - A_s)^{1/b_i} + \right.\right.$$

$$\left.\left. \frac{b_i}{2 + b_i} (1 - A_s)^{2/b_i} + \frac{b_i}{3 + b_i} (1 - A_s)^{3/b_i} + \cdots \right] \right\} \tag{3.9}$$

In this brief description of VIC-2L, we have only described the formulations in which the hydrologic parameters to be regionalized appear. For a complete description of the model, the reader is referred to Liang et al. (1994).

3.5 Runoff routing model

A unit hydrograph approach is used to account for advection and dispersion of the VIC-2L model output in the channel network. The approach was implemented in a grid network by Wetzel (1994) to account for the lateral transport of water through surface and subsurface storage reservoirs and to connect each of the modeled 1×1 grid cells via a flow network. It has been used for simulation of the Missouri, Colorado, and Columbia Rivers by Wetzel (1994), Mas et al. (1994), and Nijssen et al. (1994) respectively. The model consists of two components. The first accounts for the transport of water within a 1×1 grid cell and is referred to as within-grid routing, while the second simulates water transport along the flow network, between grid cells and is referred to as grid-to-grid routing.

The within-grid routing component accounts for the time required for runoff produced within a grid cell to reach an arbitrary outlet. The runoff generated by the VIC-2L for each grid cell, is convolved with a unit hydrograph according to the discrete convolution given by:

$$R_i = \sum_{j=1}^{i \leq J} Q_j \, H_{i-j-1} \qquad (3.10)$$

Where R is the internally routed runoff at the grid cell outlet, Q is the runoff output of the VIC-2L model, H contains the unit hydrograph ordinates, i refers to the time step of the unit hydrograph, j refers to the time step of runoff time series, and J is the total number of time steps in the runoff time series.

The internally routed runoff R_i is transported downstream through the flow network shown in Figure 2.3. For routing across a grid cell, an effective velocity of 1 m/sec was assumed, which is the lower value in the velocity range suggested by Sausen (1994). For purpose of computing the lag time, the channel lengths are computed based on the straight line distance from the center of one block to that of the next dependent on the configuration of the flow network

defined in Figure 2.3. It should be noted that the flow velocities do not represent actual channel velocities (which tend to be lower), because the actual channel lengths are much longer (by a multiple of the average sinuosity (>1)) than the straight line distances.

3.6 Parameter estimation

In most previous large scale applications, the hydrological parameters of the land surface scheme, such as the VIC-2L model and Arno model, has been either fixed globally at "reasonable values", or selected subjectively from "literature values" for appropriate land cover. Examples on these applications can be found in Wood et al. (1992), Dumenil and Todini (1992), Stamm et al. (1994), and Rowntree and Lean (1994). Previous experience in the development and application of conceptual streamflow simulation models for forecasting, can provide a useful mean with respect to model parameter parsimony, for the application of land surface parameterizations for coupled land-atmosphere models. Better methods of estimating parameters of macroscale are obviously needed.

In this section we explore two alternative approaches for estimation of the parameters of the VIC-2L model. Table 3.1 lists the hydrologic parameters of the VIC-2L model that need to be determined. The first method, complete optimization, estimates all model parameters simultaneously using a search procedure. The second method uses spatially distributed soil data directly to determine selected parameters of the VIC-2L model with the remaining parameters determined using a search procedure. For this purpose a number of ISA catchments within the Arkansas-Red River basin (LSA) were selected for calibrating the VIC-2L model using the available hydrologic, meteorologic, and distributed soil data for these catchments.

3.6.1 Objective function

The idea behind the model calibration is to select parameter values to minimize the differences between the simulated and recorded streamflows. In

this study, parameter values are optimized to minimize the difference between the monthly simulated and recoded streamflow volumes given by the following objective function:

$$OBJ = \sum_{i=1}^{n} (Qsim_i - Qobs_i)^2 \tag{3.11}$$

where $Qsim_i$ and $Qobs_i$ are the simulated and observed streamflows for month i and n is the number of time periods simulated. This objective function is the commonly used sum of squares of the differences between simulated and recorded streamflows. The model time step is daily and the daily values are aggregated to monthly values.

3.6.2 Optimization procedure

The first step in the application of a conceptual model to a basin is model calibration. The objective is to determine the model parameters such that an acceptable match is obtained between the observed and simulated streamflows. Basically two approaches can be used for the calibration of conceptual models: manual parameter fitting using trial and error and automatic fitting using an optimization algorithm. James and Burges (1982) give a comprehensive discussion of various aspects of the calibration of conceptual models.

A number of methods have been used for estimation of rainfall-runoff model parameters. Among these are the Simplex method (Nelder and Mead, 1965), the Newton-Raphson method (Gupta and sorooshian, 1985), the pattern search method of Hooke and Jeeves (1961), the simulated annealing method (Kirkpatrick et al. 1983), and the genetic method (Wang, 1991). A general experience with all these methods is the difficulty of find globally optimal parameter estimates, due to the existence of multiple optima, non-smooth objective functions in the multi-parameter space, and structural problems in rainfall-runoff models such as a high degree of interaction between some of the parameters.

Recently Duan et al. (1992) developed a global optimization scheme called

the Shuffled Complex Evolution (SCE) method which attempts to address these problems. They show that the SCE algorithm is a relatively consistent, effective and efficient optimization method capable of locating the global optimum during calibration of the Sacramento soil moisture accounting model (SAC-SMA) of the National Weather Services River Forecast System (NWSRFS).

In this study three parameter optimization methods were tested: Simplex (S), Simulated Annealing combined with Simplex (SAS), and Shuffled Complex Evolution (SCE). Sensitivity of each method to the starting point and the bounds of the parameters space was explored. The SCE method was found to be the most robust of the three methods, and was therefore selected.

3.6.3 Evaluation of conceptual model performance

The model calibration process consists of calibration, verification, and prediction. In the calibration period, model parameters are estimated on the basis of available rainfall-runoff records. During the verification period, the calibrated model is applied to the available rainfall records and computed runoff values are compared with the observed records in order to assess the predictive efficiency of the model. If the efficiency is adequate, the model can then be used for runoff prediction in the prediction period. James and Burges (1982) list three criteria to evaluate calibration of a model: subjective judgment of adequacy; statistics selected to measure of goodness of fit, and user-defined objective functions. Methods of evaluating hydrologic model performance have been suggested by Aitken (1973), James and Burges (1982), and Green et al. (1986). They generally recommend the use of statistical measures of differences between observed and simulated streamflow as a quantitative measure of calibration adequacy. The statistical performance criteria used are (Aitken, 1973; Gan and Burges, 1990):

1) Comparison between mean monthly simulated $\bar{Q}_{sim}$ and observed $\bar{Q}_{obs}$ flows:

$$\bar{Q}_{sim} = \frac{1}{n} \sum Q_{sim} \tag{3.12}$$

2) Comparison between the standard deviation of monthly simulated and observed flow

$$\sigma_{sim} = \sqrt{\frac{\sum (Q_{sim} - \bar{Q}_{sim})^2}{n-1}} \tag{3.13}$$

3) Root mean square error

$$RMSE = \sqrt{\frac{\sum (Q_{sim} - Q_{obs})^2}{n}} \times \frac{100}{\bar{Q}_{obs}} \tag{3.14}$$

4) Yearly relative error

$$V\% = \frac{\bar{Q}_{sim} - \bar{Q}_{obs}}{\bar{Q}_{obs}} \times 100\% \tag{3.15}$$

5) Coefficient of determination R^2 between the observed and simulated monthly runoff

$$R^2 = \frac{\sum (Q_{obs} - \bar{Q}_{obs})^2}{\sum (Q_{sim} - \bar{Q}_{obs})^2} \tag{3.16}$$

However, different opinions are reported as to which statistical indices are most useful. James and Burges (1982) recommended graphical comparisons. Gan and Burges (1990) reported that there is no single numeric is suitable for describing how well a particular model performs. For example, James and Burges (1982) found for average daily flow volumes that a coefficient of efficiency (a measure equivalent to R^2) greater than about 0.97 was associated well model performance. Other experience (World Meteorological Organization, (WMO)

1975) for snowmelt runoff models yielded a maximum efficiency during calibration periods of 0.93. Recently, Chiew et al. (1993) and Chiew and McMahon (1994) define an "acceptable simulation" for which the coefficient of efficiency is greater than 0.6 and the mean simulated flow within 15% of mean recorded flow. In this study we use both statistical and graphical comparisons. These statistical performance criteria will be used to evaluate the calibration of the VIC-2L model in this Chapter as well as to evaluate the performance of the regionalized VIC-2L model in Chapter 4. A "good" calibration result is defined as one for which the R^2 was higher than 0.7, and the difference in volume between the observed and simulated flows is within 10%.

3.6.4 Model calibration

Data from the 40 ISA calibration catchments described in Chapter 2 were used to estimate the parameters of the VIC-2L model. These catchments are shown in Figure 2.4 and listed in Table 2.1. The parameters were estimated using the Shuffled Complex Evolution (SCE) search method of Duan et al. (1992), where the objective function was the sum of squared differences between the simulated and observed streamflow. The model was run at a daily time step and the output was aggregated to monthly values. The parameter estimation procedure requires daily time series of the input variables (precipitation, potential evaporation (PET), and, for catchments where precipitation occurs as snow, temperature), as well as an observed output series of daily streamflow to compute the objective function. Since the data required to compute PET using an energy-based formulation such as Penman-Monteith were not available for the calibration catchments, we used Hamon's method (Hamon et al, 1954; Hamon, 1961) which requires only daily air temperature and latitude. The Hamon equation can be written as:

$$ET = C_h \, D_h^{\,2} \, P_t \qquad (3.17)$$

where ET represents the average potential evapotranspiration in inches per day; D_h is the possible hours of sunshine in units of 12 hr; P_t is the saturated water

vapour density (absolute humidity) at the daily mean temperature in grams per cubic meters; times 10^{-2}; $C_h = 0.55$.

Liang et al. (1994) compared the daily E_p computed using Hamon equation with daily E_p obtained using the Penmam-Monteith equation for the FIFE site in Kansas. These authors found that the Hamon formula gave smaller E_p estimates. Because both methods proved to be roughly proportional, E_p predictions by the Hamon method were adjusted by a scale factor fe; the scaling factor fe is added to the list of parameters to be estimated (see Table 3.1).

For fitting and validation of the VIC-2L model, the data record was divided into two periods. The first period (6 years) listed in Table 2.1 is used for parameter estimation; while the rest of the record is used for model validation. For both periods, the first year of record was used to initialize the soil moisture storage.

3.6.4.1 Complete- and sub- optimization methods

Two alternative parameter estimation methods were investigated. The first method, complete optimization, estimates all model parameters simultaneously using the SCE algorithm (Table 3.1 shows these parameters). The second method, sub-optimization, involves a two stage optimization strategy. In the first stage, we use STATSGO data directly to determine three of the parameters of the VIC-2L model (saturated hydraulic conductivity, pore size distribution index, and residual soil moisture; see Section 2.3). Figures 3.4 and 3.5 show the spatially distributed saturated hydraulic conductivity and pore size distribution index parameters respectively. In the second stage, the remaining seven parameters are determined using the search procedure.

3.6.4.2 Comparison between the complete and sub optimization methods

To compare the two methods, three aspects of the estimation procedure are considered: the number of iterations, the value of the objective function, and the goodness of fit. As expected, the number of iterations used in the second method is reduced considerably (by more than 60 percent) due to the smaller

dimension of the parameter space. Figure 3.6 shows the value of the objective function for each catchment using the two methods. In the sub-optimization method the objective function is higher because only seven parameters were optimized instead of ten, however the relative difference between the two methods is small. Objective function values for the 40 catchments range from 7 to 53,000 in the case of complete optimization, while they ranges from 8 to 63,600 in the case of sub-optimization. The average ratio of the objective function in the sub-optimization to that of the complete optimization is 1.19.

Observed and simulated streamflow based on parameters obtained using the two methods are shown in Figure 3.7 for all the catchments listed in Table 2.1. The simulated hydrographs using STATSGO parameters in conjunction with the optimization method compared favorably with the hydrographs based on complete optimization. Generally, the monthly simulated hydrographs for the large catchments and the humid ones are more acceptable than those of the small catchments and the arid ones. For example, the model performs badly for the Rayado Creek, NM (see Figure 3.7). This catchment is the smallest of all the listed catchments in Table 2.1, it has an area of 168 km^2 and at elevation of 2050 m with channel slope of about 40m/km. Both optimization methods tend to produce similar hydrographs which underestimate the spring and the summer flow. Even including the Anderson snowmelt model (1973) to account for the snow accumulation and melting for this catchment no obvious improving in the model performance is achieved. This poor performance of the model may be due to inability of the recorded precipitation to represent this particular catchment, possibly due to orgraphic effects, such as rain shadowing (the precipitation gage is at 1995 m elevation, which is lower than the streamflow gage at 2050 m).

Clearly, the performance of the model varies among the catchments. Figures 3.8 to 3.12 summarize the goodness-of-fit statistics obtained for all the catchments. The performance criteria selected are the monthly root mean square error (RMSE); the monthly coefficient of variation (CV) of the observed and simulated runoff; the mean annual observed and simulated runoff; the yearly relative error (V); and the coefficient of determination (R^2). The catchments

listed in Table 2.1 are ranked according to the lowest RMSE obtained using the complete optimization method.

Figure 3.8 shows the monthly RMSE for all the catchments listed in Table 2.1. The RMSE ranges from 21 to 96 percent with an average of 54 percent in the case of the complete optimization, while in the case of sub-optimization it ranges from 23 to 124 percent with an average of 59 percent. Generally, the RMSE for the two methods are very close in most of the catchments. The largest differences are for catchments 5 and 29 which are semi-arid.

Figure 3.9 shows the observed and simulated monthly CV using both optimization methods. The dry catchments tend to have high CVs compared to the other catchments. In general, the CVs from the two methods compare well with the observed, with the exception of some dry catchments, such as catchment 37 which has mean annual runoff of only 11.2 mm.

Figure 3.10 shows the observed and simulated mean annual runoff. As shown in this Figure eleven catchments have mean annual runoff less than 100 mm and can be considered semi-arid or arid. Figure 3.11 shows yearly relative errors, which range from 0.3 to 48 percent with a mean of 6.6 percent in the case of complete optimization. In the case of sub-optimization the relative error ranges from 0.1 to 44 percent with a mean of 7.2 percent. In both cases 31 catchments out of the 40 catchments have a relative error less than five percent. Three of the catchments have relative error greater than 20 percent; these catchments are numbers 15 , 26, and 29, all of which are arid or semi-arid.

The coefficient of determination R^2 between the observed and simulated flow ranges from 0.41 to 0.98 with an average of 0.77 for the case of complete optimization (Figure 3.12). In the case of sub-optimization, R^2 ranges from 0.41 to 0.97 with an average of 0.74. Seventy percent of the catchments have R^2 greater than 0.7 in the case of the complete optimization, while in the case of sub-optimization only sixty percent of the catchments have an R^2 greater than 0.7.

3.7 Summary

The modeling framework for simulating the water and energy budgets at both the ISA and LSA scales have been presented. Three linked models form the overall modeling strategy. These models are the snowmelt model, a macroscale land surface hydrology model (VIC-2L), and a simple runoff routing model.

A methodology for estimating the hydrologic parameters of the VIC-2L land surface model is presented. This methodology consists of two alternative estimation methods. The first, complete optimization, estimates all the hydrologic parameters of the VIC-2L model simultaneously using the SCE algorithm. The second method, sub-optimization, uses distributed soil data to estimate three of the model parameters, the remanning seven parameters are then determined using the search procedure. The simulated hydrographs as well as performance criteria of the two methods for the model compared reasonably well. Therefore, the estimated parameters using the sub-optimzation method (STATSGO in conjunction with search procedure) will be adopted in the regional methodology described in the next chapter. This means that only seven of the VIC-2L model parameters needed to be investigated for a possible regional equation and the remaining three can be obtained directly from the available distributed soil data.

Table 3.1 Hydrologic parameters of the VIC-2L land surface model

Parameter	Description
b_i	Infiltration parameter
W_{c1}	Maximum soil moisture of layer 1
W_{c2}	Maximum soil moisture of layer 2
D_m	Maximum baseflow parameter
D_s	Fraction of the maximum baseflow
W_s	Fraction of the maximum soil moisture
Fe	Evaporation factor
B_p	Pore size distribution index
K_s	Saturated hydraulic conductivity
θ_r	Residual moisture content

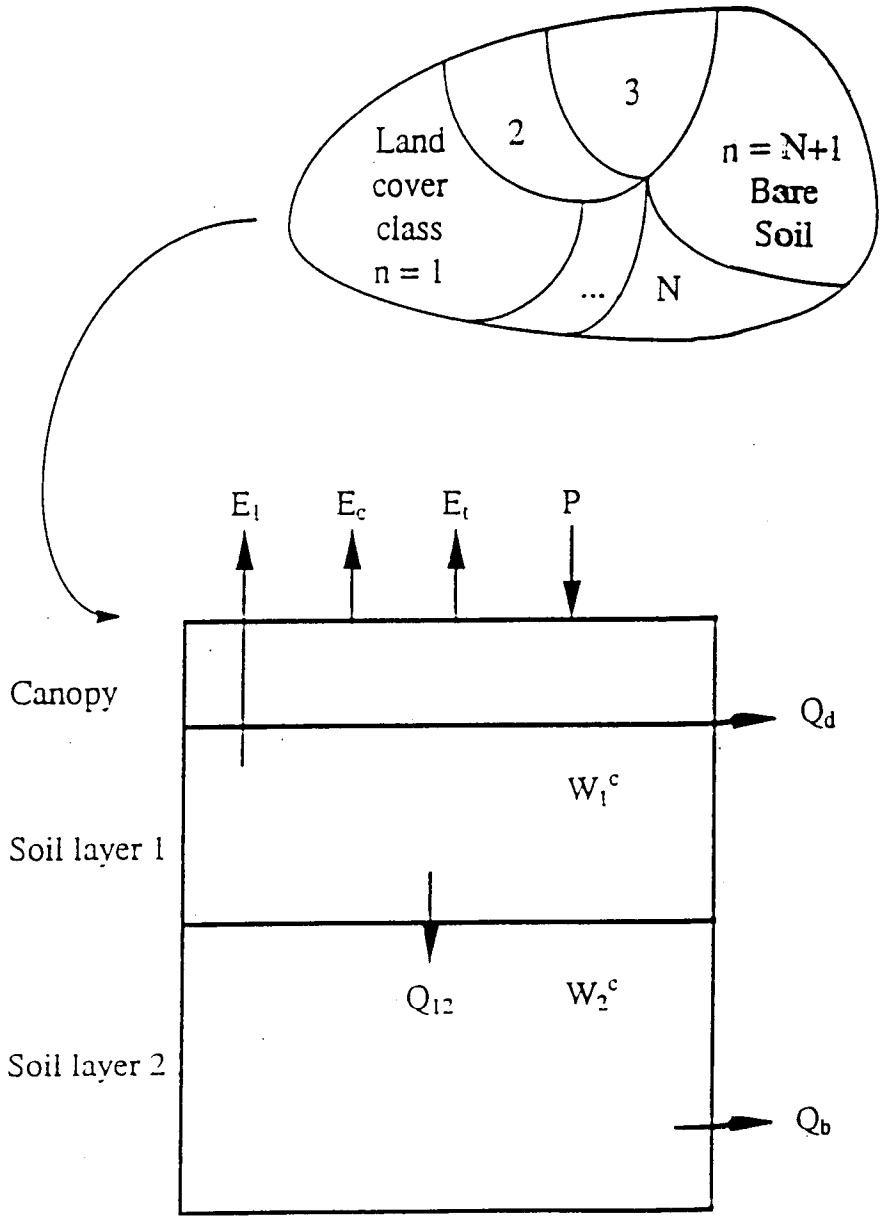

Fig. 3.1 Schematic representation of the VIC-2L model.

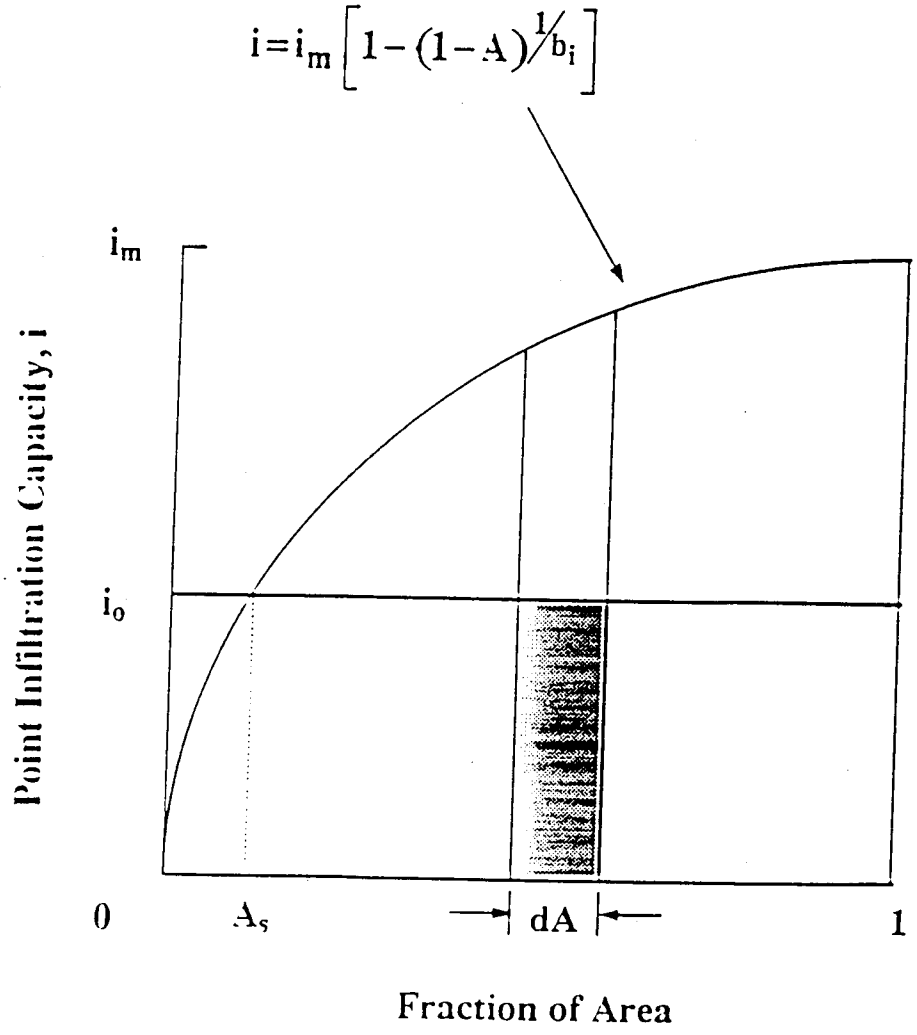

Fig. 3.2 Schematic showing the runoff and infiltration relationships as a function of grid wetness and infiltration capacity.

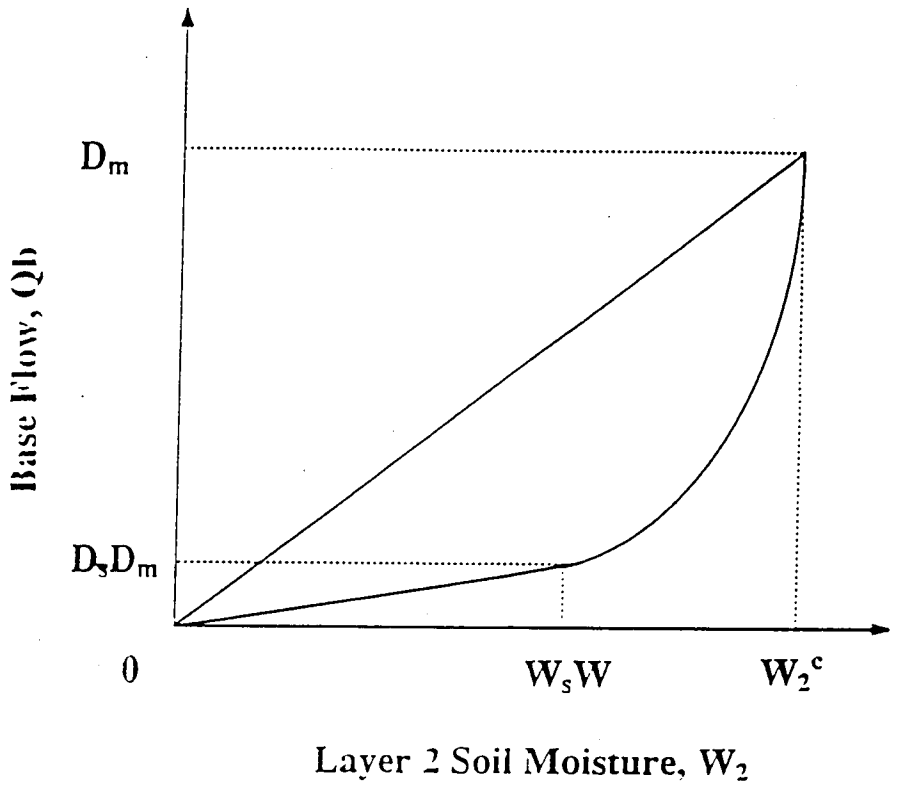

Fig. 3.3 Schematic representation of Arno nonlinear base flow

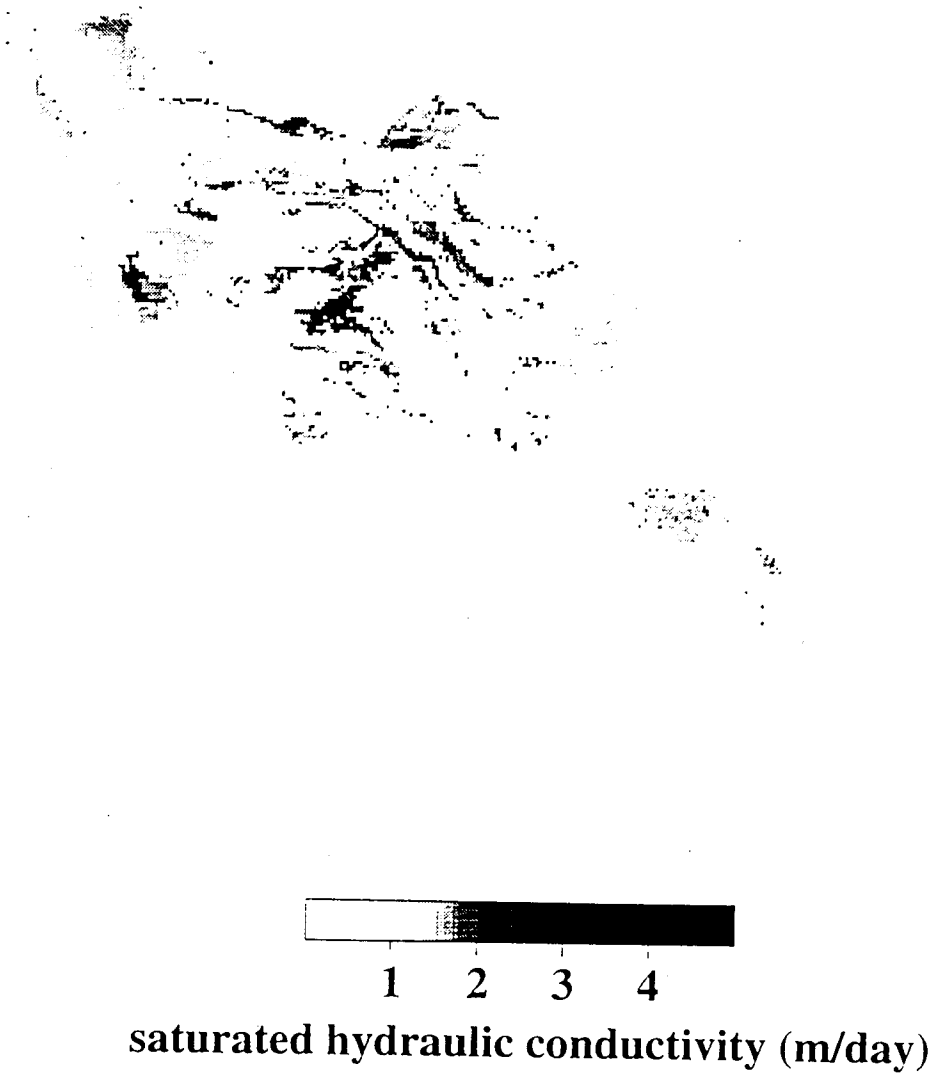

Fig. 3.4 Calculated spatial distribution of hydraulic conductivity (K_S) for the Arkansas-Red River basin derived from STATSGO data

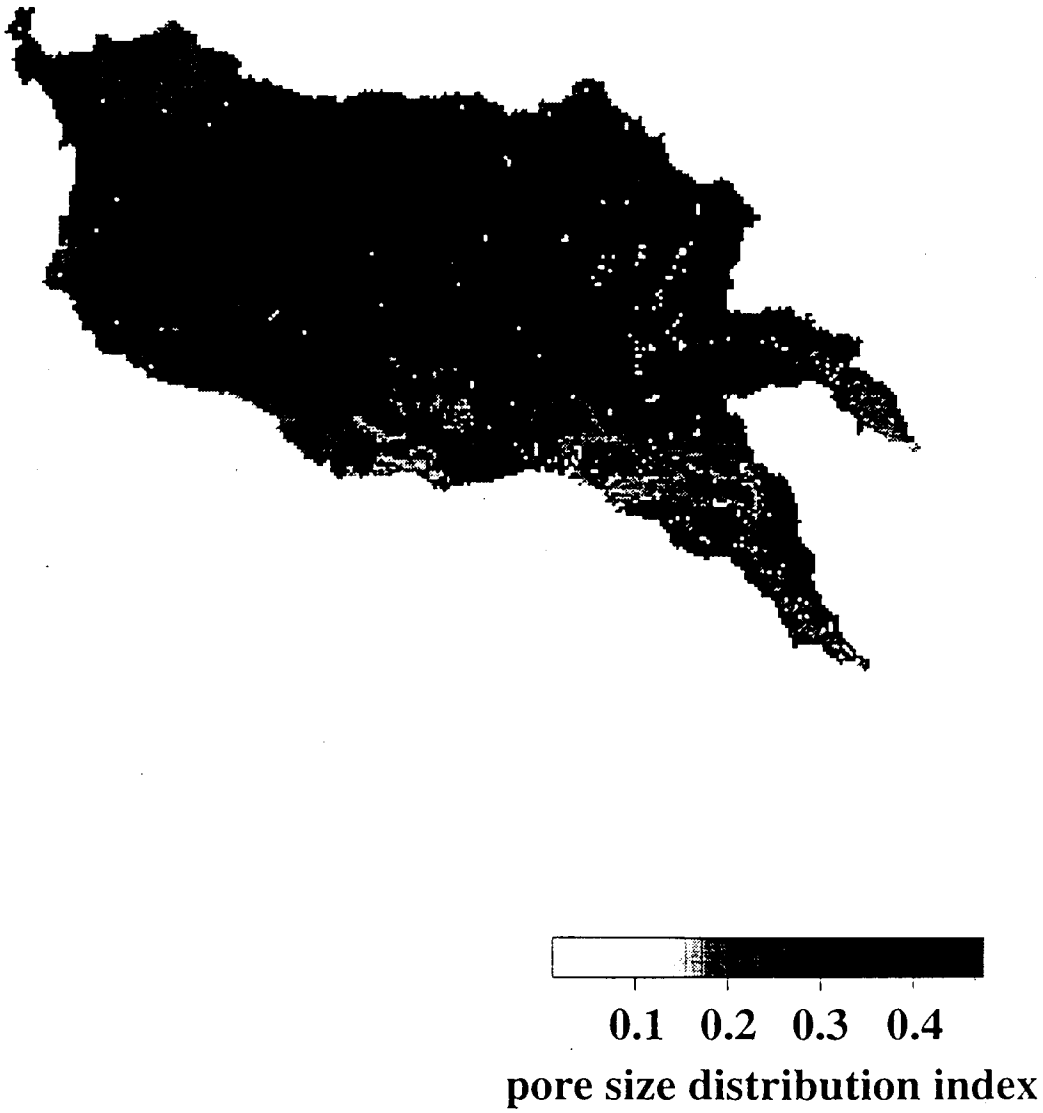

Fig. 3.5 Calculated spatial distribution of pore size distribution index (B_p) for the Arkansas-Red River basin derived from STATSGO data

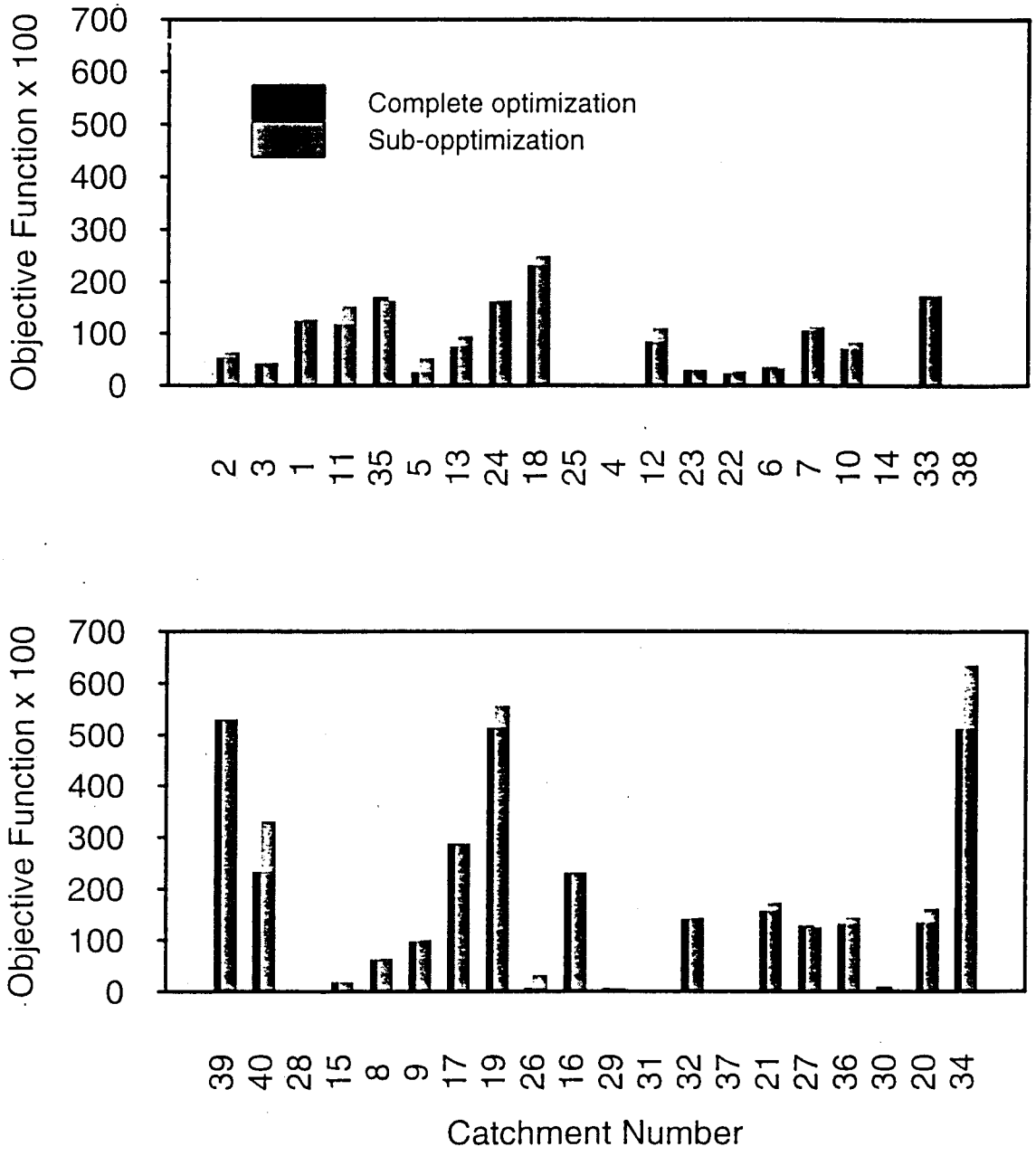

Fig. 3.6 Comparison of objective function obtained using complete and sub-optimization methods

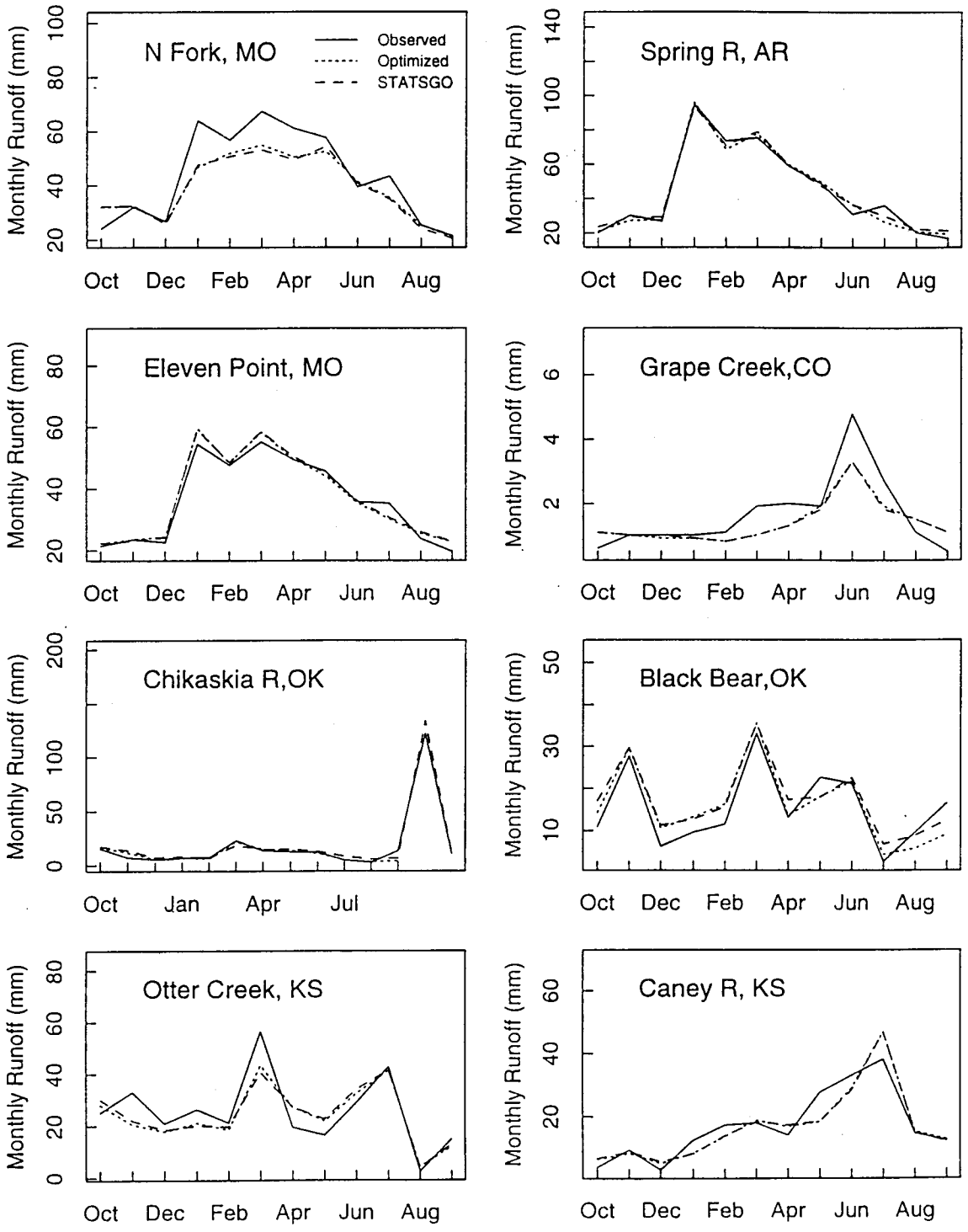

Fig. 3.7 Observed and predicted (using complete optimization) as well as predicted (using sub-optimization) mean monthly streamflow for selected calibration catchments (for the six-year calibration period).

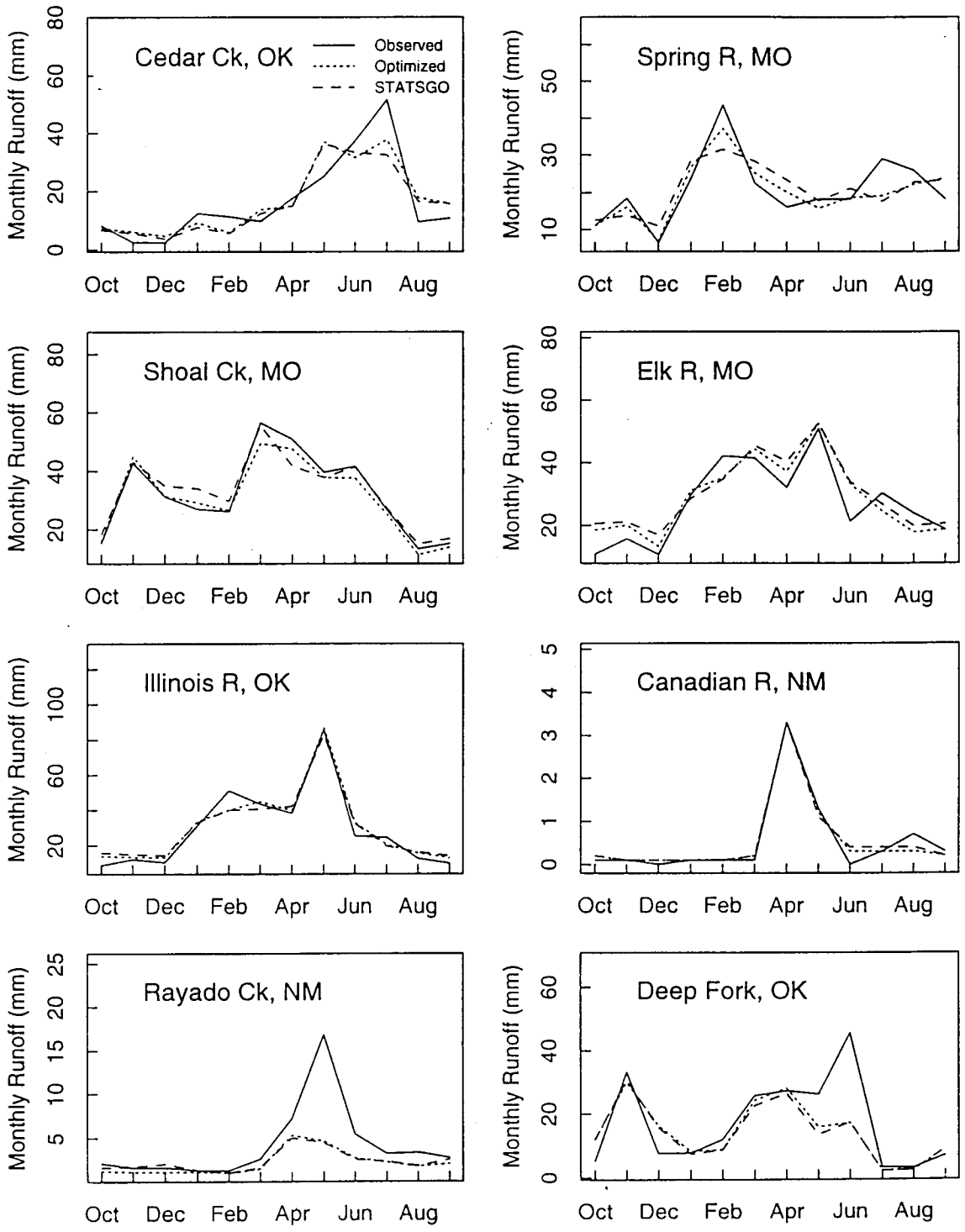

Fig. 3.7 (contd.) Observed and predicted (using complete optimization) as well as predicted (using sub-optimization) mean monthly streamflow for selected calibration catchments (for the six-year calibration period).

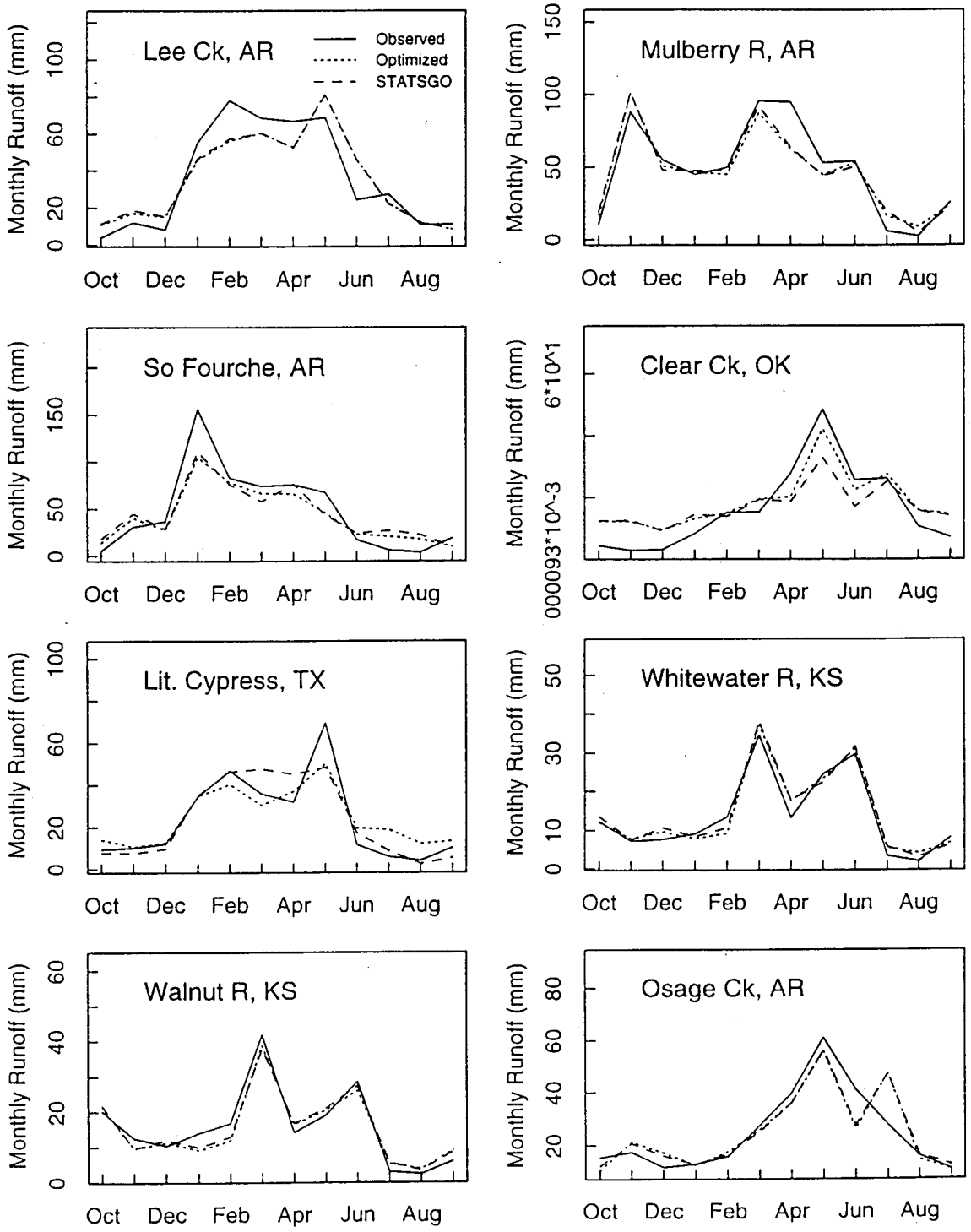

Fig. 3.7 (contd.) Observed and predicted (using complete optimization) as well as predicted (using sub-optimization) mean monthly streamflow for selected calibration catchments (for the six-year calibration period).

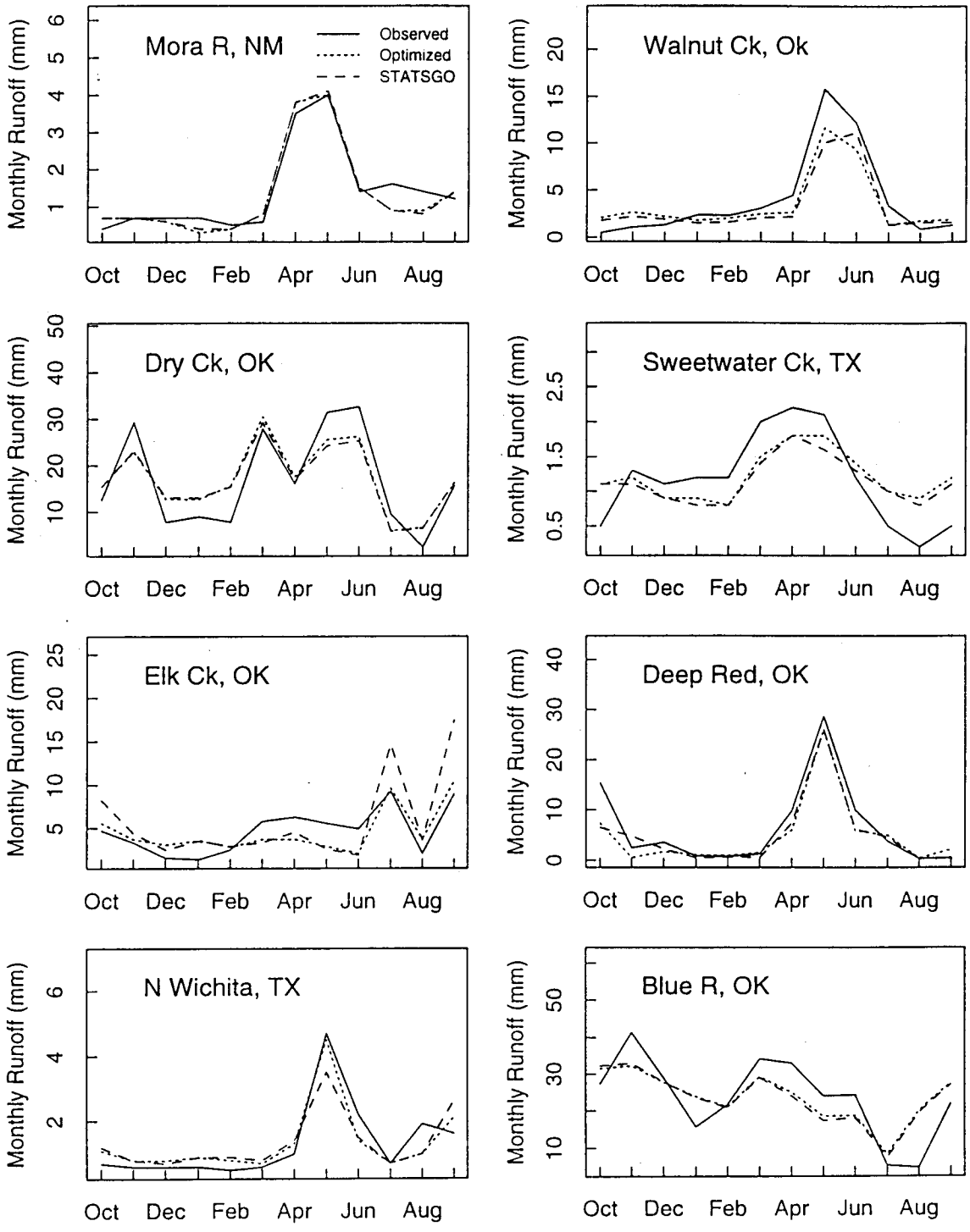

Fig. 3.7 (contd.) Observed and predicted (using complete optimization) as well as predicted (using sub-optimization) mean monthly streamflow for selected calibration catchments (for the six-year calibration period).

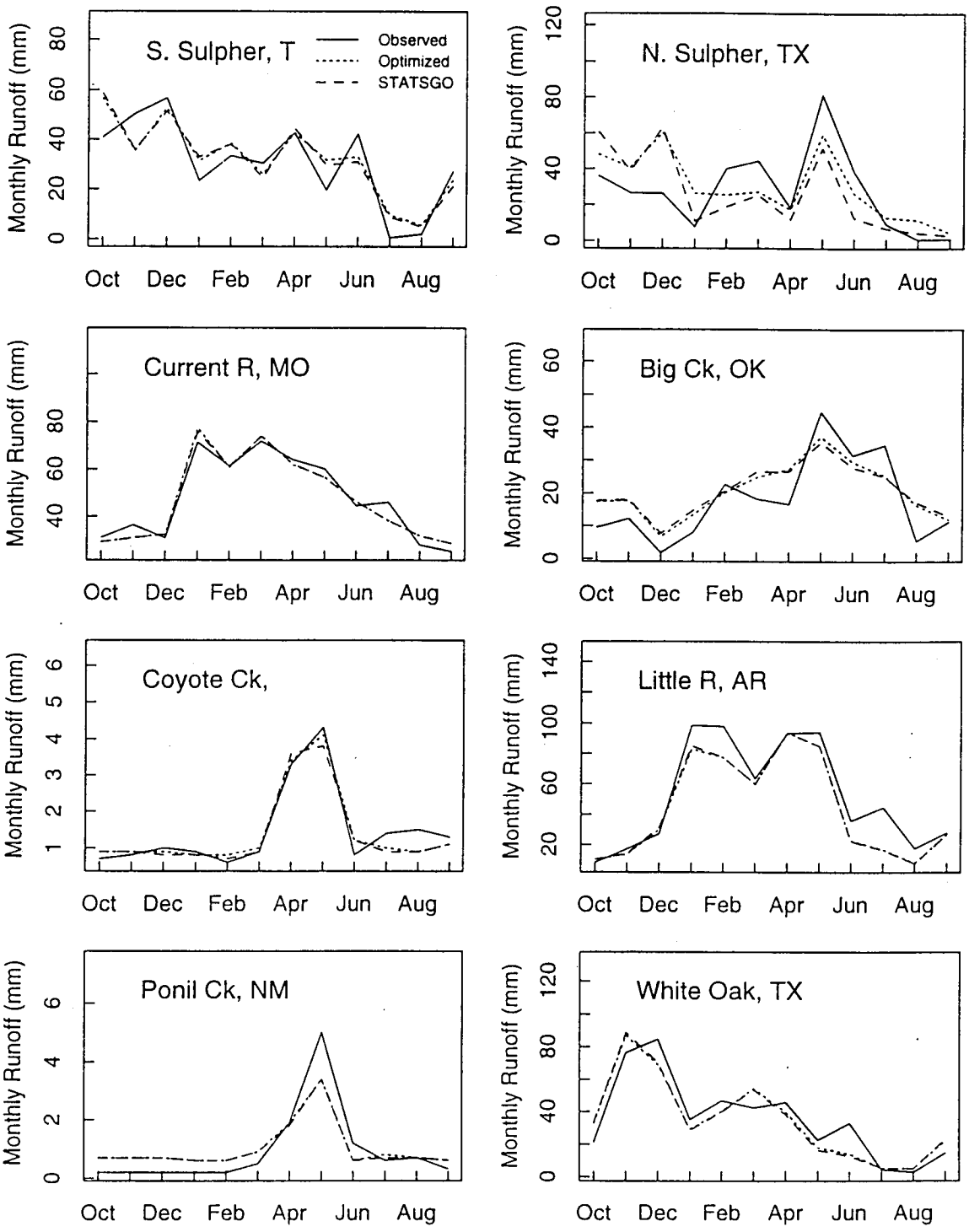

Fig. 3.7 (contd.) Observed and predicted (using complete optimization) as well as predicted (using sub-optimization) mean monthly streamflow for selected calibration catchments (for the six-year calibration period).

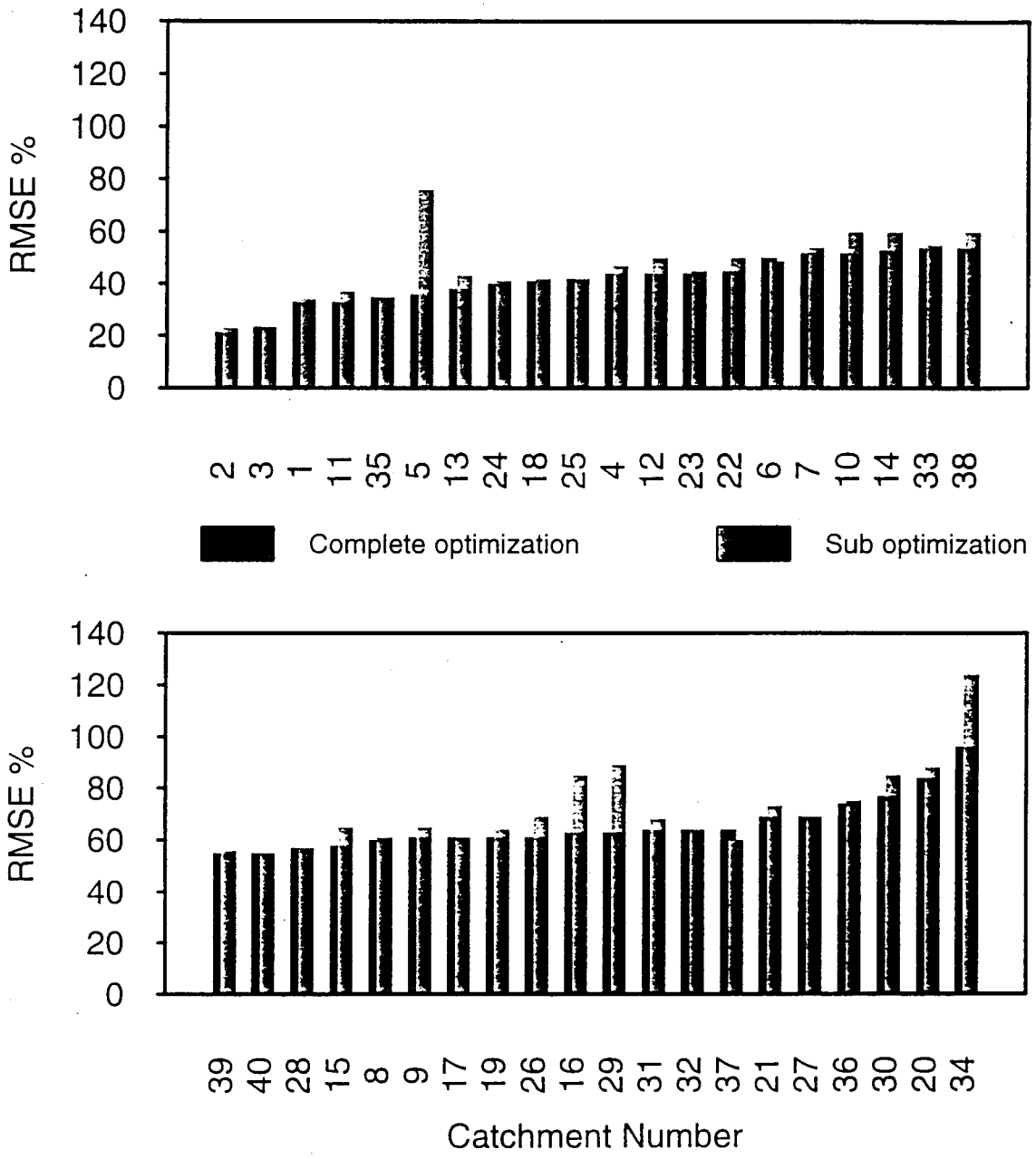

Fig. 3.8 Comparison of monthly root mean square error (RMSE) for all catchments using both complete and sub-optimization methods

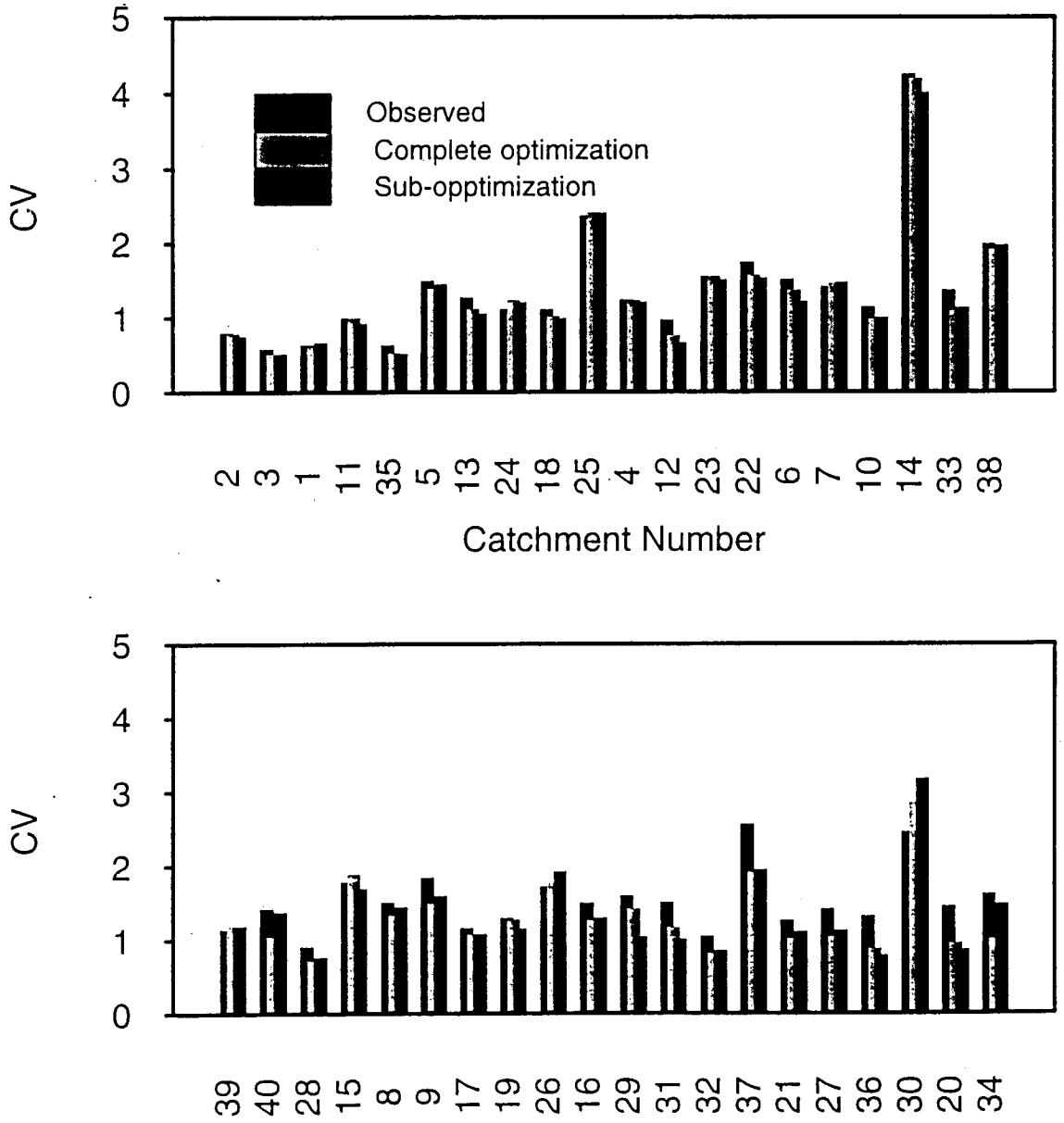

Fig. 3.9 Observed and predicted (using complete optimization) as well as predicted (using sub-optimization) coefficient of variation (CV) of monthly streamflow for all calibration catchments

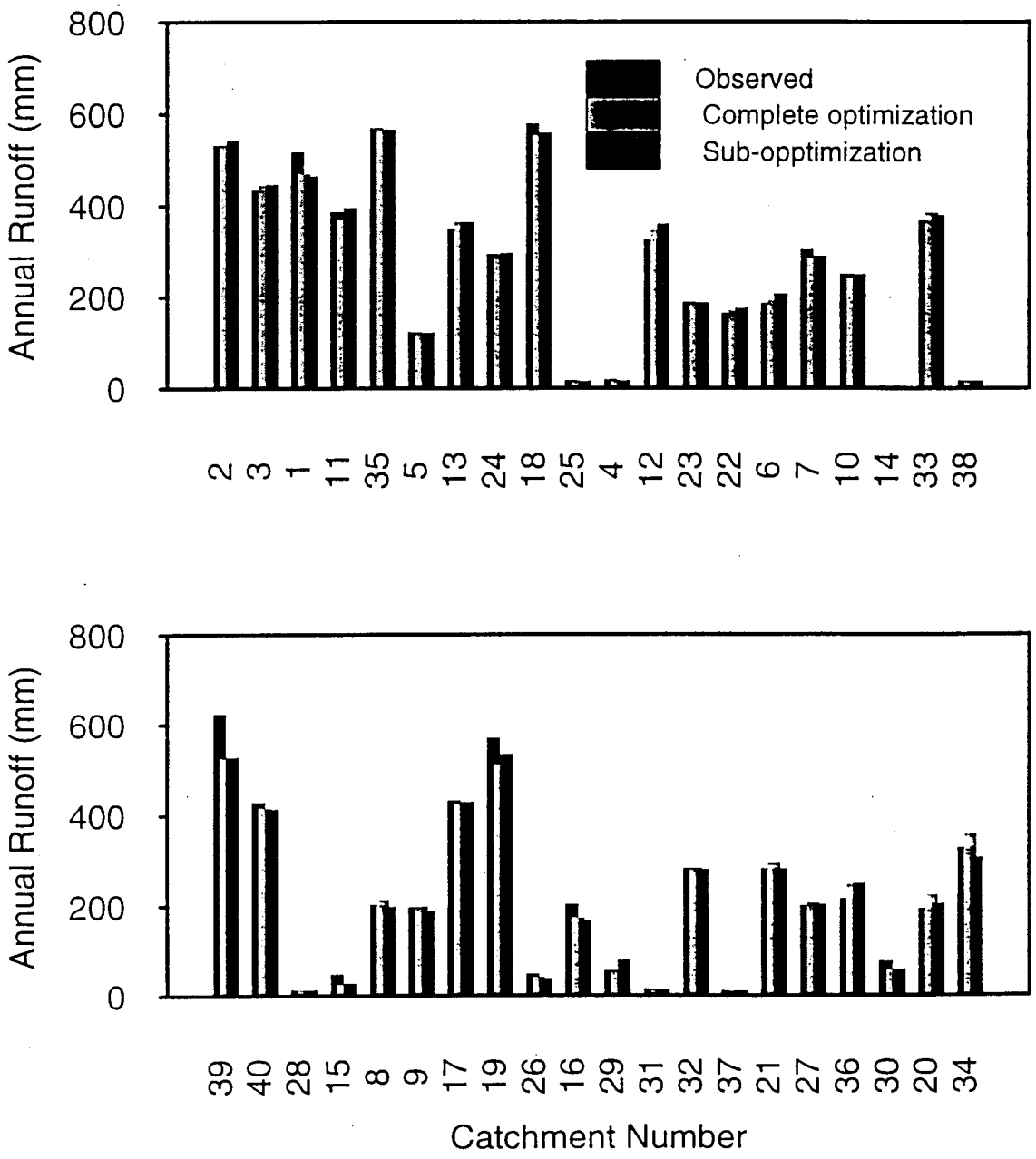

Fig. 3.10 Observed and predicted (using complete optimization) as well as predicted (using sub-optimization) mean annual runoff for all calibration catchments

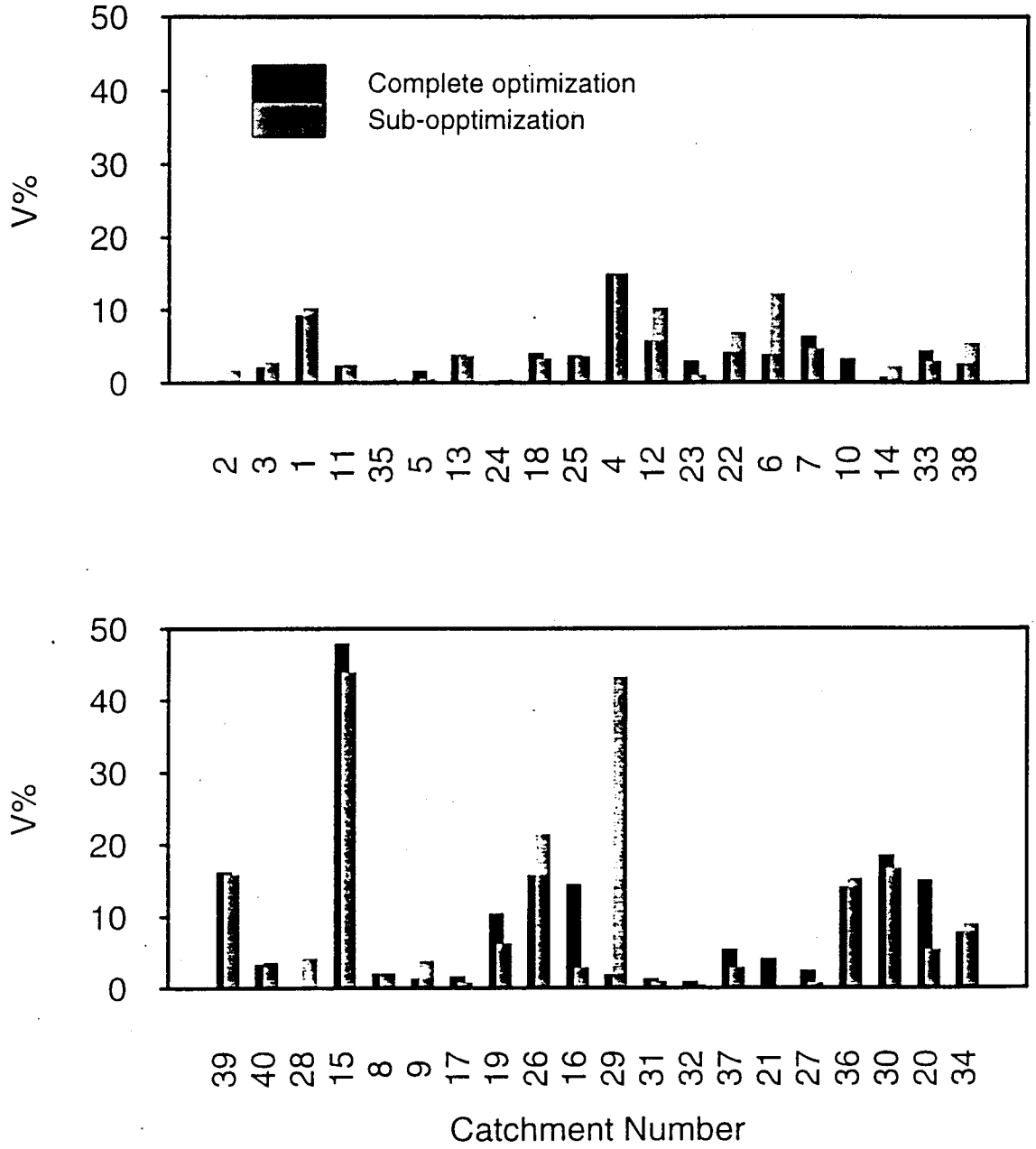

Fig. 3.11 Comparison of yearly relative error of runoff (V%) for all catchments using both complete and sub-optimization methods

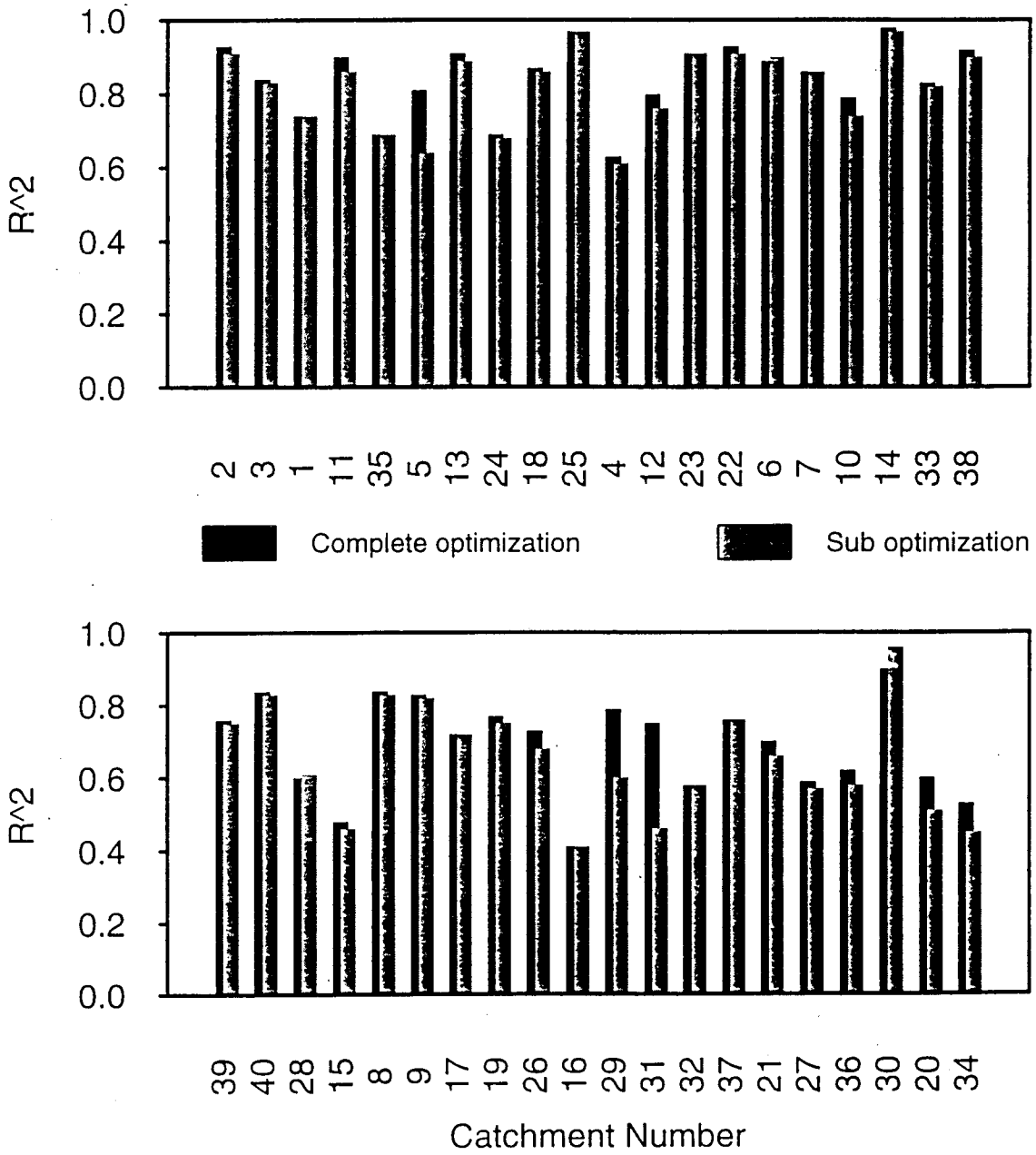

Fig. 3.12 Coefficient of determination (R^2) between the observed and simulated runoff for all catchments using both complete and sub-optimization methods

CHAPTER 4 DEVELOPMENT of REGIONAL EQUATIONS for a HYDROLOGICAL MODEL

In Chapter 3, the modeling framework was described, and the hydrological parameters of the VIC-2L model were estimated for 40 ISA catchments. In this chapter, we present a regression-based regionalization methodology for estimating the parameters of a macroscale land surface hydrology model (VIC-2L).

4.1 Introduction

Global change problems place a new set of demands on hydrologic models. Estimation of parameters for macroscale land surface schemes applicable at the scale of general circulation models used for numerical weather prediction models and climate simulation poses formidable challenges. In large scale applications, the hydrological parameters of land surface schemes, such as the Variable Infiltration Capacity two-layer (VIC-2L) model, have been either fixed globally at "reasonable" values, or they have used "literature values" for the appropriate land cover. Better methods of estimating parameters of macroscale models are obviously needed. The use of regionalization methods, "trained" using local parameters estimates and distributed land surface characteristics data bases, offers one possibility.

In this chapter, we present a methodology for regionalization of the parameters of the VIC-2L land surface hydrologic model for the GCIP Southwest Large Scale Area (LSA-SW) which essentially comprises the Arkansas-Red River basin. The approach is based on direct estimation of the hydrologic parameters of the VIC-2L model using station hydrologic and meteorological data for a set of catchments. The approach has been developed using the SCS State Soil Geographic (STATSGO) data base directly to determine three of the parameters of the VIC-2L model (saturated hydraulic conductivity, pore size distribution

index, and residual moisture content for 40 catchments within the Arkansas-Red River basin, and the remaining seven parameters are determined using the search procedure as discussed in Chapter 3. Regional equations are developed in this chapter to relate the VIC-2L model parameters to measurable physical quantities of the catchments included in distributed data bases such as digital elevation data, and the U. S. Soil Conservation Service STATSGO soils data base.

The approach is tested by application of the regionally estimated parameters to catchments not in the training data set. In Chapter 5, the regional parameter estimates are tested by applying the VIC model to the Arkansas-Red River basin at a one degree spatial scale.

4.2 Review of hydrologic regionalization

Hydrological regionalization is mainly concerned with extending records in space. It has been used for a number of years as a standard tool in hydrology to facilitate the extrapolation of data from sites at which records have been collected to others at which data are unavailable (e.g. Riggs, 1972; Mosley, 1981). Many investigations have attempted to develop regional hydrologic models for the purpose of estimating low-flow statistics at ungaged sites from readily available geomorphic, geologic, climatic and topographic parameters. Examples for low flow regionalization can be found in Tasker (1972), Vogel and Kroll (1990, 1992), and Nathan and McMahon (1990). A study area can be divided into homogeneous regions that are considered to behave in a similar fashion. Records within these regions may be extrapolated with more precision, and therefore regression equations based upon the physical attributes of the catchments may be used to predict hydrologic variables. By identifying such hydrologic regions we may explain or account for part of the variability caused by hydrologic information available in the data set.

On the other hand, regionalization of rainfall-runoff models for prediction at ungaged catchments is more difficult. The approach is typically similar in the way it attempts to develop regression relationships between the optimized

parameters of a conceptual rainfall-runoff model and catchment characteristics. A few regionalization studies have been conducted along this line. An example is the study of Jarboe and Haan (1974) who calibrated a four parameter water yield model for 17 catchments in Kentucky. They obtained errors between observed and predicted streamflow volumes of 6.5 percent for six independent catchments (the error of prediction, in percent, was defined as 100 times the average annual deviation divided by the annual observed runoff). Magette et al. (1976) calibrated the Kentucky Watershed Model on 16 catchments and reported errors between one and 860 percent for six independent catchments. The Sacramento model (Burnash et al., 1973) was also studied, and its parameters were fitted to data from eight subcatchments. The resultant regional parameters were tested and found to result in an error between observed and predicted streamflow volumes ranging from zero to 100 percent (Weeks and Ashkenasy, 1985). Weeks and Boughton (1987) developed prediction equations for a simple 3 parameter Auto-Regressive Moving Average (ARMA) model using 13 catchments; they obtained errors between observed and predicted streamflow volume of around 13 to 30 percent on four independent catchments.

These regionalization studies have various limitations. For example Jarboe and Haan (1974) state that their regionalization is limited by the catchment size (less than 40 mi^2) and by the average soil depth (less than 85 inches). Furthermore, the number of catchments used to develop the regional relationships was relatively small, e.g., 21 catchments in Magette et al. (1976), 23 catchments in Jarboe and Haan and eight catchments in the Weeks and Ashkenasy (1985) studies.

In general, regionalization approaches have been primarily useful for interpolation of parameters. There are two main reasons for the limited success in the regionalization of the rainfall-runoff models. The first is that at the catchment level, the parameters may be poorly determined (e.g. Kuczera, 1983), which makes the task of developing useful regionalization relationships more difficult. The second reason is that some parameters may not be well estimated by regional relationships.

Improving the precision of the estimated parameters must be a priority in order to increase the chance of the success of the regionalization methodology. Furthermore, Weeks and Ashkanasy (1985) indicate that sufficient data should be available to allow confidence in both model parameter estimates, and the regression parameters, although how many data are required for this is not defined. The following section gives background on the regionalization methodologies used to fulfill the second objective of this study (see Section 1.4). Subsequent sections describe the methodology that has been used in developing the regional relationships, and evaluation of the regional relationships for both the calibrated and independent catchments.

4.3 Development of regional parameter equations

Regionalization of the VIC-2L model parameters is the fundamental objective of this study. Attempts to develop regionalization relationships for rainfall-runoff models as a function of physical catchment attributes have met with limited success in the past due to poor determination of parameters at the individual catchment level. The global optimization scheme described in Chapter 3 has been shown to provide good estimates of the parameters of the VIC-2L model for a number of ISA catchments. However, there are no such well defined criteria to judge weather the estimated parameters are good or not. Because the parameters may have been estimated well but the model performance may be poor.

4.3.1 General approach

Multiple regression is the most widely used method of regional parameter estimation in hydrological applications, especially for transferring streamflow characteristics estimated at gaged sites to ungaged sites. A general linear model for multiple regression is:

$$Y = \beta_1 X_1 + \beta_1 X_2 + \ldots\ldots\ldots + \beta_p X_p$$

where Y is a dependent variable (VIC-2L parameters), X_1, X_2,.....X_p are independent variables (catchments attributes) and β_1, β_2.....β_p are unknown parameters. Alternative forms of nonlinear regression model will also be investigated by using different transformations of the dependent and independent variables. The availability of diagnostic software for model building and the ease of variable transformations, make the use of multiple regression an attractive and flexible option.

The unknown coefficients can be determined using the method of least squares (see, for example, Draper and Smith, 1981). This method is well known and need not be described in detail, though the form of the estimates are:

$$\beta = (X^T X)^{-1} X^T Y$$

Our assumption in developing the regional equations is that both the estimated VIC-2L model parameters and the physical characteristics of the catchments are considered error free. Stepwise regression procedures will be used to determine the optimum number of independent variables in the equations. As described in Sections 2.3 and 2.4, different physical catchment characteristics are available for each of the ISAs. The selection of the candidate physical catchment variables was based on the review of the literature related to low flow and rainfall-runoff model regoinalization studies. The variables available for developing the regional equations in this study are listed in Table 4.1. A statistical summary for these variables is shown in Table 4.2.

One of the most difficult problems in regression analysis is the selection of the regression model. This is because in most cases the independent variables are not statistically independent but are correlated. Therefore, one of the first steps that should be done in regression analysis is to compute the correlation matrix of the independent variables. Then the multicolinearity can be checked by comparing

each pair of the independent variables. If the correlation between two independent variables equal to unity, one of these variables must be omitted from the regression model or else the X^TX cannot be inverted. If the correlation is close to unity then the variance of $\hat{\beta}$ may very large. In this work, when pairs of variables were identified with a correlation coefficient over 0.7, the least useful of the two was removed.

Different regression models were investigated using backward elimination for the VIC-2L model parameters to select the optimum number of independent variables to be used. The criteria used to select the appropriate regression model is a high value of R^2 (multiple coefficient of determination) and a maximum number of independent variables of 12 (Hann (1977) suggests that the number of coefficients estimated should not exceed 35 percent of the number of observations). The multiple coefficient of determination (R^2) (in percent) defined as:

$$R^2 = 100(1 - \frac{SSE}{SST})$$

where SSE is the error sum of squares, SST is the total sum of squares.
Hann (1977) criteria for the maximum number of independent variables that allowed to enter the regression equation seems unreasonable. Therefore, a maximum of six variables was permitted to be added to each equation to preserve some degree of freedom within the equation. In addition, only the regression coefficients that were significantly different from zero at the five percent level of significance were included.
Five regression models were investigated:

LIN-Linear model

$$Y = \beta_1 X_1 + \beta_2 X_2 + \ldots$$

SQT1-Square root model (both dependent and independent variables are

transformed)

$$\sqrt{Y} = \beta_0 + \beta_1\sqrt{X}_1 + \beta_2\sqrt{X}_2 + \ldots$$

SQT2-Square root model (independent variables transformed only)

$$Y = \beta_0 + \beta_1\sqrt{X}_1 + \beta_2\sqrt{X_2} + \ldots.$$

LOG1-Logarithmic (base 10) model (both dependent and independent variables are transformed)

$$\log(Y) = \beta_0 + \beta_1 \log(X_1) + \beta_2 \log(X_2) \ldots$$

LOG2-Logarithmic model (independent variables transformed only)

$$Y = \beta_0 + \beta_1\log(X_1) + \beta_2\log(X_2)\ldots$$

As indicated by Draper and Smith (1981) stepwise procedures do not necessarily select the best model, but they usually select an acceptable one. However, in this study an alternative combined procedure was used in an attempt to improve the model selection. This procedure consists of two stages. In the first stage the stepwise regression procedure is run with a given level of acceptance and rejection. When the selection procedure stops, the number of variables in the final selected model (say q) can be determined. In the second stage, all possible subset regressions were performed.

The IMSL routine RBEST also provides the "best K" subsets with one predictor variable, the "best K" subsets with two predictor variables, and so on up to the single equation with all the predictor variables. The best set with q independent variables was selected from the "best q" subsets.

4.3.2 Regional equations

The general approach outlined in Section 4.3.1 was followed for regionalization of the VIC-2L model. Rather than developing regional regressions for all of the parameters, three of the VIC-2L model parameters (the saturated hydraulic conductivity K_s, the pore size distribution index B_p, and the residual soil moisture θ_r) were estimated directly using STATSGO attributes as described in Chapter 3. The remaining 7 parameters (infiltration parameter b_i, three baseflow related parameters, and the maximum soil moisture contents in layers 1 and 2) are determined via the regional relationships. The optimum values for these seven parameters of the VIC-2L model determined in Section 3.6 became the dependent variables and the watershed characteristics described in Sections 2.3 and 2.4 became the independent variables in a stepwise regression analysis. The regional equation for each parameter was selected from the best combinations of the independent variables. Five different regression models were tested for each parameter. The final regional regression equations relating the VIC-2L parameters and watershed characteristics (see Table 4.1 for independent variable definitions) are:

Infiltration parameter (b_i)

$$\sqrt{b_i} = -3.1014 + 6.4409\sqrt{TP} - 2.72485\sqrt{FC} - 0.02367\sqrt{K_s} - 0.02512\sqrt{Hgc} + 0.2736\sqrt{AI}$$

Maximum soil moisture of layer 1 (W_{c1})

$$\log(W_{c1}) = 22.74485 + 1.82587\log(EP) - 0.38307\log(Pr) - 0.36114\log(Hgb) - 0.15719\log(Hgd) - 3.33881\log(Ta) + 1.44203\log(SP1)$$

Maximum soil moisture of layer 2 (W_{c2})

$$\log(W_{c2}) = 25.96178 + 0.34052\log(Pr) - 0.35108\log(K_s) - 5.36303\log(Ta) + 2.29213\log(P1) + 0.68959\log(ST3) - 1.00362\log(SP)$$

Maximum baseflow parameter(D_m)

$$D_m = 2.99669 + 0.17131\ PS - 0.06789\ Hgc - 0.08231\ Hgd - 0.09115\ Ta + 8.21053\ T3$$

Fraction of maximum baseflow (D_s)

$$\log(D_s) = 10.33434 + 0.45269\ \log(Pr) - 0.46446\ \log(K_s) - 3.58841\ \log(NE) + 3.18517\ \log(AI) - 3.09429\ \log(P2)$$

Fraction of maximum soil moisture (W_s)

$$\log(W_s) = 2.30705 - 1.3819\ \log(PS) - 5.56545\ \log(TP) - 0.50963\ \log(Hgb) - 1.4128\ \log(T1) - 1.88042\ \log(ST2) + 2.14062\ \log(ST3)$$

Evaporation factor (Fe)

$$\text{Log(Fe)} = -20.4207 - 0.36497\ \log(EP) + 0.75752\ \log(awc) + 0.25466\ \log(Hgb) + 3.60517\ \log(Ta) + 2.57499\ \log(T1) - 1.45934\ \log(ST2)$$

4.3.3 Analysis of the regional equations

The coefficient of determination R^2, the F-test values of the regression equations, the standard errors of estimate, and the coefficient of variation of the estimates (the standard deviation of the residuals divided by the mean of the dependent variable determined from the regression equation) are given in Table 4.3. R^2 ranges from 45 to 76 percent. For example, forty five percent of the variation in the maximum baseflow parameter (D_m) is explained by the regression equation, and 76 percent of the variation in the scaling factor of the evaporation (fe) is explained by the regression equation.

The hypothesis that the regression does not explain a significant amount

of the variation in VIC-2L model parameters was rejected for all the regression models at probabilities ranging from 0.0001 to 0.0038. All of the estimated regression coefficients were significantly different from zero at the five percent level of significance.

Table 4.4 lists the independent variables (catchment attributes) used in the development of the prediction equations for the VIC-2L parameters as well as the type of regression model. Ten out of the 11 soil attributes are used in the development of the regional equations. The saturated hydraulic conductivity (k_s), the average permeability (Pr), and the hydrologic group B soil (Hgb) were the most important soil attributes. They appear in three equations. Percent sand (PS), total porosity (TP), effective porosity (EP), hydrologic group C soil (Hgc) and hydrologic group D soil (Hgd) are soil attributes of secondary important; each of them appears in two equations. The field capacity (FC) and the available water capacity (Awc) appear in one equation. We believe that the reason why FC and Awc are not among the important soil attributes is that they were taken as ratio of the water depth to the total depth of the soil which in turn resulted in an absence of clear discrimination between catchments. The absence of information about the actual soil depth in the STATSGO data base resulted in making these two attributes (FC and Awc) secondary variables in the regression equations. Percent sand does not appear in any of the equations, apparently because it is correlated with most of the derived soil attributes.

Twelve of the storm characteristics and temperature are utilized in the regional equations. The statistics of the interarrival time seems to be an important explanatory variables in the regional equations. Another important variable is the mean annual temperature, which appeared in three of the equations. The annual intensity (annual rainfall amounts divided by the total number of events (mm/day)) appeared in two of the equations, and it is the most important variable in prediction of the infiltration parameter (b_i). The storm depths in Season 1 and Season 2 appear in one equation, as does the storm depth standard deviation of Season 1 and Season 3.

The seven regional relationships described in Table 4.4 were used to

calculate the parameters for the 34 calibration watersheds. Figure 4.1 compares the estimated (using the regional relationships) and the calibrated (locally optimized) parameters of the VIC-2L model. Generally, there is good agreement between the calculated parameters from the two methods. R^2 ranges from 45 percent for the maximum baseflow parameter D_m to 76 percent for the evaporation scaling factor (fe) (see Table 4.3).

4.4 Calibration catchment predictions

Useful information about the adequacy of the prediction equations and the ability of the model to simulate runoff using regional parameters can be obtained by testing the equations on the calibration catchments. In previous regionalization studies (Jarboe and Haan, 1974; Magette et al., 1976; Weeks and Ashkenasy, 1985; and Weeks and Boughton, 1987) the main criteria used as a measure for the goodness-of-fit of the regional relationships is the percentage error between the observed and simulated streamflow volume. Comparisons of observed and simulated hydrographs based on regional parameters are almost totally absent in the literature. Therefore, the measure of performance reported in Section 3.6.3 will be used here.

The parameters of VIC-2L calculated from the prediction equations were used to simulate runoff for the 34 calibrated catchments. The average annual observed runoff and the average annual simulated runoff were calculated, and the difference between these two quantities (average annual deviation) was computed. The error of prediction (in percent) was defined as 100 times the average annual deviation divided by the annual observed runoff. The RMSE was used to rank the 34 catchments (Figure 4.2). The monthly root mean square error ranges from 27 to 145 percent with an average of 75 percent, which compared quite well with the RMSE obtained using locally sub-optimized parameters. The coefficients of variation of the monthly streamflow also compared well to those of the observed and locally sub-optimized flows (Figure 4.3). Figure 4.4 shows the annual observed and simulated runoff using the regional parameters as well as using the locally optimized parameters. A

comparison was made of the error produced in the simulated average annual runoff on the calibrated catchments using the optimum model parameters and the error produced using the calculated parameters (Figure 4.5). The annual relative error ranges from 1 to 48 percent using the regional parameters, while it ranges from 0.1 to 44 percent using the locally optimized parameters. Eighteen of the calibrated catchments have a relative error less than 5 percent, and only five of them have a relative error greater than 20 percent.

An average of the percentage errors was computed by adding the absolute percentage error for each watershed and dividing by the number of watersheds. The average error of prediction obtained using the optimum parameters on the calibrated catchments was 7.3 percent, and using the calculated parameters was 15.9 percent. The coefficient of determination (R^2) between the observed and simulated flow using the regional relationships ranged from 16 to 90 percent with an average of 68 percent (Figure 4.6). Figure 4.7 shows the observed monthly mean and simulated mean using the regional relationships as well as those using the optimization method.

The model performance using the regional equations on the calibrated catchments was generally quite good. The exceptions are catchments No. 15 (Rayado Creek, NM); No. 16 (Deep Fork, OK); and No. 17 (North Wichita Creek, TX). These catchments have the lowest coefficients of determination among all the 34 catchments in the optimization procedure (R^2 less than 50 percent). This is reflected the poor performance of the regional equations as well. Both Rayado Creek and North Wichita Creek are arid catchments with mean annual runoff of 49 and 16 mm, respectively. Deep Fork is a semi-humid catchment with mean annual runoff of 203 mm; it has a relative error of -12 percent. The model simulations for this catchment tend to be biased upward in winter and downward in the spring and the summer. Grape Creek, CO, an alpine catchment, also had poor model performance using both the locally optimized parameter and the regional parameters. Both sets of parameters tended to underestimate the observed streamflows by 15 and 39 percent, respectively.

4.5 Test catchment predictions

The relationships developed in the previous section were tested using the six independent (i.e. not used for parameter estimation) catchments given in Table 2.1. The VIC-2L model parameters for the six catchments were computed using the regional characteristics in conjunction with regional equations. Streamflow was then simulated for the same calibration period, and the resulting simulated streamflows were compared with observations as well as the simulated flow using the locally estimated parameters for these catchments (see Table 4.5). The model performance was generally best for the humid test catchments and worst for the driest ones. For the Current River, MO; Little River, AR; and White Oak, TX (all which had observed runoff greater than 400 mm), the regional and locally estimated parameters performed almost the same. The regional parameters performed poorly for the arid catchments, Coyote Creek, NM; and Ponil Creek, NM. The mean annual runoff for Coyote Creek is 17.3 mm and for Ponil Creek is 11.2 mm, and both have mean elevation greater than 2500 m. The RMSE and R^2 obtained using the regional equations is very close to those obtained by using the locally estimated parameters as shown in Table 4.5 with exception of these two arid catchments.

Figure 4.8 and Table 4.5 show the long-term mean historical streamflow for all the six test catchments as well as the mean simulated streamflow for the same period based on locally optimized parameters, and simulated streamflow for the same period using parameters based on the regional equations. In the case of the humid catchments, the hydrographs estimated using the regional parameters compared reasonably well with those estimated using the optimized parameters. The regional equations performed much worse than locally optimized parameters for the arid catchments.

4.6 Summary

This chapter summarizes preliminary results of a regionalization methodology developed for estimation of the parameters of the VIC-2L macroscale land surface hydrology model. The approach uses distributed land

surface characteristics from climate data and the SCS STATSGO soils data base. A key component of the methodology is extraction from the STATSGO data base of soil attributes used to explain, via regional regression, parameters estimated locally for 34 gaged catchments within the Arkansas-Red river basin. Regional relationships have been developed for the VIC-2L model using multiple linear regression. The optimum parameters of the VIC-2 model for 34 catchments in the Arkansas-Red River basin were used as dependent variables in regression equations; candidate independent variables include 28 summary measures derived from the soils, and climate data. The parameters calculated from the regional equations were used to simulate runoff for the 34 calibrated catchments. The model performance using the regional equations on the calibrated catchments was generally quite good. These relationships were tested by comparing observed and simulated runoff records from 6 watersheds that are not included in the 34 watersheds used for calibration. The results show that the regional relationships can be satisfactorily applied to other independent catchments.

In the next chapter, the VIC-2L model is applied to the Arkansas-Red River basin at the one degree spatial scale. This implementation uses the regional equations together with STATSGO-based saturated hydraulic conductivity, pore size distribution index, and residual soil moisture.

Table 4.1 Description of catchment variables

Variable		Description	Units
		Soil variables	
1	PS	Percent sand	-----
2	PC	Percent clay	----
3	TP	Total Porosity	m/m
4	EP	Effective Porosity	m/m
5	FC	Field capacity	m/m
6	K_s	Saturated hydraulic conductivity	mm/day
7	Hgb	Hydrologic group B	%
8	Hgc	Hydrologic group C	%
9	Hgd	Hydrologic group D	%
10	awc	Available water capacity	m/m
11	Pr	Average permeability	cm/hr
		Precipitation and Temperature variables	
12	Ta	Average temperature	F
13	Tm	Mean maximum temperature	F
14	P	Mean annual precipitation	mm
15	AI	Mean annual intensity	mm/day
16	NE	Mean annual number of event	days
17	P1	Season 1 mean storm depth	mm
18	P2	Season 2 mean storm depth	mm
19	P3	Season 3 mean storm depth	mm
20	SP1	Season 1 standard deviation of storm depth	mm
21	SP2	Season 2 standard deviation of storm depth	mm
22	SP3	Season 3 standard deviation of storm depth	mm
23	T1	Season 1 interarrival time	days
24	T2	Season 2 interarrival time	days
25	T3	season 3 interarrival time	days
26	ST1	Season 1 standard deviation of interarrival time	days
27	ST2	Season 2 standard deviation of interarrival time	days
28	ST3	Season 3 standard deviation of interarrival time	days

Table 4.2 Summary statistics for all catchment variables

Variables		Minimum	Maximum	Mean	St. dev
1	PS	9.42	34.06	21.15	1.18
2	PC	5.25	61.76	23.26	2.38
3	TP	0.45	0.52	0.48	0.00
4	EP	0.08	0.28	0.19	0.01
5	FC	0.18	0.40	0.29	0.01
6	K_s	4.86	1137.0	116.0	34.6
7	Hgb	4.53	74.6	34.3	3.38
8	Hgc	0.17	63.56	30.89	3.09
9	Hgd	1.31	88.00	27.12	3.94
10	awc	8.13	20.20	14.05	0.60
11	Pr	6.77	218.7	72.6	10.05
12	Ta	93.5	113.7	107.5	0.82
13	Tm	76.0	96.0	90.8	0.86
14	P	312	1267	907	47.0
15	AI	2.54	12.7	10.01	0.43
16	NE	56.0	101.0	81.3	2.31
17	P1	4.44	13.97	10.52	0.42
18	P2	5.33	16.71	12.25	0.46
19	P3	3.66	13.94	9.47	0.51
20	SP1	6.78	17.04	13.82	0.46
21	SP2	6.88	23.72	16.76	0.65
22	SP3	4.09	18.26	12.71	0.71
23	T1	3.28	7.23	4.36	0.18
24	T2	3.75	6.48	4.62	0.12
25	T3	3.85	12.41	6.24	0.40
26	ST1	3.53	9.58	5.07	0.27
27	ST2	4.20	9.55	5.79	0.22
28	ST3	4.28	14.0	7.43	0.49

Table 4.3 Significance of the regional relationships

Parameter	R^2	F	Standard Error	C.V.
b_i	57	7.3	0.13	32.0
W_{c1}	63	7.6	0.25	4.8
W_{c2}	71	10.8	0.24	4.0
D_m	45	4.5	1.23	55.0
D_s	54	6.6	0.54	9.2
W_s	74	14.2	0.27	48.0
fe	76	12.7	0.18	115.7

R^2 (percent of the variation in the VIC-2L parameters which is explained by the regression equation)

F (F-test valuess of the regression equations)

C.V. (coefficient of variation of the estimated parameters)

Table 4.4 Analysis of the Regional Relationships

Independent variables		b_i	W_{c1}	W_{c2}	D_m	D_s	W_s	fe
1	PS				√		√	
3	TP	√					√	
4	EP		√					√
5	FC	√						
6	K_s	√		√		√		
7	Hgb		√				√	√
8	Hgc	√			√			
9	Hgd		√		√			
10	AWC							√
11	Pr		√	√		√		
12	Ta		√	√				√
13	Tm				√			
15	AI	√				√		
16	NE					√		
17	P1			√				
18	P2					√		
20	SP1		√					
22	SP3			√				
23	T1						√	√
25	T3				√			
27	ST2						√	
28	ST3			√			√	√
N		5	6	6	5	5	6	6
Model		SQT1	LOG1	LOG1	LIN	LOG1	LOG1	LOG1

Table 4.5 Regionalization results for 6 independent catchments, showing mean annual runoff (Q); error of prediction (V%); coefficient of determination (R^2); and monthly root mean square error (RMSE).

Catchment	Run	Q (mm)	V%	R^2	RMSE
1 Current R, MO	Observed	569.3			
	Optimized	565.7	0.6	69	0.35
	Regional	556.6	2.2	67	0.37
2 Big Cabin Ck, Ok	Observed	216.4			
	Optimized	249.6	-15.3	58	0.67
	Regional	191.5	11.5	55	0.75
3 Ponil Creek, NM	Observed	11.2			
	Optimized	11.9	-2.9	76	0.60
	Regional	21.7	-92.0	25	
4 Coyote Creek,	Observed	17.3			
	Optimized	16.5	5.5	90	0.60
	Regional	17.3	0.0	5	0.82
5 Little River, AR	Observed	624.6			
	Optimized	528.8	15.9	75	0.56
	Regional	490.7	21.9	75	0.62
6 White Oak Ck, TX	Observed	428.7			
	Optimized	414.2	3.7	83	0.55
	Regional	393.1	8.5	81	0.59

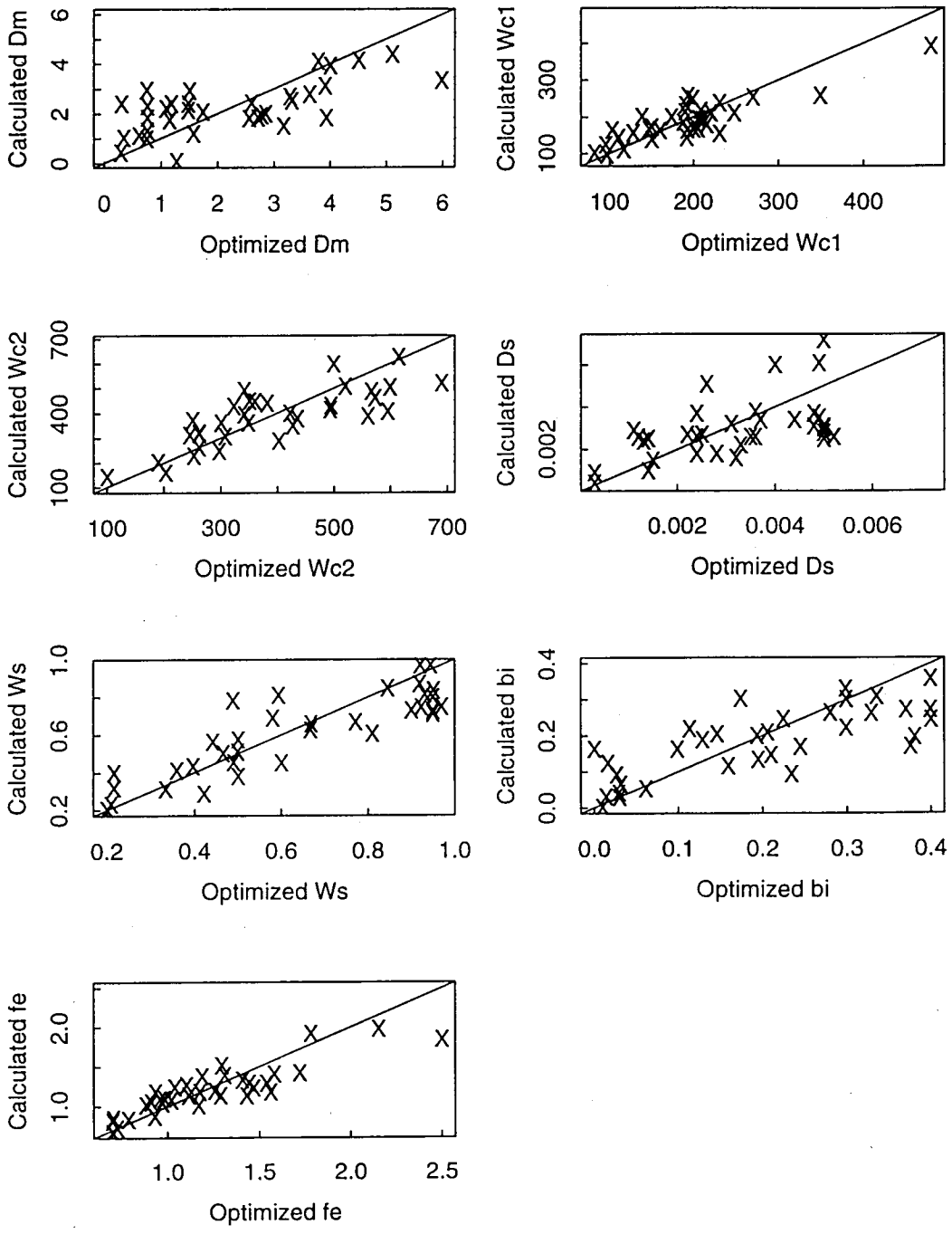

Fig. 4.1 Comparison between locally optimized and calculated regionalized VIC-2L model parameters.

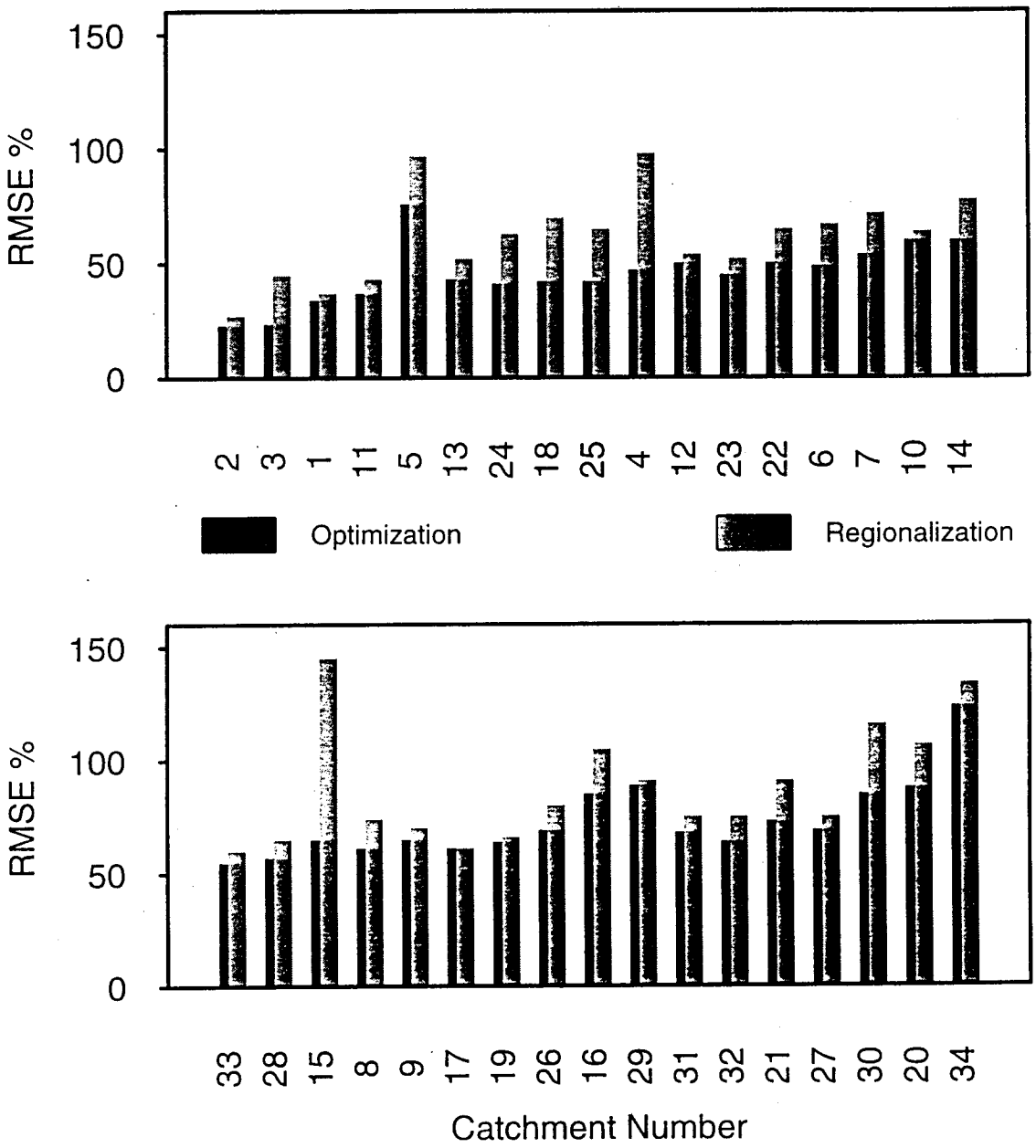

Fig. 4.2 Comparison of monthly root mean square error (RMSE) for all catchments using both locally optimized parameters and regional parameters

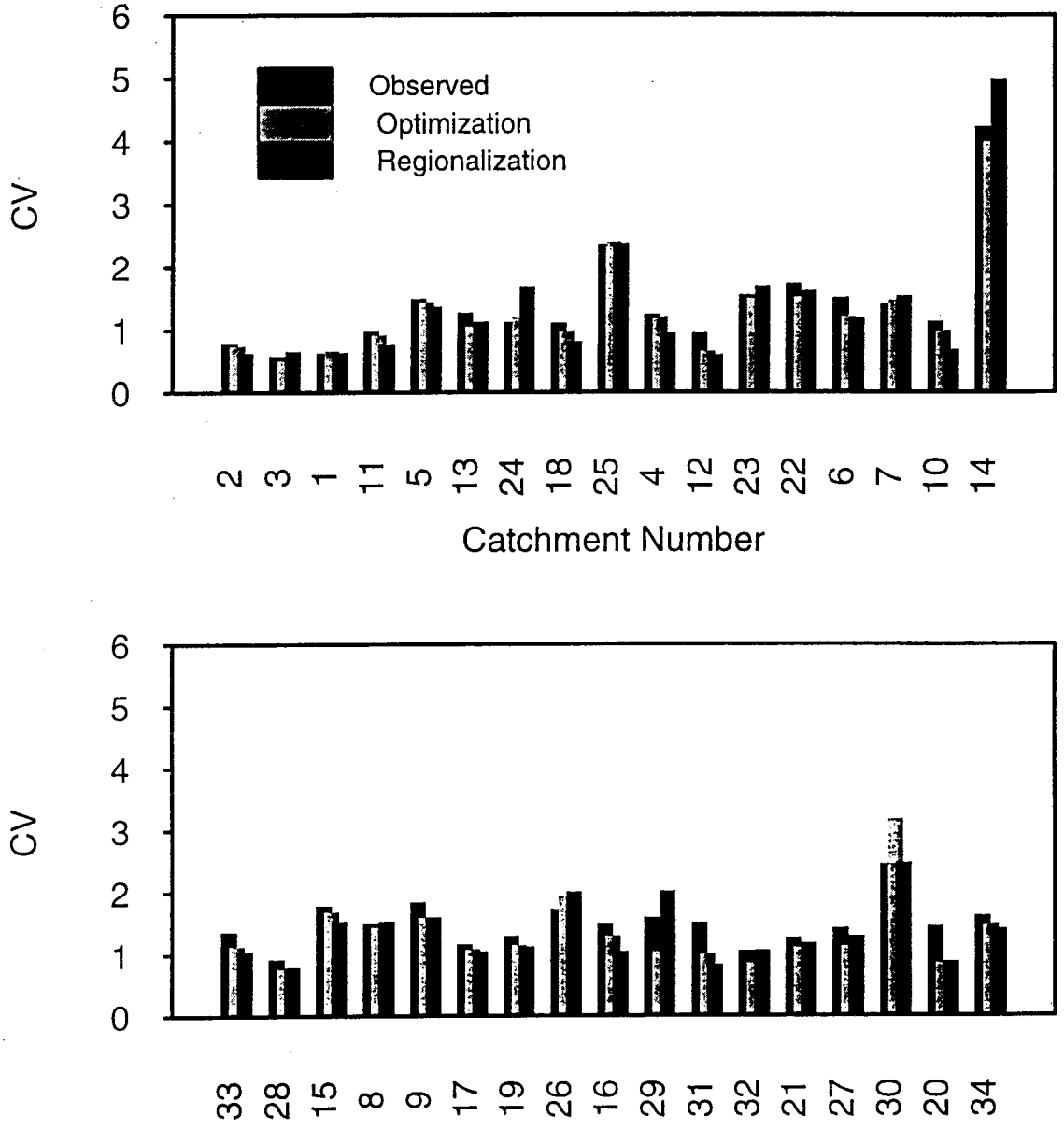

Fig. 4.3 Observed and predicted (using locally optimized parameters) and predicted (using regional parameters) coefficient of variation (CV) of monthly streamflow for all calibration catchments

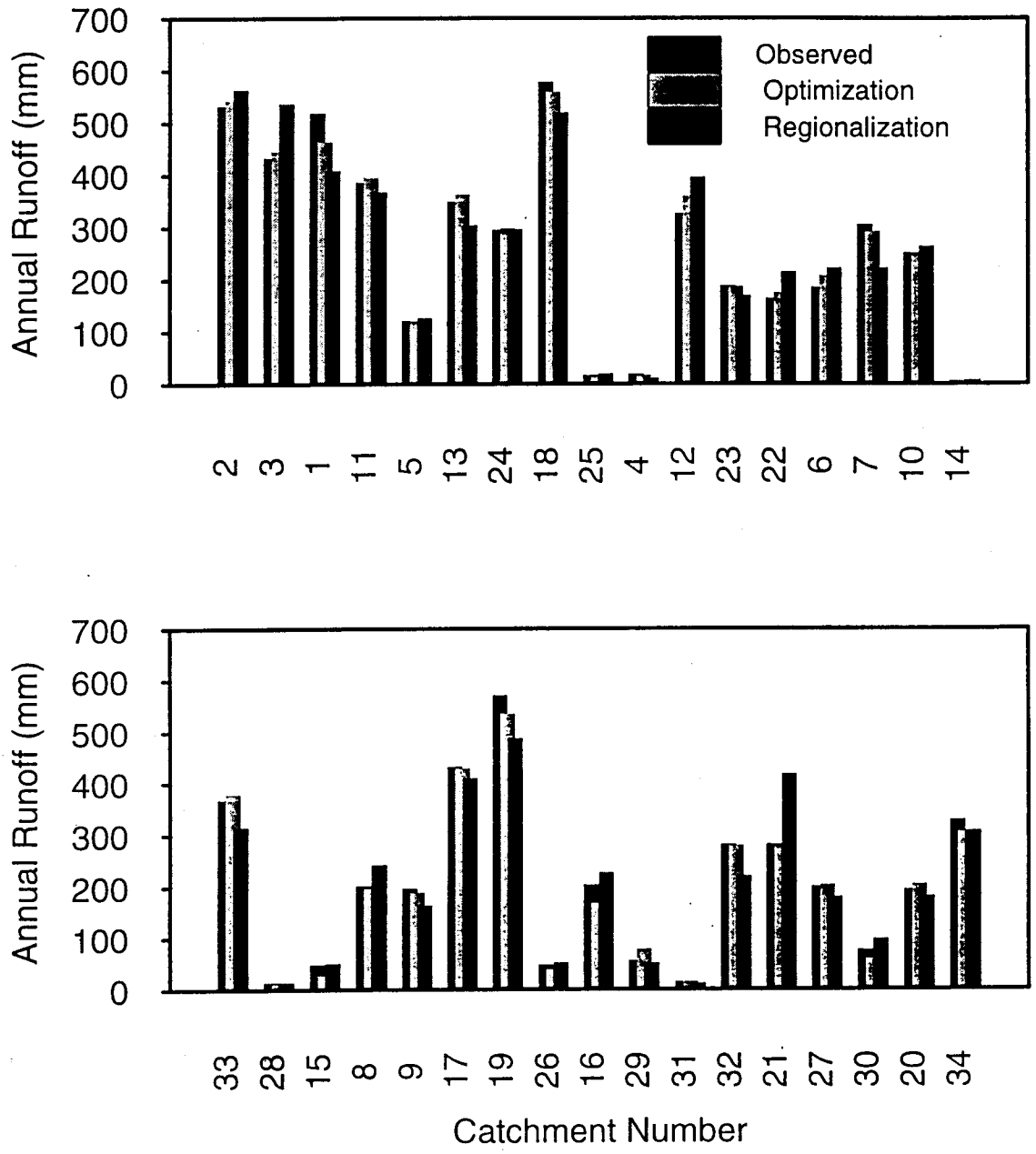

Fig. 4.4 Observed and predicted (using locally optimized parameters) and predicted (using regional parameters) mean annual runoff for all calibration catchments

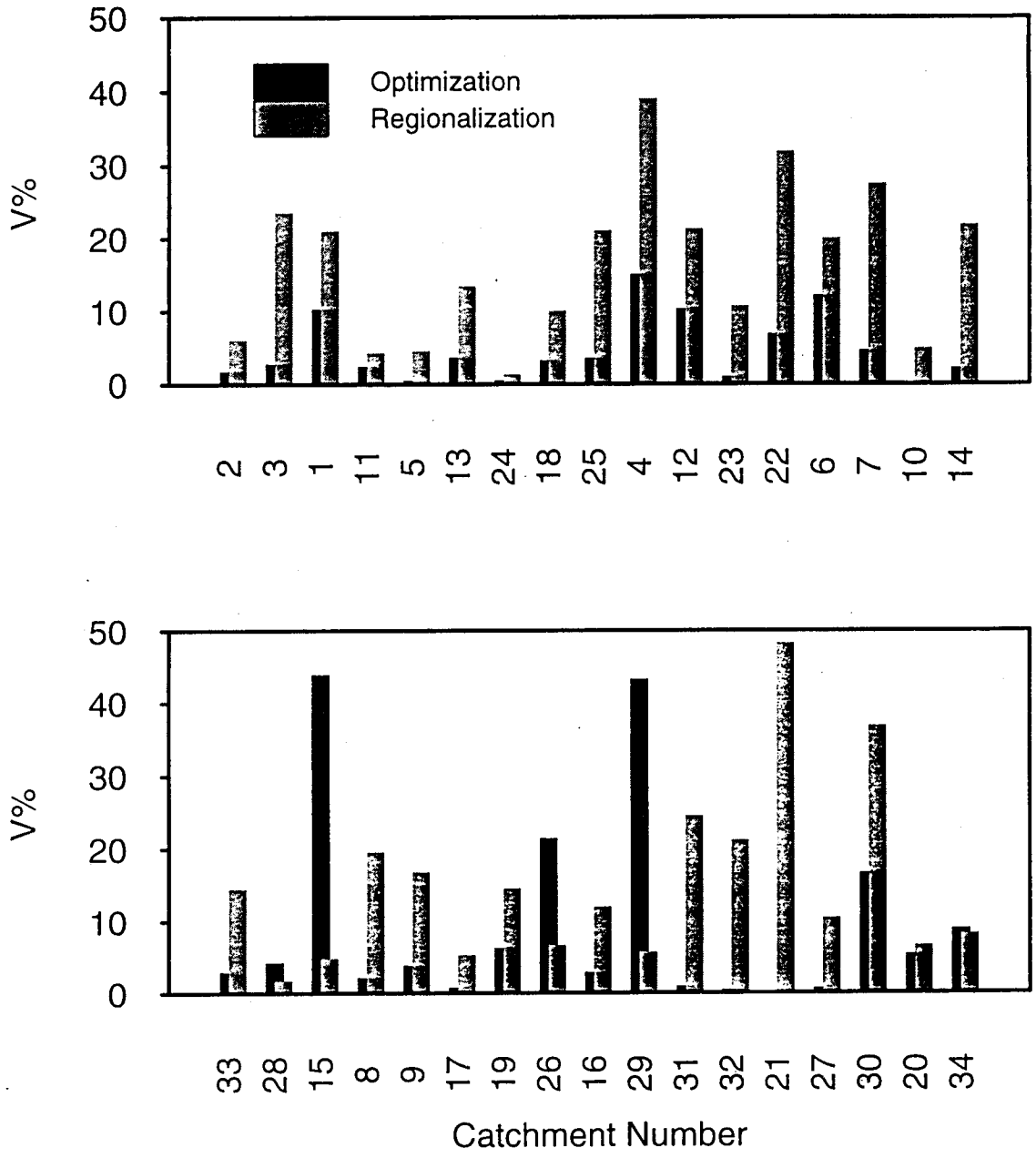

Fig. 4.5 Comparison of yearly relative error of runoff (V%) for all catchments using both locally optimized and regional parameters

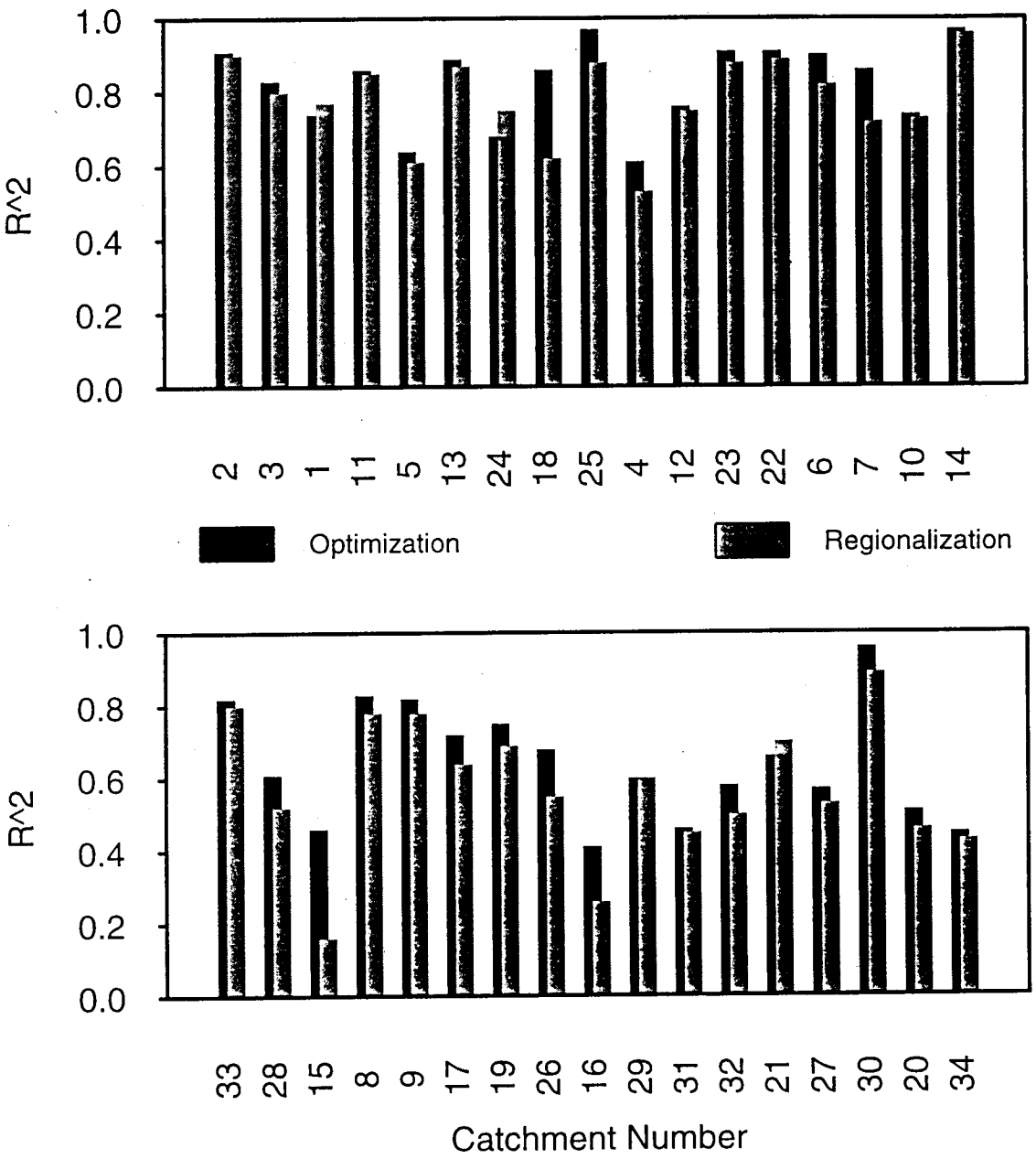

Fig. 4.6 Coefficient of determination (R^2) between the observed and simulated runoff for all catchments using both locally optimized and regional parameters

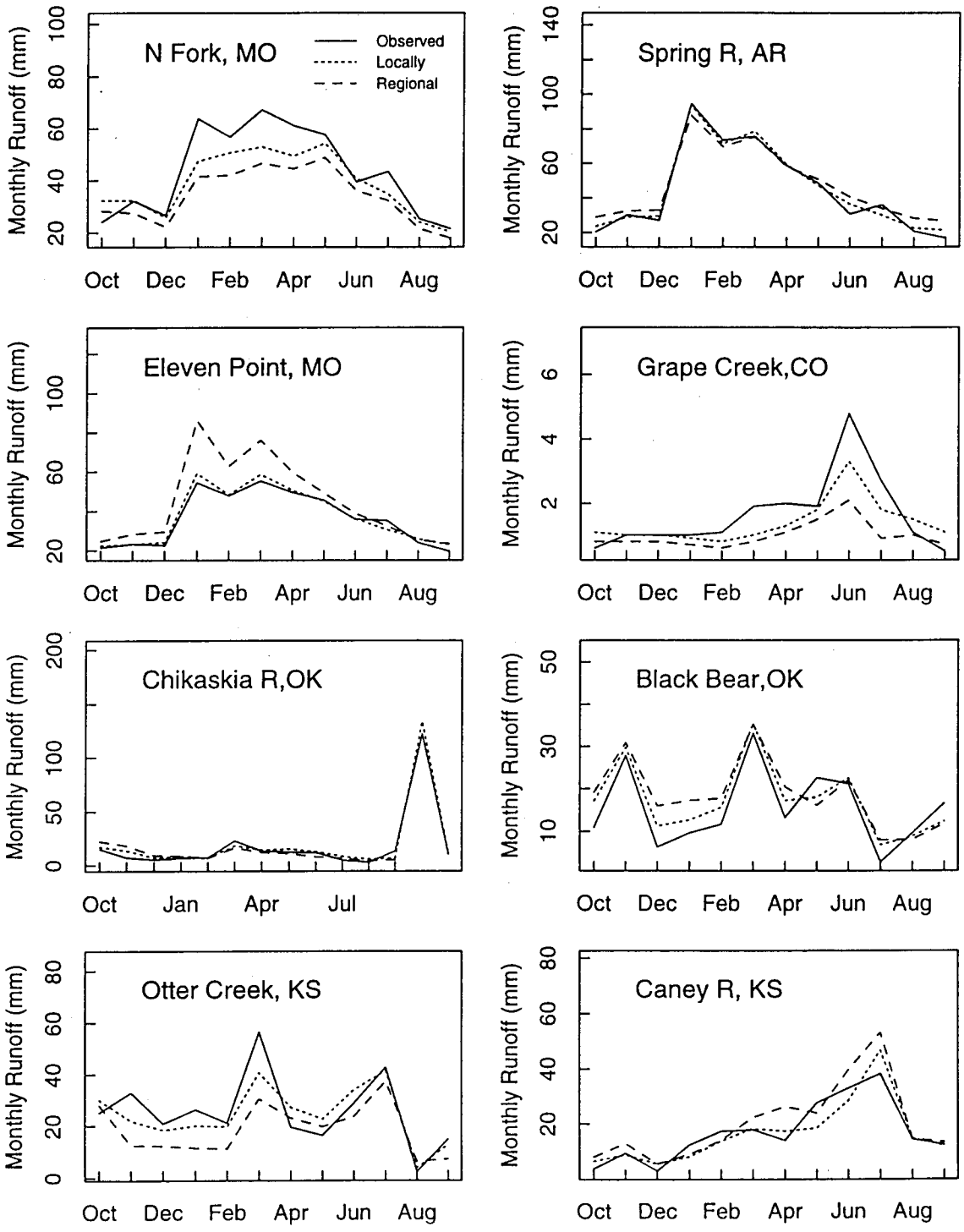

Fig. 4.7 Observed and predicted (using locally optimized parameters) as well as predicted (using regional parameters) mean monthly streamflow for selected calibration catchments.

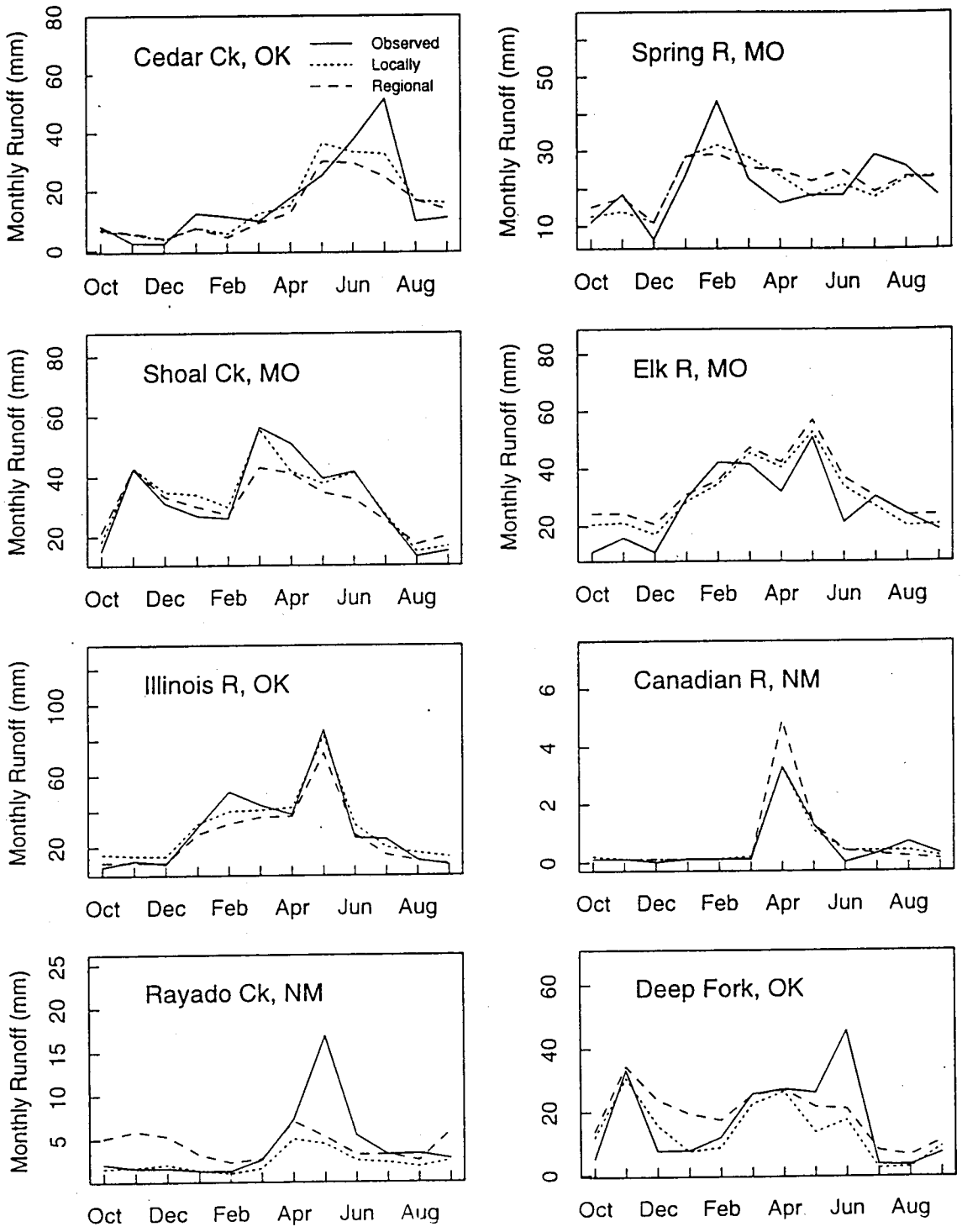

Fig. 4.7 (contd.) Observed and predicted (using locally optimized parameters) as well as predicted (using regional parameters) mean monthly streamflow for selected calibration catchments.

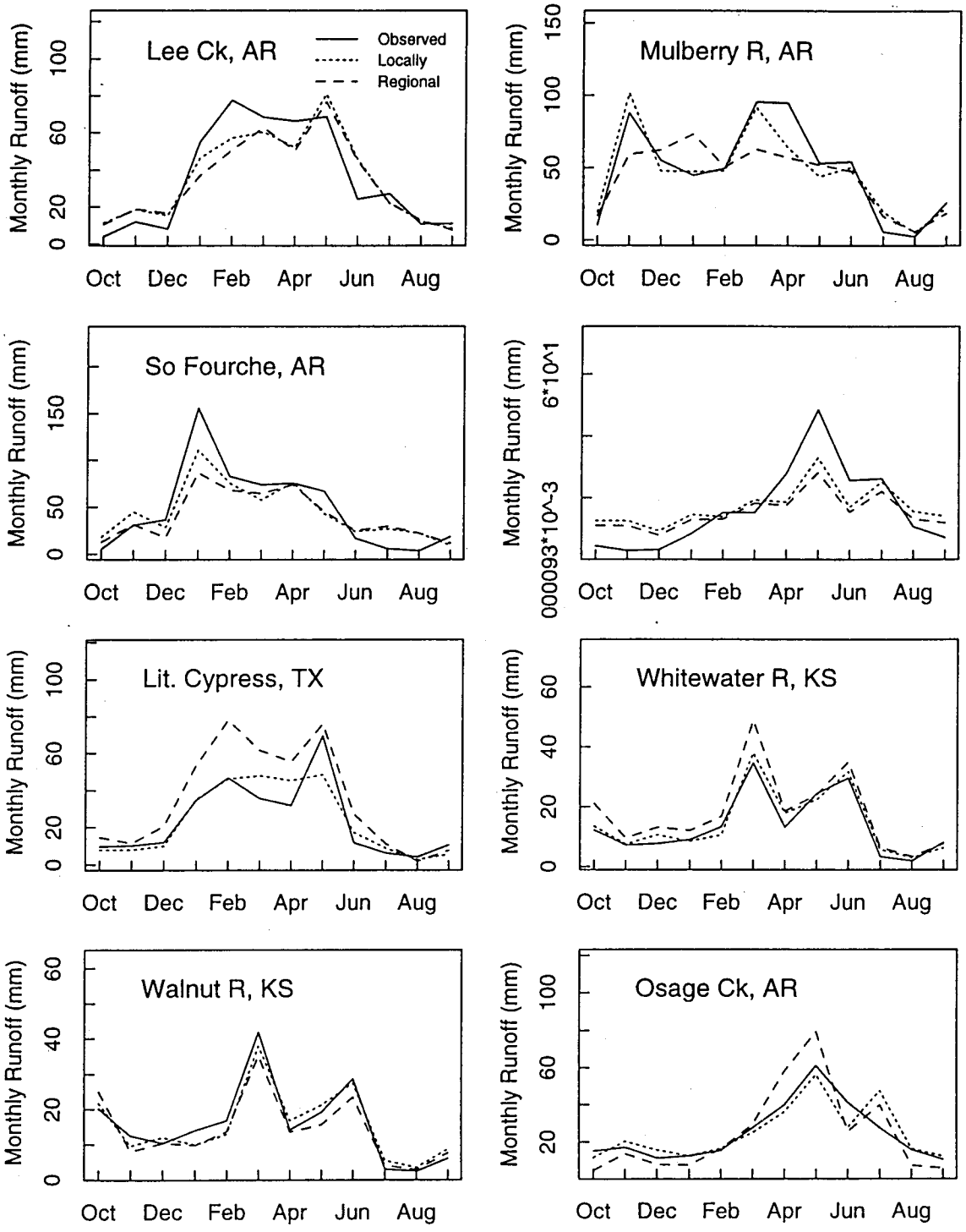

Fig. 4.7 (contd.) Observed and predicted (using locally optimized parameters) as well as predicted (using regional parameters) mean monthly streamflow for selected calibration catchments.

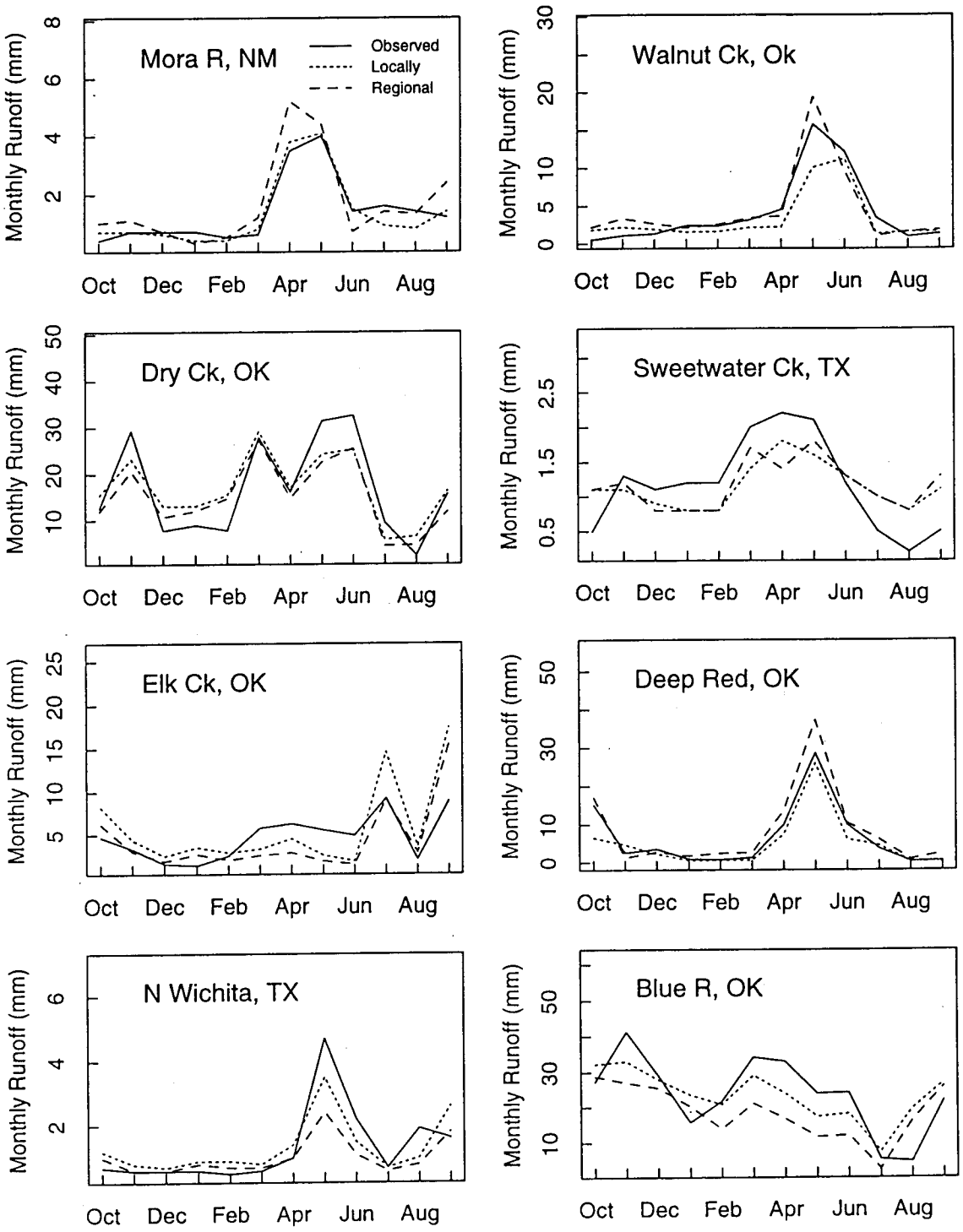

Fig. 4.7 (contd.) Observed and predicted (using locally optimized parameters) as well as predicted (using regional relationships) mean monthly streamflow for selected calibration catchments.

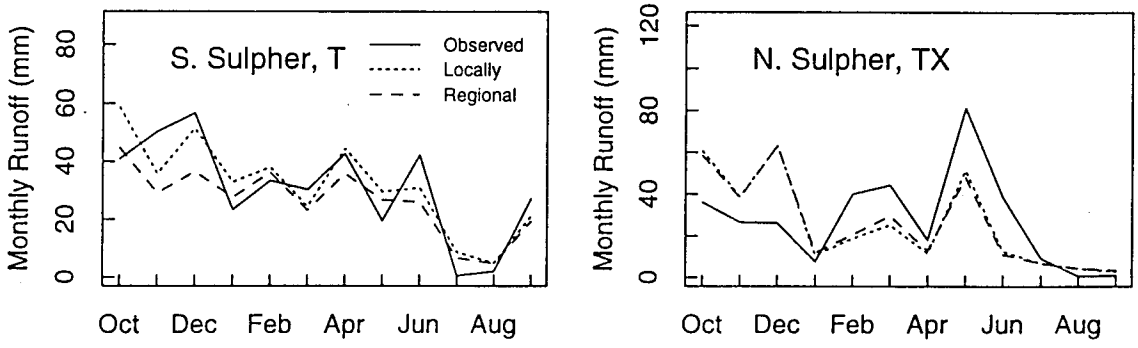

Fig. 4.7 (contd.) Observed and predicted (using locally optimized parameters) as well as predicted (using regional parameters) mean monthly streamflow for selected calibration catchments.

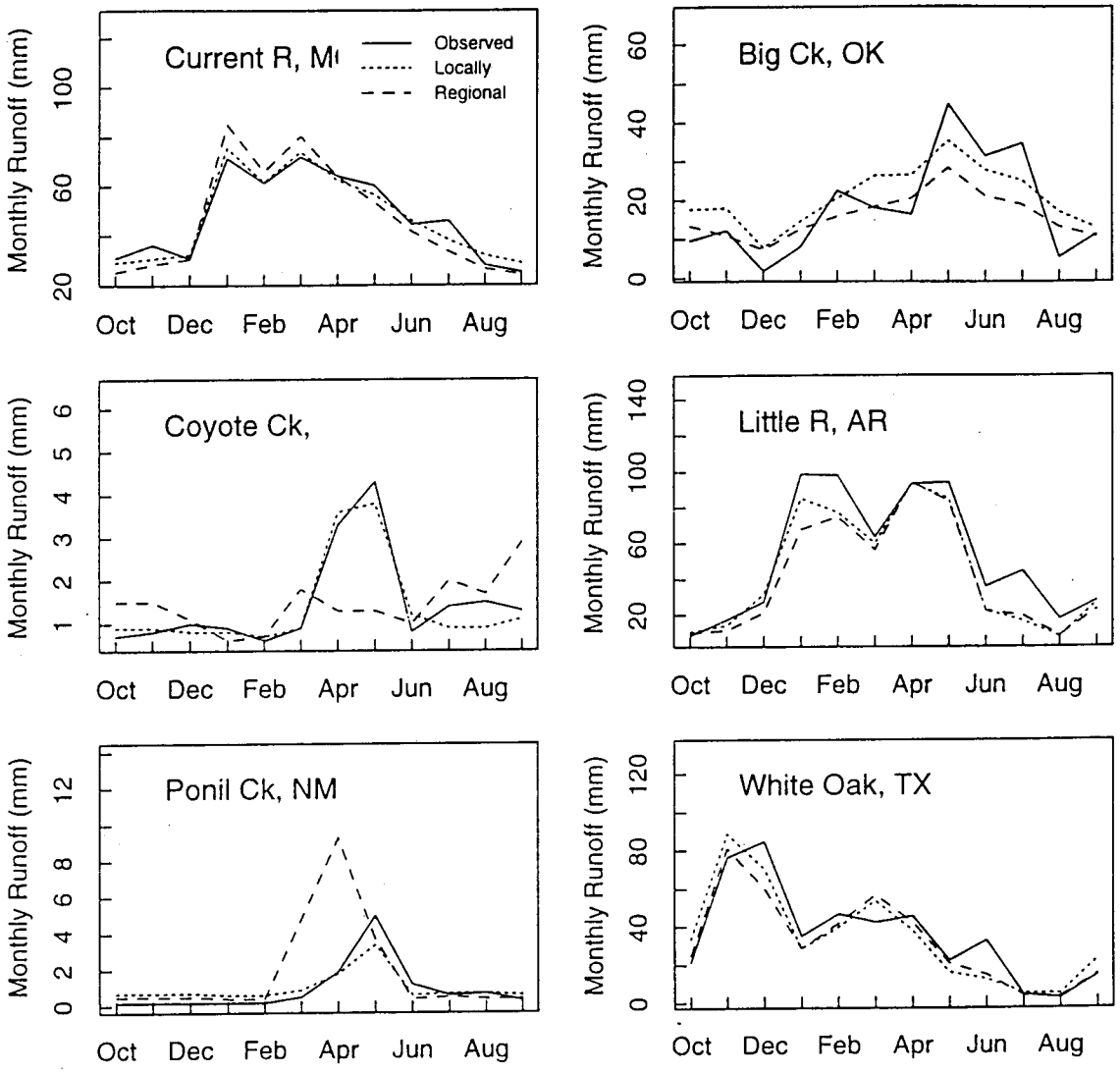

Fig. 4.8 Observed and predicted (using locally optimized parameters) as well as predicted (using regional parameters) mean monthly streamflow for the six test catchments.

CHAPTER 5 APPLICATIONS of GRID BASED VIC-2L MODEL

In Chapter 3 modelling and parameter estimation strategies were described for a land surface hydrological model (VIC-2L) applicable to predict moisture and energy balances for large continental rivers. In Chapter 4 a regional parameter estimation method for the VIC-2L model was developed. In this chapter, three applications of the grid-based VIC-2L model for the Arkansas-Red River basin are described.

5.1 Introduction

Determining the space-time variability of hydrological processes and energy fluxes over a continental scale area is a challenging task. The fluxes of heat and moisture across the land/atmosphere interface may vary over a range of spatial scales due to the inhomogeneity of land surface (WMO, 1992). Land surface inhomogeneities include differences in soil type, vegetation cover, topography, water content, depth of the water depth, precipitation, and land use. In general the heterogeneity of the land surface increases with the horizontal scale of the simulation domain. Typically, one grid cell of mesoscale model represent a domain of 10-100 km^2, while one GCMs grid square usually represents a domain of around 250,000 km^2 (Avissar and Verstraete, 1990). Accordingly, developing and testing macroscale hydrological models appropriate for modeling the water and energy fluxes at the scale of large continental rivers (for example, the GCIP southwest Large Scale Area (LSA) which essentially comprises the Arkansas-Red River basin) are needed. For reliable estimates of these fluxes for the GCIP LSAs, the information gained from the application of the macroscale hydrological model at intermediate scale area (ISA) catchments must be incorporated at the LSA application. An example of such information is the spatial variability of the parameters of macroscale hydrologic models, such as VIC-2L, within the LSA. The regional relationships that relate the hydrological

parameters of the VIC-2L model to land surface attributes are described in Chapter 4. They provide a means for estimating the spatial variability of the VIC-2L parameters within the LSA.

In this chapter we describe three applications of a grid network version of the two-layer Variable Infiltration Capacity (VIC-2L) model applied at one degree resolution. These applications are illustrated for the GCIP southwest LSA. In the first application (Abdulla et al., 1995a) the grid network model is run off-line at a daily time step, forced by precipitation and potential evapotranspiration which is computed using a temperature-based algorithm. By off-line implementation we mean that no attempt was made to account for feedbacks from the land surface to the atmosphere, e.g. by incorporation of the VIC-2L as a land surface scheme in a GCM. The gridded hydrologic parameters of the VIC-2L model are estimated using two methods. The first is the STATSGO based approach described in Chapter 3. The second is linear interpolation of locally optimized parameters for the 40 calibrated ISA catchments (see Chapter 3).

In the second application, the model is also run at a daily time step, but in this case the gridded hydrological parameters are estimated using both the STATSGO based approach and the regional equations developed in Chapter 4. The purpose of this application is to test the performance and the ability of the VIC-2L model to simulate the large scale water balance components using regional parameters (Abdulla and Lettenmaier, 1995).

In the third application (Abdulla et al., 1995b) the VIC-2L model is tested for its ability to simulate large scale sensible and latent heat fluxes in the Arkansas-Red River basin. In this application the full energy balance version of the model is used. The model is run off-line at a three hour time step, forced by gridded station data from NCDC Surface Airways data (including wind speed, relative humidity, temperature, surface pressure and total sky cover) as well as incoming longwave and shortwave radiation estimated using empirical methods. The hydrological parameters are obtained using the regional equations developed in Chapter 4.

5.2 Case Study I: Water balance estimation using interpolated parameters

In this section we describe the application of an approach for gridded parameter estimation of the two-layer Variable Infiltration Capacity (VIC-2L) model of Liang et al. (1994) for the GCIP LSA-SW region (Arkansas-Red River basins). The approach is based on the results of the parameter estimation strategy described in Chapter 3. Seven of the gridded hydrological parameters of the VIC-2L model are linearly interpolated from the locally optimized parameters for the 40 ISA calibration catchments, as described in Section 3.4. The remaining three are estimated directly at the one degree scale using the U.S. Soil Conservation Service State Soil Geographic Data Base (STATSGO). The gridded hydrological parameters (i.e. the interpolated parameters as well as those obtained from STATSGO) are then used in an off-line grid implementation of VIC-2L at a one degree scale for the entire Arkansas-Red River basin.

The three models described in Chapter 3 are linked as shown in Figure 5.1. The approach can be summarized as follows (Figure 5.1): i) the snow accumulation and ablation model is run for each of the four elevation bands in each grid cell. Inputs to the snow model include daily time series of precipitation and temperature as well as the digital elevation data and snow model parameters, the outputs are time series of snow pack outflow and rainfall; ii) the VIC-2L model is run for each grid cell, using the elevation band-averaged snow model output as input as well as the daily potential evapotranspiration and hydrological and vegetation parameters. Outputs of the VIC-2L model are total runoff, evapotranspiration, and soil moisture time series; iii) the runoff from each grid box is then routed from grid cell to grid cell through the entire channel network based on simple distance and travel time assumptions.

The approach is tested by comparison of monthly streamflow predicted by the gridded VIC-2L model routed from box-to-box throughout the entire channel network using a simple uniform velocity (no channel dispersion) routing scheme.

The model predicts streamflow at selected locations where naturalized streamflow (regulation effects removed) for a 38 year period (1948-1986) have been estimated by the Tulsa District of the Department of the Army Corps of Engineers. In addition, the model-generated catchment-total evapotranspiration for the 14 year period October 1972 - November, 1986 is compared with total evapotranspiration derived from an atmospheric moisture budget analysis of the Arkansas-Red basin (Bradley et al., 1995).

5.2.1 Grid parameter estimation

The VIC-2L model was developed for application over large areas, such as the domain of mesoscale numerical weather prediction models. For this purpose, the Arkansas-Red River basin was divided into 61 cells of size one degree latitude by one degree longitude (see Figure 2.3). For each grid cell, two kinds of parameters are needed. The first type, which are related to vegetation and its interaction with the atmosphere, include minimum canopy resistance, leaf area index LAI[n,m] (n=1, 2,....., N; m=1, 2,....., 12) for each surface cover class, the zero plane displacement height, roughness length, and the relative fraction of roots in each of the two soil layers. Figure 2.6 shows the distribution of the six major vegetation classes for the Arkansas-Red River basin. Each of the vegetation covers is associated with a set of these parameters (see Table 5.1). The leaf area index is calculated for each month and each vegetation class as described in Section 2.5; the other vegetation parameters are determined using literature for each of the vegetation cover class. For example, the zero plane displacement height (d_0) and the roughness length (z_0) are important parameters in calculation of the aerodynamic resistance r_w. They are estimated based on canopy height (h) as follows (Calder, 1993):

$$d_0 = 0.63\ h \tag{5.1}$$

$$z_0 = 0.1\ h \tag{5.2}$$

The relative fraction of roots in each of the two soil layers are taken from

literature values for each vegetation cover. Minimum canopy resistance r_c is taken as 100 s/m as used by Liang et al. (1994). Table 5.1 lists these parameters for each of the vegetation classes. For more details as to the specific function of each of these parameters, the reader is referred to Liang et al. (1994).

The second type of the VIC-2L model parameters are hydrological, including the saturated hydraulic conductivity, the pore size distribution index, the infiltration shape parameter, the three baseflow related parameters, and the maximum soil moisture contents in layer 1 and 2 (see Table 3.1). As shown in Section 3.3.4 and Figure 3.7, the simulated hydrographs using STATSGO parameters in conjunction with the optimization method compare favorably with the hydrographs based on complete optimization. This result was encouraging, and motivated us to use the STATSGO-based approach because it avoids the problem of transferring parameters from the ISAs to the LSA for some of the parameters. Accordingly, two of the hydrological parameters (see Figures 3.4 and 3.5) can be determined directly using STATSGO data such as (the saturated hydraulic conductivity and pore size distribution index). From the three STATSGO based parameters, only the saturated hydraulic conductivity and the pore size distribution index were used directly in the model. The Brooks-Corey residual water content, which is given as a fraction of water volume to soil volume, was not directly used in the model, because the information about the actual soil thickness is not available in STATSGO. Instead it was taken as a fraction (in this case 0.3) of the maximum soil moisture for each layer.

To determine the remaining hydrological parameters for each grid box, the estimated hydrological parameters from the ISAs, estimated as described in Section 3.3.4 for the 40 calibration catchments, were interpolated spatially. We found that in some cases, in particular near the edge of the LSA where the ISA estimates had to be extrapolated, rather than interpolated, unrealistic values resulted which were reset to the average value estimated from the closest catchments. Figures 5.2a-d shows the spatial distributions of four of the interpolated parameters: maximum soil moisture of layer 1 and layer 2, maximum base flow, and the infiltration parameter. For more details as to the

specific function of each of these parameters, the reader is referred to Liang et al. (1994).

5.2.2 Implementation of grid-based VIC-2L model

Using parameters estimated for each grid cell as described in the previous section, the VIC-2L model was implemented off-line (see Figure 5.1). In its usual configuration, VIC-2L performs the complete surface energy and water balances, in which case the model is driven by downward solar and longwave radiation, in addition to surface meteorological variables. In the off-line version, the surface energy balance is not performed, and the driving variables are precipitation, temperature, and potential evapotranspiration. When it is applied in fully coupled (water and energy balance) mode, VIC-2L uses the energy-based snow accumulation and ablation model of Wigmosta et al. (1994). However, in the off-line version, absent the driving variables required for the energy-based model, we instead used the temperature index snow accumulation and ablation model of Anderson (1973), which is a part of the National Weather Service River Forecast system. The only data requirements of Anderson's model are precipitation, surface air temperature, and elevation.

To account for orographic effects on precipitation, and elevation dependence of temperature, each grid cell was divided into four elevation bands, using 30 arc second digital elevation data. Daily time series of precipitation, and maximum and minimum temperature from the climatological stations in each grid cell (usually two) were used. The precipitation time series for each station were normalized by their annual means, and grid cell averages of the normalized precipitation series were constructed. The average normalized time series were then rescaled by the mean annual areal precipitation for the grid cell (in this study it is taken as the annual mean of the two precipitation stations). The temperature for each station was lapsed to the mean elevation of the grid cell, using a lapse rate of 6 $^{\circ}$C/km, which is approximately the psuedo-adiabatic lapse rate at the mean elevation of LSA-SW . The form of precipitation is determined based on the mean temperature of each elevation band. Where there were two stations in the grid cell, the temperatures, lapsed to the grid cell mean

elevation, were averaged. The grid cell average temperature, corrected for elevation, was then lapsed to the elevation of each of the four bands.

Since the data required to compute PET using an energy-based formulation such as Penman-Monteith were not available for each grid, we used Hamon's method (Hamon et al, 1954; Hamon, 1961) which requires only daily air temperature and latitude (Eq. 3.17). The potential evaporation predicted by Hamon's method were adjusted by a scaling factor. This scaling factor was based on comparison of the annual E_p estimated by the Hamon's equation with the annual E_p estimated by four other empirical methods. These methods are: Blaney-Criddle as modified by the FAO (Doorenbos and Pruitt, 1977), Hargreaves (Hargreaves et al., 1985), radiation (Doorenbos and Pruitt, 1977), and Penman as modified by the FAO (Doorenbos and Pruitt, 1977). Four Surface Airways stations where climatological data required by the four methods are collected, were selected to represent the different climates within the Arkansas-Red River basin. The scaling factor for each station was taken as the ratio of the average annual Ep estimated from each method to the annual Ep estimated using Hamon equation. Then the scaling factor for each station was taken as the average of the scaling factor from the four methods. The factors ranged from 1.25 for the humid area to 2.0 for the arid area.

The output of the snow accumulation and ablation model is rain plus melt (precipitation on bare ground plus snowmelt) for each elevation band at 6 hour time steps. The rain plus melt series were aggregated to a daily time step and averaged over the four elevation bands to provide the input to the VIC-2L model.

The unit hydrograph approach of Wetzel (1994) and Mas (1995) was used to account for lagging and dispersion of the VIC-2L model output in the channel network. The method applies one unit hydrograph to VIC-2L output for a grid cell, and another to streamflow entering the grid cell from adjacent cells. For simplicity, a triangular unit hydrograph was used for flow originating within the grid cell, and a simple lag (based on effective channel velocity and channel length) was used for flow crossing a cell.

5.2.3 Results

5.2.3.1 Streamflow evaluation

The grid-based model for LSA-SW was run for the period October, 1948 to September, 1987 using the estimated parameters as described in Section 5.2.1. The unit hydrograph values used are given in Table 5.2. These values are the same as those used in the Missouri River simulations performed by Wetzel (1994). For routing flow across a grid cell, we assumed an effective velocity of 1 m/sec (assumed to be constant in space and time), which is the lower value in the velocity range suggested by Sausen (1994). For purposes of computing the lag time, the channel lengths were computed based on the straight line distance from the center of one block to that of the next dependent on the configuration of the flow network defined in Figure 2.3. The flow velocities do not represent actual channel velocities (which tend to be lower), because the actual channel lengths are longer than the straight line distances, typically by a factor equal to the average sinuosity (> 1).

The streamflow volumes resulting from the routing model were accumulated to monthly totals. Although the naturalized streamflow data used for validation purposes are available at a daily time step, the data at this time step are problematic due to inherent assumptions about travel times that must be made in the streamflow naturalization process. Monthly averaging reduces many of these problems. It also has the effect that errors in the VIC-2L simulations due to assumptions about channel distances and travel times are minimized.

Figures 5.3 and 5.4 show the observed and the simulated mean monthly streamflow, the monthly streamflow time series, and the coefficient of variation of the monthly streamflows for the furthest downstream locations in the Arkansas and Red River basins, respectively. Table 5.3 provides similar information for the other locations shown in Figure 2.3. Given the relatively unsophisticated method used to obtain the hydrologic model parameters, the model performs well. A general characteristic of the simulated hydrographs is that they tend to underestimate the peak seasonal flow. Also, the model

underestimate the mean monthly flow for February through May, and overestimate it for August through November. Although the peak is slightly underpredicted, mean annual volume is well simulated as shown in Table 2.3 for 10 gauging stations (6 of them for Arkansas River and the remaining for the Red River). Generally, the simulated annual flow is greater than the observed annual flow for 8 of these stations. At the mouth of the Arkansas River (Little Rock) the relative error is 7.3 percent and the mouth of the Red River (Shreveport) the relative error is -12 percent.

5.2.3.2 Regional evapotranspiration evaluation

Figure 5.5 shows the spatial distribution of the mean of 38 years of evaporation and runoff for the Winter (October to March) and the Summer (April to September) for LSA-SW using the grid-based model (VIC-2L). In both seasons the runoff and evaporation increases from West to East, following the mean precipitation gradient. As shown in Table 5.4, at the scale of the Arkansas-Red River basins, the evaporation for the summer is approximately twice that for the winter, while the runoff for the two seasons is approximately the same.

Figure 5.6 shows the associated spatial distribution of the evaporation and runoff ratios for both seasons. The runoff ratio (runoff/precipitation) increases in the West-to-East direction for both seasons. The evaporation ratio (evaporation/precipitation) for the winter is lowest in the Eastern part of the region, while the summer is highest in Eastern part of the region. The average evaporation ratio for the Arkansas-Red basin is approximately 0.70 in the winter and just under 1.0 for the summer. Typically this ratio tends to be about four times the winter runoff ratio and eight times the summer runoff ratio.

Figure 5.7 shows the annual mean geographic distribution of the processes involved in the water balance analysis using the VIC-2L model. Precipitation (upper panel) is characterized by an increasing west to east gradient. The driest region is the western part where the annual precipitation is less than 1 mm/day. Modeled evaporation (middle panel) is fairly consistent with the precipitation; about 85 percent of the annual precipitation is evaporated. Modeled annual

runoff (lower panel) is also affected by large east-west gradients of the precipitation and the evaporation. Most of the generated runoff is from the eastern region. The largest amount occurs in the western part of the region.

Figure 5.8 shows the annual runoff and annual evaporation ratios. The runoff ratio increases in general from west to east. On the other hand the evaporation ratio is highest in the western part and lowest in the eastern part of the region.

Figure 5.9 shows the monthly hydrologic cycle budget for the Arkansas-Red River basin. The upper panel shows the mean monthly value for each of the water balance components. The dominant component in the water balance is precipitation, which is slightly larger during the summer than the winter. The highest values are in May (104 mm) followed by June (86 mm). The lowest three months are December (34 mm), January (26 mm), and February (35 mm). The evaporation is highest during the summer, and slightly exceeds precipitation in June and July. This is possible because of the moisture that was stored in the plant root zone of the soil during the preceding months of the year. Runoff is the smallest component of the water cycle. The highest values are for May (13 mm), April (12.6 mm), March (11.2 mm), and June (11 mm). The lowest runoff is in August (4 mm). The lower panel of Figure 5.9 shows the coefficient of variation of the monthly water balance components. The runoff tends to be more variable than precipitation and the evapotranspiration (ET); the variability of ET in turn is less than that of precipitation.

The VIC-2L model-generated catchment-total ET from October 1972, through September 1986, was compared with total ET derived from an atmospheric moisture budget of the Arkansas-Red basin by J. A. Smith (Princeton University). The atmospheric water budget was estimated (see Abdulla et al., 1995) using the following equations:

$$\frac{\partial W}{\partial t} + \nabla \cdot \mathbf{Q} = E - P \tag{5.3}$$

$$\mathbf{Q} = \int_{300\text{mb}}^{p_s} q\mathbf{V}\frac{dp}{g} \tag{5.4}$$

where W is precipitable water (liquid equivalent of water vapor in the atmospheric column), $\nabla \cdot \mathbf{Q}$ is the water vapor flux divergence, E is evapotranspiration, $\mathbf{V}$ is the horizontal wind velocity, p_S is the surface atmospheric pressure, g is the gravitational acceleration, and P is precipitation. Radiosonde data were analyzed by J.A. Smith and his colleagues to compute the storage change within the atmospheric column and water vapor convergence terms. Figure 5.10 shows the location of the atmospheric sounding stations and the footprint of the atmospheric column used in the analysis. The point radiosonde data were interpolated onto 1 degree grids within the atmospheric column, and used to compute the storage change within the atmospheric column and water vapor convergence terms on a daily time step. These were then aggregated to the monthly time step for the monthly water budget. Details of the method used in the water budget computations are provided in Bradley et al. (1995).

Monthly precipitation for the basin was obtained by accumulating the daily precipitation (see Section 5.2.2) used in the hydrological model simulations. Monthly evapotranspiration was then computed as a residual in the atmospheric water budget. Figure 5.11 shows the monthly average vapor convergence term from the 16 years of analysis. There appears to be a well defined seasonal cycle, except for April which is much smaller than either March or May. April tended to have daily values with rather high convergence or divergence and a small net convergence as shown in the figure. The storage change terms are typically an order of magnitude smaller than the convergence terms. There is, however, a systematic seasonal progression in the storage change terms that if neglected leads to minor biases in the seasonal cycle of the water budget.

Figure 5.12a shows the monthly times series for the ET estimates for the hydrologic model and the atmospheric budget. Generally, the January ET values from the atmospheric budget tend to be lower than those of the VIC-2L model, and sometimes the atmospheric budget ET values are negative. In the

case of the VIC-2L model the ET is always greater than zero. Figure 5.12b shows the mean monthly ET, spatially integrated over the entire Arkansas-Red basin. The mean monthly estimates agree quite closely from late winter to mid-summer. However, the VIC-2L model estimates less evaporation in the Fall and more in mid-winter, than the atmospheric budget. Figure 5.12c shows the coefficient of variation of the monthly ET. The VIC-2L model estimates of the coefficient of variation are lower than those derived from the atmospheric budget, especially in winter.

Table 5.4 also summarizes the statistics of the seasonal and annual spatially averaged ET and runoff for the atmospheric budget along with the hydrological model. The mean seasonal estimates agree very closely; to within 5 percent in the winter and less than 1 percent for summer. However, the atmospheric model estimates of the coefficient of variation are greater than those of the VIC-2L model for both seasons. On an annual basis, the results from both models are extremely close; the estimated total annual ET from the atmospheric model is 619 mm and for the VIC-2L model it is 614 mm. These results indicate that at the scale of the Arkansas-Red River basin, the atmospheric budget and land surface hydrologic models provide comparable estimates of regional ET.

5.3 Case Study II: Water balance estimation using regional parameters

In this section, the regional parameter relationships developed in Chapter 4 are used in the validation of the VIC-2L model as well as to test its ability to simulate the water balance components. The only difference between this section and Section 5.2 is that the model is driven by the regional parameters determined by using the explanatory variables for each grid box and the regional relationships developed in Chapter 4, while in Section 5.2 we used the interpolated parameters. Nothing else was changed in the modelling strategy, including the vegetation parameters, which are the ones given in Table 5.1.

5.3.1 Grid cell regional parameters

The regional parameter estimation methodology developed in Chapter 4 for ISAs was used to determine the spatial distribution of the VIC-2L model parameters for each grid box in the Arkansas-Red River basin (Figure 2.3). For this purpose the soil attributes were aggregated using the procedure described in Section 2.3. Climatological data (i.e. storm characteristics) were estimated from the climatological stations in the grid cell. Figures 5.13a-d shows the spatial distribution for some selected parameters of the VIC-2L model. Figures 5.13a and 5.13b show the spatial distribution of the maximum soil moisture of layer 1 (W_{c1}) and layer 2 (W_{c2}), respectively. W_{c1} ranges from 85 to 385 mm with a mean value of 185 mm. On the other hand W_{c2} ranges from 155 to 897 mm with a mean value of 412 mm. Figure 5.13c shows the spatial distribution of the maximum baseflow parameter (D_m), which ranges from 0.2 to 10 mm/day. The highest values are in the western region at high elevations, while the lower values are associated with flatter areas in the eastern part of the region. Figure 5.13d shows the spatial distribution of the infiltration parameter (b_i). This parameter is affected by the climatological gradient; it generally increases from west to east similar to the distribution of the precipitation (about 40 percent of the variation in this parameter is explained by the annual rainfall intensity). Similar to Section 5.2, two of the hydrological parameters (see Figures 3.4 and 3.5) were determined directly using STATSGO data (the saturated hydraulic conductivity and pore size distribution index).

5.3.2 Results

The grid-based VIC-2L was run for the period October, 1948 to September, 1987 using the regional parameters estimated in Section 5.3.1. The modelling strategy and the parameters for the snow melt model as well as the routing model are identical to those used in Section 5.2. Because the hydrological parameters of the VIC-2L model form the only difference between the application presented in this section and that presented in Section 5.2, the results using the regional parameters will be presented as a direct comparison to those obtained using the interpolated parameters (Section 5.2). In the following

subsections, the simulated hydrograph, the annual and the seasonal water balance components are presented.

5.3.2.1 Simulated hydrograph

Figures 5.14 and 5.15 show the observed and the simulated mean monthly streamflow time series, and the coefficient of variation of the monthly streamflows for the furthest downstream locations in the Arkansas and Red River basins, respectively. The model performed reasonably well using the regional parameters, in particular, the performance was considerably better than that shown in Figures 5.3 and 5.4. Although the peak is slightly underpredicted, the mean annual volume was well simulated. Table 5.5 lists the observed and the simulated annual runoff based on the regional parameters and the interpolated parameters (Section 5.2) for ten gaging stations shown in Figure 2.3. In general there was considerable improvement in the simulated annual runoff for all the gauging stations by using the regional parameters. For example, at the outlet of the Arkansas River (Little Rock) the relative error in the runoff volume is -1.3 percent in the case of the regional parameters compared to 7.3 percent in the case of the interpolated parameters. At the outlet of the Red River (Shreveport) the relative error is 1.7 percent in the case of the regional parameters compared to -12 percent in the case of interpolated parameters. The average absolute relative error in the simulated annual runoff for the ten gauging stations is 10 percent in the case of the regional parameters and 20 percent in the case of the interpolated parameters.

5.3.2.2 Annual water balance components

The patterns of the annual mean geographic distribution of the processes involved in the water balance analysis obtained using the regional parameters are similar to those obtained using the interpolated parameters (Figure 5.7). No significant difference exists in the spatially integrated means of the annual runoff and evaporation using both sets of parameters (see Table 5.4 and Table 5.6). On the other hand, there is a significant difference in the means of these processes on the basis of individual grid cells. To evaluate this difference, the 61 grid cells

shown in Figure 2.3 are divided into four climate conditions according to their mean annual precipitation (see Figure 5.16):

i) Arid (Annual Precipitation ($\bar{P} < 280$ mm)

ii) Semi-arid ($280 \leq \bar{P} < 600$ mm)

iii) Sub-humid ($600 \leq \bar{P} < 1000$ mm)

iv) Humid ($\bar{P} \geq 1000$ mm)

The climate classification here is selected subjectively based only on the annual precipitation, similar classification are considered by Kuhl and Miller (1992) in their study of the seasonal runoff for the world's largest rivers.

Figures 5.17a and 5.17b show the annual percent differences in the runoff ratio and the evaporation ratio, respectively. The percent difference of the annual runoff ratio (PDRR) is defined as:

$$PDRR = \left(\frac{ARR_r - ARR_i}{ARR_r}\right) \times 100 \tag{5.5}$$

where ARR_r is the estimated annual runoff ratio using the regional parameters, and ARR_i is the estimated annual runoff ratio using the interpolated parameters. As can be seen in Figure 5.17, the percent differences in the runoff ratio (range from 0 to 100 percent) are much larger than those of the evaporation ratios (range from zero to 10 percent). The largest percent difference in the runoff ratio occurs in the most arid part of the region which is the north-west corner. In the case of the evaporation ratio, the largest difference occurs in the humid area (the eastern part of the region).

Figures 5.18a and 5.18b show the histograms of the percent difference in the runoff and the evaporation ratios, respectively, between the two approaches (i.e. the interpolation and the regional) for all the 61 grid cells shown in Figure 5.16. Eight of the grid cells have greater than 50 percent difference in the annual runoff ratio, seven of them are arid or semi-arid grid cells. All the humid grid cells have less than 40 percent difference in the annual runoff ratio. On the other hand, most of the grid cells have differences less than 5 percent in the annual evaporation ratio. Only 9 of the grid cells (all of them are humid and sub-humid) have five to ten percent difference in the evaporation ratio.

Figures 5.19 a and b show the simulated annual runoff ratios using the regional and interpolated parameters, respectively. Although the generated histogram of the runoff ratio are slightly different, the lower and the upper limit for each climate condition are very similar. For example, the annual runoff ratio for the humid grid cells ranges from .15 to .3 in both histograms. The arid and semi-arid grid cells have modeled annual runoff ratio ranging from 0.001 to .15. The distributions of the sub-humid grid cells in both histograms are slightly different. In the case of the regional parameters the runoff ratio for the sub-humid cells ranges from .1 to .25, while in the case of the interpolated parameters the runoff ratio ranges from .05 to .2. Figures 5.19c and d show the annual evaporation ratio histograms using the regional and the interpolated parameters, respectively. In both runs, the evaporation ratio for the humid grid cells ranges from .7 to .85 and for the arid and semi-arid it ranges from .85 to 1.0.

A question may arise from these results: why is the percent difference in the annual evaporation ratio between the two runs relatively small compared to those of the runoff ratio? As shown in Figure 5.18 most of the grid cells have an evaporation ratio ranging from 0.85 to 1.0, and most of the grid cells have a runoff ratio less than 0.2. These results indicate that the hydrological processes in the Arkansas-Red River basin are mainly water rather than energy limited, especially at the annual scale. This explains why the percent differences in the evaporation ratios are mostly less than 10 percent. In other words, the annual model estimated ET, is only slightly affected by the differences between the hydrological parameters in the two runs. On the other hand, the percent differences in the annual runoff ratio between the two runs are generally larger, mainly due to the differences between the hydrological parameters used in both runs. To some extent these results are consistent with the sensitivity analysis of the VIC-2L model parameters conducted by Liang (1994). She found that the leaf area index, the minimum stomatal resistance, and the soil porosity have the greatest influence on the model output of total annual runoff and annual evaporation. Since in this study the vegetation parameters in the two runs are held constant, the soil porosity may play an important role in the simulated

runoff difference between the two runs. The soil porosity is not directly used in this study, but it is related to the maximum soil moisture in layers 1 and 2 as follows:

$$\text{maximum soil moisture} = \text{porosity} \times \text{soil depth} \tag{5.6}$$

Liang (1994) also found that the drainage parameters (D_s and W_s) had minimal effects on the monthly and annual evaporation and annual runoff. The monthly runoff distribution varies significantly with these parameters. Since in our case the two parameter sets are completely different for all grid cells, it is difficult to know which parameters are most responsible for differences in simulated runoff. However, from these results (see Figure 5.18), it is clear that the runoff is strongly affected by the hydrological parameters. One reason is that all the hydrological parameters (listed in Table 3.1) are involved in the runoff formulation, while only some of them are used in the evaporation formulation. This may increase the chance of having large differences between the two runs in the case of runoff. For example, three of the drainage parameters (D_s, D_m, and W_s (see Table 3.1)) are used only in the runoff formulation. These parameters appear in the baseflow formulation as follows:

$$Q_b = \left(\frac{D_s D_m}{W_s W_{c2}}\right) W^{-} \tag{5.7}$$

Testing the combination of these parameters $\left(k_1 = \frac{D_s D_m}{W_s W_{c2}}\right)$ for eight of the grid cells in which the percent difference in the runoff ratio between the two runs was greater than 40 percent, showed that ratio of k_1 ranged from 1:4 to 1:30 in these cells. Seven of these grid cells are exterior cells and most of them are semi-arid. For such grid cells, the hydrological parameters are mainly extrapolated which may cause a higher possibility for the parameters to be different. For the other grid cells where the difference in the runoff ratio was less than 40%, the k_1 values in the two runs were quite close. Generally, it is found that for the arid and semi-arid area the simulated runoff difference between the two runs are more sensitive to the difference in the two sets of the parameters than that for humid and sub-humid area. This also evident from the

poor performance of the regional equation in semi-arid and arid catchments as shown in Chapter 4. The higher sensitivity of the runoff ratio in the western part of LSA-SW results from the greater sensitivity of ruonff in arid and semi-arid catchments to the infiltration parameterization.

5.3.2.3 Seasonal water balance

Figure 5.20 shows the seasonal spatial distribution of the percent difference in the generated runoff and evaporation ratios between the two runs. In general the largest percent difference in the evaporation ratio is in the eastern part of the area (humid and sub-humid), and it is greater in the winter than in the summer. On the other hand the distribution of the percent difference in the runoff ratio in the winter and the summer are very similar. Figure 5.21 shows the histograms of the percent difference in the runoff and the evaporation ratios between the two runs for both winter and summer. The percent difference in the evaporation ratio ranges from 0 to 16 percent in the winter and it is highest in the humid and sub-humid cells. In the summer, the percent difference in the evaporation ratio ranges from 0 to 11 percent. The percent difference in the runoff ratio ranges from 0 to 100 percent for both winter and summer, but only 13 grid cells have differences greater than 40 percent.

Figure 5.22 compares the histograms of the evaporation ratio for both winter and summer using the two sets of parameters. The summer evaporation ratio from the two runs has a narrower range than that in winter. It ranges from 0.85 to 1.1 in the summer and from .4 to 1.05 in winter. Similarly the range in runoff ratio in the summer is narrower than that in winter (Figure 5.23). The runoff ratio ranges from 0.01 to 0.4 in winter and from 0.01 to .25 in summer.

Table 5.6 also summarizes the statistics of the seasonal and annual spatially averaged evaporation and runoff for the atmospheric budget along with the VIC-2L model. The results reported in Table 5.7 (using the regional parameters) are close to the results reported in Table 5.4 (using the interpolated parameters). The evaporation in the winter is about 2 mm lower than that in

Table 5.4. The statistics for the summer runoff are the same in both Tables. The spatially averaged winter runoff using the regional parameters is 57.3 mm, while it is 54.6 mm using the interpolated parameters.

On an annual and seasonal basis the evaporation results of the VIC-2L model using both the interpolated and the regional parameters are close to those obtained using the atmospheric budget. Although the results discussed above show that there are some differences in the simulated runoff and evaporation using the two sets of parameters, there is no difference in spatially averaged seasonal and annual evaporation between the two runs at the scale of the Arkansas-Red River basin. The results reported in Tables 5.4 and 5.7 indicate that atmospheric budget and the VIC-2L model (using the two sets of parameters) provide comparable estimates of the regional evaporatranspiration. These results imply that at the scale of the Arkansas-Red River and for the climatological conditions (semi-arid to sub-humid climate), the output of any of these models will be controlled by the available soil water, and the hydrological processes for these climate conditions are mainly water limited.

5.4 Case Study III: Water and energy balance estimation

In this application the VIC-2L model was tested for its ability to simulate the full land surface energy balance of the Arkansas-Red River Basin. As in Sections 5.2 and 5.3, the basin was partitioned into sixty-one grid cells (one degree resolution). Station precipitation and temperature were used to construct input precipitation and snowmelt time series. As described in Section 5.4.1.2 clear sky incoming shortwave radiation was predicted using an empirical equation, then the clear sky radiation was reduced according to cloud cover gridded from NCDC Surface Airways data. Downward longwave radiation was computed using the empirical equation of the Tennessee Valley Authority (TVA) (1972) based on humidity, temperature, and cloud cover gridded from NCDC data. Soil and vegetation parameters were the same as in Sections 5.2 and 5.3. The model generated catchment-total latent heat fluxes are tested by comparison with total evaporation derived from an atmospheric moisture budget of the

Arkansas-Red River basin. The grid network model was run off-line at a three hour time step and driven by the gridded station data described above.

The differences between this application and the previous applications described in sections 5.2 and 5.3 are: i) the time step is 3 hour in this case while in the previous cases it was daily; and ii) the VIC-2L performs the complete surface energy and water balances, driven by downward solar and longwave radiation, in addition to surface meteorological variables, while in the previous applications (Sections 5.2 and 5.3) only water balance computations were performed.

5.4.1 Model Input data

5.4.1.1 Surface airways data:

Observed hourly meteorological data were used for a 4-year period (1984-1987) for 26 NCDC Surface Airways stations distributed across the Arkansas-Red River basin to force the grid-based VIC-2L model. Table 5.7 lists these stations and Figure 5.24 shows their locations. The meteorological data include

1) Surface temperature (C°)
2) Wind speed (m/sec)
3) Relative humidity (%)
4) Surface pressure (mb)
5) Total sky cover (%)

For each station the data were regrouped from an hourly to a 3 hour time step by taking the arithmetic average. Missing data were estimated using either the data from the same station or the closest station depending on the length of the missing period. In the case of one missing value, the value was estimated by linear interpolation of the value before and after the missing time step. When more than one consecutive value was missing, values from the closest station were used to replace the missing value. The value from the closest station was adjusted by the ratio or the difference between the long term means of the two stations.

Corrected station data were interpolated to the 1 degree grid mesh using an inverse squared distance scheme, which is a simple version of the spherical adaptation of Shepared's (1968, 1984) numerical approximation method (Willmott et al., 1985). The gridded meteorological data were used in two ways in the VIC-2L model:

i) some of these data are used only to calculate the shortwave and longwave radiation based on sky cloud cover

ii) other data such as the wind speed and surface pressure are needed in the Penman-Monteith evapotranspiration algorithm.

5.4.1.2 Shortwave radiation

The principal source of heat for evapotranspiration is solar radiation, RS. RS, when measured at the earth's surface, includes both direct and diffuse shortwave radiation and is termed "global radiation". Many techniques have been developed to estimate the incident solar radiation. The general approach of most of these methods is to first find the clear sky solar radiation by using the top of atmosphere downward radiative flux and reducing this amount based on the climatological clear sky atmospheric transmittance. Then, for cloudy conditions, an empirical relationship is employed which relates the percent cloud cover to an attenuation in the incident solar radiation.

The following empirical approach is used here, in which the hourly (or any length period) extraterrestrial radiation can be estimated according to Duffie and Beckman (1980) as:

$$R_{ah} = [12(60)/\pi]\ G_{sc}\ d_r\ [\cos(\phi)\cos(\delta)[\sin(\omega_2) - \sin(\omega_1)] + (\omega_2\text{-}\omega_1)\sin(\phi)\sin(\delta)] \quad (5.8)$$

where R_{ah} is hourly extraterrestrial radiation in MJm^{-2}; G_{sc} is the solar constant, 0.08202 $MJm^{-2}min^{-1}$ (1.959 cal $cm^{-2}min^{-1}$); and d_r is the relative distance of the earth from the sun as defined in Eq. 5.10; ϕ is the grid cell latitude and δ is the declination, in radians; ω_2 is the solar time angle at the end

of the hourly period, and ω_1 is the solar time at the beginning of the hourly period, calculated as:

$$\omega_1 = \omega - \pi/24 \tag{5.9a}$$

$$\omega_2 = \omega + \pi/24 \tag{5.9b}$$

where ω is the solar time at the midpoint of the hourly period in radians (noon = 0, afternoon is positive, morning is negative). The relative distance from the earth to sun, given by

$$d_r = 1 + 0.033 \cos(2\pi J/365) \tag{5.10}$$

where J is the Julian day ($1 \leq J \leq 365$ or 366).

The hourly values of clear-sky solar radiation, R_{soh}, can be estimated using the procedure of Hottel (1976) where:

$$R_{soh} = (\tau_b + \tau_d) R_{ah} \tag{5.11}$$

τ_b is atmospheric transmittance of direct-beam shortwave radiation and τ_d is atmospheric transmittance of diffuse shortwave radiation. Different values can be estimated for these transmittance dependent on the climate (i.e. Tropical, Midlatitude summer, Midlatitude winter, and Subartic summer), grid elevation, latitude, and the time of the year. For cloudy conditions, an empirical relationship is employed which relates the percent cloud cover to attenuation in the incident solar radiation (Bras, 1990):

$$R_d = (1\text{-}0.65\ N^2)\ \tau_d * R_{ah} \tag{5.12}$$

where R_d is the direct radiation under cloudy conditions, ($\tau_d * R_{ah}$) direct radiation under clear sky conditions and N is the fraction of cloud covered sky.

The approach was evaluated using hourly pyranometer measurements of incoming solar radiation for the First ISLSCP Field Experiment (FIFE) site for a

number of ("golden" and "silver") days selected from Intensive Field Campaigns 2, 3, and 4. Figure 5.25 compares pyranometer measurements of incoming solar radiation at FIFE and empirically estimated radiation. The root mean squared error between the estimated and the measured values is 120 W/m^2 or about 22% of the average observed value. When the skies are clear over the site (golden day) the estimation procedure performed much better. The errors on cloud days are due, in part to the accuracy of the cloud cover estimates, which were taken from Topeka which is about 75 km from the FIFE site.

5.4.1.3 Longwave radiation

Downward longwave radiation is emitted by the atmosphere and depends strongly on emissivity as well as air temperature and the water content in the atmosphere. The presence of clouds also increases the longwave radiation due to additional radiation emission from the base of the clouds. Longwave radiation was calculated by using the equation suggested by Bras (1990) and taken from TVA (1972), which takes into account the effect of clouds

$$R_l = K_c \, E_a \, \sigma \, Ta^{\,4} \tag{5.13}$$

where K_c an empirical cloud correction is applied (TVA, 1972; Bras, 1990):

$$K_c = (1+0.17N^2) \tag{5.14}$$

and

$$E_a = 0.74+0.0049 \, e \tag{5.15}$$

where E_a is the atmospheric emissivity, e is vapor pressure, Ta is the surface air temperature, σ is Stefan-Boltzman constant, and N is the fraction of the total sky cloud cover. Similar approaches were used by Arola and Lettenmaier (1995) and Zoin et al. (1995).

5.4.2 Implementation

Using the regional hydrological parameters described in Section 5.3.1 and the vegetation parameters described in Section 5.2.1, the grid-based VIC-2L model was implemented off-line to perform complete surface energy and water balances. In this case, the VIC-2L model was driven by gridded incoming radiation, air temperature, wind, humidity, cloud cover, surface pressure, and precipitation. The output was gridded fluxes of latent and sensible heat, surface and subsurface runoff, and soil moisture (see Figure 5.26).

The first 9 months of the simulation period (January 1984 to September 1987) was taken as a warm up period. Because daily precipitation data were available from the data set described in Section 2.3, precipitation was assumed to be uniform over the daily reporting period, and 3-hour values were obtained by dividing the daily totals by 8. Shortwave and longwave radiation were estimated using temperature and cloud cover data as described in Sections 5.4.1.1 and 5.4.1.2. Other meteorological forcing data such as wind speed, surface pressure, relative humidity, and surface temperature were interpolated from the Surface Airways data as described in Section 5.4.1.1. The time of observation of all the forcing data, taken from the Surface Airways data, are consistent. The first time step of each day starts at midnight local time (i.e. the first time step is from midnight to 3 a.m. local time).

Unlike the applications in Sections 5.2 and 5.3, the potential evapotranspiration was calculated using an energy based formulation (Penman-Monteith Equation) instead of a temperature-based formulation (Hamon Equation). The energy-based snow routine was disabled, however, because only a few grids have perennial snow accumulation, and those areas where is snow is most important have minimal effects on the basin water balance, which is controlled by the humid eastern part of the basin. The initial soil moisture for layers 1 and 2 was taken as the soil moisture prediction for January 1, 1984 from the run in Section 5.3 (which was for the period October 1948 to September, 1987).

The results in this section are for the period October 1984 to September 1987. In addition, the results are presented as direct comparisons between two runs. The first run, which is termed the "Water balance run", consists of the last three years of the simulation reported in Section 5.3, in which the model was driven by daily precipitation, and temperature. The potential evapotranspiration was calculated using a temperature-based method. In the second, "full-energy run", the model was forced by a three-hour time step of meteorological and climatological data described in the previous sub-sections. The potential evapotranspiration was calculated using an energy based formulation (Penman-Monteith Equation). The average precipitation of this period is 120 mm greater than the average precipitation for the 38 years period presented in Sections 2.2 and 2.3.

Figures 5.27 a and b shows the spatial distribution of percent differences in the annual runoff and evaporation ratios between the two runs (water balance and full-energy runs), respectively. Similarly, Figure 5.28 shows the histogram of these differences for all the 61 grids. Although the two runs have the same hydrologic and vegetation parameters, the percent differences in the runoff and evaporation ratios are similar to the percent difference between the two runs described in Sections 5.2 and 5.3 (see Figure 5.18). Although the two runs have different time steps, types of forcing (input) data, and types of formulation used in the model, the results compare well at the monthly and annual time scales. The percent differences in the annual evaporation ratio ranged from 0 to 18 percent; about half of the grid cells show less than 5 percent difference in the evaporation ratio. Only 14 grid cells (sub-humid to humid) have greater than 10 percent differences in the annual evaporation ratio. On the other hand, the percent differences in the runoff ratio range from 0 to 100 percent. Most of the grid cells are within 40 percent difference. The runoff component is of concern to society; hence improvements in representing this would be beneficial. Figure 5.29 shows the histograms of the annual runoff and evaporation ratios using both runs. The ranges of the histograms are similar in both runs, but the distributions of the grid cells are slightly different in the two runs.

Figure 5.30 shows the mean seasonal spatially distributed latent and sensible heat fluxes. The seasonal distributions of these fluxes show a clear dependence on soil moisture. For example, for both Winter and Summer, the latent heat flux is larger in the western part (Humid) than eastern part (arid). On a seasonal bases the latent heat in the Summer is much larger than the Winter. On the other hand, sensible heat flux show more dependence on the soil moisture. In this case, the sensible heat flux decrease in west-east direction. The sensible heat flux in the summer is larger than that of the winter. The distribution of both fluxes in the Arkansas-Red River basin are consistent and capture most of the physical characteristics of this area.

5.4.3. Spatially integrated water and energy budgets

The model generated spatially integrated evapotranspiration from October 1985 through September 1987, was compared with total evaporation derived from an atmospheric moisture budget of the Arkansas-Red River basin (Eqs. 5.3 and 5.4). Figure 5.31 shows the three-year monthly ET, spatially integrated over the entire Arkansas-Red River basin. In general the generated monthly ET from the two runs (i.e. the water balance run and the full-energy run) are in a good agreement with those derived from the atmospheric budget.

The largest difference in the evaporation estimates from the VIC model and the atmospheric budget occurs in the summer of 1987 as shown in Figure 5.31 For the summer 1987 the total vapor net convergence was -180 mm, while for the summer of 1986 was $+25$ mm, and for summer 1985 was -96 mm. The best agreement between the two models is for year 1986 where the net convergence is the lowest. The mean monthly estimates of the VIC-2L model for Winter period (October to April) is slightly lower than the atmospheric budget. During the Summer period (May, July, August and September) the VIC-2L model estimates is lower than the atmospheric budget. The largest difference between the two models is in July in which the VIC-2L model estimates is about 77 mm (in the two runs) while for the atmospheric budget is about 105 mm.

Table 5.8 compares the seasonal spatially averaged evaporation and runoff for the VIC-2L model runs along with atmospheric budget. In the winter, the

VIC-2L model runs (water balance run and the full-energy run) produce ET estimates that are very close to the atmospheric budget estimates. The ET ratios for winter are 0.61 (using the water balance run), and 0.59 (using the full energy run), and 0.64 (from the atmospheric budget). In the summer, there is significant difference in the ET estimates between the VIC-2L model and atmospheric budget. For example the ET ratios for the summer are 0.99 (using the water balance run), 0.96 (using the full-energy run), and 1.16 (using the atmospheric budget). The spatially averaged runoff from the two runs are comparable. The estimated winter runoff ratio is about 0.25 using the water balance run and 0.26 using the full-energy run. The summer runoff ratio is 0.11 using the water balance run and 0.1 using the full energy run.

5.5 Summary

This chapter has summarized testing of the VIC-2L land surface scheme through the application to the Arkansas-Red River basin using spatially distributed parameters estimated via a regionalization scheme. The approach uses distributed land surface characteristics from digital elevation data and the SCS STATSGO soils data base, and vegetation cover from the EPA Global Ecosystems Database. Key components of the methodology are extraction from the STATSGO data base of soil attributes used to determine two of the model parameters and a regionalization scheme from which the remaining parameters were determined.

Three applications of the grid-based version of VIC-2L model to LSA-SW at the one degree spatial scale were described in this chapter. The first two applications are related to estimation of the water balance components using both the interpolated and regional parameters. The third application is related to estimation of the water and energy balances using the regional parameters. The differences between the first two applications and the third one are the time step, types of forcing data, and types of model formulation.

Simulated monthly mean hydrographs for the Arkansas River are in reasonably good agreement with the observed hydrographs, although the seasonal

peak flows (late spring) are underestimated, and the fall and winter low flows are overestimated. The magnitude of the bias is less for the humid, eastern part of the basin than the more arid west. The average absolute relative error in the simulated annual runoff for ten gauging stations is 10 percent in the case of the regional parameters and 20 percent in the case of the interpolated parameters.

There were no significant differences in the model-generated catchment-total water balance components using both sets of parameters. However, there were significant differences in the water balance components for individual grid cells. The largest relative difference in the runoff ratio occurred in the most arid grid cells, while the largest differences in the evaporation ratio occurred in the humid cells. In general, the model estimated ET (most of the grid cells have differences less than five percent) is only slightly affected by the differences between the hydrological parameters in the two runs.

The evaporation predicted by the VIC-2L model compared well with that derived from an atmospheric moisture budget of the Arkansas-Red River basin. VIC-2L model is tested in this application for its ability to simulate large scale energy and water fluxes in the Arkansas-Red River basin. VIC-2L shows promising results for simulating large scale fluxes of latent and sensible heat, being able to capture both magnitude and timing of these fluxes for the hydro-climatic environmental of the Arkansas-Red River basin.

Table 5.1 Vegetation parameters for the Arkansas-Red River basin

Parameter	Short Grass	Tall Grass	Woodland	Deciduous Forest	Evergreen Forest	Alpine
d_0 (m)	0.02	0.15	0.3	2.0	2.0	0.01
z_0 (m)	0.13	0.95	1.9	12.6	12.6	0.06
f_1	1.0	0.8	0.6	0.5	0.5	1.0
f_2	0.0	0.2	0.4	0.5	0.5	0.0
r_{min} (s/m)	100	100	100	100	100	100
LAI 1	1.9	2.1	2.8	1.9	3.4	0.4
LAI 2	2.2	2.3	2.9	2.1	3.4	0.3
LAI 3	2.8	3.1	3.5	2.9	3.5	0.4
LAI 4	3.6	4.1	4.9	4.9	3.7	0.6
LAI 5	3.4	4.0	5.2	5.0	4.0	0.8
LAI 6	3.3	3.7	5.1	5.0	4.4	1.5
LAI 7	3.4	3.7	4.8	4.6	4.4	1.6
LAI 8	3.2	3.2	4.4	4.3	4.3	1.5
LAI 9	3.3	3.3	4.2	3.8	4.2	1.3
LAI 10	2.8	2.9	3.5	2.7	3.7	0.8
LAI 11	2.5	2.7	3.2	2.5	3.5	0.5
LAI 12	2.1	2.3	2.9	2.1	3.4	0.4

Table 5.2 Unit hydrograph values used for the Arkansas-Red Basin

Time Step (day)	0	1	2	3	4	5	6	7
U.H.Value	0.	.095	.19	.286	.214	.143	.072	.0

Table 5.3 Observed and estimated mean annual runoff (in thousands of acre-feet) for the Arkansas-Red River basin using the interpolated parameters of the VIC-2L model

Gauging Station	Area km^2	Observed (taf)	Simulated (taf)	Error %
Neosho R at Fort Gibson	32362	5895	4809	18.4
Verdigris R at Inola	20489	3514	1718	51.1
Arkansas R at Kaw	120512	2425	3218	-32.7
Arkansas R at Haskell	195475	5616	6098	-8.6
Canadian R at Eufaula	123221	3672	3396	7.5
Arkansas R at Little Rock	409297	28774	26686	7.3
Red R at Texoma	87497	3296	3788	-14.9
Red R at De Kalb	107257	8241	9815	-19.1
Red R at Fulton	120289	12739	15361	-20.6
Red River at Shreveport	141587	17612	19733	-12.0

Table 5.4 Seasonal and annual comparison of the atmospheric and the VIC-2L evaporation estimates using interpolated parameters

	Winter		Summer		Annual	
	Atmos.	VIC	Atmos.	VIC	Atmos.	VIC
Mean evaporation (mm)	191	181	428	433	619	614
CV evaporation	0.33	0.16	0.16	0.12	0.148	0.108
Evaporation Ratio	0.68	0.65	0.96	0.97	0.864	0.855
Mean Runoff (mm)		54.6		51.4		106
CV Runoff		0.48		0.31		0.37
Runoff Ratio		0.20		0.12		0.14

Table 5.5 Comparison of simulated mean annual runoff using interpolated and regional parameters of the VIC-2L model

Gauging Station	Obs.	Interpolated		Regional	
	flow	flow	V%	flow	V%
Neosho R at Fort Gibson	5895	4809	18.4	5016	14.9
Verdigris R at Inola	3514	1718	51.1	2085	40.7
Arkansas R at Kaw	2425	3218	-32.7	3046	-25.6
Arkansas R at Haskell	5616	6098	-8.6	6168	-9.8
Canadian R at Eufaula	3672	3396	7.5	3681	-0.2
Arkansas R at Little Rock	28774	26686	7.3	29143	-1.3
Red R at Texoma	3296	3788	-14.9	3358	-1.9
Red R at De Kalb	8241	9815	-19.1	8417	-2.1
Red R at Fulton	12739	15361	-20.6	13274	-4.2
Red River at Shreveport	17612	19733	-12.0	17321	1.7

Table 5.6 Seasonal and annual comparison of atmospheric and the VIC-2L estimates of evaporation using regional parameters

	Winter		Summer		Annual	
	Atmos.	VIC	Atmos.	VIC	Atmos.	VIC
Mean evaporation (mm)	191	179	428	433	619	612
CV evaporation	0.33	0.16	0.16	0.12	0.148	0.106
Evaporation Ratio	0.68	0.64	0.96	0.97	0.864	0.852
Mean Runoff (mm)		57.3		51.5		109
CV Runoff		0.54		0.32		0.41
Runoff Ratio		0.21		0.12		0.15

Table 5.7 Surface Airways stations

	Station	State	Lat.	Long.
1	Abilene	TX	32.42	-99.68
2	Amarillo,	TX	35.23	-101.70
3	Dallas-Fort Worth	TX	32.90	-97.03
4	Lubbock	TX	33.65	-101.82
5	Midland	TX	31.95	-102.18
6	Oklahoma City	OK	35.40	-97.60
7	Roswell	NM	33.30	-104.53
8	Longview	TX	32.35	-94.65
9	Tucumcari	NM	35.18	-103.60
10	San Angelo Mathis	TX	31.37	-100.50
11	Fort Smith	AR	35.33	-94.37
12	Dodge City	KS	37.77	-99.97
13	El Paso	TX	31.80	-106.40
14	Lufkin Angelina	TX	31.23	-94.75
15	Alamosa Bergman	CO	37.45	-105.87
16	Colorado Springs	CO	38.82	-104.72
17	Pueblo	CO	38.28	-104.52
18	Albuquerque	NM	35.05	-106.62
19	Columbia	MO	38.82	-92.22
20	Springfield	MO	37.23	-93.38
21	Little Rock	AR	34.73	-92.23
22	Shreveport	LA	32.47	-93.82
23	Wichita	KS	37.65	-97.43
24	Russel	KS	38.87	-98.82
25	Tulsa	OK	36.20	-95.90
26	Dallas-Hinsley Fld	TX	32.73	-96.97

Table 5.8 Seasonal Comparison of atmospheric budget and the VIC-2L evaporation estimates based on: i) water balance formulation (VIC/W);and ii) full-energy balance fromulation (VIC/WE)

	WINTER (October thru March)				
	Evaporation			Runoff	
	Atmo	VIC/W	VIC/WE	VIC/W	VIC/WE
Mean evaporation	230.8	219.2	212.4	90.7	6.6
CV evaporation	0.18	0.11	0.12	0.27	1.73
Evaporation Ratio	0.64	0.61	0.59	0.25	0.02
	SUMMER (April thru September				
Mean evaporation	560.7	476.4	461.9	51.2	50.4
CV evaporation	0.14	0.04	0.01	0.20	0.05
Evaporation Ratio	1.16	0.99	0.96	0.11	0.10

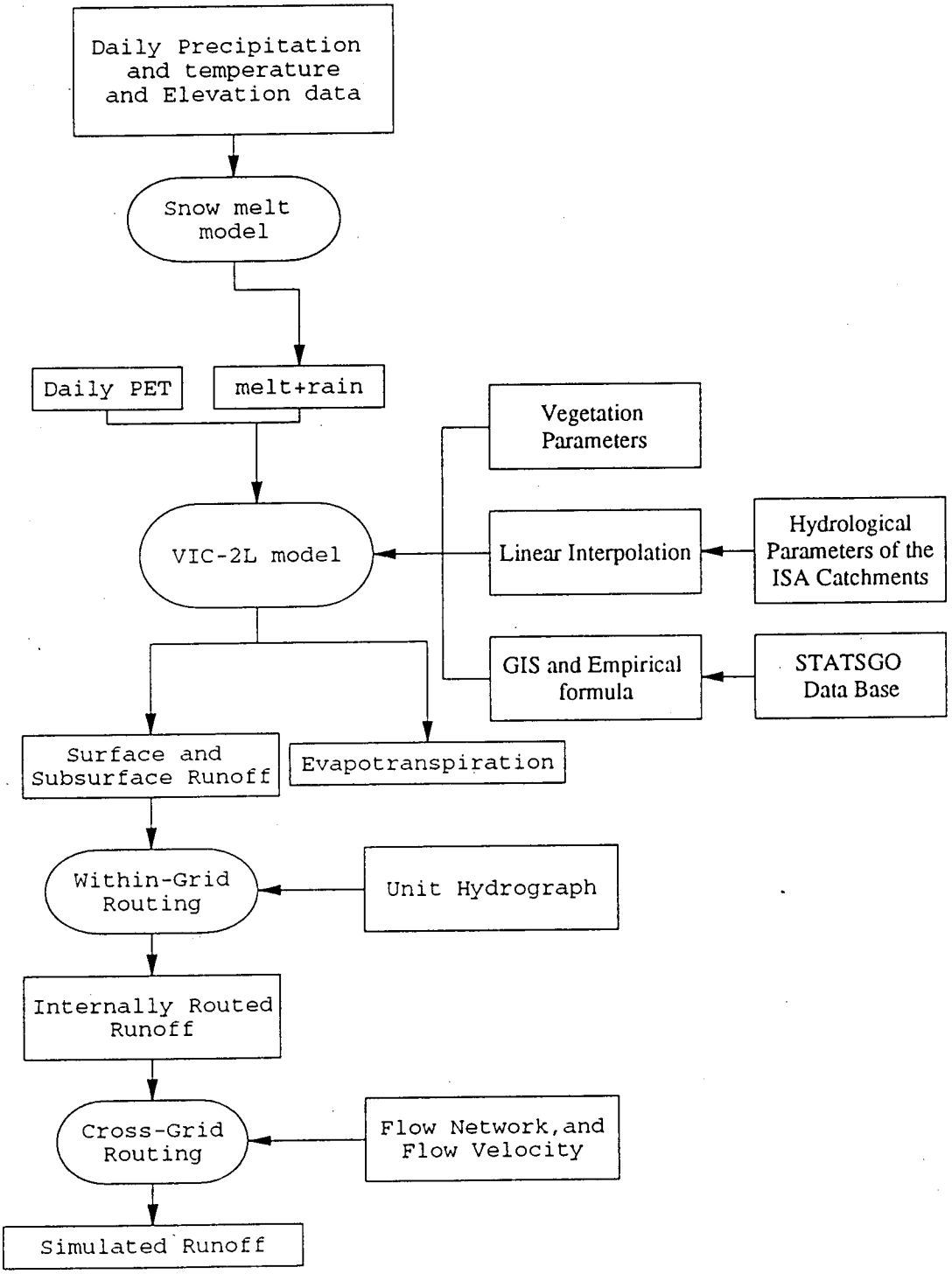

Fig. 5.1 Modeling approach

a) Maximum soil moisture parameter (Wc1)

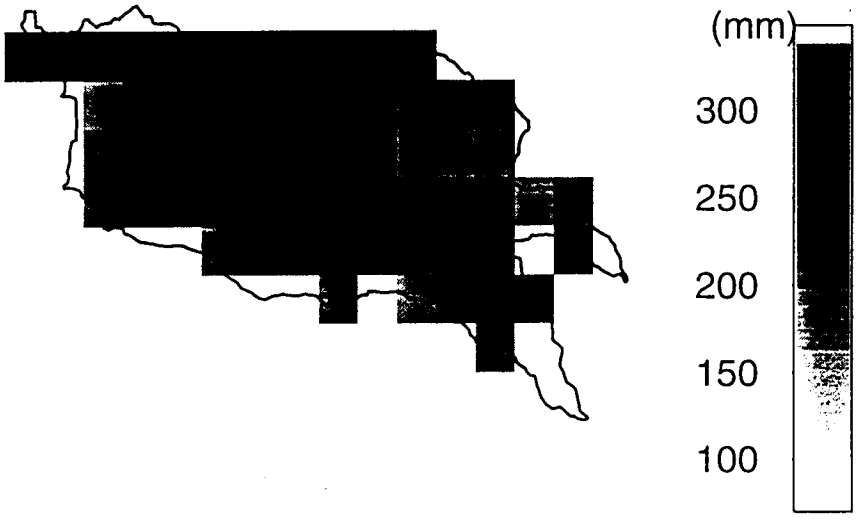

b) Maximum soil moisture parameter (Wc2)

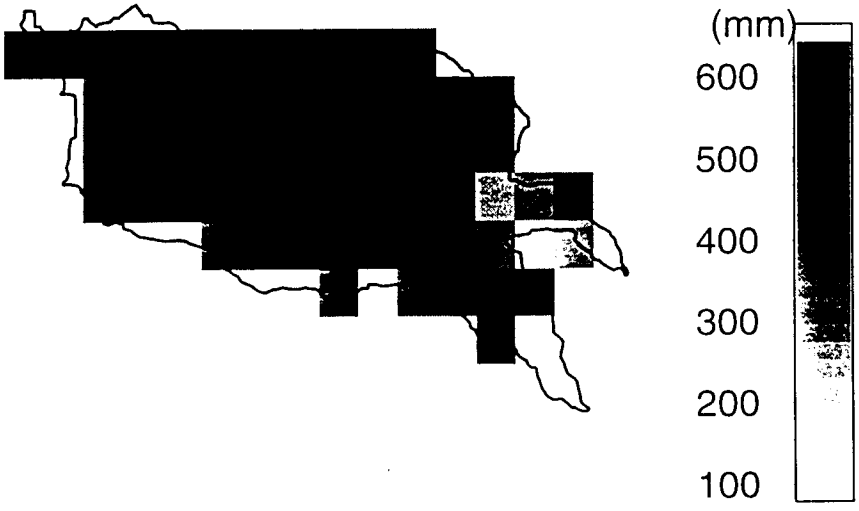

Fig. 5.2 Linearly interpolated maximum soil moisture parameters of a) layer 1; b) layer 2

c) Maximum baseflow parameter (Dm)

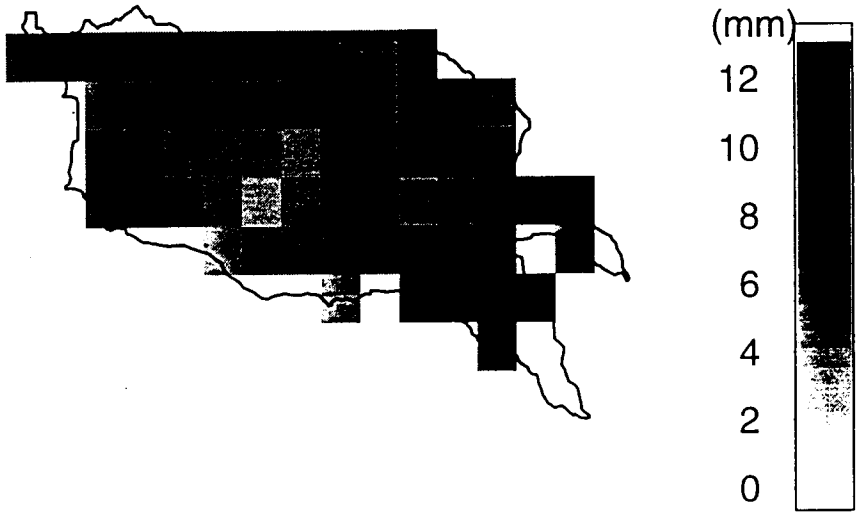

d) Infiltration parameter (bi)

Fig. 5.2 Linearly interpolated: c) maximum baseflow parameter;
d) infiltration parameter

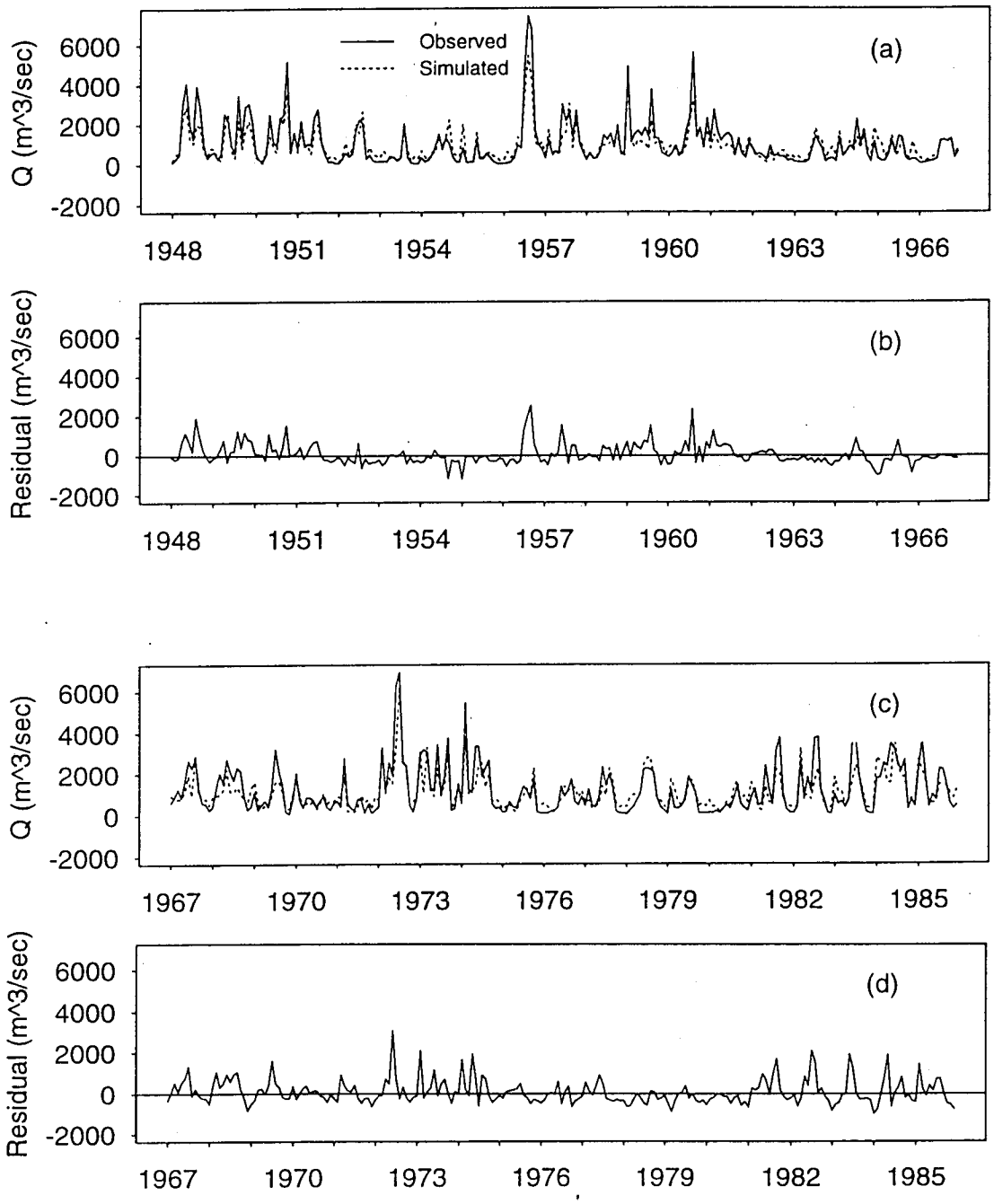

Fig. 5.3 Observed and simulated monthly streamflow for Arkansas River at Little Rock using the interpolated parameters: (a) simulation period (1948-1966); (b) residual (1984-1966); (c) simulation period (1967-1986); (d) residual (1967-1986)

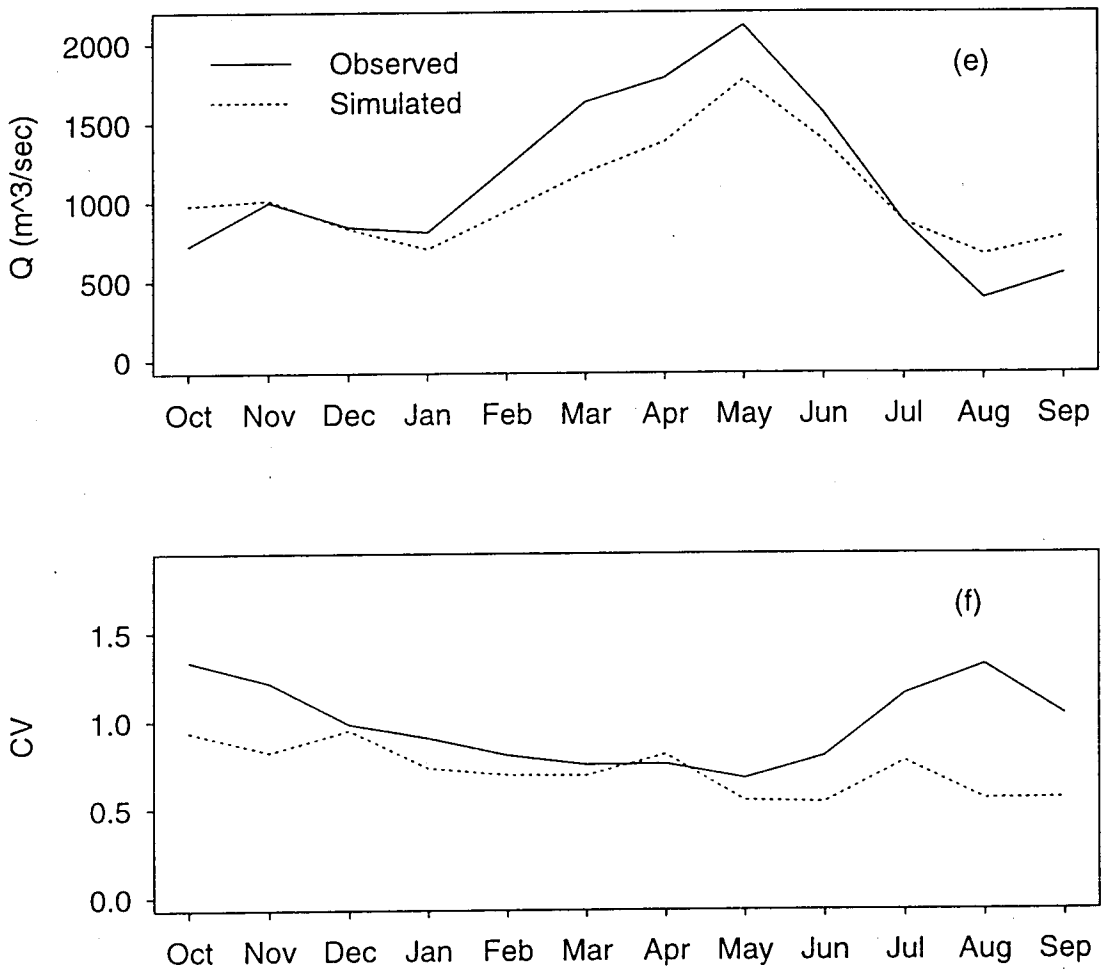

Fig. 5.3 (contd) (e) mean monthly streamflow for the period (1948-1986); (f) coefficient of variation of monthly streamflow for the period (1948-1966)

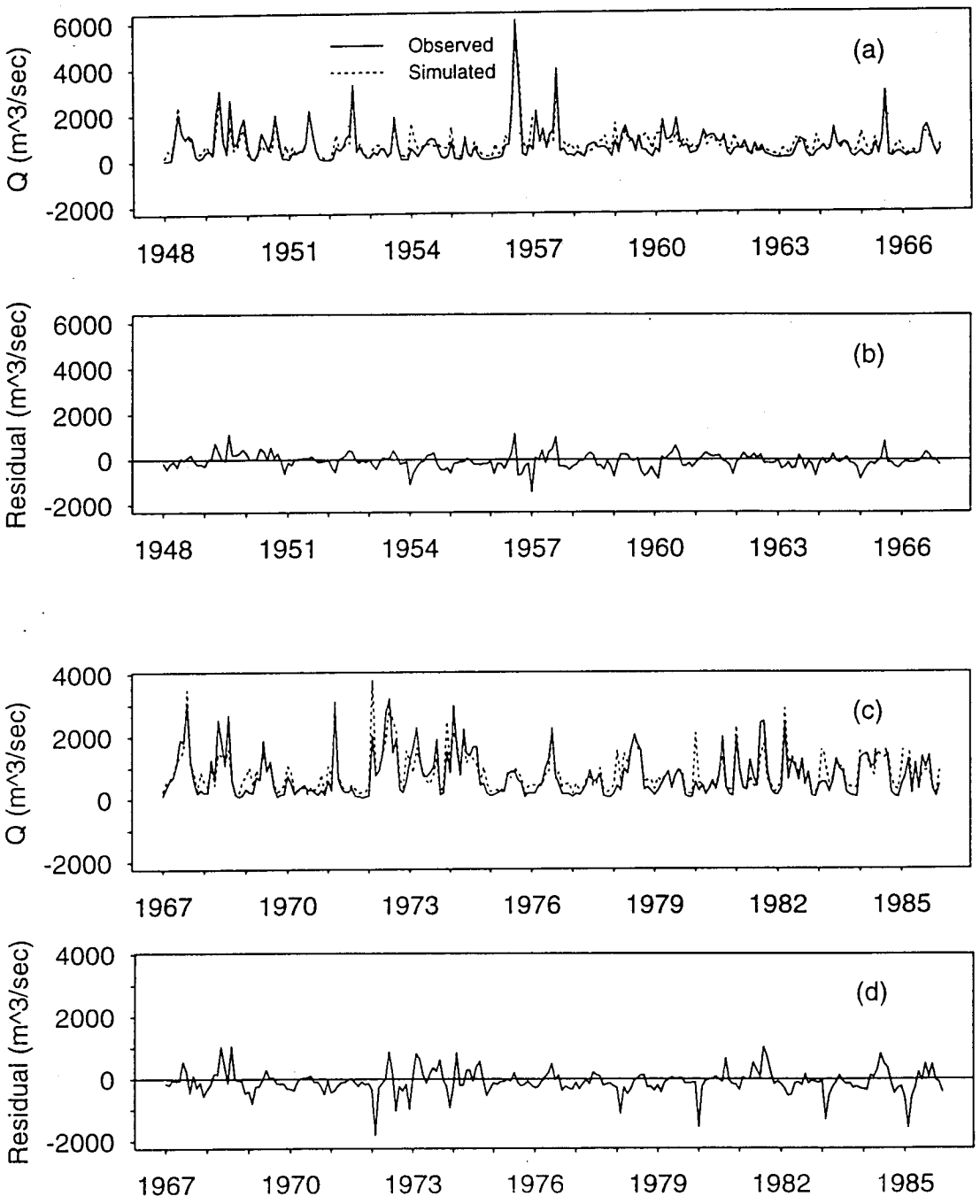

Fig. 5.4 Observed and simulated monthly streamflow for the Red River at Shreveport using the interpolated parameters: (a) simulation period (1948-1966); (b) residual (1984-1966); (c) simulation period (1967-1986); (d) residual (1967-1986)

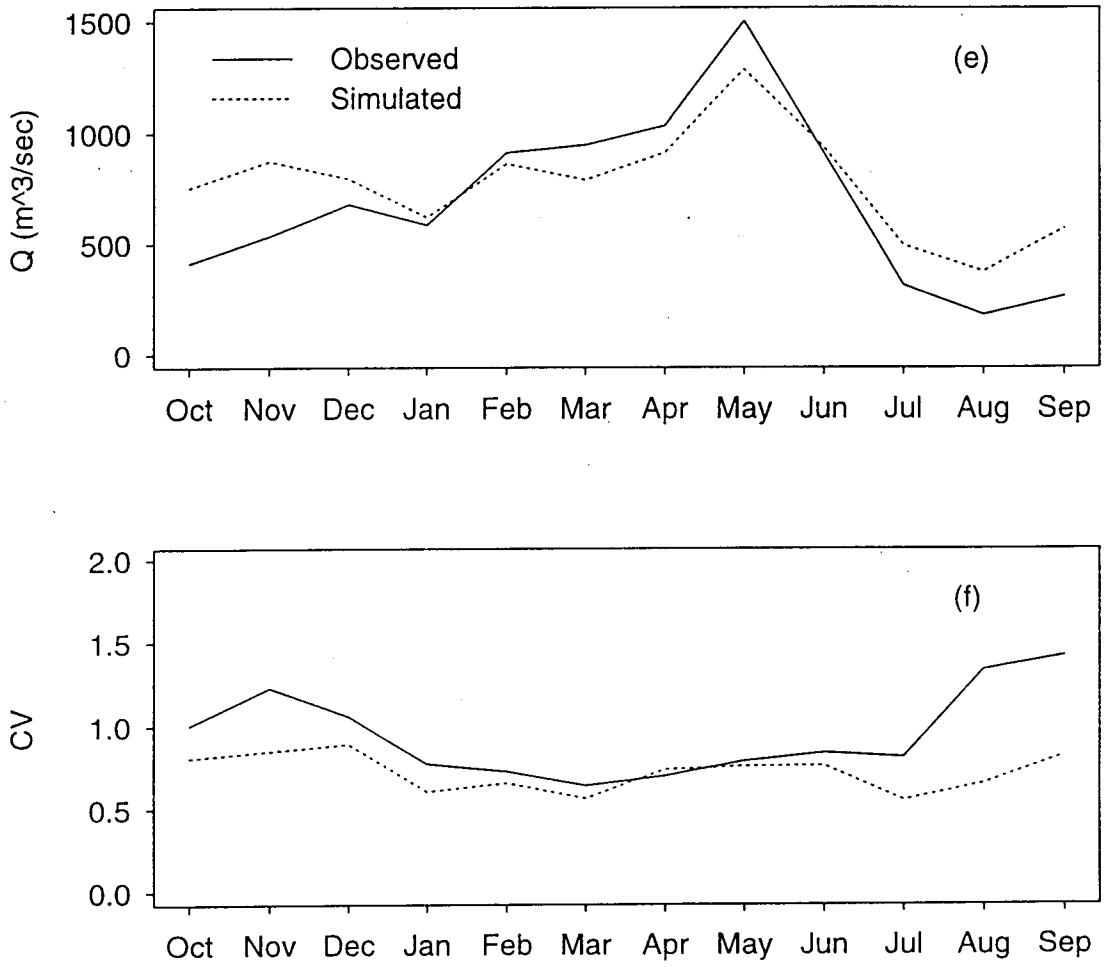

Fig. 5.4 (contd) (e) mean monthly streamflow for the period (1948-1986); (f) coefficient of variation of monthly streamflow for the period (1948-1966)

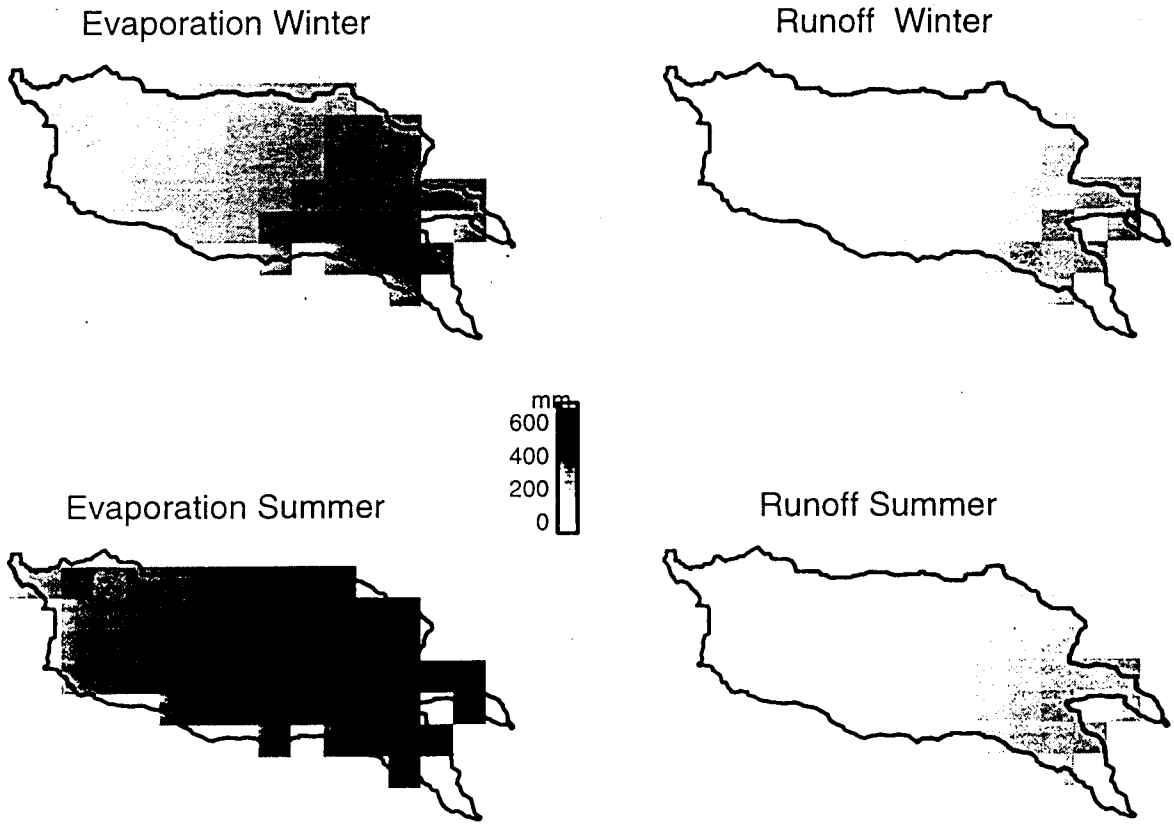

Fig. 5.5 Distribution of the mean evaporation and runoff for winter (October to March) and summer (April to September)

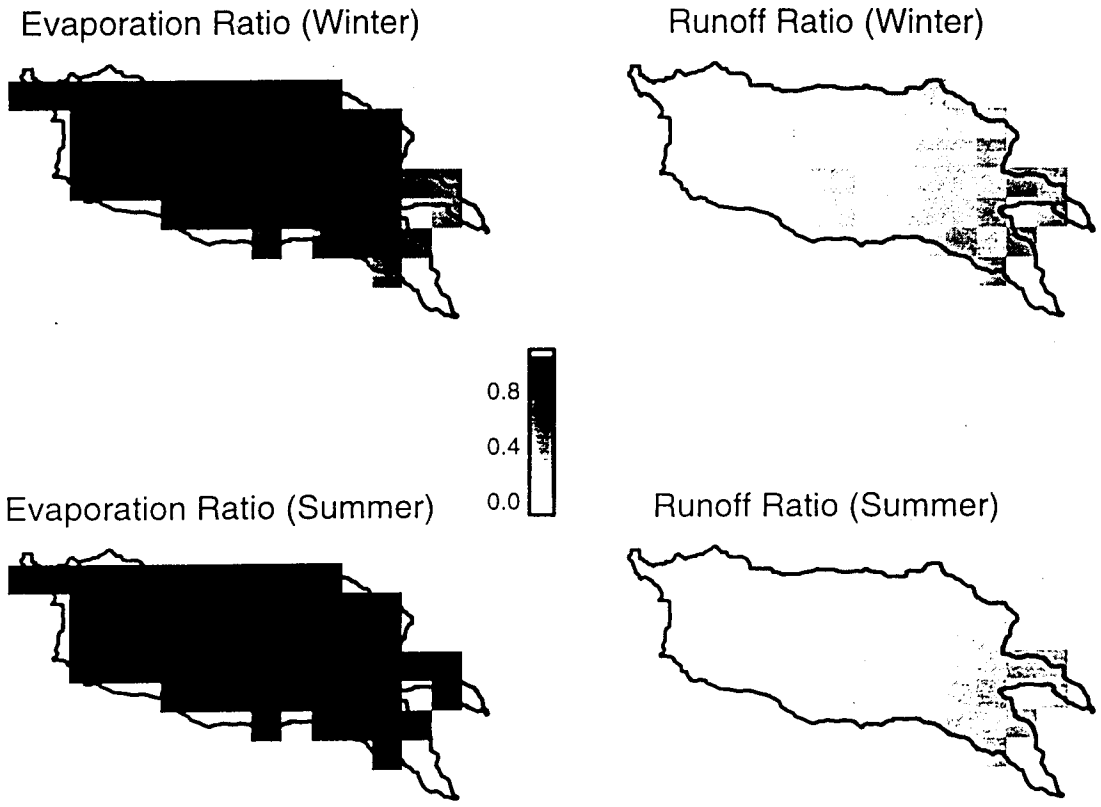

Fig. 5.6 Distribution of the evaporation and runoff ratios for winter (October to March) and summer (April to September)

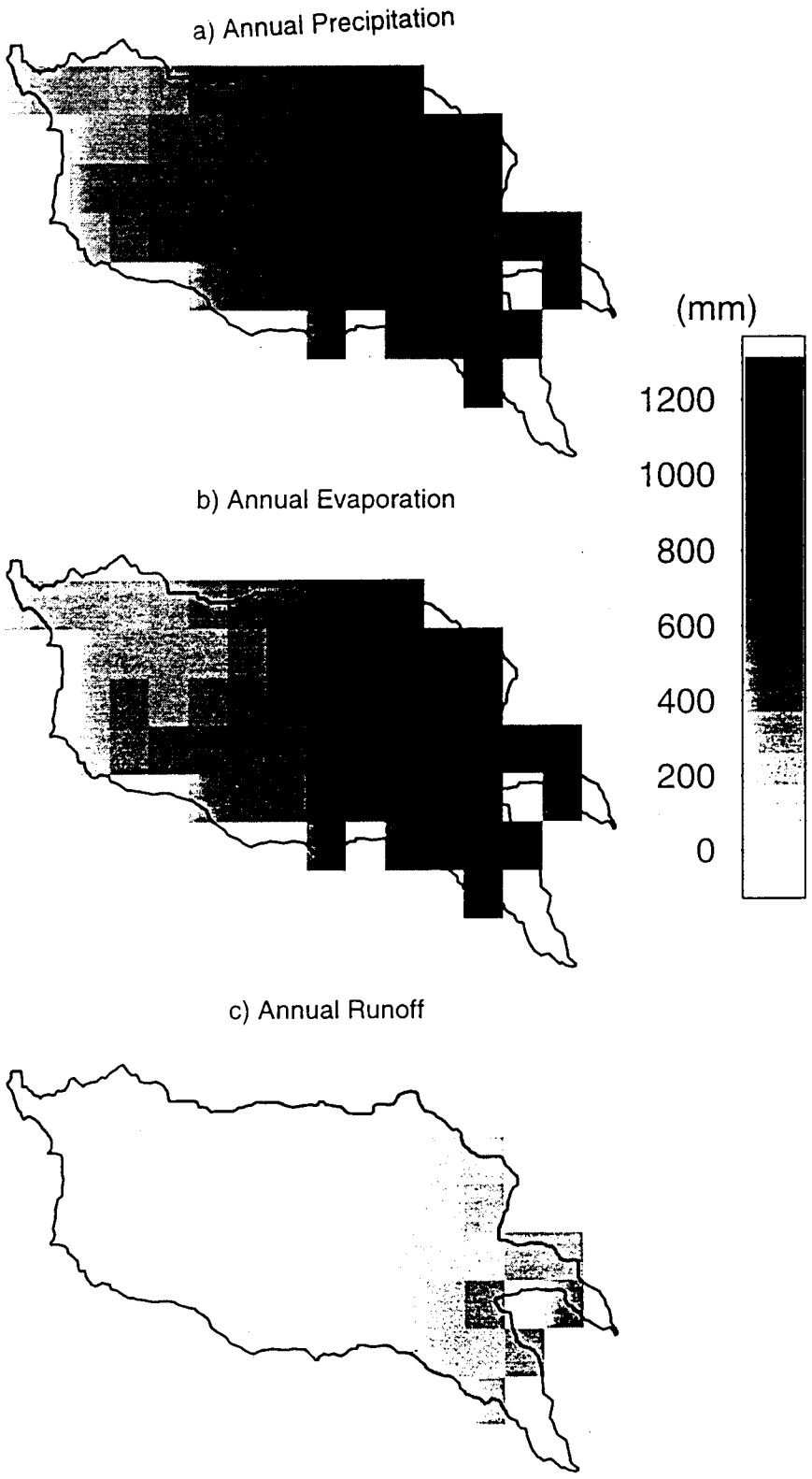

Fig. 5.7 Arkansas-Red River annual mean geographic distribution of water balance components; precipitation (upper panel);. evaporation (middle panel); and runoff (lower panel)

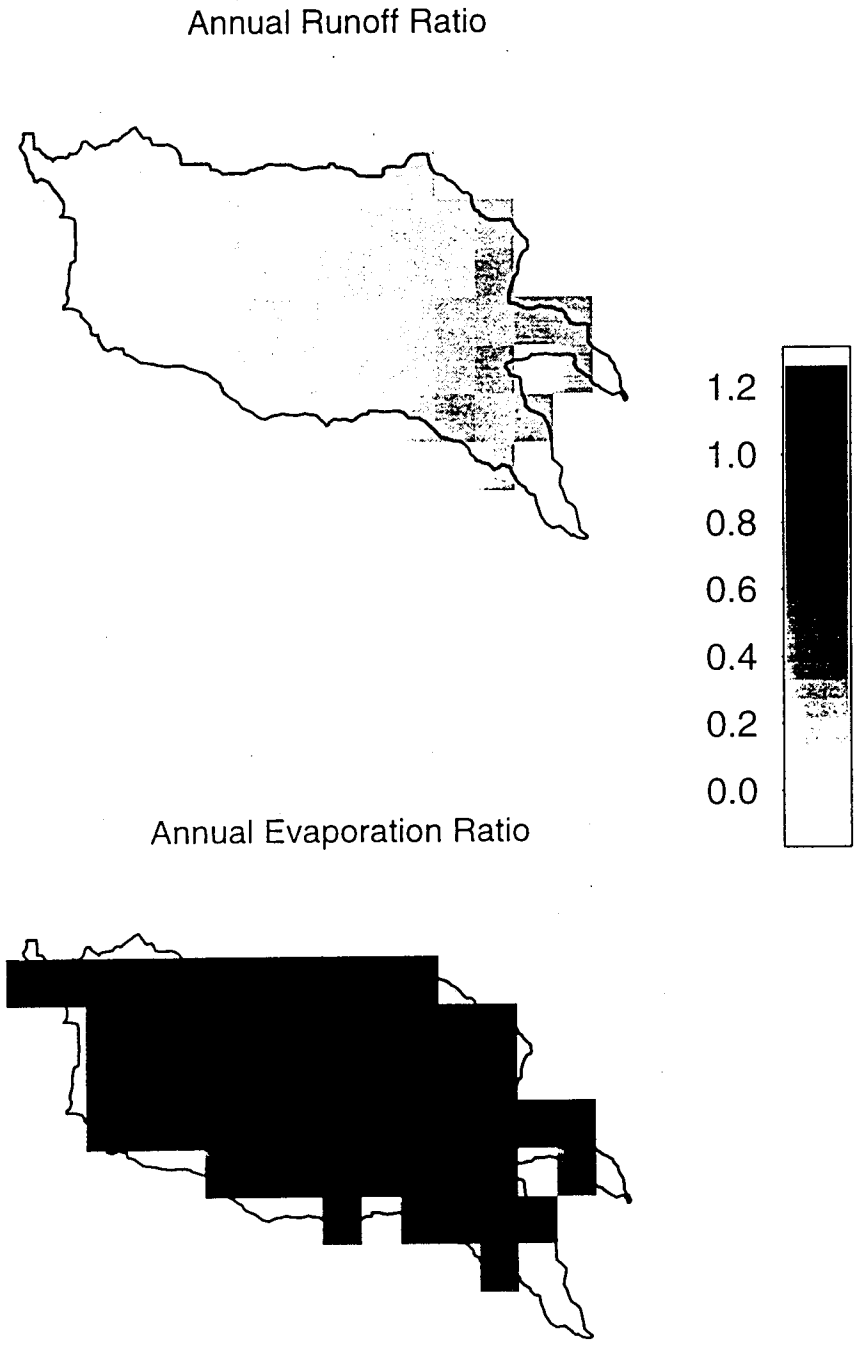

Fig. 5.8 Arkansas-Red River basin annual geographic distribution of runoff ratio (upper panel) and evaporation ratio (lower panel)

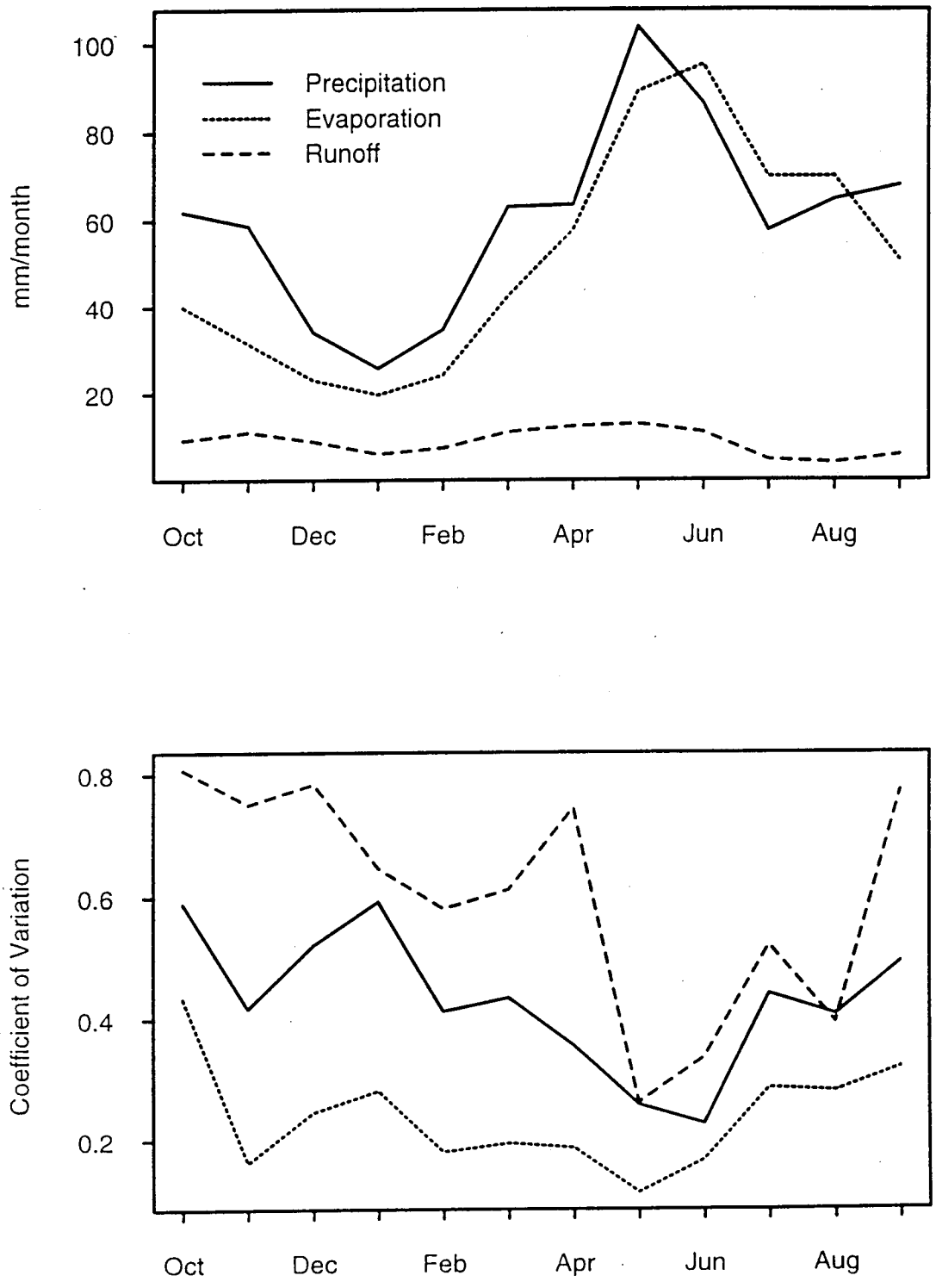

Fig. 5.9 The Arkansas-Red River basin mean monthly hydrologic cycle components (upper panel); and their coefficient of variations (lower panel)

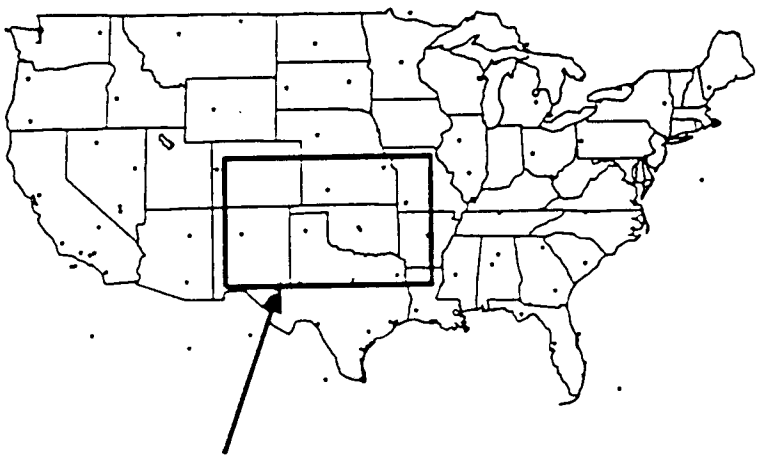

Fig. 5.10 Location of radiosonde sounding stations and domain used in the atmospheric budget analysis

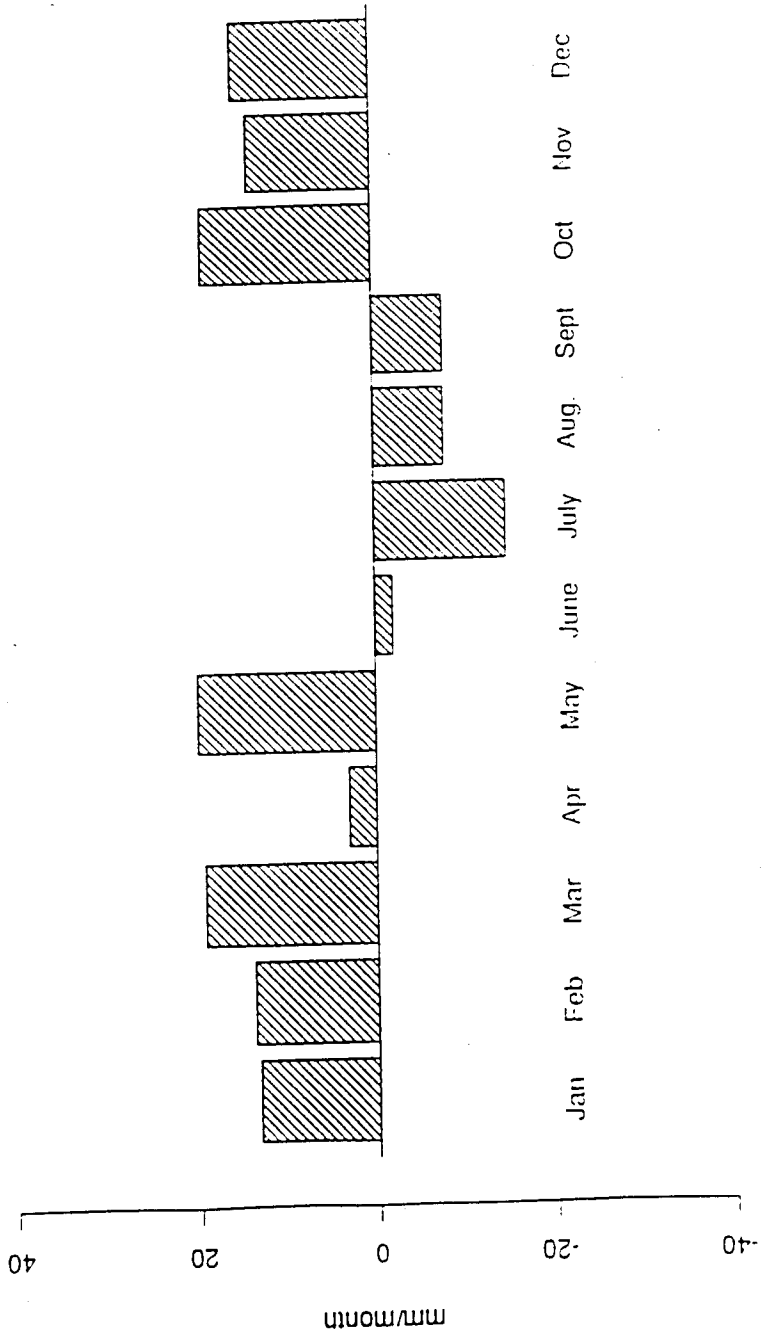

Fig. 5.11 Average monthly vapor convergence based on monthly atmospheric budget analysis (1973-1989).

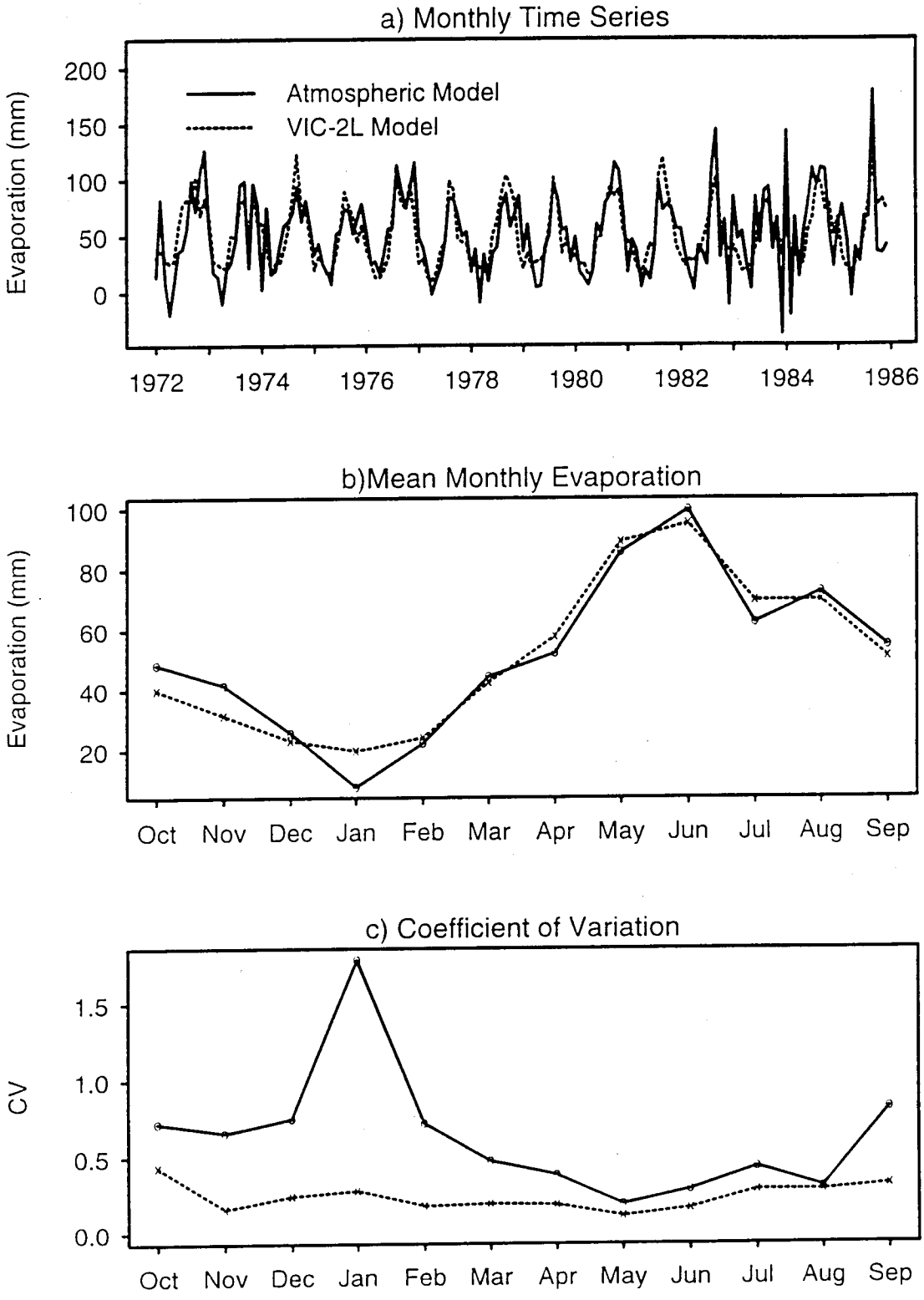

Fig. 5.12 Monthly evaporation predicted by atmospheric budget analysis and the VIC-2L model: a) Evaporation monthly time series; b) Mean monthly evaporation; c) Coefficient of variation

a) Maximum soil moisture parameter (Wc1)

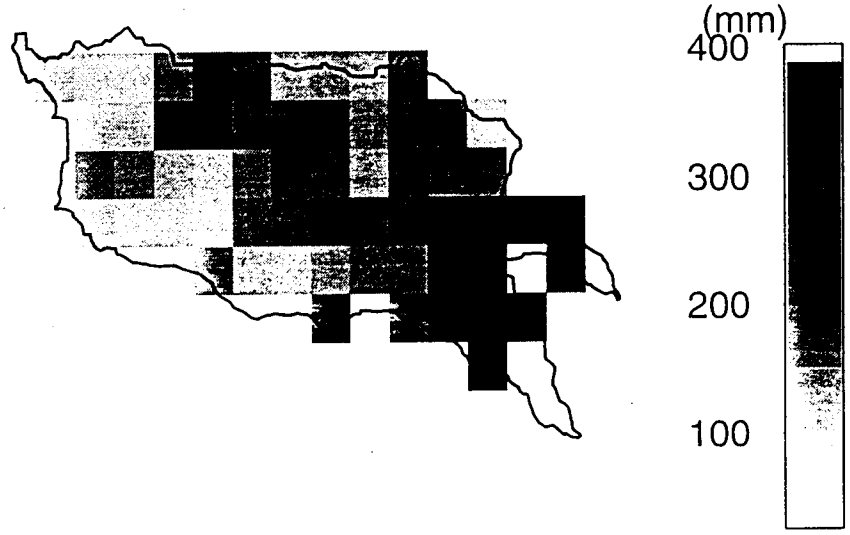

b) Maximum soil moisture parameter (Wc2)

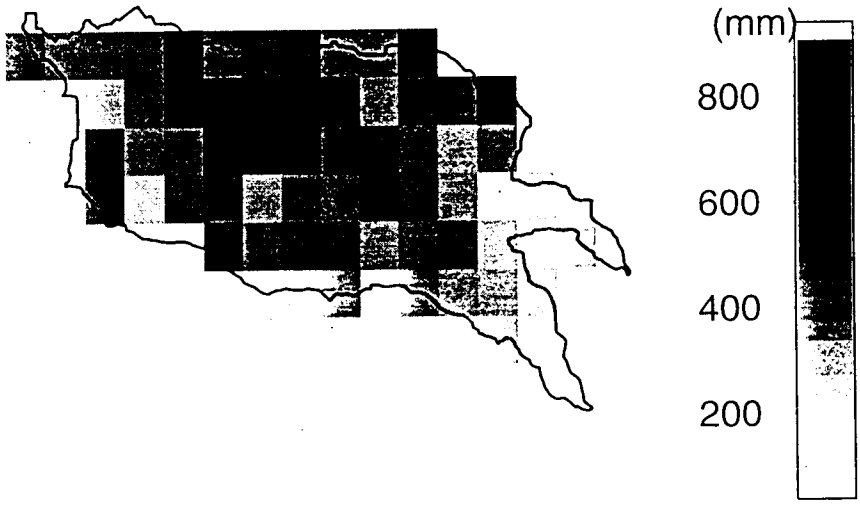

Fig. 5.13 Spatial distribution of the regional estimates of the maximum soil moisture parameters of a) layer 1; b) layer 2

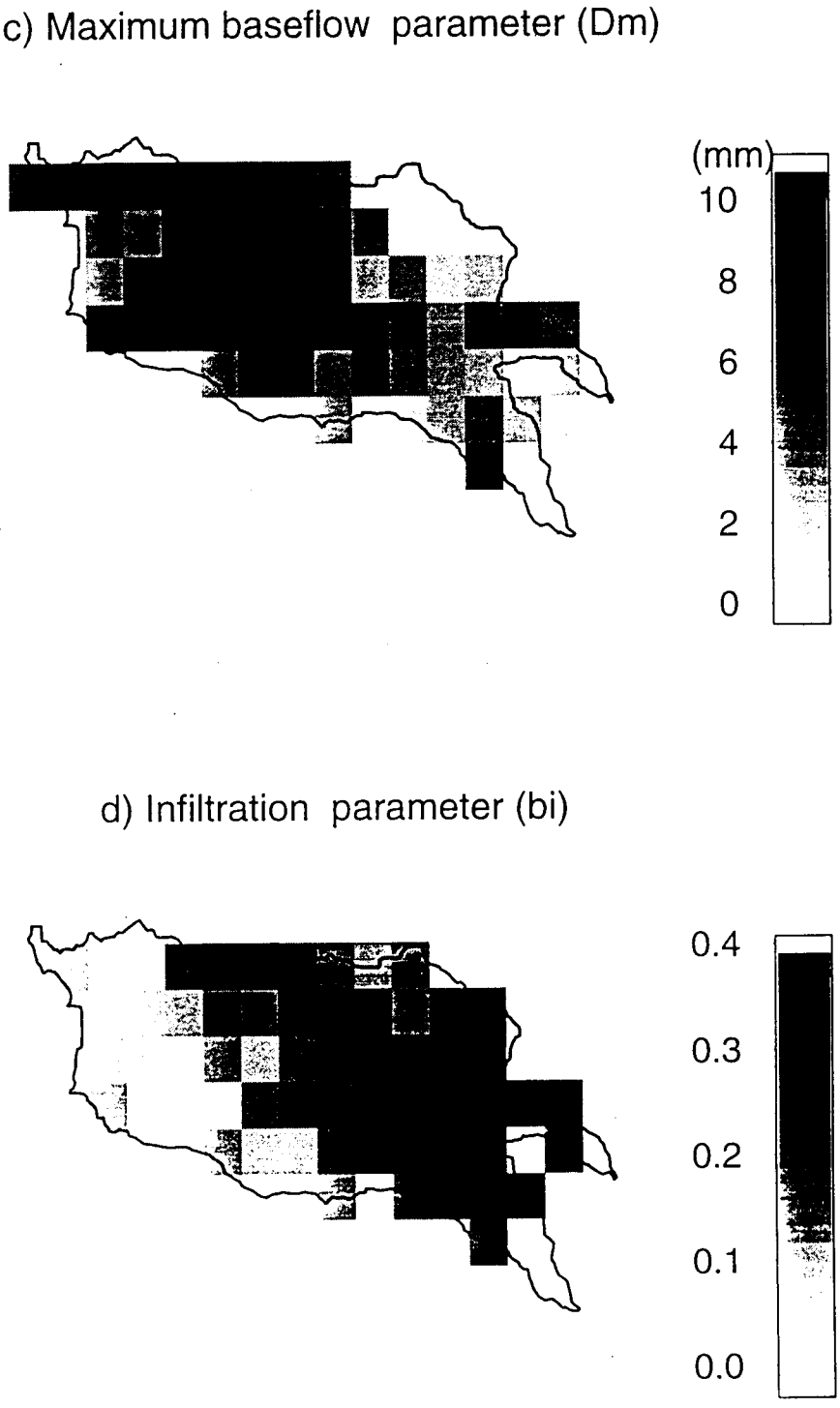

Fig. 5.13 Spatial distribution of the regional estimates of c) the maximum baseflow parameter; d) the infiltration parameter

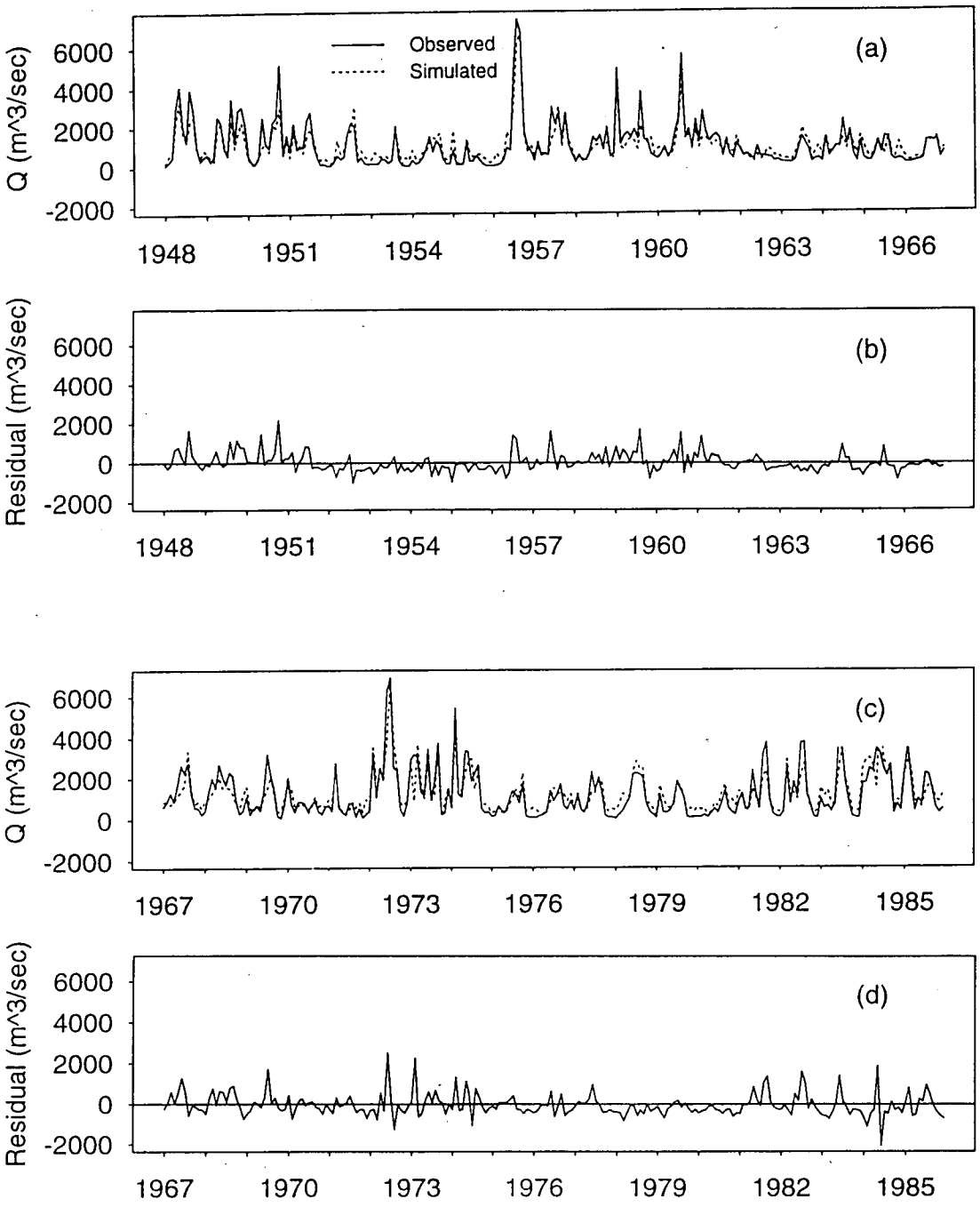

Fig. 5.14 Observed and simulated monthly streamflow for Arkansas River at Little Rock using the regional parameters: (a) simulation period (1948-1966); (b) residual (1984-1966); (c) simulation period (1967-1986); (d) residual (1967-1986)

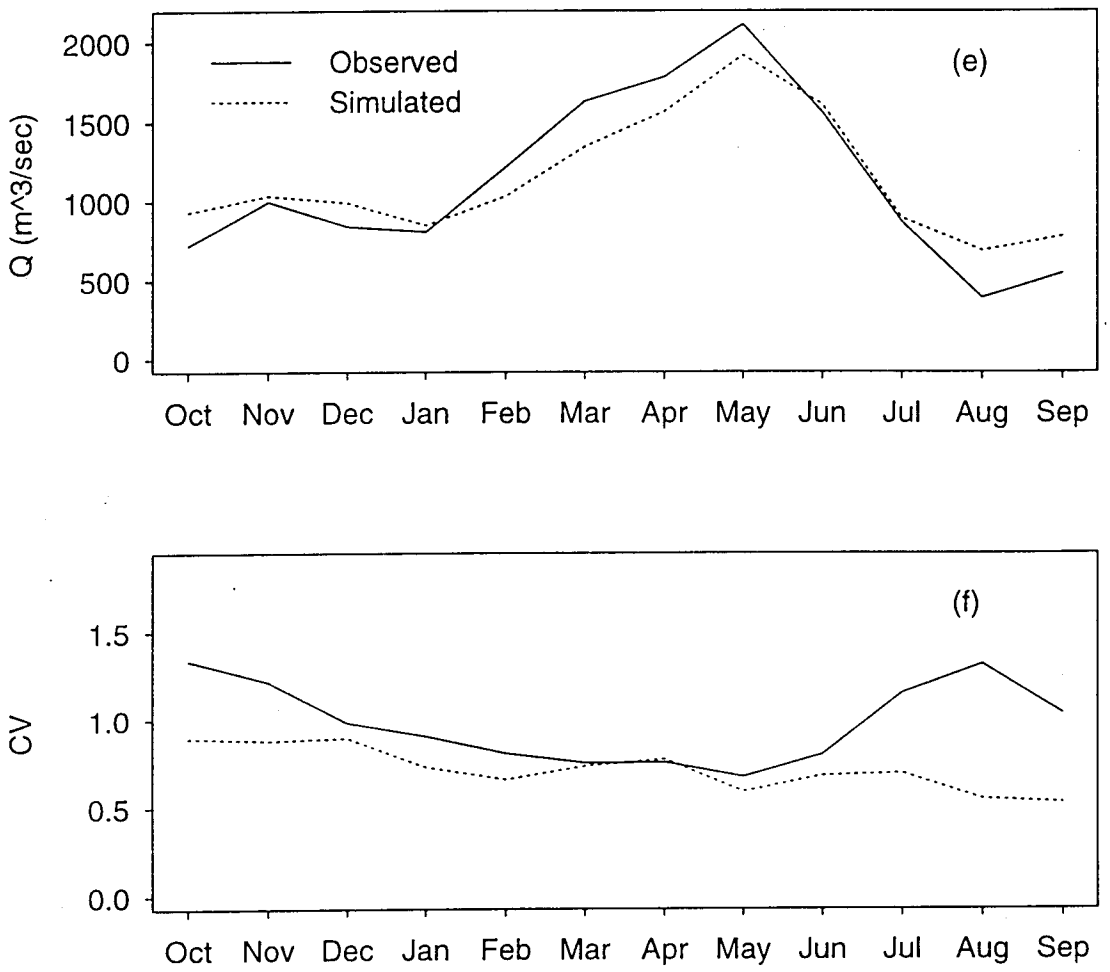

Fig. 5.14 (contd) (e) mean monthly streamflow for the period (1948-1986); (f) coefficient of variation of monthly streamflow for the period (1948-1966)

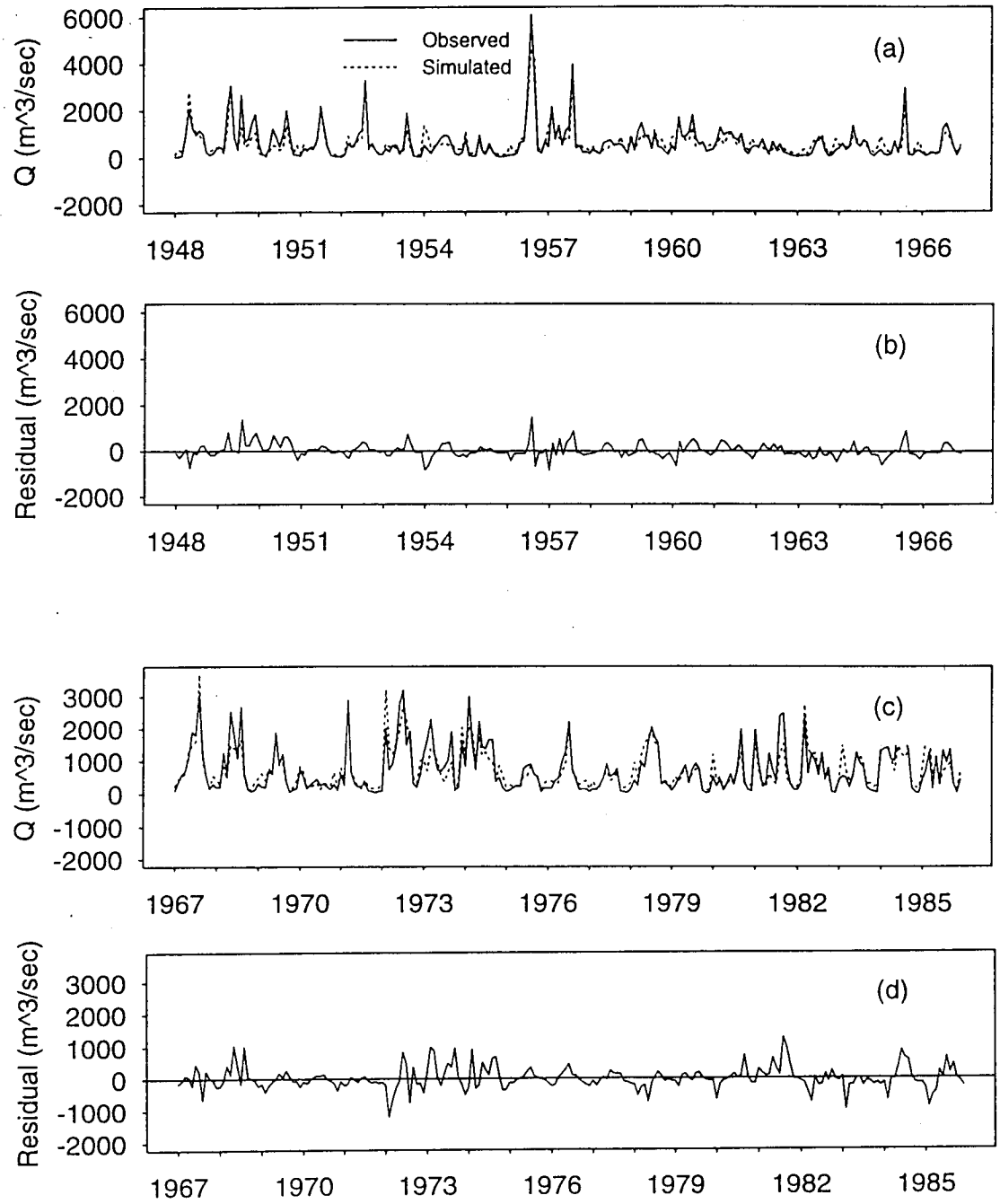

Fig. 5.15 Observed and simulated monthly streamflow for Red River using the regional parameters: (a) simulation period (1948-1966); (b) residual (1984-1966); (c) simulation period (1967-1986); (d) residual (1967-1986)

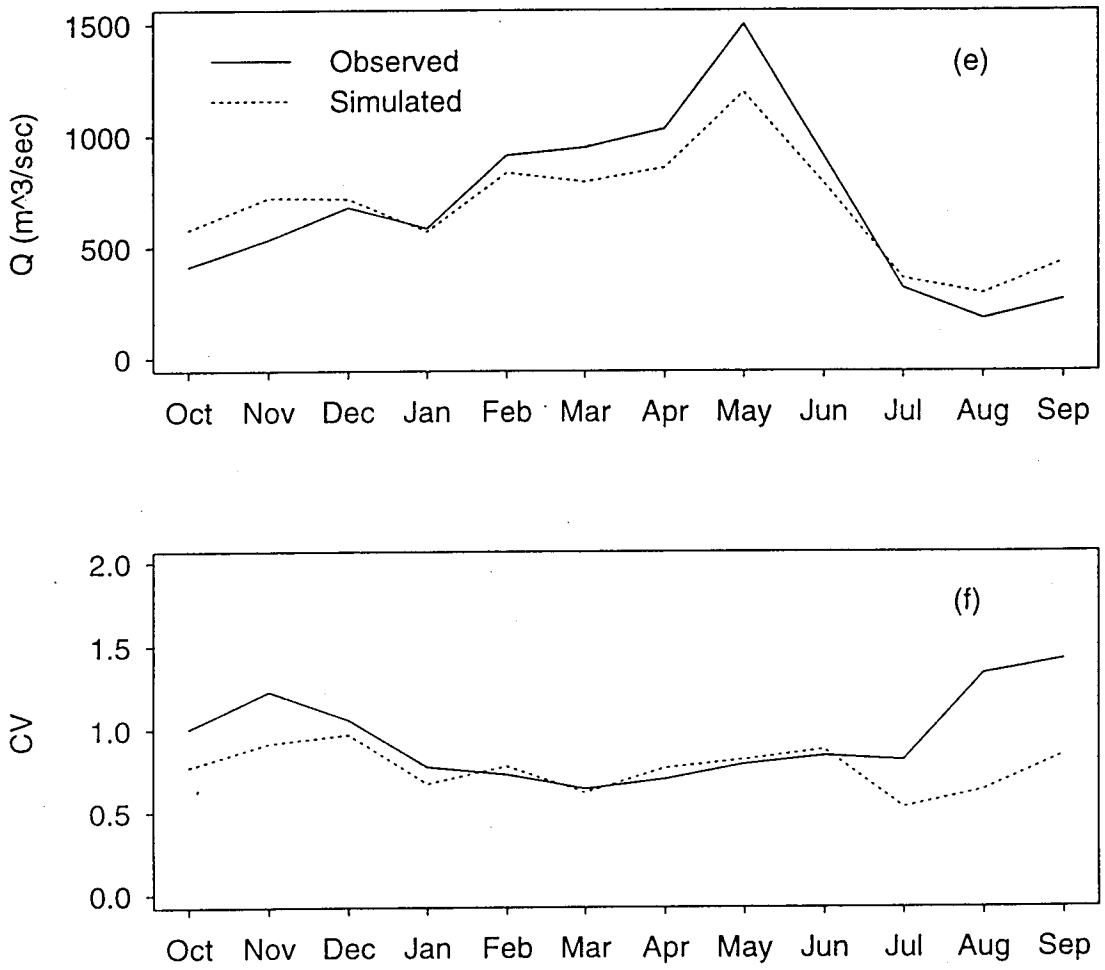

Fig. 5.15 (contd) (e) mean monthly streamflow for the period (1948-1986); (f) coefficient of variation of monthly streamflow for the period (1948-1966)

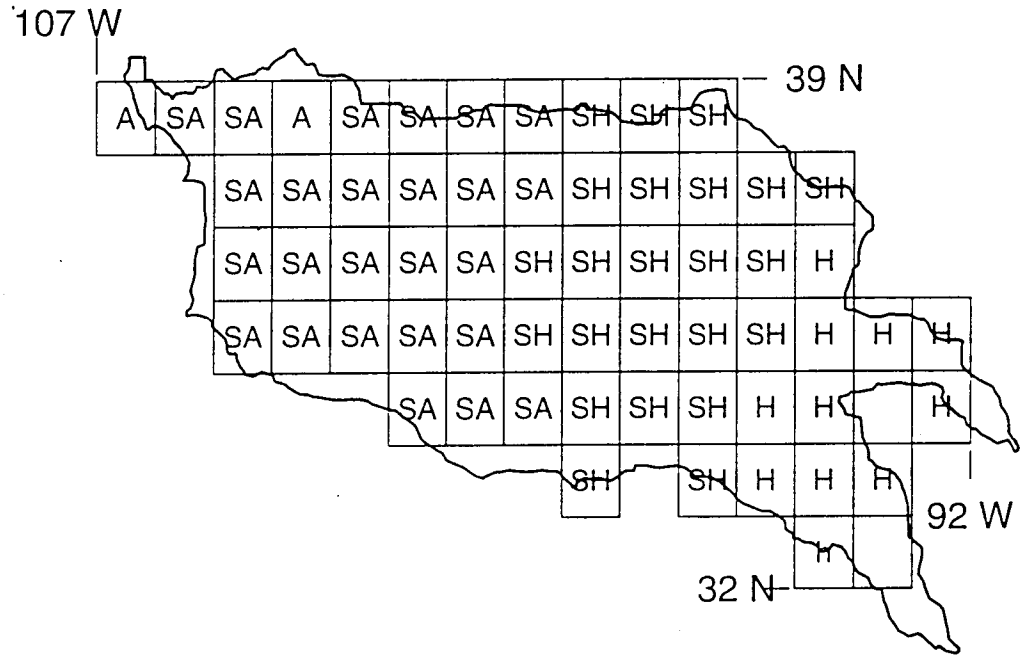

Fig 5.16 Climate classification: i) A: Arid (Annual Precipitation ($\bar{P}$) ≤ 280 mm); ii) SA: Semi-arid (280 mm $< \bar{P} \leq 600$ mm); ii) SH: Sub-humid (600 mm $< \bar{P} \leq 1000$ mm); iv) H: humid ($\bar{P} > 1000$ mm)

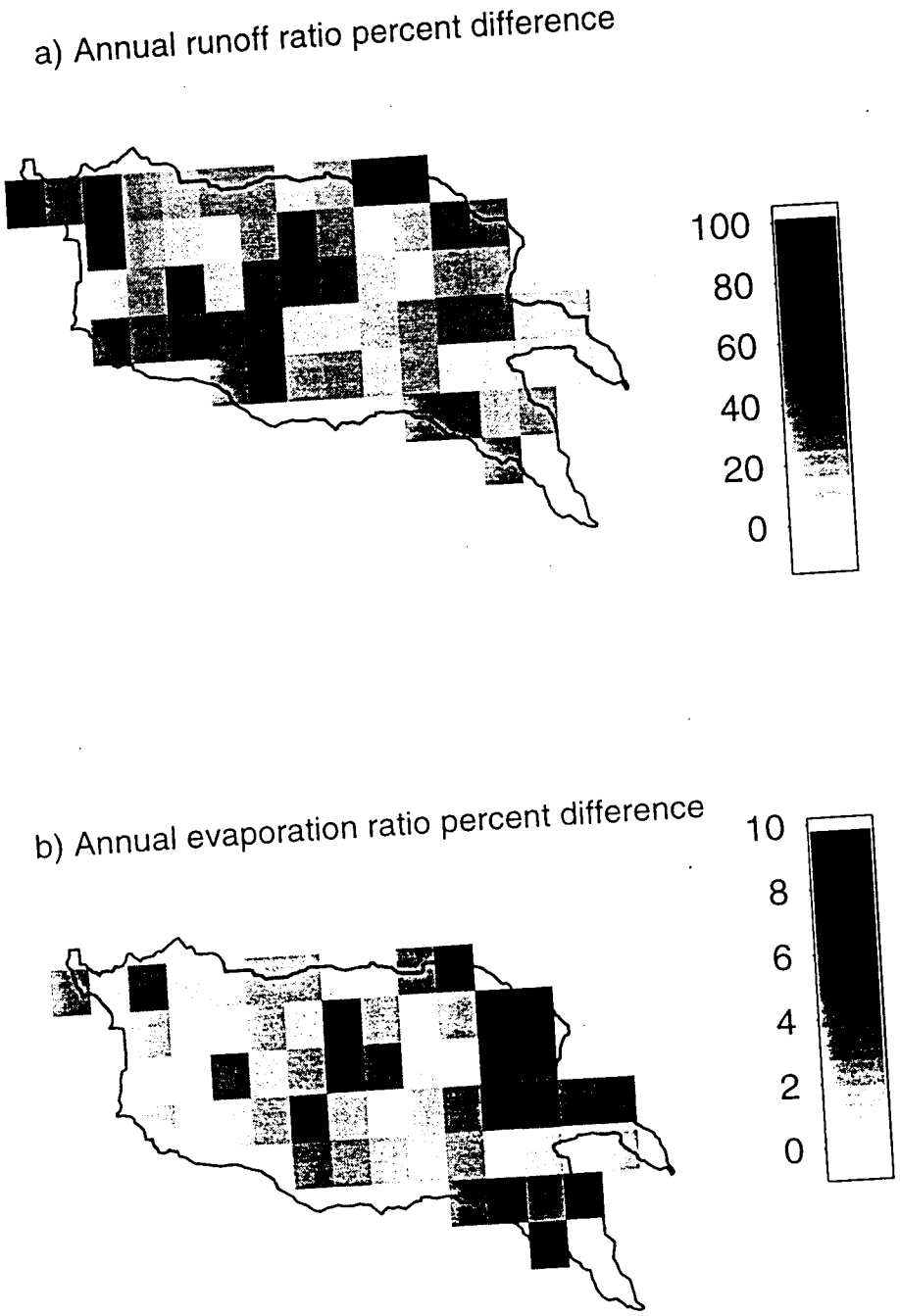

Fig 5.17 Spatial distribution of percent differences in a) annual runoff ratio obtained using the interpolated and regional parameters; b) annual evaporation ratio obtained using the interpolated and regional parameters

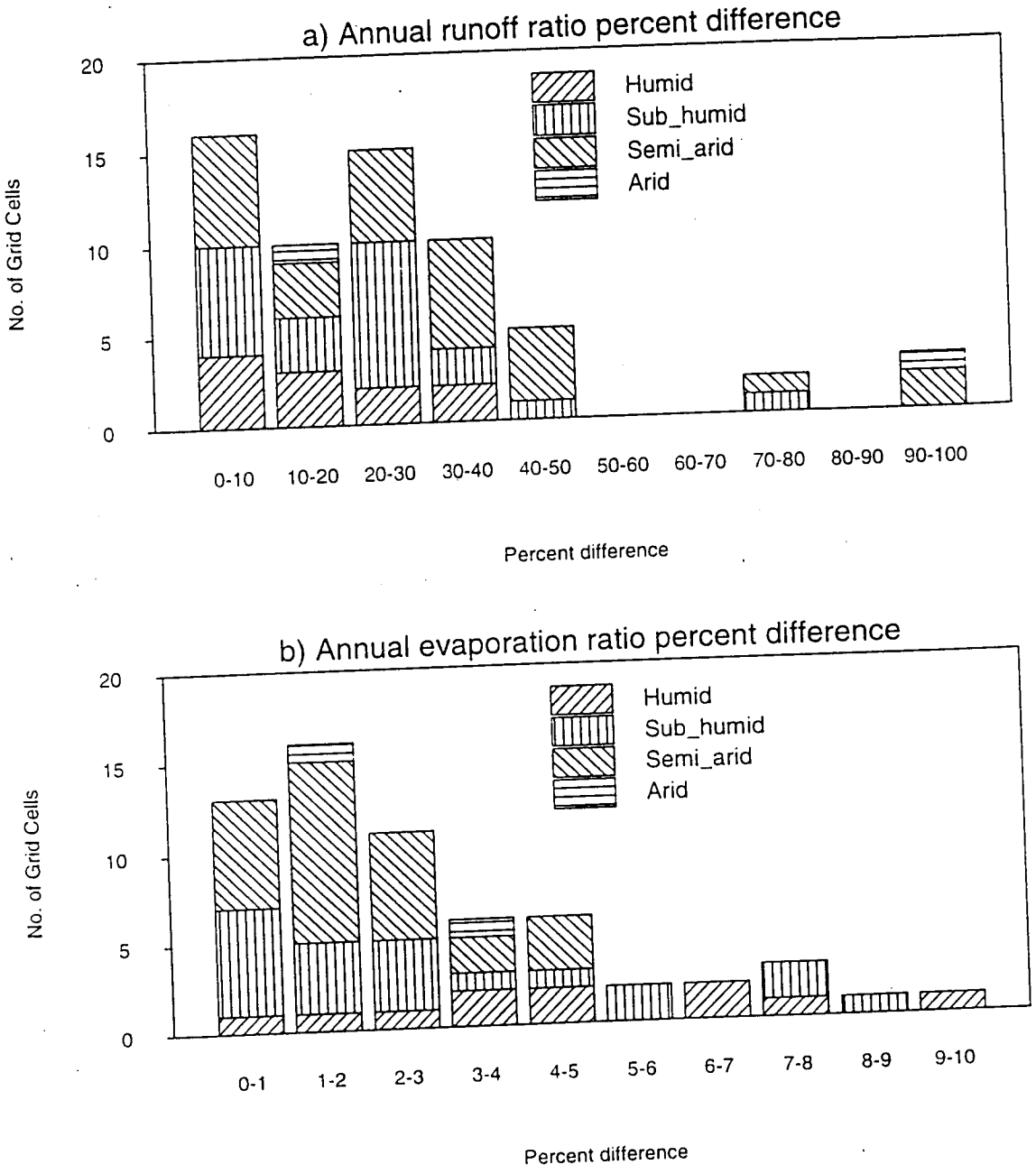

Fig 5.18 Histogram of percent difference in a) annual runoff ratio obtained using the interpolated and the regional parameters; b) annual evaporation ratio

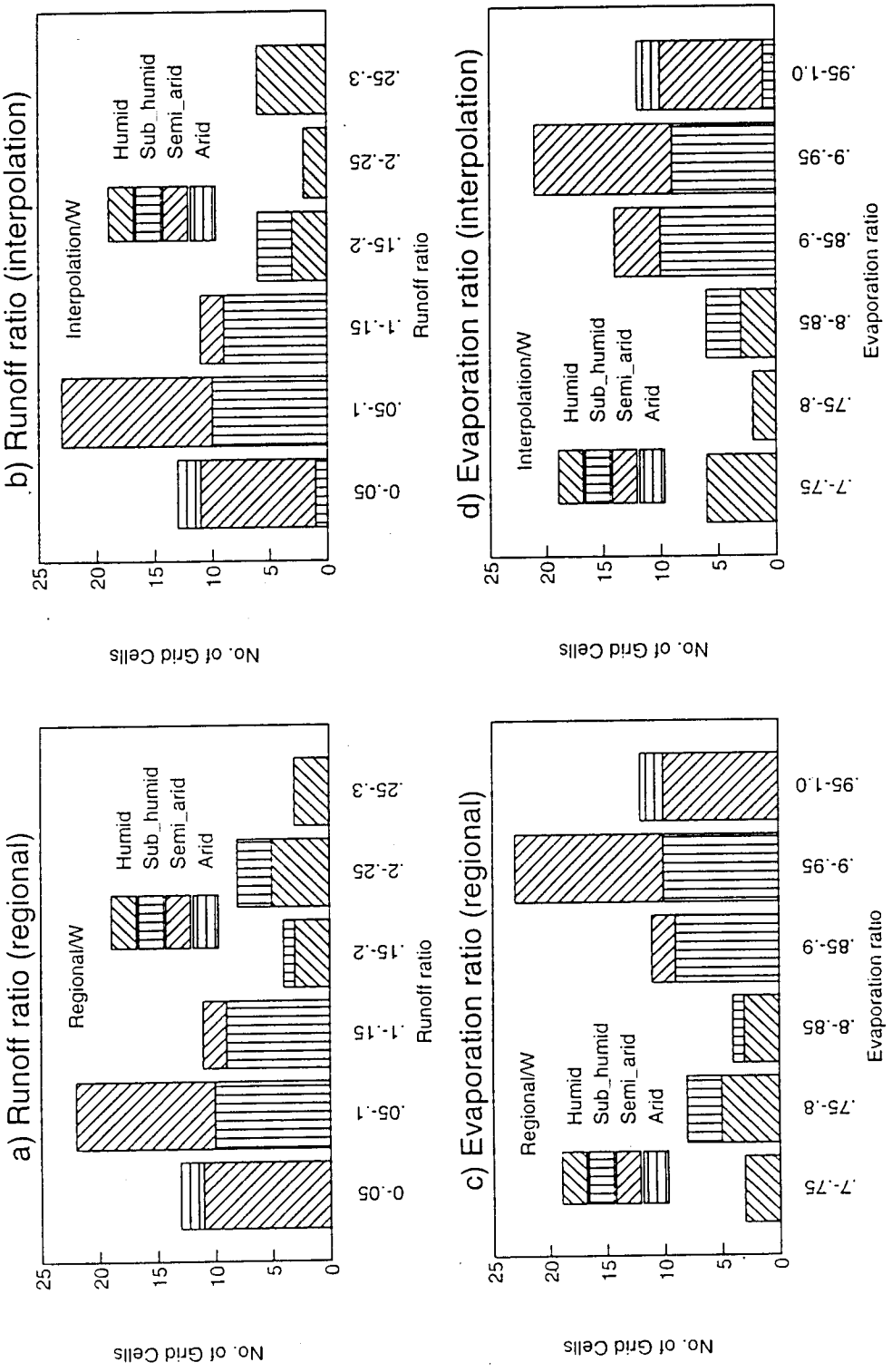

Fig 5.19 Simulated annual a) runoff ratio using interpolated parameters; b) runoff ratio using regional parameters; c) evaporation ratio using interpolated parameters; d) evaporation ratio using regional parameters

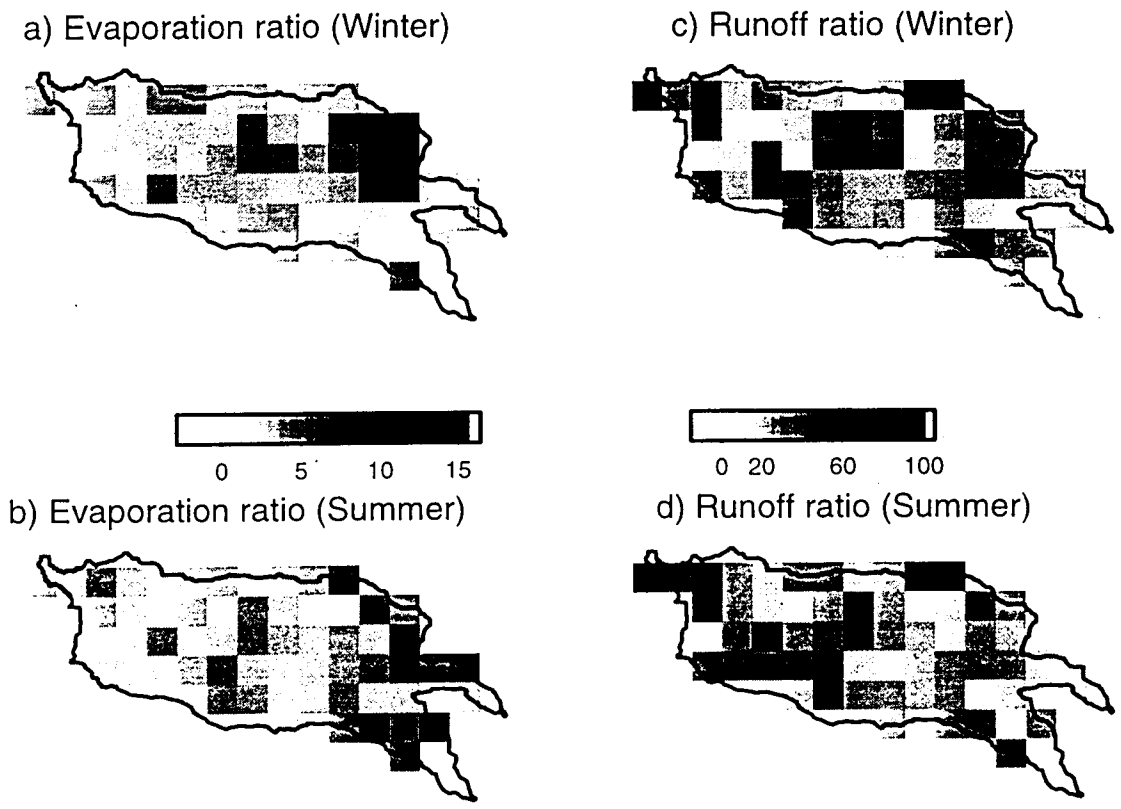

Fig. 5.20 Spatial distribution of percent difference in: a) winter evaporation ratio; b) summer evaporation ratio; c) winter runoff ratio; and d) summer runoff ratio using regional and interpolated parameters

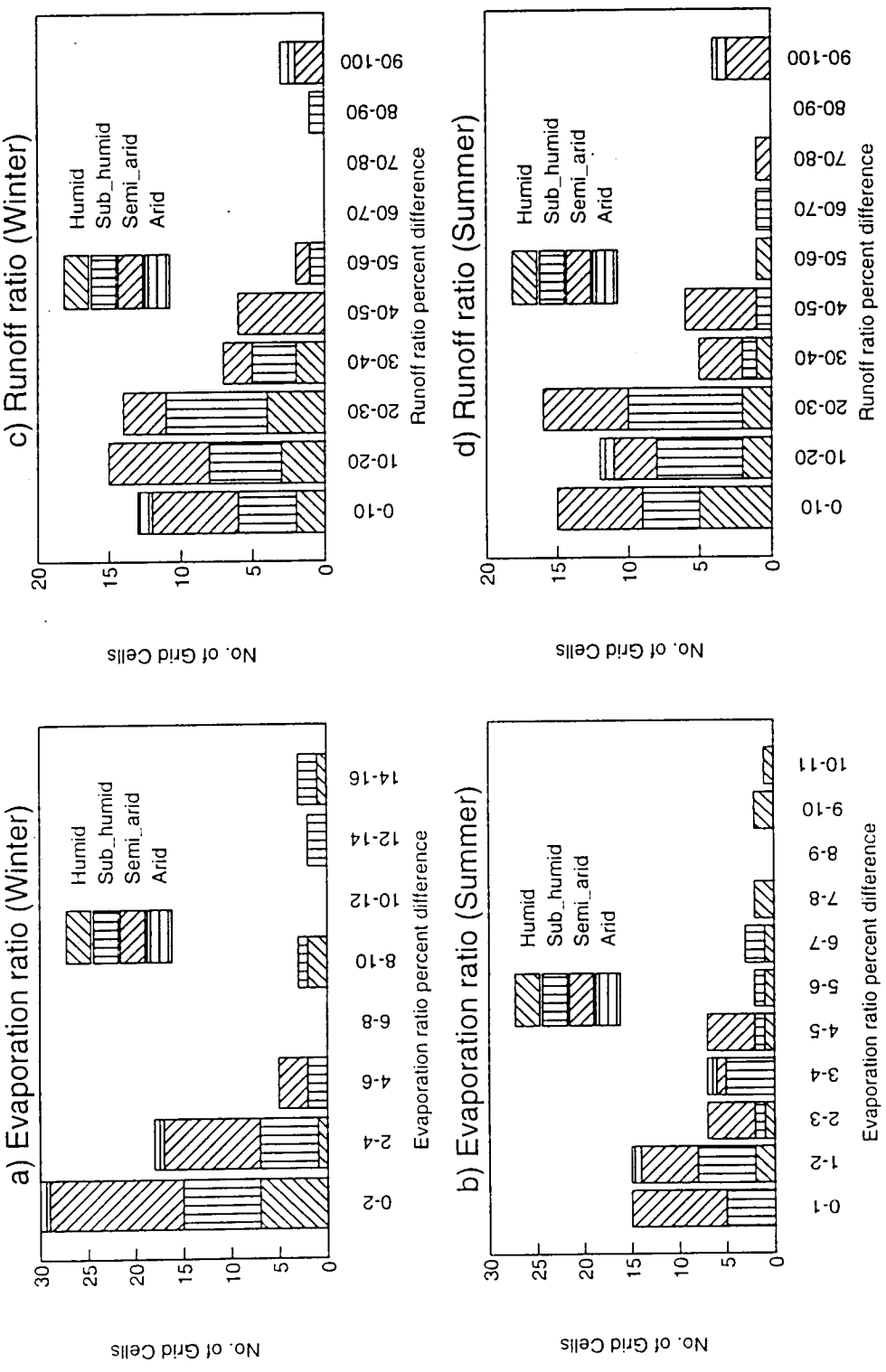

Fig. 5.21 Distribution of percent difference in a) winter evaporation ratio; b) summer evaporation ratio; c) winter runoff ratio; and d) summer runoff ratio using regional and interpolated parameters

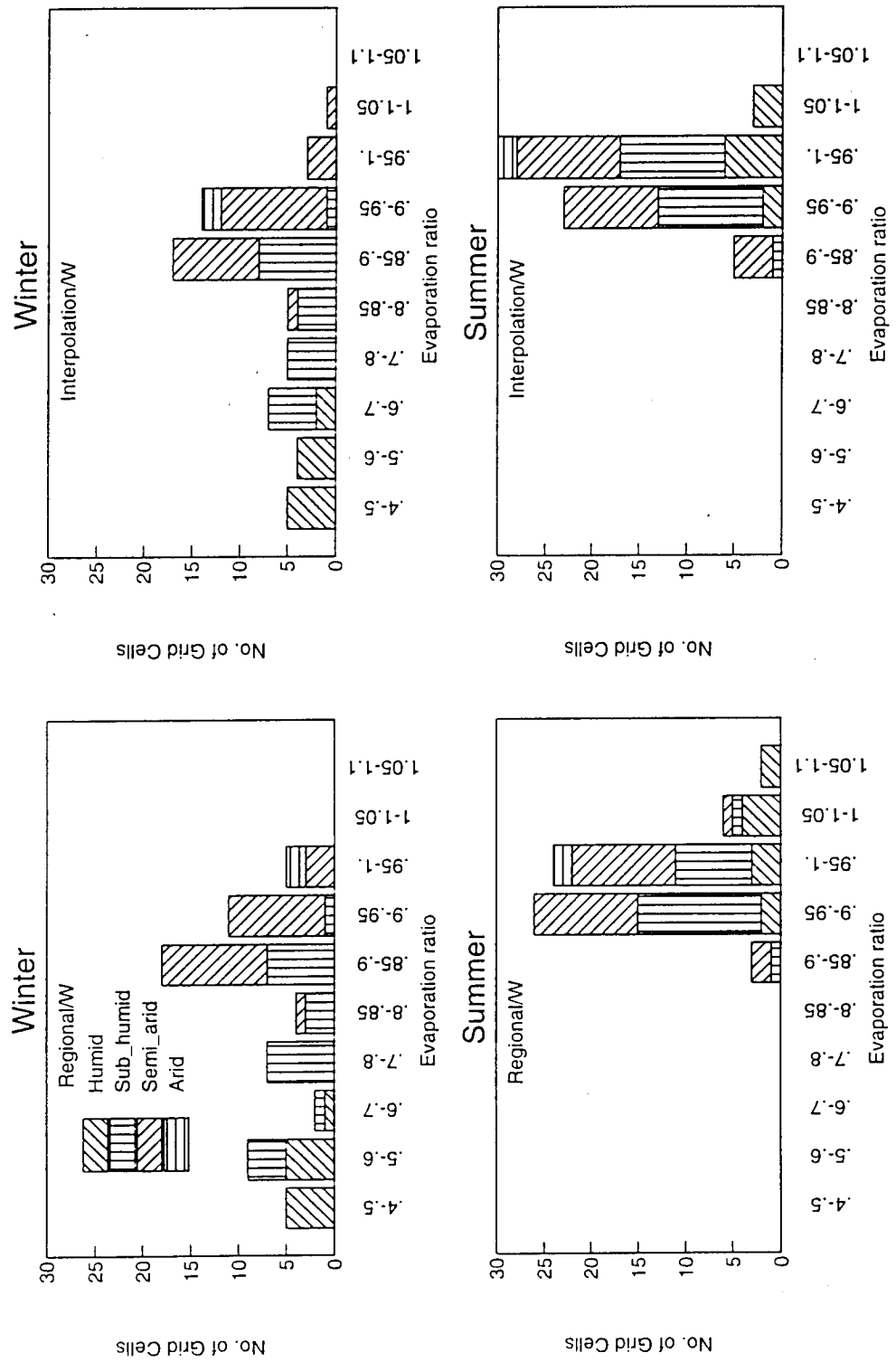

Fig. 5.22 Distribution of winter and summer evaporation ratios using regional and interpolated parameters

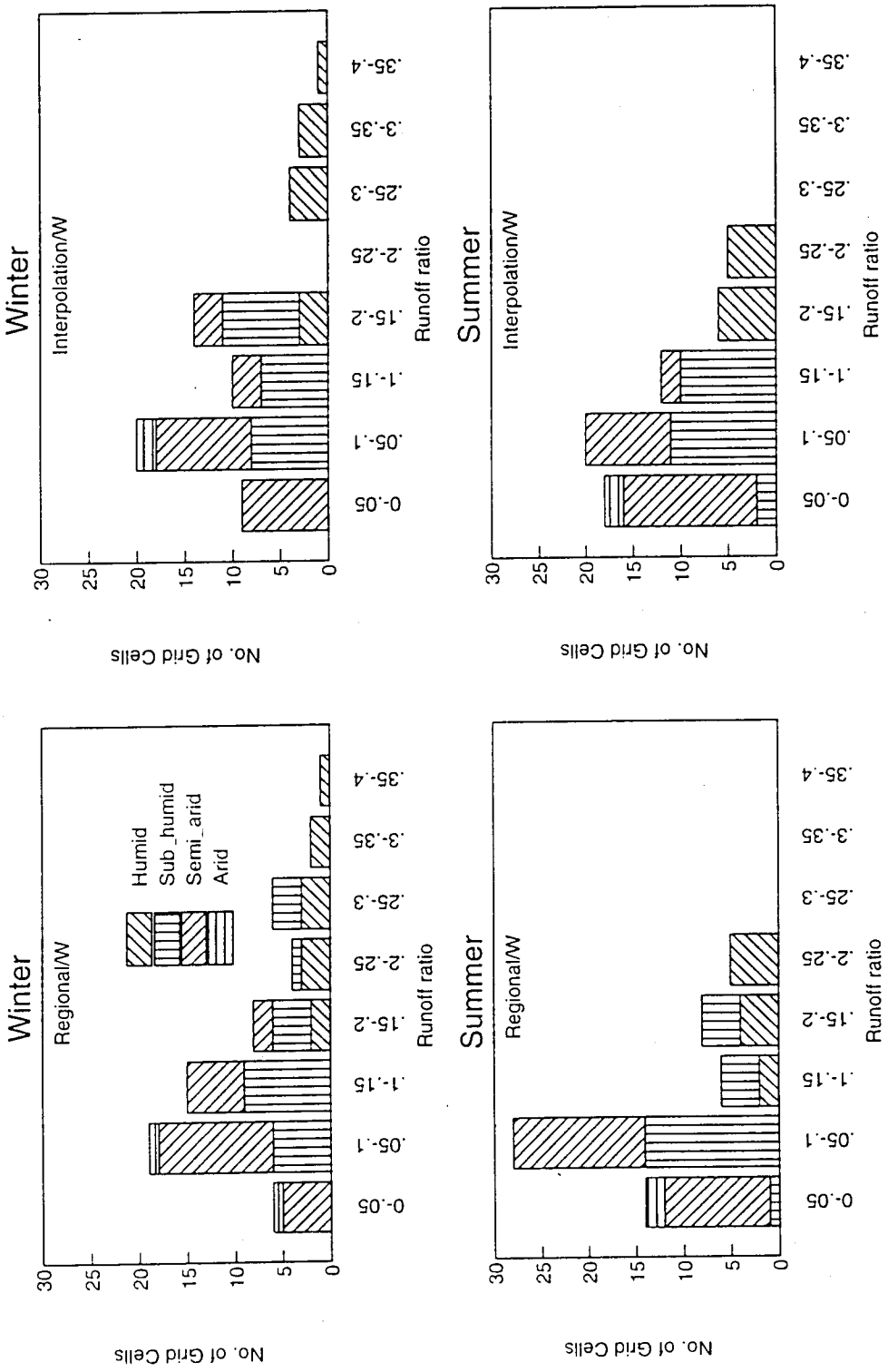

Fig. 5.23 Distribution of winter and summer runoff ratios using regional and interpolated parameters

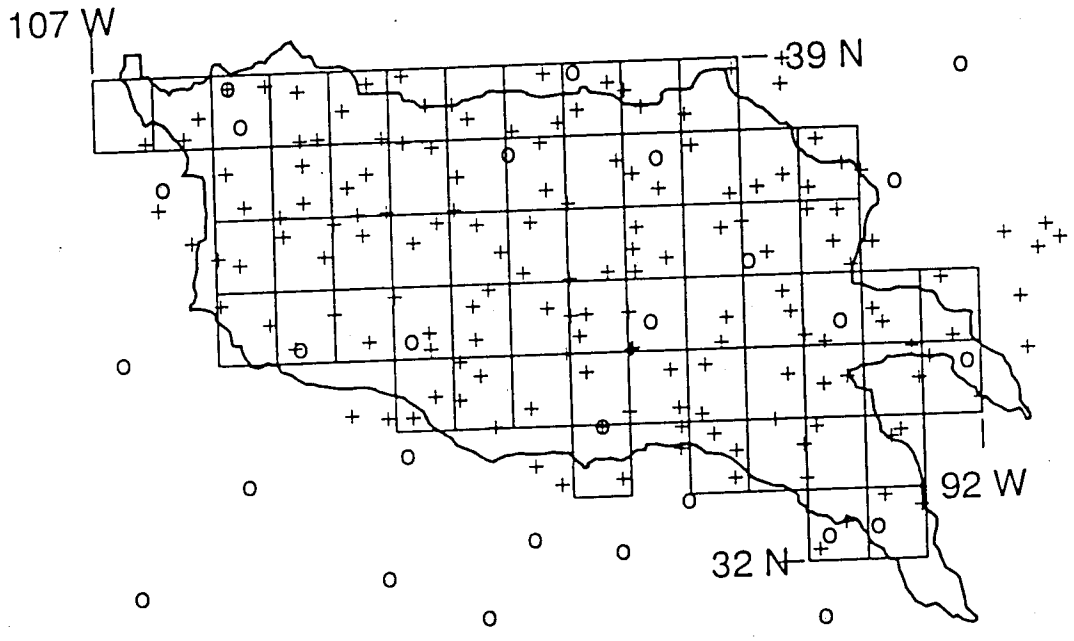

Fig. 5.24 Location of Surface Airways stations

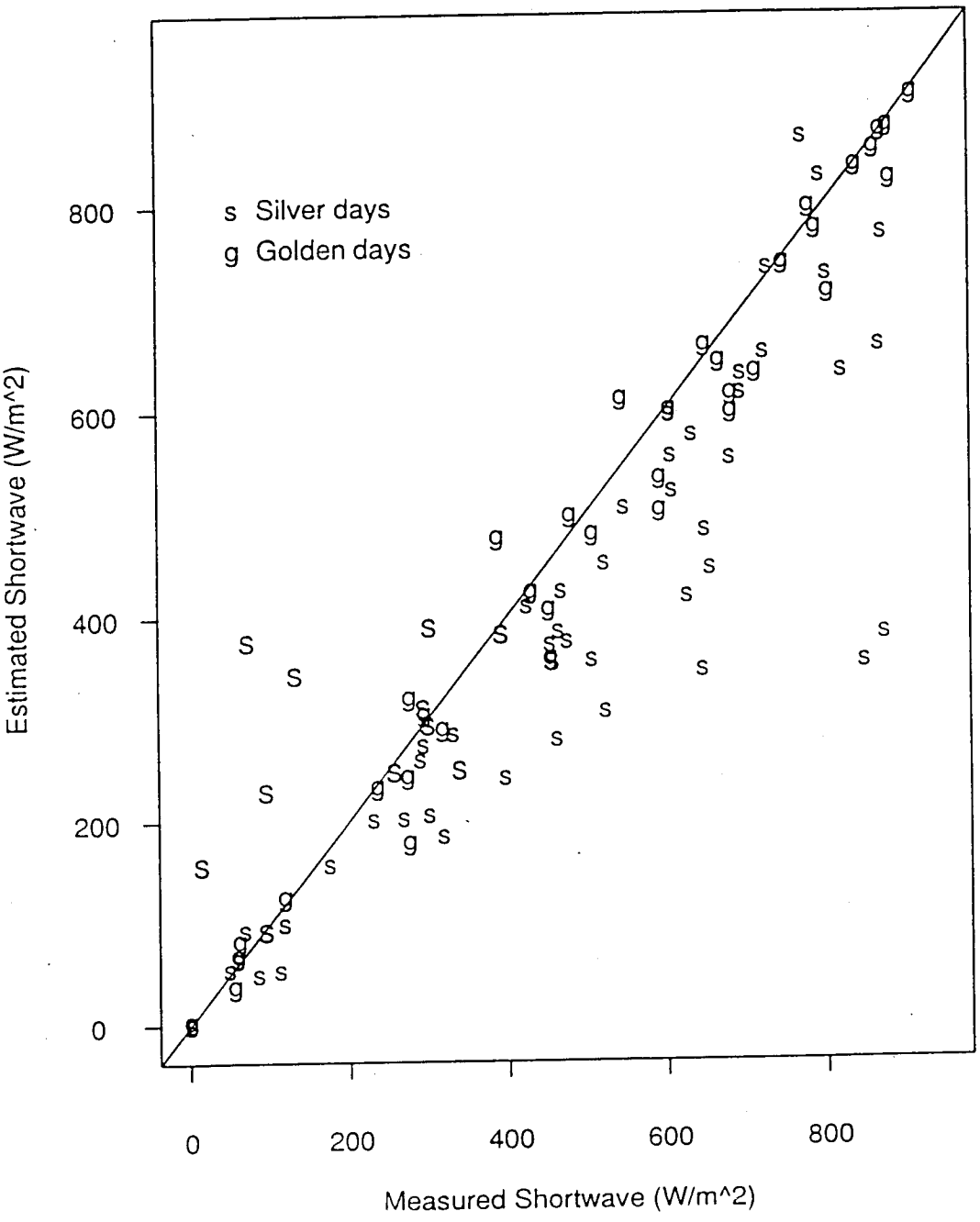

Fig. 5.25 Estimated and observed hourly incoming shortwave radiation, for a number of days of the summer 1985, at the FIFE site, Kansas

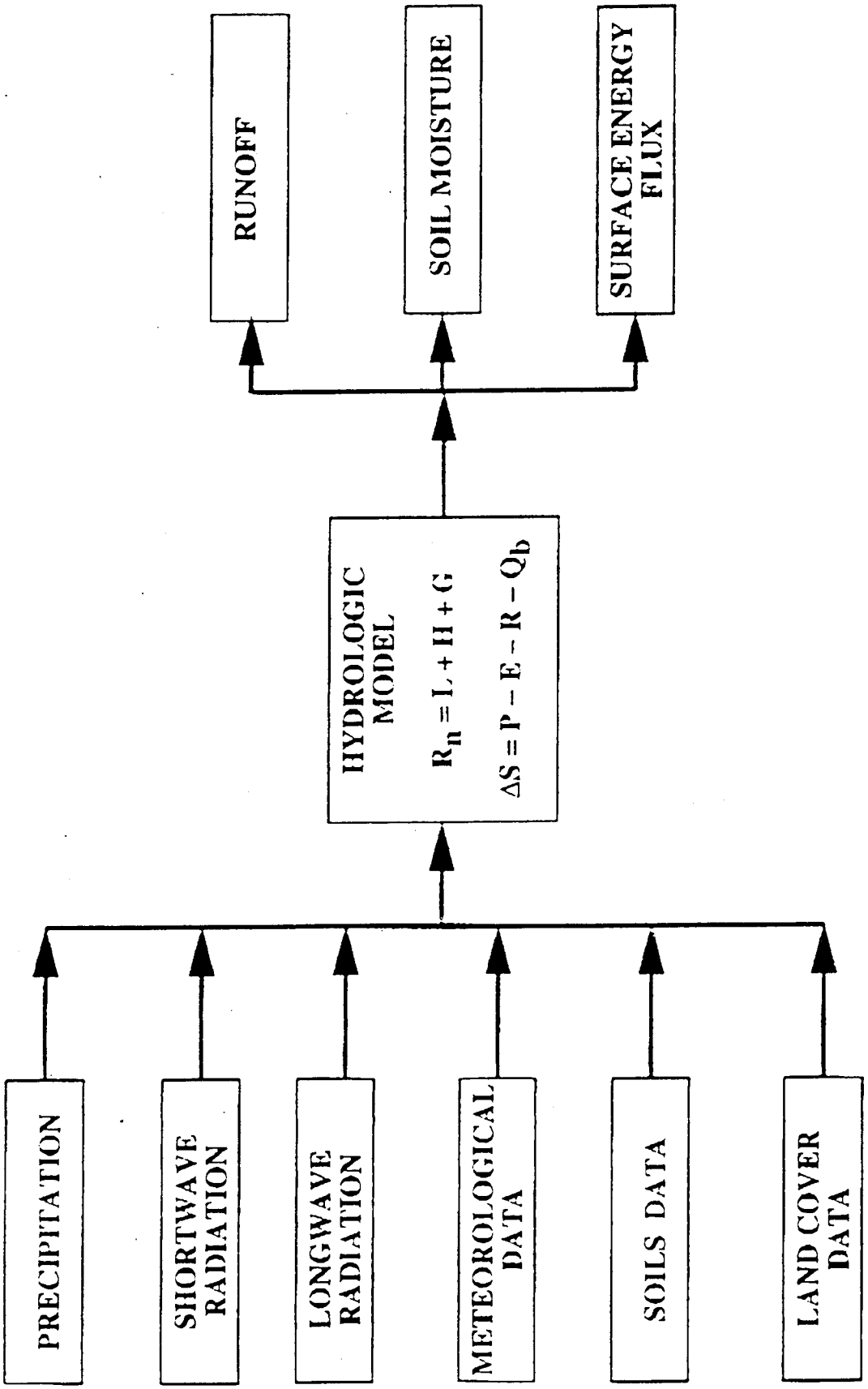

Fig. 5.26 Forcing data and output of the VIC-2L model

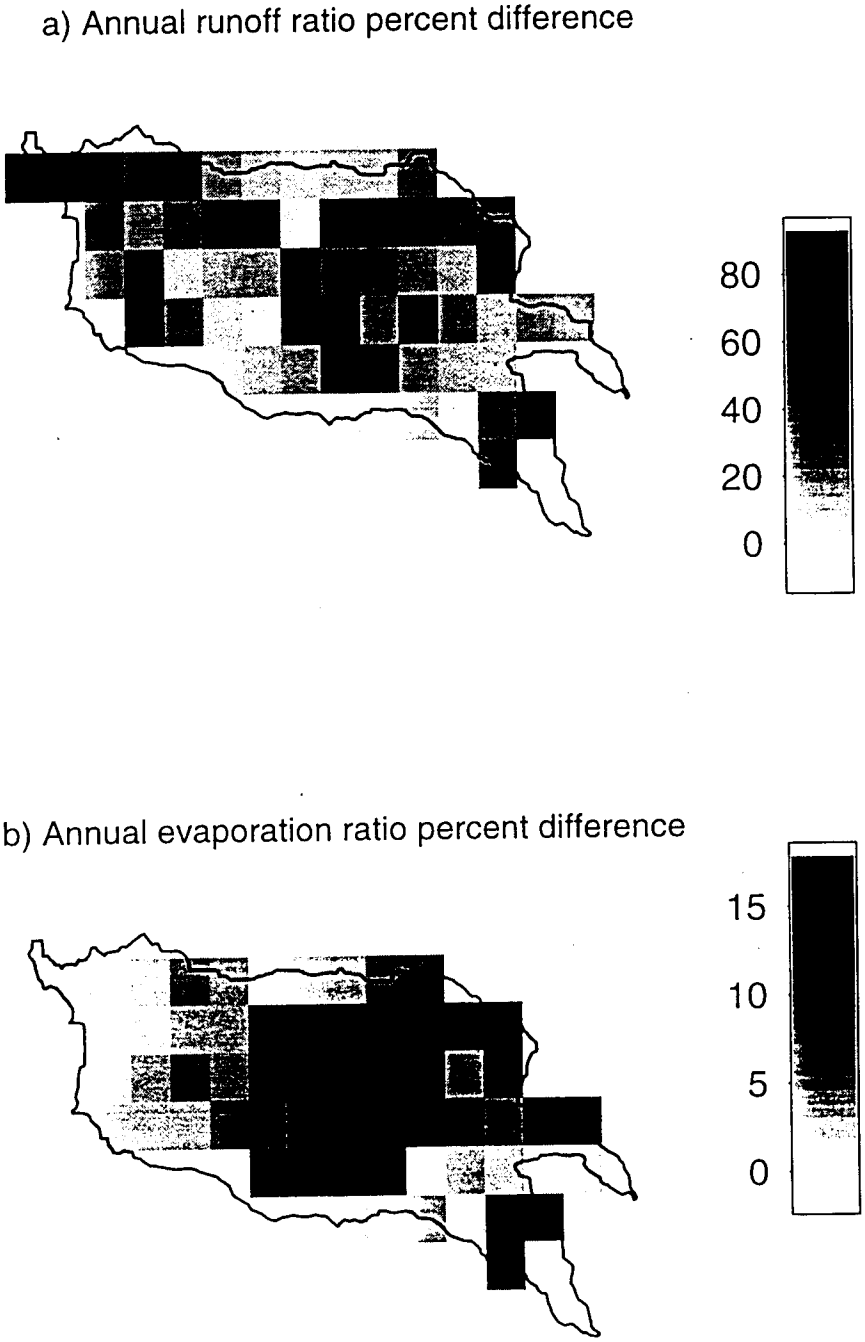

Fig 5.27 Spatial distribution of percent difference between water balance and full-energy balance runs: a) annual runoff ratio; and b) annual evaporation ratio

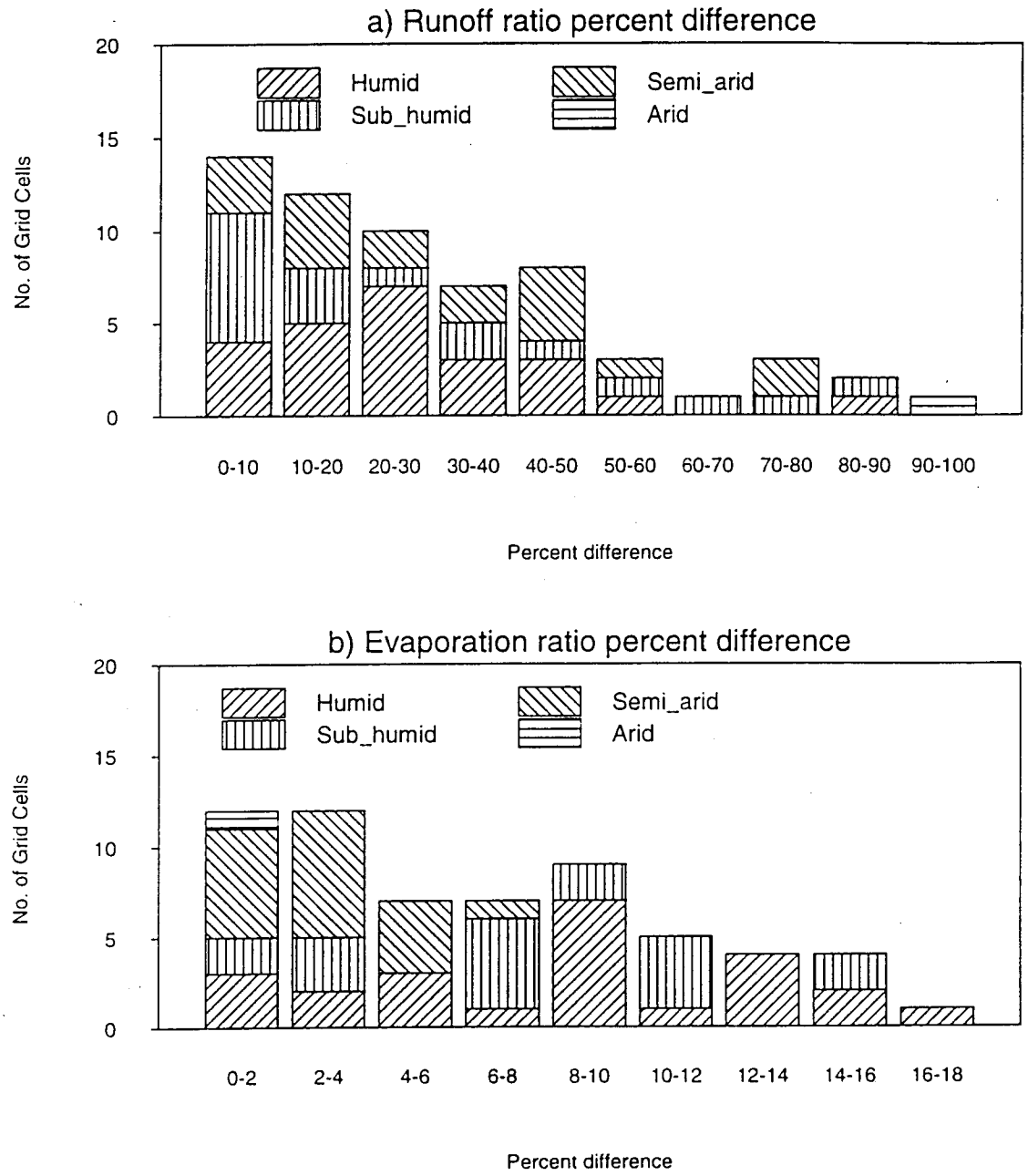

Fig 5.28 Histograms of percent difference between water balance and full-energy balance runs: a) annual runoff ratio; and b) annual evaporation ratio

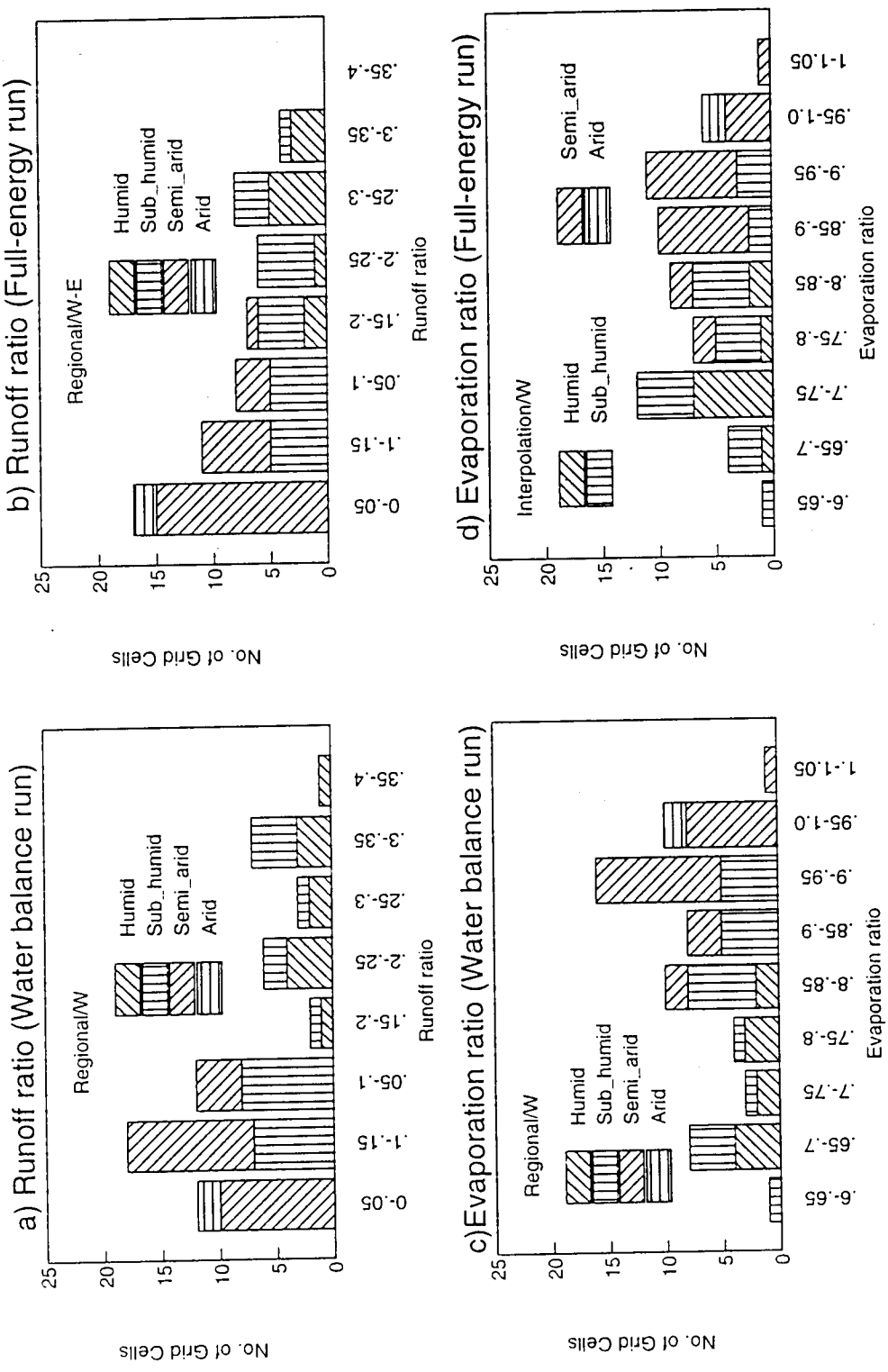

Fig. 5.29 Histograms of annual runoff and evaporation ratios using water balance and the full-energy balance runs

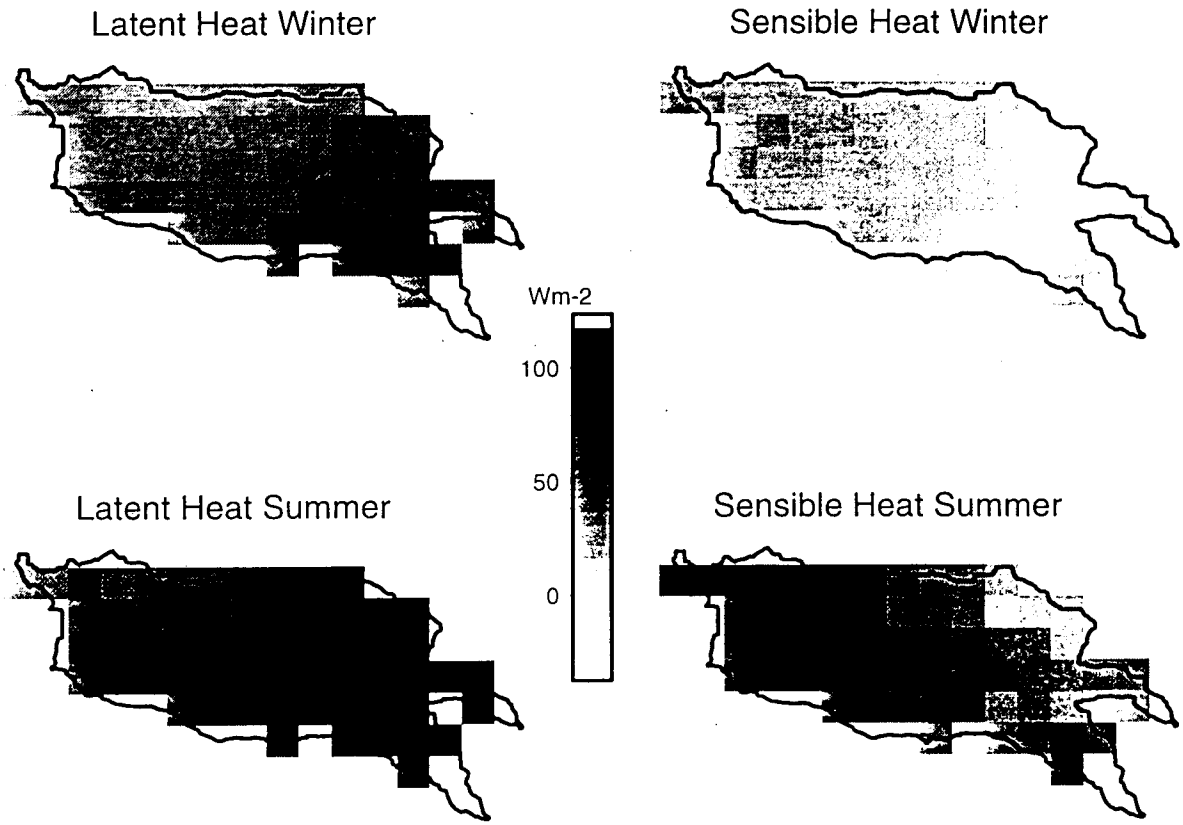

Fig. 5.30 Distribution of mean winter and summer latent and sensible heat fluxes

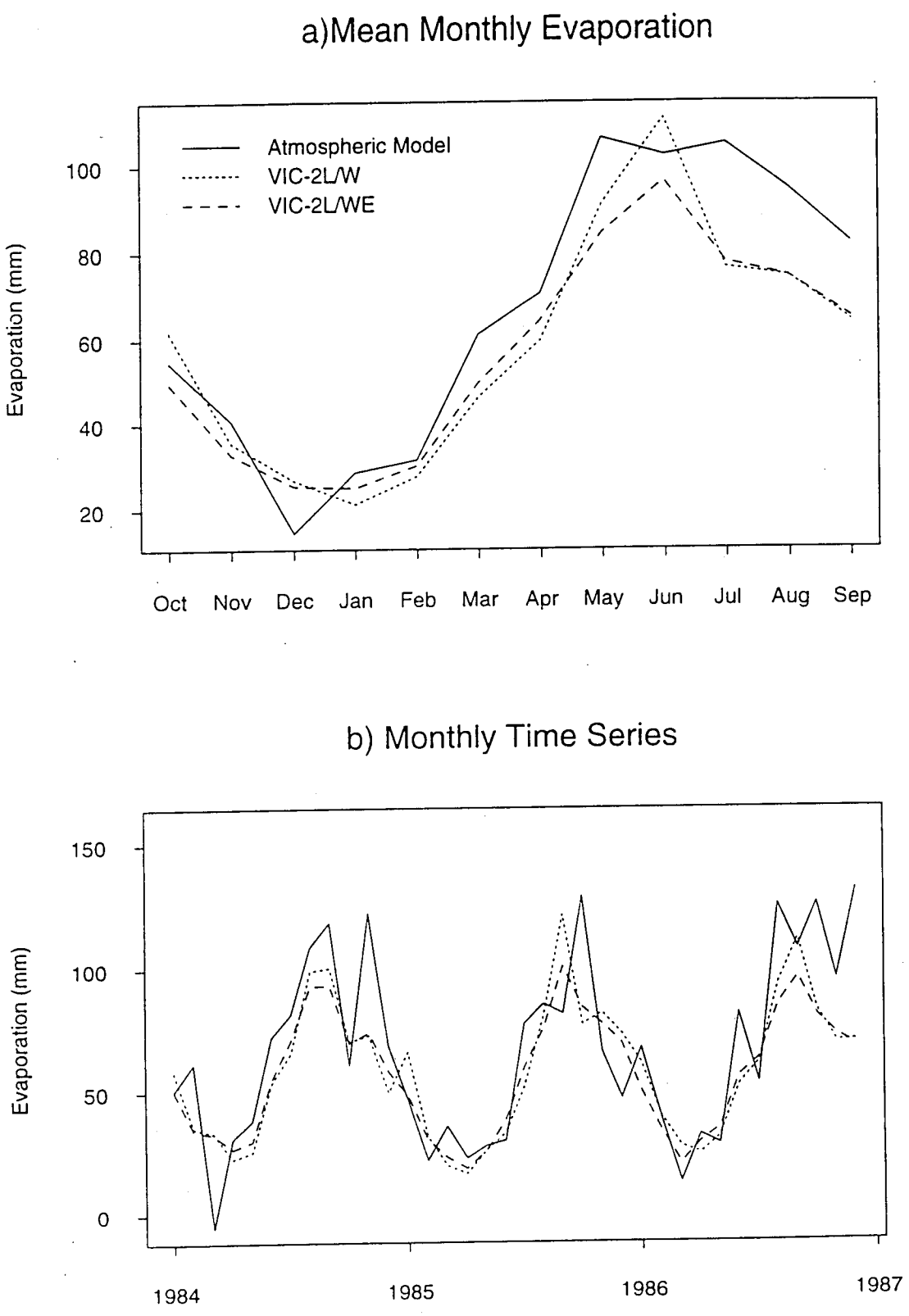

Fig. 5.31 Comparison VIC-2L and atmospheric budget evaporation estimates for Arkansas-Red River basin: a) mean monthly evaporation, b) monthly time series

CHAPTER 6 CONCLUSIONS AND RECOMMENDATIONS FOR FUTURE WORK

6.1 Summary

Large scale hydrology problems place a new set of demands on hydrologic models. Estimation of parameters for macroscale land surface schemes applicable at the scale of general circulation models used for numerical weather prediction models and climate simulation poses formidable challenges. In large scale applications, the hydrological parameters of land surface schemes, such as the Variable Infiltration Capacity two-layer (VIC-2L) model, have been either fixed globally at "reasonable" values, or they have used "literature values" for the appropriate land cover. Better methods of estimating parameters of macroscale models are obviously needed. The use of regionalization methods, using local parameters estimates and distributed land surface characteristics data bases, offers one possibility.

In addition, determining the space-time variability of hydrological processes and energy fluxes over a continental scale area is a challenging task because the fluxes of heat and moisture across the land/atmosphere interface may vary over a range of spatial scales due to the inhomogeneity of land surface. Accordingly, developing and testing macroscale hydrological models appropriate for modeling the water and energy fluxes at the scale of large continental rivers (for example, the Arkansas-Red River basin) are needed. For reliable estimates of these fluxes at the LSA, the information gained from the application of the macroscale hydrological model at intermediate scale area (ISA) catchments must be incorporated at the LSA application. An example of such information is the spatial variability of the parameters of the macroscle hydrologic model within the LSA.

A methodology has been presented for regionalization of the parameters of the VIC-2L land surface hydrologic model for the GCIP Southwest Large Scale

Area (LSA-SW) which essentially comprises the Arkansas-Red River basin. The approach is based on direct estimation of the hydrologic parameters of the VIC-2L model using station hydrologic and meteorological data for a set of catchments. Two alternative approaches for estimation of the parameters of the VIC-2L model were investigated. The first method, complete optimization, estimates all model parameters simultaneously using a search procedure. The second method uses spatially distributed soil data directly to determine selected parameters of the VIC-2L model with the remaining parameters determined using a search procedure. Key components of the methodology are extraction from the STATSGO data base of soil attributes used to determine two of the model parameters. The simulated hydrographs as well as performance criteria of the two methods for the model compared well. Therefore, the estimated parameters using the sub-optimization method (STATSGO in conjunction with search procedure) were used in the regional methodology described in the Chapter 4. This means that only seven of the VIC-2L model parameters needed to be investigated for a possible regional equation and the remaining three can be obtained directly from the available distributed soil data. The two-stage optimization worked reasonably well as indicated by different performance measures. For example, the mean of the R^2 between the observed and simulated streamflow for 14 of the catchments was 0.75 for the complete optimization and 0.69 for the two-stage optimization. The mean absolute relative error for the two methods was similar (3% and 9%, respectively), even though higher objective function values resulted for the two-stage method, the two-stage procedure yielded a substantial reduction in the number of iterations (by a factor of 5, on average).

Regional equations were developed to relate the VIC-2L model parameters to measurable physical quantities included in data bases such as digital elevations, climatological data, and the U. S. Soil Conservation Service STATSGO soils data base. The optimum parameters of the VIC-2L model for 34 catchments in the Arkansas-Red basin were used as dependent variables in regression equations. The independent variables represent easily determinable watershed characteristics. The relationships provide means by which the

parameters of rainfall-runoff models can be estimated in the absence of local hydrological data. The approach was tested by application of the regionally estimated parameters to catchments not in the data set used to estimate regional parameters.

In addition, three applications of a grid network version of the two-layer Variable Infiltration Capacity (VIC-2L) model applied at one degree resolution were presented. These applications were illustrated for the Arkansas-Red River basin. In the first application the grid network model was run off-line at a daily time step, forced by precipitation and potential evapotranspiration computed using a temperature-based algorithm. The gridded hydrologic parameters of the VIC-2L model were estimated using two approaches. The first is the STATSGO based approach. The second is linear interpolation of locally optimized parameters for the 40 calibrated ISA catchments.

In the second application, the model was also run at a daily time step, but in this case the gridded hydrological parameters were estimated using both the STATSGO based approach and the regional equations developed in Chapter 4. The purpose of this application is to test the performance and the ability of the VIC-2L model (using the regional parameters) to simulate the large scale water balance components.

In the third application the VIC-2L model was tested for its ability to simulate large scale sensible and latent heat fluxes in the Arkansas-Red River basin. In this application the full energy balance version of the model was used. The model was run off-line at a three hour time step, forced by gridded station data from surface airways data (including wind speed, relative humidity, temperature, surface pressure and total sky cover) as well as incoming longwave and shortwave radiation estimated using an empirical methods.

6.2. Conclusions

The major conclusions of this research are:

(1) A regression approach was used to predict the parameters of a coupled

water and energy balance model applicable to continental rivers. For the Arkansas-Red River basin, the regression equations explained about 45 to 76 percent of the variation in the parameters of the VIC-2L model.

(2) Of the ten soil attributes and twelve climatological characteristics tested as candidate explanatory variables in the regional equations, the saturated hydraulic conductivity (k_s), the average permeability (Pr), and the hydrologic group B soil (Hgb) were the most important soil attributes. Storm interarrival time, and mean annual temperature were also important explanatory variables.

(3) the spatial distribution of several of the VIC-2L parameters (including the infiltration parameter and the maximum baseflow parameter) are controlled by the climatological and the topographic gradient in the Arkansas-Red River basin.

(4) The model performance, tested by comparing observed and simulated runoff records from 6 watersheds not included in the 34 calibration watersheds, was generally quite good for humid and sub-humid catchments. However simulations of streamflow for the arid and most semi-arid catchments were generally poor.

(5) Simulated monthly mean hydrographs for the Arkansas-Red River basin using regional parameter estimates were in reasonably good agreement with the observed hydrographs, although the seasonal peak flows (late spring) tended to be underestimated, and the fall and winter low flows overestimated. The magnitude of the bias is less for the humid, eastern part of the basin than the more arid west.

(6) The evaporation predicted by the VIC-2L model compared well with that derived from an atmospheric moisture budget of the Arkansas-Red River basin; the evaporation budget was relatively insensitive to the two forms of regional parameter estimates that were tested. However, there were significant differences in the means of the water balance components for individual grid cells. The largest relative differences in the runoff ratios occurred in the most

arid part of the region, while the largest differences in the evaporation ratios occurred in the humid area. These results indicate that the hydrological processes in the Arkansas-Red River basin are mainly water rather than energy limited, especially at the annual scale.

6.3. Recommendations for future work

The results of this study suggest a number of research topics related to the current work that are worthy of future exploration. Six specific suggestions for follow up work related to model validation and implementation of the results of this work into GCMs simulations are described briefly.

6.3.1 Calibration

The catchments for which the VIC-2L model performance was worst were either snow dominated or arid. The model needs to be tested for more catchments with these characteristics, with the following considerations:

i) In the case where meteorological data are not available to calculate E_p via the Penman-Monteith method, it is recommended to use the Hargreaves's (1985) equation instead of Hamon's (1961) equation (both are temperature index methods). This should eliminate the use of the scaling factor for E_p. Preliminary analysis of the Hargreaves equation indicates that it gives estimates of E_p comparable with those obtained using the Penman equation.

ii) The difficulty in obtaining good calibration results in arid and semi-arid areas may be related to the optimization criteria used which depend entirely on minimizing the difference between the observed and simulated runoff. In these areas where the annual runoff ratios are small (e.g. less than 0.15), calibration using streamflow data alone may be insufficient. One solution may be to include the estimated actual evaporation (where available) as another optimization criteria.

iii) It is preferable to use the reparameterized drainage parameters of the VIC-2L model as suggested by Abdulla and Lettenmaier (1995b) in parameter search procedures.

6.3.2 How sensitive would the VIC-2L be to the STATSGO attributes?

Another area that should be investigated is the sensitivity of the regional parameters to the soil attributes used as explanatory variables. In other words, if data for catchments or grids were obtained using different spatial sampling, how would this affect the resulting parameters, and how sensitive would the VIC-2L model performance be to the changed parameters? In addition, detailed analyses are needed to assess the accuracy of the STATSGO derived soil attributes. Two types of analyses may be possible: i) to study the effect of different sampling resolution on the derived average values; and ii) to compare the difference in the derived soil attributes from STATSGO to those obtained from a high resolution data base. One possible data base that could be used is the Soil Survey Geographic (SSURGO) data base which is available for some parts of the Arkansas-Red River basin. The SSURGO data base provides the most detailed level of information and was designed primarily for farm and landowner, township, and county natural resources planning and management.

6.3.3 Spatial variability in the precipitation

This study did not deal with the issue of spatial variability in the precipitation, and for simplicity, only the spatial average values were used. The importance and effects of the spatial variability in precipitation on catchment hydrologic response have been addressed by various authors including Entekhabi and Eagleson (1989), Famiglietti and Wood (1990), and Henderson-Sellers and Pitman (1992). Liang et al. (1995) have developed a closed form derived distribution approach to account for the spatial variability of precipitation in the VIC-2L model. It would be of interest to evaluate the effects of precipitation spatial variability on the VIC-2L model predictions. One possibility is to use the hourly precipitation data from NEXRAD (Next Generation Weather Radar)

network of WSR-88D (Weather Surveillance Radar -1988 Doppler) radars which are available for most of the Arkansas-Red river basin at 4 km × 4 km resolution.

6.3.4. Validation of large scale surface fluxes

The regional parameter estimates for the VIC-2L model were only applied to Arkansas-Red River basin. It would be desirable to test the procedure for larger areas with different surface characteristics and climate conditions, such as snowmelt dominated areas. In addition, observed data, where available over a large area, should be used to validate the large scale fluxes such as those presented in Section 5.4. Large scale field studies which have included aircraft measurements of surface fluxes and soil moisture, research radars, and soundings could provide a useful data for the validation of these fluxes obtained in Section 5.4. An example is the data from HAPEX-MOBILHY (Hydrological Atmospheric Pilot Experiment) which were collected over an area on the order of 100 × 100 km.

6.3.5 Global transferability of VIC-2L model and implementation in GCMs

To test the global performance of the VIC-2L model, the effects of feedbacks from GCMs should be investigated. Therefore, implementation of the VIC-2L model into a GCM is a logical next step in the model's evaluation. Among the difficulties encountered during the implementation of a land surface scheme within a meteorological model are the specification of surface parameters over the entire simulation domain. The regional equations developed in this study can be used to assist in the specification of model parameters, especially if the training region is expanded.

6.3.6. Regional equations assuming two or more homogeneous regions

One of the difficulties in estimating regional parameters is parameter heterogeneity, especially in the recession part of the hydrograph. Clustering techniques might be a useful alternative to regression-based methods in this respect. For instance, catchments might be classified into, for example, three

groups, such as Group 1 for catchments that tend to be dominated by linear baseflow recession, Group 2 for catchments that tend to behave nonlinearly in the recession part of the hydrograph, and a third group for catchments that are dominated by both kind of recession sequences. Although this method has the potential for superior results, it requires a relatively large sample size.

REFERENCES

Abbott, M.B., J.C. Cunger, P.E. O'Connell, and J. Rasmussen, An introduction to the European Hydrological System- Systeme Hydrologique Europeen, "SHE", 1: History and philosophy of a physically-based, distributed modelling system, *J. of Hydrology*, 87,45-59, 1986.

Abdulla, F.A., and D.P. Lettenmaier, Development of regional equations for parameterization of land surface schemes, *paper presented at American Geophysical Union Fall meeting, San Francisco,* December, 1994.

Abdulla, F.A., D.P. Lettenmaier, E.F. Wood, and J.A. Smith, Application of a macroscale hydrologic model to estimate the water balance of the Arkansas-Red River basin, accepted for publication, *J. Geophys. Res.*, 1995a.

Abdulla F.A., B. Nijssen, D.P. Lettenmaier, E.F. Wood, and J.A. Smith, Modeling large scale surface energy fluxes in the Arkansas-Red River basin using VIC-2L model, paper presented at the European Geophysical Society, General Assembly 1995, Hamburg, Germany, 1995b.

Ahuja, L.R., D.K. Cassel, R.R. Bruce, and B.B. Barnes, Evaluation of spatial distribution of hydraulic conductivity using effective porosity data, *Soil Science 148*, 404-411, 1989.

Anderson, E.A., "National Weather Service River Forecast System -- Snow accumulation and ablation model", NOAA Technical Memorandum HYDRO-17, U.S. National Weather Service, Silver Spring, MD, 1973.

Aitken, A.P., Assessing systematic errors in rainfall-runoff models, *J. Hydrol., 20*: 121-136, 1973.

Arola A., and D.P. Lettenmaier, Effects of subgrid spatial heterogeneity on

GCM-scale land surface energy and moisture fluxes, accepted for publication, *J. Clim.*, 1995.

Avissar, R., and R.A. Pielke, A parameterization of heterogeneous land surface for atmospheric numerical models and its impact on regional meterology, *Mon. Weather Rev., 117*, 2113-2136, 1989.

Becker, A., and B. Pfuetzner, Larger-scale hydrological modelling for regional transferring of hydrological information, *Regionalization in hydrology* (Proceedings of the Ljubjana Symposium, April 1990). IHAS Publ. no. 191, 1990.

Betts, A.K., J.H. Ball, and A.C.M. Beljaars, Comparison between the land surface response of the ECMWF model and the FIFE-1987 data, *Q.J.R. Meteorol. Soc., 119*, 975-1001, 1993.

Beven, K.J., A. Calver, and E.M. Morris, The Institute of hydrology distributed model, Rep. 98, Inst, of Hydrol., Wallingford, United Kingdom, 1987.

Bradley, A.A., J.A. Smith, and M.L. Baeck, "Hydroclimatology of the 1993 Mississippi River Floods", submitted to *Water Resour. Res.*, 1995.

Bras, R., *Hydrology, An introduction to Hydrologic Science*, Adison-Wesley, 643 pp., 1990.

Brooks, R.H., and A.T. Corey, Hydraulic properties of porous media, *Hydrol. Pap. 3*, Colo. State Univ., Ft. Collins, 1964.

Burnash, R.J., R.L. Ferral, and R.A. McGuire, A generalized streamflow simulation system-Conceptual modeling for digital computers, report, Joint Fed. State River Forecast Center, U.S. Nat. Weather Serv. and Calif. Dep. of Water Resour., Sacramento, Calif., 1973.

Calder, I.R., Hydrologic effects of land-use change, Chapter 13 in *Handbook of Hydrology*, D.R. Maidment, ed., McGraw-Hill, Inc., U.S., 13, 1993.

Charney, J., W. Quirk, S. Chow and J. Kornfield, A comparative study of the effects of albedo change on drought in semi-arid regions, *J. Atmos. Sci., 34*, 1366-1385, 1977.

Crawford, N.H., and R.K. Linsely, Digital simulation in hydrology: Stanford Watershed Model IV, Department of Civil Engineering Stanford University, *Tech. report no. 39*, July 1966.

Delworth, T., and S. Manabe, The influence of soil wetness on near-surface atmospheric variability, *J. Clim.*, 1447-1462, 1989

Dickinson, R.E., A. Henderson-Sellers, P.J. Kennedy, and M.F. Wilson, "Biosphere-atmosphere transfer scheme (BATS) for NCAR Community Climate Model", *NCAR Technical Note, NCAR/TN-275+STR*, Boulder, Colorado, 1986.

Dickinson, R.E., A. Henderson-sellers, and P.J. Kerredy, "Biosphere-atmosphere transfer scheme (BATS) version 1e as coupled to the NCAR Community Climate Model", *NCAR Tech.Note, TN-387+STR*, 1993.

Dooge, J.C., Looking for hydrologic laws, *Water Resour. Res.*, *22*(9), 46S-58S, 1986.

Doorenbos, J., and W.O. Pruitt, Guidelines for predicting crop water requirements, *FAO Irrig. and Drain. Paper No. 24, 2nd ed.*, FAO Rome, Italy, 1977.

Draper, N.R., and H. Smith, *Applied Regression Analysis*, 2nd ed., John Wiley, New York, 1981.

Duan, Q., S. Sorooshian, and V. Gupta, Effective and efficient global optimization for conceptual rainfall-runoff models, *Water Resour. Rec.*, *28*(4), 1015-

1031, 1992.

Duffie, J.A., and W.A. Beckman, *Solar engineering of thermal processes*, John Wiley and Sons, New York, 1980.

Dumenil, L., and E. Todini, A rainfall-runoff scheme for use in the Hamburg climate model, in *Advances in Theoretical Hydrology, A Tribute to James Dooge,* O'Kane. Ed., pp. 129-157, European Geophys. Sco., Series on Hydrological Sciences, 1, Elsevier, Amstedam, 1992.

Eagleson, P.S., The emergence of global-scale hydrology, *Water Resour. Res., 22*(9), 7S-14S, 1986.

Entekhabi, D., and P.S. Eagleson, Land surface hydrology parameterization for atmospheric general circulation models including subgrid scale spatial variability, *J. Clim., 2*, 816-831, 1989.

Famiglietti, J.S., and E.F. Wood, Evapotranspiration and runoff from large areas; Land surface hydrology for atmospheric general circulation models, in *Land Surface-Atmosphere Interactions for Climate Modeling: Observations, Models, and Analysis,* E.F. Wood, Ed., pp. 179-204, Kluwer Academic Publishers, 1991.

Francini. M., and M. Pacciani, Comparative analysis of several conceptual rainfall-runoff models, *J. Hydrol., 122,* 161-219, 1991.

Gan, T.Y., and S.J. Burges, An assessment of a conceptual rainfall-runoff modele's ability to represent the dynamics of small hypothetical catchment: 1 models, model properties, and experimental design, *Water Resour. Res., 26*(7), 1595-1604, 1990.

Giorgi F., and L. O. Mearns, Approaches to the simulation of regional climate change: A Review, *Rev. Geophys., 29*, pp. 191-216, 1991.

Gupta, V.K., and S. Sorooshian, The automatic calibration of conceptual catchment models using derivative-based optimization algorithms, *Water Resour., Res.*, *21*(4), 473-485, 1985.

Grant, P.J., Low flow characteristics on three rock types of the east coast, and the translation of some representative basin data, *J. Hydrol.*, *10*(1), 22-35, 1971.

Haan, C.T., *Statistical Methods in Hydrology*, The Iowa State University Press, 1977.

Hamon, R.W., L.L. Weiss, and W.T. Wilson, Insolation as an empirical function of daily sunshine duration, *Mon. Weather Rev., 82,* 141-146, 1954.

Hamon, R.W., Estimating potential evapotranspiration, *J. Hydraulics Div., 87*, 107-120, 1961.

Hargreaves, G.H., and Z.A. Samani, Reference crop evapotranspiration from temperature, *Applied Engrg. in Agric.*, *1*(2): 96-99, 1985.

Henderson-Sellers, A., and A. Pitman, Land-surface schemes for future climate models: specification, aggregation, and heterogeneity, *J. Geophys. Res. 97*(D3), 2687-2696, 1992.

Hooke, R., and T.A. Jeeves, Direct search solutions of numerical and statistical problems, *J. Assoc. Comput. Mach.*, *8*(2), 212-229, 1961.

Hottel, H.C., A simple model for estimating the transmittance of direct solar radiation through clear atmosphere, *Solar Energy, 18*:129, 1976.

James, L.D., and S.J. Burges, Selection, calibration, and testing of hydrologic models, in *Hydrologic Modeling of small Watersheds,* edited by C. T. Haan, H. P. Johnson, D L. Brakensiek, Am. Soc. Ag. Eng., St-Josefph, Mich., 437-472, 1982.

Jarboe, J.E. and C.T. Haan, Calibrating a water yield model for small ungaged watersheds, *Water Resour. Res.*, *10*(2), 256-262, 1974.

Karl, T.R., C.N. Williams, F.T. Quinlan, and T.A. Boden, "United States Historical, Climatology Network (HCN) serial temperature and precipitation data", NDP-019/R1, Carbon Dioxide Research Program, Oak Ridge National Laboratory, Oak, Tennessee, 1990.

Kindwell, K.B., Global vegetation index User's Guide, NOAA/NESDIS/SDSD, Satellite Data Services Division Princeton Executive Square, Washington, D.C., 1990.

Kirkpatrick, S., C.D. Gelatt, and M.P. Vecchi, Optimization by simulated annealing, *Science, 220*, 671-680, 1983.

Kuczera, G., Improved parameter inference in catchment models, 1, Evaluating parameter uncertainty, *Water Resour. Res.*, *19*(5), 1151-1162, 1983.

Kuhl, C.S., J.R. Miller, Seasonal river runoff calculated from a global atmospheric model, *Water Resour. Res., 28*(8), 2029-2039, 1992.

Lettenmaier, D.P., and Sheer, D.P., Climatic sensitivity of California water resources, *J. Water Resour. Plann. Manage., 117*: 260-272, 1991.

Liang, X., A two-layer variable infiltration capacity land surface represenation for general circulation models, Water Resources Series, *Technical Report No., 140*, University of Washington, Seattle, Washington, U.S.A., 1994.

Liang, X., D.P. Lettenmaier, E.F. Wood, and S.J. Burges, "A simple hydrologically based model of land surface water and energy fluxes for GCMs", *J. Geophys. Res. 99*(D7), 14,415-14,428, 1994.

Lull, H.W., and W.E. Sopper, Factors that influence streamflow in the northeast, *Water Resour. Res.*, *2*(3), 371-379, 1966.

Lytle D.J., N.B. Bliss, and S.W. Waltman, Interpeting the State soil geographic data base, presented in Proceeding second International Conference/Workshop on Integrating Geographic Information Systems and Environmental Modeling, Breckenridge, Colorado, 1994.

Magette, W.L., V.O. Stanholz, and J.G. Cair, Estimating selected parameters for the Kentucky watershed from watershed characteristics, *Water Resour. Res.*, *12*(3), 472-476, 1976.

Mahouf, J.F., E. Richard, and P. Mascart, The influence of soil and vegetation on the development of mesoscale circulation, *J. clim. Appl. Meteor.*, *26*, 1483-1495, 1987.

Manabe, S., J. Smagorinsky, and R.J. Strickler, Simulated climatology of a general circulation model with a hydrological cycle, *Mon. Weather Rev.*, *93*, 769-798, 1965.

Manabe, S., Climate and ocean circulation I. The atmospheric circulation and the hydrology of the earth surface, *Mon. Weather Rev.*, *97*, 739-774, 1969.

Mas E.V., Assessing the hydrologic impacts of climate change on a contintental-scale watershed: An application to the Colorado River Basin, M.S. thesis, Department of Civil Engineering and Operations Research, Princeton University, June, 1995.

McMahon, T.A., and A. Diaz, Methods of computation of low streamflow. *Studies and Reports in Hydrology No. 36* (UNESCO, Paris), 95pp, 1982.

Mintz, Y., The sensitivity of numerically simulated climates to land-surface boundary conditions, in *Global climate,* J.T. Houghton, Ed., pp. 79-105, Cambridge Univ. Press, 1984.

Minzenmayer, F.E., "STATSGO/GRASS Interface User's Guide Version 1.2", USDA-SCS Internal Publication, Lincoln, Nebraska, 200 pages, 1992.

Mosley, M. P., Delimitation of New Zealand Hydrologic regions, *J. Hydrol., 49,* 173-192, 1981.

Nathan, R.J., and McMahon, T. A., Identification of homogeneous regions for the purpose of regionalization, *J. Hydrol., 121,* 217-238, 1990.

Nelder, J.A., and R., Mead, A simplex method for function minimization, *The Computer J., 7,* 308-313, 1965.

Nijssen B., D.P. Lettenmaier, F.A. Abdulla, S.W. Wetzel, and E.F. Wood, Simulation of runoff from continental-scale River basins using a grid-based land surface scheme, submitted to *Water Resour. Res.,* 1995.

Ookouchi, Y., M. Segal, R.C. Kessler, Evaluation of soil moisture effects on the generation and modification of mesoscale circulations, *Mon. Weather Rev.,* 2281-2291, 1984.

Olson, J.S., J.A. Watts, and L. J. Allison, "Carbon in live vegetation of major world ecosystems", U.S. Department of Energy, DOE/NBB-0037, No. TR004, U.S. Department of Energy, Washington, DC, 1983.

Rawls, W.J., and D.L. Brakensiek, Prediction of soil water retention properties for hydrologic modeling, in *Watersheds in the eighties,* ASCE, 293-299, 1985.

Riggs, H.C., Low-flow investigations, *Techniques of Water Resources Investigation of the*

U.S. Geol. Surv., Book 4, Chapter B1, U.S. Geol. Surv., Washington D.C., 1972.

Riggs, H.C., Regional analysis of streamflow techniques. *Techniques of Water Resources Investigation of the U.S. Geol. Surv.*, Book 4, Chapter B3, U.S. Geol. Surv., Washington D.C., 1973.

Rowntree, P.R., Review of GCMs as a basis for predicting the effects of vegetation change on climate, in *Forests, Climate, and Hydrology- Regional Impacts*, E.R.C. Reynolds and F.B. Thompson, Eds, pp. 162-196, The United Nations Univ., 1988.

Rowntree, P.R., and J. Lean, Validation of hydrological schemes for climate models against catchment data, *J. Hydrol.,155,* 301-323, 1994.

Sausen, R., S. Schubert, and L. Dumenil, A model of river runoff for use in coupled atmosphere-ocean models, *J. Hydrol., 155*, 337-352, 1994.

Sellers, P.J., Y. Mintz, Y.C. Sud, and A. Dalcher, Asimple biosphere model (SiB) for use within general circulation models, *J. Atmos. Sci., 43*(6), 505-531, 1986.

Sellers, P.J., and J.L. Dorman, Testing the simple biosphere model (SiB)using point micrometeorological and biophysical data, *J. Appl. Meteor., 26*, 622-651, 1987.

Shepard, D. Computer mapping: the SYMAP interpolation algorithm, in *Spatial Statistics and Models*, (Gaile G.L., and C. Willmott, eds.), Dordrecht: D. Reidel Publishing: 133-146, 1984.

Shuttleworth, W.J., The role of hydrology in global science, *IAHS Publication, 204*, 361-375, 1991.

Slack, J. R., A.M. Lumb, and J. M. Landwehr, Hydro-Climatic Data Network

(HCDN): A U. S. Geological Survey streamflow data set for the United States for the study of climatic variations, 1874-1988., *U. S. Geological Survey Open-File Report 92-129,* 1992.

Stamm J.F., E.F. Wood and D.P. Lettenmaier, Sensitivity of a GCM simulation of global climate to the representation of land surface hydrology, *J. Clim.,* 7(8), 1218-1239, 1994.

Sud Y.C., P.J. Sellers, Y. Mintz, M.D. Chou, G.K. Walker, and W.E. Smith, Influence of the biosphere on the global circulation and hydrologic cycle - a GCM simulation experiment, *Agric. Forest Meteor., 52,* 133-180, 1990.

Sugawara, M., I. Watanabe, E. Ozaki, and Y. Katsuyame, Reference manual for the TANK model, National Research Center for Disaster Prevention, Tokyo, 1983.

Tasker, G. D., Simplified testing of hydrologic regression regions, *J. Hydrc. Div.,* Proc., ASCE, 108(HY10): 122-128, 1972.

TVA (Tennessee Valley Authority), Heat and mass transfer between a water surface and the atmosphere, Norris, Tenn.: Tennessee Valley Authority, Laboratory report no. 14, Water resources research report no. 0-6803, 1972.

Vogel, R.M., and C.N. Kroll, The value of streamflow record augmentation procedures in low-flow and flood-flow frequency analysis, *J. Hydrol., 125,* 259-276, 1991.

Vogel, R.M., and C.N. Kroll, Regional geohydrologic-geomorphic relationships for the estimation of low-flow statistics, *Water Resour. Res., 28*(9), 2451-2458, 1992.

Wang, Q.J., The genetic algorithm and its application to calibrating conceptual rainfall-runoff models, *Water Resour. Res., 27(9),* 2467-2471, 1991.

Wallis, J.R., D.P. Lettenmaier, and E.F. Wood, A daily hydroclimatological data set for the continental United States, *Water Resour. Res.*, *27*,1657-1633, 1991.

Weeks, W.D., and N.M. Ashkanasy, Regional parameters for the Sacramento model: a case study, *Civil Engin. Trans., Instit. Engin., Aust., CE 27*: 305-313, 1985.

Weeks, W.D. and W.C. Boughton, A simple ARMA hydrologic model for ungaged catchments in Queensland, *Civil Engin. Trans., Instit. Engin. Aust., CE 29:* 85-95, 1987.

Wetzel, S., "A hydrological model for predicting the effects of climate change", B.S. Thesis, Department of Civil Engineering and Operations Research, Princeton University, Apr., 1994.

Wigmosta, M.W., L.W. Vail, and D.P. Lettenmaier, A distributed hydrology-vegetation model for complex terrain, *Water Resour. Res. 30*(6), 1665-1679, 1994.

Willmott, C.J., C.M. Rowe, and W.D. Philpot, Small-scale climate maps: A sensitivity analysis of some common assumptions associated with grid point interpolation and contouring, *The American Cartographer, 12*(1),5-16, 1985

Wood, E.F., Global scale hydrology: Advances in land surface modeling, *Reviews Geophys., Supplement,* 193-201, 1991.

Wood, E.F., D.P. Lettenmaier, and V.G. Zartarian, A land-surface hydrology parameterization with subgrid variability for general circulation models, *J. Geophys. Res., 97*(D3), 2717-2728, 1992.

Zektser, I.S., and H. A. Loaiciga, Ground water fluxes in the global hydrologic cycle: past, present, and future, 1992.

Zhao, R.J., Flood forecasting method for humid regions of China, *East China College of Hydraulic Engineering,* 1977.

Zion, M.S., E.F. Wood, R. Dubayah, Estimation of incoming shortwave and longwave radiation for use in modeling the surface energy balance, submitted to *Water Resour. Res.*, 1995.

APPENDIX A
EXAMPLE CALCULATION OF SOIL CLAY PERCENTAGE USING STATSGO DATA

STATSGO data are provided in a probabilistic form, i.e., the attributes are assigned to probability intervals, rather than points. In the STATSGO data base, each geographic unit (e.g., state) is broken down into a number of map units. Map units contain a unique set of soil attributes, but need not be spatially contiguous. Each map unit consists of a set of what are termed maps, which in turn consist of a set of categories. In the following example we perform our calculations for one map unit, which is assumed to consist of six maps and seven categories. Each map contains one of the seven categories, which in the case of this example is a percent areal coverage, but could also be the value of a soil property, for instance, bulk density, in which case the categories would correspond to bulk density intervals. For this example, we take the categories (percent areal coverage) to be Category 0: 0, Category 1: >0 to 10, Category 2: 11 to 20, Category 3: 21 to 40, Category 4: 41 to 60, Category 5: 61 to 80, Category 6: 81 to 100).
Now say that the maps are assigned to categories as follows:

Map	Associated Category (areal coverage in %)
Map 1 (0 to 5%)	Cat 0: (0 category not met)
Map 2 (5.1 to 10%)	Cat 4 (41 to 60%)
Map 3 (10.1 to 20%)	Cat 2 (11 to 20%)
Map 4 (20.1 to 30%)	Cat 3 (21 to 40%)
Map 5 (30.1 to 40%)	Cat 1 (0 to 10%)
Map 6 (>40%)	Cat 0 (0 category not met)

What does the above table mean? For the selected map unit the percentage of

clay ranges from 5.1 to 40% (because Map 6 is not used, i.e., there is no part of the map unit with clay content in excess of 40 percent). 41 to 60 percent (Category 4) of the map unit has clay content ranging from 5.1 to 10 percent clay (Map 2). 11 to 20 percent (Category 2) of the map unit has 10.1 to 20 percent clay (Map 3), and so on.

We then compute the mid point for each of the above maps and their associated categories:

Midpoint of the Map	Midpoint of associated category
Map 1 (2.5%)	CatMap 1 = 0%
Map 2 (7.5%)	CatMap 2 = 50%
Map 3 (15%)	CatMap 3 = 15%
Map 4 (25%)	CatMap 4 = 30%
Map 5 (35%)	CatMap 5 = 5%
Map 6 (>40%)	CatMap 6 = 0%

Then we compute the average of the attribute of interest (percent clay) for the map unit:

$$\text{Average percent clay} = \frac{\sum_{i=1}^{6} \text{Mapi CatMapi}}{\sum_{i=1}^{6} \text{CatMapi}} = 12.25\%$$

In subsequent computations of derived quantities, such as the hydraulic conductivity, we assign the average attribute computed as above to each pixel falling within the given map unit.